

Personalised medicine for pancreatic cancer: using endoscopic ultrasound-guided biopsy for the development of a personalised pre-clinical model of disease

Student: William Berry

Supervisors: Professor Brendan Jenkins and Dr Daniel Croagh

Doctor of Philosophy Thesis

Student number [REDACTED]

Monash University

Hudson Institute of Medical Research

Centre for Innate Immunity and Inflammatory Disease, Cytokine Signalling Laboratory

Monash Health, Department of Surgery

Table of Contents

DECLARATION	VI
ACKNOWLEDGEMENTS	VIII
LIST OF FIGURES	IX
ABBREVIATIONS	XII
PUBLICATIONS, PRESENTATIONS AND AWARDS	XIV
ABSTRACT	1
CHAPTER 1: INTRODUCTION	3
1.1 PANCREATIC CANCER TREATMENT	3
1.2 MOLECULAR PROFILE OF PC	6
1.3 METHODS FOR ISOLATING GENETIC MATERIAL FROM HUMAN PC SAMPLES	8
1.4 PERSONALISED THERAPY IN PC.....	14
1.5 PRE-CLINICAL MODELS IN PC	16
1.5.1 <i>Genetically-engineered mouse models (GEMMs)</i>	16
1.5.2 <i>Xenograft models</i>	17
1.6 TARGETING <i>KRAS</i> WILD TYPE TUMOURS.....	21
1.8 SUMMARY.....	23
1.9 TABLES AND FIGURES.....	24
CHAPTER 2: METHODS	58
2.1 HUMAN SPECIMEN COLLECTION	58
2.2 GENETIC WORK.....	59
2.2.1 <i>Genomic DNA (gDNA) and RNA extraction</i>	59
2.2.2 <i>Gene mutation analyses</i>	59
2.2.3 <i>Reverse transcription (RT)-polymerase chain reaction (PCR)</i>	59
2.2.4 <i>Transcriptome profiling</i>	60
2.2.4 <i>In silico molecular analyses</i>	61

2.3 PROTEIN WORK.....	61
2.3.1 Immunohistochemistry	61
2.3.2 Histological and cytological analyses	61
2.3.3 Protein lysates from tissue	62
2.3.4 Lowry protein assay	62
2.3.5 Western blot	63
2.4 ANIMAL WORK.....	64
2.4.1 Porcine specimen collection and FNA needle comparison	64
2.4.2 Patient-derived xenograft and treatment	64
2.5 STATISTICAL ANALYSES AND COMPUTATIONAL ANALYSIS OF MOLECULAR METADATA	66
2.6 FIGURES.....	67
CHAPTER 3: DEFINING THE UTILITY OF EUS GUIDED FNA FOR THE GENETIC CHARACTERISATION OF PANCREATIC CANCER	71
3.1 OPTIMISATION OF GENOMIC DNA AND TOTAL RNA EXTRACTION FROM EUS FNA SAMPLES	72
3.2 OPTIMISATION OF SAMPLE COLLECTION	73
3.3 HIGH EPITHELIAL CELL CONTENT OF PC EUS FNA-DERIVED SAMPLES.....	74
3.4 COMPARISON OF GDNA DERIVED FROM FIXED TISSUE AND ADDITIONAL BIOPSIES.	75
3.5 DETECTION OF ONCOGENIC <i>KRAS</i> MUTATIONS IN GDNA DERIVED FROM FIXED TISSUE AND ADDITIONAL BIOPSIES	76
3.6 GENETIC YIELD WITH DIFFERENT EUS FNA NEEDLES.....	77
3.7 DISCUSSION	78
CHAPTER 4: TRANSCRIPTOME PROFILE OF PANCREATIC CANCER USING EUS FNA.....	95
4.1 EUS-FNA-DERIVED RNA QUALITY CONTROL FOR RNASEQ	97
4.2 TRANSCRIPTOME PROFILE OF PC TO INFORM DIAGNOSIS.....	98

4.3 MOLECULAR PROFILING TO GUIDE TREATMENT SELECTION IN PC.....	99
4.4 DISCUSSION	102
CHAPTER 5: USING A NOVEL PATIENT-DERIVED XENOGRAFT MODEL TO DEMONSTRATE EFFICACY OF PANITUMUMAB IN <i>KRAS</i> WILD TYPE TUMOURS	145
5.1 ESTABLISHING A PATIENT-DERIVED XENOGRAFT USING EUS FNA SAMPLES OF PC	146
5.2 <i>KRAS</i> GENOTYPING OF PDX TUMOURS	147
5.3 TREATMENT WITH PANITUMUMAB	147
5.4 CHANGES IN CELL PROLIFERATION AND CELL DEATH ON TREATMENT.....	148
5.5 CHANGES IN EGFR SIGNALLING PATHWAY ACTIVATION	149
5.6 DISCUSSION	150
CHAPTER 6	169
6.1 SUMMARY.....	169
6.2 EUS FNA IN MOLECULAR MEDICINE.....	170
6.3 PRE-CLINICAL DISEASE MODELS FOR PERSONALISED MEDICINE IN PC.....	172
6.4 <i>KRAS</i> WILD TYPE DISEASE AND PANITUMUMAB TREATMENT.....	175
6.5 NOVEL TARGETS FOR PERSONALISED THERAPY.....	176
6.6 TARGETING INFLAMMATION IN PC	178
6.7 CONCLUSION	181
APPENDIX	191
APPENDIX 1: RT-QPCR PRIMERS.....	191
APPENDIX 2: R CODE FOR RNASEQ DATA ANALYSES	194
APPENDIX 3: ANTIBODIES	195
APPENDIX 4: BUFFERS AND SOLUTIONS	196
APPENDIX 4: MANUFACTURERS	197
APPENDIX 5 - JOURNAL ARTICLE:.....	198

BERRY, W., ET AL. ENDOSCOPIC ULTRASOUND-GUIDED FINE-NEEDLE ASPIRATE- DERIVED PRECLINICAL PANCREATIC CANCER MODELS REVEAL PANITUMUMAB SENSITIVITY IN KRAS WILD-TYPE TUMORS. <i>INTERNATIONAL JOURNAL OF CANCER</i> (2017).....	198
APPENDIX 6 - BOOK CHAPTER: METHODS IN MOLECULAR BIOLOGY: INFLAMMATION AND CANCER. BERRY, W. , CROAGH, D. CHAPTER: UTILITY OF ENDOSCOPIC ULTRASOUND- GUIDED FINE-NEEDLE ASPIRATION FOR PRECLINICAL EVALUATION OF THERAPIES IN CANCER.....	213
APPENDIX 7 – PROFESSIONAL DEVELOPMENT	228
REFERENCES	233

Declaration

This thesis contains no material that has been accepted for the award of any other degree or diploma in any university, and to the best of my knowledge and belief, contains no material published or written by another person, except where due reference is made in the text. Where the work in this thesis is part of joint research, the relative contributions of the respective persons are listed in the text.



William Berry (PhD Candidate)
Monash University
Faculty of Medicine, Nursing and Health Sciences

Cancer and Immune Signalling Laboratory
Centre for Innate Immunity and Infectious Diseases
Hudson Institute of Medical Research

Department of Upper GI Surgery
Monash Health

Notice 1

Under the Copyright act 1968, this thesis must be used only under the normal conditions of scholarly fair dealing. In particular no results or conclusions should be extracted from it, nor should it be copied or closely paraphrased in whole or in part without the written consent of the author. Proper written acknowledgement should be made for any assistance obtained from this thesis.

Notice 2

I certify that I have made all reasonable efforts to secure copyright permissions for third-party content included in this thesis and have not knowingly added copyright content to my work without the owner's permission.

Acknowledgements

I would like to sincerely thank both my wonderful supervisors, Brendan and Dan, for showing me how to be a diligent researcher, and inspiring me throughout my PhD. I am incredibly proud of what we have achieved together and excited for the future of this project.

To everyone in the Jenkins laboratory and CiiiD for their generous guidance, and enduring friendship I am extremely thankful.

Finally, I would like to say a big thank-you to my family, friends, and my beautiful partner without whom I would not have been able to start or finish this foolish endeavour.

List of figures

Figure 1.1: Treatment options and outcomes in PC

Figure 1.2: Forest plot using Phase III clinical trials in PC

Figure 1.3: Percentage of patients who received different treatment options for pancreatic cancer from The Cancer Genome Atlas

Figure 1.4: EUS FNA cytology technique.

Figure 1.5: Venn diagram showing the differences between the genes up regulated in PC in two published diagnostic gene signatures.

Figure 1.6: Flow diagram illustrating how genetically engineered mouse models progress from normal pancreas through pre-malignant conditions to PC.

Figure 1.7: Xenograft models in PC.

Figure 1.8: Epidermal growth factor signaling pathway and the mechanism of action of Panitumumab.

Figure 1.9: Pancreatic cancer progression model from normal pancreatic epithelium through to intra-epithelial neoplasia and adenocarcinoma.

Figure 2.1: Schematic overview of study methodology from collecting patient samples, to processing for genetic extraction or xenograft and downstream data generation and analyses.

Figure 3.1: Comparison of DNA / RNA isolation methods for EUS FNA samples.

Figure 3.2: RNA yield for each isolation method.

Figure 3.3: RNA yield for each collection method.

Figure 3.4: Gene expression analyses of the high epithelial cell content, of pancreatic origin, in EUS FNA-derived PDAC samples.

Figure 3.5: Detection of *KRAS* mutation in FFPE and additional biopsies.

Figure 3.6: EUS FNA needle comparisons.

Figure 4.1: Quality control assessment of EUS FNA-derived RNA from Monash Biobank cohort.

Figure 4.2: RNAseq contrasting the transcriptome of PC (N = 40) and normal pancreas (N = 5)

Figure 4.3: Heatmap indicating the gene expression of genes in two diagnostic gene lists (Rodriguez and Bhasin, Table 4.2) for independent transcriptome profile datasets.

Figure 4.4: Gene set enrichment results for Bhasin, et al gene list.

Figure 4.5: Gene set enrichment results for Rodriguez, et al gene lists of up- (top) and down-regulated genes (bottom).

Figure 4.6: Incidence of mutations potentially targetable with existing chemotherapy agents in TCGA

Figure 4.7: Transcriptome profile contrasting localised and metastatic PC.

Figure 4.8: Heatmap of TCGA data demonstrating unsupervised hierarchical clustering of *KRAS* wild type tumours and tumours with DNA repair pathway mutations.

Figure 4.9: Transcriptome profile of *KRAS* wild type and mutant tumours

Figure 4.10: Gene set enrichment analysis for *KRAS* wild type and mutant tumours in TCGA dataset.

Figure 4.11: Transcriptome profile of tumours with and without a DNA repair pathway mutation (*BRCA1/2*, *PALB2*, *ATM*).

Figure 4.12: Overall survival of TCGA cohort, with and without molecular targets.

Figure 5.1: Immunostaining on two PDX displaying H & E stain

Figure 5.2: Differential responsiveness of EUS FNA-derived *KRAS* wild type (WT) and *KRAS* mutant (MUT) PDXs to anti-EGFR therapy

Figure 5.3: Differential responsiveness of EUS FNA-derived *KRAS* wild type and *KRAS* mutant PDXs to anti-EGFR therapy

Figure 5.4: Reduced cellular proliferation in panitumumab-treated *KRAS* wild type PDX tumours.

Figure 5.5: TUNEL staining for treated PDX tumours.

Figure 5.6: Western blots with the indicated antibodies for EGFR signaling pathways in protein lysates from treated tumours

Figure 6.1: A flow diagram demonstrating the potential utility of personalised pre-clinical disease models that capture inter-tumoural heterogeneity

Figure 6.2: Pancreatic cancer progression model from normal pancreatic epithelium through to intra-epithelial neoplasia and adenocarcinoma.

Figure 6.3: TLR2 signalling pathway via MyD88 activates multiple signalling molecules

Abbreviations

AKT	Protein kinase B
ATP4A	Adenosine triphosphatase 4A
BRCA	Breast cancer susceptibility gene
CDKN2A	Cyclin-dependent kinase inhibitor 2A
cDNA	Copy DNA
CK	Cytokeratin
Ct	Threshold cycle
DNA	Deoxyribonucleic acid
EGF	Epidermal growth factor
EGFR	Epidermal growth factor receptor
ERK	Extracellular signal-regulated kinase
EUS-FNA	Endoscopic ultrasound guided fine needle aspirate
GC	Gastric cancer
GEO	Gene expression omnibus
Gp130	Glycoprotein 130 receptor
H. Pylori	Helicobacter Pylori
hENT1	Human equilibrative nucleoside transporter 1
HER2	Human epidermal growth factor receptor 2
IL	Interleukin
IMPACT	Individualised molecular pancreatic cancer therapy
JAK	Janus Kinase
KRAS	Kirsten Rat sarcoma, a protein or gene
MAGIC trial	Medical Research Council Adjuvant Infusional Chemotherapy Trial
MAPK	Mitogen-activated protein kinase
NF-κB	Nuclear factor kappa-light-chain-enhancer of activated B cells
p-STAT3	Phosphorylated STAT3
PALB2	Partner and localiser of BRCA2
PanIN	Pancreatic intraepithelial neoplasia
PCNA	Proliferating cell nuclear antigen
PCR	Polymerase chain reaction
PDAC	Pancreatic ductal adenocarcinoma
PDX	Pancreatic and duodenal homeobox factor
PDX	Patient-derived xenograft

RNA	Ribonucleic acid
RT-qPCR	Real time quantitative polymerase chain reaction
SMAD4	SMAD family member 4
SOCS3	Suppressor of cytokine signalling 3
STAT3	Signal transducer and activator of transcription 3
TCGA	The Cancer Genome Consortium
TFF	Trefoil factor
TLR	Toll like receptor
TNF	Tumour necrosis factor
TP53	Tumour protein 53
TUNEL	Terminal deoxynucleotidyl transferase dUTP nick end labelling
Tyr757	Tyrosine 757
USA	United States of America
VEGF	Vascular endothelial growth factor

Publications, presentations and awards

Journal article:

Berry, W., et al. Endoscopic ultrasound-guided fine-needle aspirate-derived preclinical pancreatic cancer models reveal panitumumab sensitivity in KRAS wild-type tumors. *International journal of cancer* (2017). – (Appendix 5)

Book chapter:

Methods in molecular biology: Inflammation and cancer.. **Berry, W.,** Croagh, D. *Chapter: Utility of endoscopic ultrasound-guided fine-needle aspiration for preclinical evaluation of therapies in cancer – Accepted – (Appendix 6)*

PRESENTATIONS	
Year	Details
2017	Departmental oral presentation: <ul style="list-style-type: none"> Alfred Health – Department of Medical Oncology, Department of Radiation Oncology, Journal Club meeting. Berry, W., et al. <i>Endoscopic ultrasound-guided fine-needle aspirate-derived preclinical pancreatic cancer models reveal panitumumab sensitivity in KRAS wild-type tumors.</i>
2016	Oral presentation: <ul style="list-style-type: none"> Australian and New Zealand Hepatic, Pancreatic and Biliary Association, Annual Meeting, Gold Coast - Berry, W., et al. <i>Endoscopic ultrasound-guided fine-needle aspirate-derived preclinical pancreatic cancer models reveal panitumumab sensitivity in KRAS wild-type tumors</i>
2016	Poster presentation: <ul style="list-style-type: none"> Australian and New Zealand Hepatic, Pancreatic and Biliary Association, Annual Meeting, Gold Coast (Poster presentation) – Berry, W., et al. <i>Transcriptome profiling of pancreatic cancer to identify treatable phenotypes for personalised medicine</i>
2016	Poster presentation: <ul style="list-style-type: none"> Monash Health Translational Precinct research week - Berry, W., et al. <i>Transcriptome profiling of pancreatic cancer to contrast localised and metastatic disease</i>
2016	Oral presentation: <ul style="list-style-type: none"> Monash University Three Minute Thesis competition – Berry, W. <i>Advancing personalised medicine for pancreatic cancer</i>
2016	Grand round presentation: <ul style="list-style-type: none"> Monash Health – Grand Rounds, Gastroenterology Department. Berry, W. <i>Advancing personalised medicine for pancreatic cancer</i>

2016	<p>Oral presentation:</p> <ul style="list-style-type: none"> • Monash Health, Department of Surgery – Marshall Prize. Berry, W., et al. <i>Transcriptome profiling of pancreatic cancer to contrast localised and metastatic disease</i>
2015	<p>Oral presentation:</p> <ul style="list-style-type: none"> • UGI Tumour group, Southern Melbourne Integrated Cancer Service, Monash Comprehensive Cancer Consortium. Croagh, D. Berry, W. <i>Pancreatic Cancer Database: Using EUS FNA to personalise pancreatic cancer therapy – Preliminary studies</i>
2015	<p>Poster presentation:</p> <ul style="list-style-type: none"> • Monash Health research week, poster presentation – Berry, W., et al. <i>Fine needle aspirate as a means of characterising gene expression of pancreatic cancer</i>
2014	<p>Oral presentation:</p> <ul style="list-style-type: none"> • Royal Australian College of Surgeons – Annual Surgeons Meeting 2014 - Berry, W., et al. <i>Fine needle aspirate as a means of characterising gene expression of pancreatic cancer</i>
2014	<p>Oral presentation:</p> <ul style="list-style-type: none"> • Australian and New Zealand Hepatic, Pancreatic and Biliary Association, Annual Meeting, Queenstown (Free papers) – Berry, W., et al. <i>Fine needle aspirate as a means of characterising gene expression of pancreatic cancer</i>

AWARDS		
Year	Name of Award/ Prize/ Scholarship	Institution
2015 - 2017	Australian Postgraduate Award	Monash University, NHMRC
2016	<p>Australian and New Zealand Hepatic, Pancreatic and Biliary Association - Free papers</p> <ul style="list-style-type: none"> • Best presentation 	ANZHPBA – Annual meeting 2016
2016	<p>Three minute thesis competition:</p> <ul style="list-style-type: none"> • Centre for Innate Immunity and Immune Disease 1st Prize • School of Clinical Sciences 3rd prize 	Monash University, Hudson Institute of Medical Research
2014	<p>Medical student prize</p> <ul style="list-style-type: none"> • Best presentation 	Royal Australian College of Surgeons – Annual Surgeons Meeting 2014

Abstract

Background

Pancreatic cancer (PC) is largely refractory to existing therapies used in unselected patients, thus emphasising the pressing need for new approaches for patient selection in personalised medicine. There are numerous potential targets for personalised therapy that have been treated in other cancers, including *KRAS* wild type disease, DNA-repair pathway mutations, *HER2* amplification, and *BRAF* mutation. In addition, localised disease is amenable to treatment with pancreatic resection and remains the only treatment to extend median survival beyond one year. *KRAS* mutations occur in 85-96% of PC patients and confer resistance to epidermal growth factor receptor (EGFR) inhibitors (e.g., panitumumab) in other malignancies, suggesting that *KRAS* wild type PC patients may benefit from targeted panitumumab therapy, indeed this is the most prevalent of the targets mentioned above.

Methods

I used tumour tissue procured by endoscopic ultrasound-guided fine-needle aspirate (EUS FNA) to compare the in vivo sensitivity in patient-derived xenografts (PDXs) of *KRAS* wild type and mutant PC tumours to panitumumab, and to profile the molecular signature of these tumours in patients with metastatic or localised disease. In addition, I used The Cancer Genome Atlas (TCGA) to investigate the molecular characteristics of PC in tumours with and without specific molecular targets (e.g. *KRAS* wild type).

Results

RNAseq of EUS FNA-derived tumour RNA from localised (n = 20) and metastatic (n = 20) PC cases revealed a comparable transcriptome profile. Screening the *KRAS*

mutation status of tumour genomic DNA obtained from EUS FNAs stratified PC patients into either *KRAS* wild type or mutant cohorts, and the engraftment of representative *KRAS* wild type and mutant EUS FNA tumour samples into NOD/SCID mice revealed that the growth of *KRAS* wild type, but not mutant, PDXs was selectively suppressed with panitumumab. Furthermore, *in silico* transcriptome interrogation of TCGA-derived *KRAS* wild type (n = 38) and mutant (n = 132) PC tumours revealed 391 differentially expressed genes.

Conclusion

Taken together, my study validates EUS FNA for the application of a novel translational pipeline comprising mutation screening and pre-clinical therapeutic trials using PDXs, applicable to all PC patients, as a tool to evaluate personalised therapy. Specifically, these results suggest that there are no molecular changes that occur in metastatic disease that predispose these tumours to the more aggressive phenotype. Finally, the result from my PDX experiment suggest that as a novel targeted therapy for PC, anti-EGFR therapy in may be successful for patients with *KRAS* wild type tumours.

Chapter 1: Introduction

Pancreas cancer (PC) is regarded as one of the most lethal malignancies, and ranks as the fourth most common cause of cancer-related death worldwide [1,2]. The prognosis is dire; among solid tumours PC has the worst 5-year-survival rate at only 5% [3,4]. This is in part due to advanced disease at the time of presentation, with only 20% of patients diagnosed at an early enough stage that they are suitable for surgical resection [5], but PC at all stages of disease remains refractory to non-surgical treatments. Main known risk factors for PC include cigarette smoking [6], alcohol [7], family history of PC [8] and familial cancer syndromes [9]. Pancreatic ductal adenocarcinoma (PDAC) accounts for over 90% of PC [10], with the remaining 10% made up of several rare exocrine and endocrine tumours of the pancreas, PDAC is the focus of this thesis and will be referred to as PC throughout the text [11].

1.1 Pancreatic cancer treatment

In 1935 Whipple, et al [12] published a report demonstrating the survival benefit of pancreatic resection for PC. Since then resection has been the best treatment option for PC and is indicated for patients with disease localised to the pancreas. In these patients resection can extend median survival to 18-27 months [5,13]. In 1996 gemcitabine was shown to be more effective than other existing chemotherapy regimens (i.e. 5-fluorouracil) [5]. Up until this time medical treatments had been used in a restrained way, as they were largely ineffective, and associated with frequent undesirable adverse effects [13-15]. Gemcitabine has since been the mainstay for non-resectable PC until very recently (Figure 1.1), although several treatments have reached Phase II/III clinical trials, only three trials have demonstrated an

improvement in survival compared to gemcitabine monotherapy (Table 1.1A and 1.1B, Figure 1.2): gemcitabine and nab-paclitaxel [16]; gemcitabine and erlotinib [17]; and FOLFIRINOX (a combination of folinic acid, 5-fluorouracil, irinotecan and oxaliplatin) [18]. In practice, FOLFIRINOX is favoured as it gives the greatest potential for survival benefit, but its use is reserved for patients with higher performance status because of an undesirable side-effect profile. Furthermore, there is no published data on the use of FOLFIRINOX in patients over 71 years of age and with an ECOG (Eastern Cooperative Oncology Group) performance status greater than 1. As such, the majority of patients still receive gemcitabine monotherapy, which has a lower risk of adverse effects [18].

Together, the literature shows that despite numerous Phase III clinical trials, surgery remains the most effective treatment against PC. However, it can only be offered to those 20% of patients who have localised disease and a good performance status. Therefore, there is an urgent need for more effective non-surgical treatments.

Another area of difficulty for clinicians treating patients with PC is the lack of data comparing treatments to anything other than “standard therapy” (gemcitabine monotherapy). For example, there is no trial directly comparing the two most promising therapies: nab-Paclitaxel and FOLFIRINOX. A recent meta-analysis of PC treatments has attempted to address this: Chan, et al [19] compared 16 randomised control trials that used gemcitabine monotherapy as a control treatment arm, and by creating a hazard ratio for each treatment relative to gemcitabine from all studies, as well as using a Bayesian multi-treatment analysis, they compared treatments. The authors conclude that FOLFIRINOX has the highest probability of being the most successful treatment (83%), followed by gemcitabine and nab-paclitaxel (11%), gemcitabine and erlotinib (3%) and gemcitabine and S-1 (3%). However, the studies included in the analysis are not necessarily comparable, and the patient cohorts vary in terms of age, stage and performance status [19]. Although this is theoretically

addressed within the Bayesian analysis, comparing patient cohorts with vast differences in these key criteria makes the results of the analysis less valid.

More recently, Neoptolemos, et al [20] performed a Phase 3, open-label multi-centre randomised trial including 730 patients across 92 centres in Europe. Neoptolemos, et al demonstrate that for patients undergoing pancreatic resection with adjuvant chemotherapy capecitabine in combination with gemcitabine, compared to gemcitabine alone improved overall survival to 28.0 months compared to 25.5 months. However, the addition of capecitabine to these adjuvant chemotherapy regimes increased the rate of adverse events to 226/359 (63%) compared with the adverse event rate with gemcitabine alone 196/366 (54%). These data suggest capecitabine is beneficial to patient overall survival in the adjuvant.

Current clinical practice reflects the recommendations from the literature. Patients who are ineligible for surgery will receive FOLFIRINOX or gemcitabine and nab-paclitaxel if they have good performance status before treatment (Figure 1.1). For those with poorer performance status they are typically trialled on gemcitabine or 5-fluorouracil monotherapy with adjuvant radiotherapy. Figure 1.3 shows the proportion of patients on the different treatment options for PC in The Cancer Genome Atlas (TCGA) cohort from around the world. However, TCGA only included patients eligible for surgical resection, thus omitting patients with locally advanced or metastatic disease (Tables 1.2 and 1.3). As a result, TCGA cohort has a wide variety of treatments reflecting those used as adjuvant chemotherapy to pancreatic resection.

Taken together, clinical trials and clinical practice both demonstrate the significant challenge PC presents and further highlight that advanced PC remains largely refractory to treatment.

1.2 Molecular profile of PC

One of the difficulties in treating PC is the complex molecular profile leading to wide inter-tumoural heterogeneity. For instance, genome-wide association studies (GWAS) on large cohorts ($n > 5,000$) of PC patients and control individuals have identified numerous PC susceptibility loci. These contain a variety of genes, some of which have previously been implicated in oncogenesis (e.g. *BCAR1*, *KLF14*, *PDX1*, *TERT*) [21]. More recently, whole-exome sequencing and whole genome sequencing analyses of resected tumour tissue from a smaller PC patient cohorts ($n = 109$; $n = 456$; and $n = 150$) reported that 24 genes were significantly mutated in at least ~5% of cases, some of which not only provided prognostic value in terms of disease pathology or patient survival (e.g. *KRAS*, *RBM10*), but also identified patients who may respond to targeted therapies (e.g. *BRAF*, *PIK3CA*), providing “a roadmap for precision medicine” [22-24]. Notably, the high genetic diversity of PC tumours provides a rational explanation for the relatively slow progress in the development of novel and effective chemotherapies for PC, especially since all new treatments have previously been tested on unselected PC patient populations [10,16,18,25-27]. In addition, Bailey, et al [23] reported that PC clustered into four distinct cancer subtypes (squamous, pancreatic progenitor, immunogenic and aberrantly differentiated endocrine exocrine), and these correlated with histopathological classification of these tumours (e.g. adenosquamous carcinoma and mucinous adenocarcinoma). This already can inform prognosis, with the squamous subtype demonstrating a median survival of only 13.3 months post-resection, compared to 23.7 – 30.0 months in the other subtypes [23].

Perhaps the most clinically relevant application of these data is on personalising cancer therapy. By identifying subtypes of PC and exploring the differences in the molecular pathways that are active in each subtype, clinicians can

begin to understand which therapies are likely to be effective in these distinct disease phenotypes. Furthermore, this substantiates the theory that the molecular profile of individual tumours holds the key to explaining why some patients have an exceptional response to therapy and why some patients do not respond at all. Accordingly, personalised therapeutic approaches based on the genetic profile of individual tumours provide the opportunity to vastly improve patient outcomes [28]. Taken together, it is estimated that 15% of PC patients will have a treatable target within the molecular profile of their tumour [23,26].

Personalising therapy has been successful in other malignancies, where drugs have been used in particular subsets of tumours with susceptible phenotypes. Examples include HER2-positive breast cancer and trastuzumab [29,30], *BRAF* mutation in melanoma and BRAF/MEK inhibitor combination therapy [31-33], and *KRAS* wild type tumours in colorectal and lung cancer are sensitive to anti-epidermal growth factor receptor therapies [34,35]. Despite the potential of such approaches, a recent report by Chantrill, et al [36] highlighted obstacles for implementing personalised therapy trials for PC. Specifically, in this study, they presented progress of the Individualized Molecular Pancreatic Cancer Therapy (IMPACT) Trial, which enrolled patients with resectable PC. At the time of surgery tumour tissue was taken for genetic analysis to identify potentially treatable targets, following which each cohort would then be randomised to either targeted or standard therapy. However, no enrolled patients reached the treatment phase due to either the patient declining randomisation or deterioration, and therefore becoming ineligible for treatment. One obstacle was that genetic targets occurred in low percentages of patients, so the participants within each phenotypic group were only a fraction of the enrolled cohort. Another problem was the difficulty in isolating high quality tumour-derived genetic material (genomic DNA (gDNA) and/or RNA) in sufficient quantities for subsequent molecular profiling. Linked to this was the heavy reliance upon tissue primarily from archival formalin-fixed, paraffin-embedded (FFPE) samples for gDNA extraction,

most of which were derived from surgical resections which are possible in only 20% of all PC patients [36]. Accordingly, there is an urgent and unmet need to improve methodologies for the robust isolation of high quality genetic material in a timely manner from the vast majority of PC patients.

1.3 Methods for isolating genetic material from human PC samples

Unlike more accessible anatomical sites, the pancreas is difficult to sample without invasive surgery, therefore, to date, genetic studies in PC have largely focused on surgical resection specimens. Isolating genetic material from fresh surgical specimens can be easily done, and there is adequate material for gDNA, RNA and protein extraction from a single sample. However, since only 20% of patients are eligible for surgery, current genetic studies exclude the majority of patients and do not address the potential differences between advanced disease (inoperable) and localised disease (operable). In addition, as personalised therapy becomes more relevant for PC patients, isolating genetic material will be imperative for directing treatment in all PC patients (not just the 20% eligible for surgery). By contrast the current method for confirming a tissue diagnosis of PC is endoscopic ultrasound-guided (EUS) fine-needle aspiration (FNA) is offered to the majority of patients with various stages of disease. There are concerns of lack of cellular material within the EUS FNA samples because of the histological characteristics of PC, having stromal content of approximately 70% [37]. However, epithelial cancer cells are more easily aspirated than stromal cells [38,39] and cellularity can be confirmed by immediate onsite cytology, thus providing a relatively rapid cytological diagnosis for PC [40] (Figure 1.4). This highlights the importance of using EUS FNA to isolate genetic material to direct personalised medicine as most PC patients undergo EUS FNA. Of

note, EUS FNA has been used to provide tissue for genetic analysis for PC and other cancers, thus highlighting its potential for the isolation of genetic material to direct personalised medicine. However, up until now the clinical utility of using this technique for genetic information has been limited, largely due to issues with low tissue quantities leading to suboptimal yields of genetic material, as well as sample contamination with non-malignant cells [36,41-45]. Nonetheless, the inherent advantage of EUS FNA is the ability to sample tumours from patients who are ineligible for surgical resection, giving clinicians the ability to obtain tissue which would otherwise be unavailable [5]. As a result, genetic studies have largely focused on surgically derived tissue and thereby excluded the majority of patients who present with advanced disease.

Preliminary studies sought to use EUS FNA-derived DNA to identify *KRAS* mutation, which is found in approximately 80-90% of PC, to improve diagnostic rates compared to EUS FNA cytology alone [41,42,46-51]. A recent meta-analysis on the topic pooled 8 studies and determined that combining standard EUS FNA cytological diagnostic processes with *KRAS* testing increased the sensitivity of PC diagnosis from 80.6% to 88.7%, and reduced the false-negative rate by 55.6% [41]. Therefore, these analyses confirmed the utility of genetic testing of samples for enhancing diagnostic accuracy; it also shows that EUS FNA can be used for isolation of gDNA from PC [41]. However, a potential problem is that in many of these studies, isolated gDNA was from diagnostic specimens that were formalin-fixed paraffin-embedded (FFPE) tissue, formalin fixation can result in nucleic acid fragmentation and FFPE tissue frequently is exhausted by the diagnostic process. This formalin induced fragmentation completely degrades RNA and can reduce yield and quality of gDNA, thereby reducing the potential for the method to detect mutations in tumoural gDNA and eliminating the ability to measure gene expression. As such, this might indicate that the sensitivity of EUS FNA and *KRAS* mutation would further improve to above 88.7% if more reliable gDNA extraction techniques were used. However, with the

diagnostic sensitivity improving to 88.7%, the improvement in diagnostic rate is comparable to that seen when implementing more convenient methods such as on site cytology, which also improves the sensitivity of EUS FNA from 80% to 88% [52,53].

A similar meta-analysis specifically looked at the use of *KRAS* mutation assay to aid the diagnosis of cystic lesions [54]. This is because cystic lesions can be more difficult to diagnose with cytology alone compared to solid lesions [55]. In this meta-analysis the overall sensitivity of cytology alone was only 42% [54], and in previous meta-analyses sensitivity has been shown to be 35 - 63% [55,56]. In these analyses 8 studies that included *KRAS* status as a diagnostic adjuvant were identified, and the authors found that sensitivity improved to 71% with the molecular analysis used in conjunction with conventional cytology. The authors acknowledge that these findings may be subject to bias as only patients with a verified diagnosis on surgical resection could be included. However, this same bias would apply to the accuracy of cytology alone, therefore these findings strongly indicate that the addition of a molecular adjuvant is beneficial to diagnostic accuracy.

Similarly, there has been interest in using EUS FNA-derived RNA to identify a malignant gene expression signature that could be used for diagnosis. For example Rodriguez and colleagues examined whether it was possible to use EUS FNA-derived RNA to diagnose PC in the place of cytology [57]. In this study 48 patients were enrolled, but 9 of these had insufficient RNA for further analysis. This study used RNAseq to profile malignant and benign samples and generate a gene signature to differentiate these two diagnoses. A training set of 13 patient samples was used to generate a gene signature that differentiated benign and malignant samples. On a separate set of 23 patients (15 malignant and 8 benign) the signature was found to have a sensitivity of 0.87 and a specificity of 0.75, however, this doesn't include the 19% of samples (9/48 samples) that had insufficient RNA yields to include in the analysis. Once again, this was a retrospective study that selected for

patients with confirmed diagnoses; therefore the diagnostic value of this gene signature in samples where cytological diagnosis is “borderline” or “inconclusive” cannot be assessed. As mentioned previously, cytology alone is highly specific and has a sensitivity approaching 90% when on site cytology is available. Therefore, this study shows that EUS FNA-derived RNA can be used for meaningful genetic analysis, however, there are shortcomings related to low RNA yields in some cases. In addition, transcriptome profiling of EUS FNA-derived RNA failed to demonstrate any utility as a diagnostic tool. However, it may prove useful in terms of identifying other useful gene signatures, such as predicting sensitivity to chemotherapy. In other malignancies FNA-derived RNA has been used for gene expression analysis, and these studies have also shown that RNA yields are highly variable due to the nature of the biopsy technique [58,59]. It is worth noting that attempts to derive a diagnostic gene signature from surgical specimens have also resulted in similar accuracy [60], suggesting that the biopsy technique is not to blame for this failure, rather the nature of PC genetics and the potential for tumoural heterogeneity. Therefore, this study is evidence that EUS FNA-derived RNA can indeed be used to provide meaningful gene expression and transcriptome data.

Together, the findings from studies investigating *KRAS* mutation and transcriptome profiling demonstrate that EUS FNA can be used to obtain high quality gDNA and RNA. Therefore, EUS FNA-derived genetic material has the potential to help personalise medicine for PC patients.

To this end, a recent study used a Human Comprehensive Cancer GeneRead™ DNAseq Targeted Panel V2 (Qiagen Inc., Valencia, CA) which detects mutations across the exome (coding regions) of 160 genes frequently mutated in malignancy [61]. Included in this panel are a number of “targetable mutations”, where there is a specific therapy that has been effectively used in selected patients who have tumours with the susceptible variant (e.g. *BRAF*, *BRCA*, *PALB*, *ERBB1* and *ERBB2*). Although the authors reported that they did not identify any tumours with

“targetable mutations” there are a number of tumours that do in fact have potential treatments that could be applied. Namely, *KRAS* wild type tumours that can be treated with anti-EGFR antibodies [34,36,44,62,63] occurred in 6.9% of patients; and *ATM* mutation has been associated with DNA repair pathway impairments that could be susceptible to DNA-damaging agents [36,64]. In addition, the nature of the cancer panel analyses does not allow for copy number variant, which could identify more targets for personalised therapy (e.g. *HER2* amplification). The most important finding in this study was a comparison of EUS FNA-derived and surgically-derived DNA, which revealed that 83.3% (15/18 patients) had 100% gene mutational concordance, and allelic frequency was 34% and 35% in EUS FNA-derived and surgically-derived DNA respectively. Together, this validates the use of EUS FNA for identifying mutations in PC gDNA and shows that the tumour cell content in both sample types is similar. Ultimately, this study demonstrates that personalised therapy based on the mutation status of particular target genes can indeed be directed by EUS FNA-derived gDNA.

However, as the overwhelming majority of work has been done using resection specimens for genetic analysis, this makes comparisons with previous datasets problematic. Although it has been demonstrated that allelic frequency is comparable between EUS FNA-derived and surgically derived DNA, it is unclear what the impact sampling methods has on non-tumoural cell content and gene expression. For instance, EUS FNA samples typically contain blood, inflammatory cells and even intestinal wall epithelial cells, whereas, surgical specimens contain large areas of stromal tissue and no intestinal wall cells at all. This means that new gene expression studies using EUS FNA-derived material need to acknowledge and account for these differences. In addition, false-negatives in diagnosis also will impact on genetic analysis, where a failure to sample an adequate population of tumour cells. There are significant reservations therefore, around the interpretation of EUS FNA-derived genetic material. In studies using surgical resection specimens,

samples are acquired in the presence of surgeon and pathologist, whereby the tumour is identified and a sample taken. Subsequently, a frozen section can be performed at this site to quantify tumour cellularity in the sample that is to be used for the isolation of genetic material, or microdissection would be performed to maximise tumour cellularity [10,23,65]. These conditions can be closely matched with on-site cytology, and subsequent diagnostic cytology identifying only highly cellular samples to be used for genetic analyses. However, these concerns around cellularity cannot be completely allayed, as EUS FNA has a sensitivity of less than 90% and this is largely due to sampling error failing to obtain sufficient tissue for a conclusive diagnosis.

The obvious advantage of EUS FNA is the ability to obtain tissue from all patients, whereas the advantage of surgical specimens is that they are a known quantity. I have briefly addressed the similarities between the two sample types in terms of mutational concordance, but what of the differences? Diagnostic gene signatures have been used for both resection specimens and EUS FNA samples to distinguish PC from non-malignant tissue (pancreatitis or normal pancreas). Bhasin, et al [60] performed a meta-analysis on 12 microarray studies that contrasted PC with normal pancreas using RNA obtained from resection specimens. The authors identified a 5-gene signature that had a sensitivity and specificity of 95% and 89% respectively. Comparing these 5 genes to the list of up-regulated genes generated through similar analyses on EUS FNA-derived RNA by Rodriguez, et al [57], I observed that no genes were common to both gene lists (Table 1.4 and Figure 1.5). This suggests that EUS FNA and surgical samples are two distinct sample types and cannot be included in the same analyses. Interestingly, Moffitt, et al [66] used transcriptome profiling of tumour samples and adjacent normal tissue to perform a “virtual microdissection” to compare tumour at primary and metastatic sites. They demonstrated that previously reported differences in the transcriptome profiles of primary and metastatic tumours were likely due to contamination with surrounding

tissue and that the tumour profiles remain similar despite anatomical location changing during metastasis [66]. Overall, this suggests that differences seen in transcriptome profile between EUS FNA and resection specimens may reflect differences in the nature and degree of “contaminating” cells rather than differences in the tumour profile. Although the sampling techniques in both cases are adequate and isolate representative tumour cells, the contamination with surrounding normal tissue in both cases will obscure the profile of the tumour.

Overall, EUS FNA has only recently emerged as a candidate technique for isolating PC genetic material and therefore as a means for biomarker identification. The advantage of EUS FNA compared to surgical resection specimens is the ability to include patients with advanced disease, which in PC makes up the overwhelming majority. In addition, the ability to obtain tissue early in the clinical course of the disease facilitates the procurement of chemo-naïve tissue. Given the success in obtaining both gDNA and RNA and translating these into meaningful genomic and transcriptomic data, EUS FNA is poised to identify and characterise known and novel therapeutic biomarkers. New trials of personalised therapy in PC should endeavour to use EUS FNA to direct treatment.

1.4 Personalised therapy in PC

As previously mentioned, personalising therapy is a promising option in PC because patients do not respond uniformly to current treatment options. The wide inter-tumoural heterogeneity has led researchers to believe that an individualised approach to therapy is what is needed to address the current shortcomings in PC therapy. Importantly, personalised therapy is further advanced in other malignancies, which can guide researchers in PC to use these successful therapies in PC with

similar molecular profiles. Table 1.5 shows the prevalence of potential molecular targets and the corresponding therapy that can be used in a targeted fashion. Although some of these therapies have failed to demonstrate a survival advantage in unselected populations, by only targeting patients with amenable molecular profiles, treatment efficacy, and therefore patient outcomes, may improve substantially.

As previously mentioned, the failings of the IMPaCT trial of personalised therapy resulted in none of the 93 patients enrolled actually being treated with targeted therapy [67]. There were several contributing factors that highlight the difficulty of performing trials of personalised therapy in PC. The first problem was the low frequency of targetable mutations, the most prevalent of which was *KRAS* wild type disease occurring in 14/93. Another problematic factor was the delay between sampling mutation status result; this meant that before enrolled patients knew whether they would be eligible for a targeted treatment, they had started an alternative treatment or deteriorated that excluded them from the trial. These study design issues could be overcome by establishing treatment efficacy in a pre-clinical disease model before human clinical trials. Pre-clinical disease models have the potential to isolate these rare disease variants (e.g. *KRAS* wild type disease) using either genetically engineered cell lines or mouse models or patient-derived methods such as organoid and xenograft models. Using pre-clinical models to prove treatment efficacy before human trials may increase the rate of patients agreeing to randomisation, and additionally, may streamline study designs to use more targeted sequencing panels that may expedite mutation results.

1.5 Pre-clinical models in PC

There are a number of techniques used to model human PC and test therapies in the laboratory before applying them to patients in clinical trials.

1.5.1 Genetically-engineered mouse models (GEMMs)

Insights into the molecular basis of PC have been gained over recent years through the use of several models of PC based on conditional genetically modified mice (Table 1.6). These have the advantage of allowing specific genetic alterations (such as the commonly activated *Kras* allele) that lead to PC, usually incorporating a phenotype that progresses from normal pancreas epithelium, through the various stages of PanIN, ultimately resulting in PDAC (Figure 1.6). Despite the advantage of such models to capture PC development from the initiating normal epithelium, GEMMs cannot however capture the inter-tumoural heterogeneity seen amongst PC patient tumours. This is because such models are based on a few genetic alterations in the main disease drivers (e.g. *Kras*) leading to cell transformation and cancer development, but this does not represent tumours that harbour different disease drivers. One striking feature of these models (Table 1.6) is the reliance upon *Kras* mutations, which implies that all mouse model studies are not relevant to approximately 15% of patients with *KRAS* wild type tumours. Furthermore, these models fail to capture intertumoural heterogeneity, and don't necessarily capture rare disease phenotypes, such as those targeted in the IMPaCT personalised therapy trial.

An advantage of GEMMs, are the ability to capture the longitudinal nature of PC from chronic pancreatitis, to pre-malignant intra-epithelial neoplasia, and

ultimately invasive carcinoma. Furthermore, this allows for the model to replicate early disease and late metastatic disease.

Taken together this means that the advantage of GEMM models is the ability to study in detail the mechanisms of specific pathways involved in tumourigenesis, but the great failing of the methodology is the inability to re-capture the individuality of human disease.

1.5.2 Xenograft models

A method that has the potential to capture the individuality of patient tumours is xenograft modelling. Xenograft studies involve the growth of cancer cells in an immune-deficient mouse. These cancer cells are usually taken from either an immortalised cell-line or patient specimen (patient-derived; Figure 1.7A). Xenografts have been shown to retain the molecular characteristics of the original tumour cells (whether from patient samples or cell-lines) [68,69]. The unique advantage of xenograft studies therefore, is to capture inter-tumoural heterogeneity, which makes xenograft models a tool to demonstrate a biological response to personalised therapies designed to target specific tumour molecular profiles [70]. As such, in recent years the rate of publication of xenograft studies has soared in PC, with 338 and 294 studies published in 2015 and 2016 respectively (Figure 1.7B).

The potential clinical utility of xenografts is evidenced by a study to demonstrate efficacy for FOLFIRINOX before it was applied in the clinic [71]. Specifically, in this study pieces of grafted tumours were implanted into BALB/c mice, then initiated treatment on days 3-14, continuing treatment for 179 days or until the mice reached another ethical endpoint (tumour size >2000mg or toxicity). Notably, all mice were tumour free in the “early stage disease” (defined as treatment started on day 3, post implantation) and those with “advanced stage disease” (defined as treatment started on day 14, post implantation) had delayed tumour growth, but didn’t

prevent tumour growth, in all mice. By contrast, the response rate in human disease is 30% [18], this shows that xenograft data is useful in predicting treatment activity, but has a tendency to over-estimate the treatment effects.

An advantage of PDX models is that through tumour passage, identical tumours can be subjected to multiple treatments; therefore experiments can directly compare the efficacy of multiple treatment strategies for one patient's tumour. This has been used at Johns Hopkins to personalise therapy in PC [64]; where PC patients undergoing pancreatic resection had pieces of their tumour implanted in nude mice, and once the graft was established the tumour was passaged to expand the colony creating several mice with identical tumours matched to the original patient [64,72]. A variety of therapies can then be tested on that patient's tumour, from which the most effective treatment for the patient can then be selected should recurrence occur post-operatively [64,72]. In one example, a PDX was found to be sensitive to DNA-damaging agents, and the same therapy was given to the patient and they demonstrated an exceptional response to these agents [64]. Villaroel and colleagues [64] used surgical resection specimens to establish xenografts, which were then used to conduct individual trials of various therapies. Importantly, surgery delays recurrence and therefore allows time for the xenograft to establish and the treatment experiments to be completed before targeted therapy is to be initiated in the patient. However, this study does not mention engraftment rates, which would impact the number of patients who could potentially benefit from this practice. In one patient DNA sequencing analysis revealed the tumour had a mutation in the *PALB2* (Partner and localiser of *BRCA2*) gene. Since *BRCA* is involved in DNA repair when cross-linking damage occurs, malignancies with mutations of *BRCA* and associated genes result in DNA progressing through more error-prone pathways, and this leads to sensitivity to DNA-damaging agents (e.g. mitomycin C and platinum's) [73-77]. Villaroel and colleagues' study is an example of the potential for PDX studies to quickly translate to positive results in clinical practice and could inform a clinical trial

of DNA-damaging agents in patients with *BRCA*-associated gene mutation [64]. Indeed, Waddell, et al show *BRCA 1/2* mutation may occur in as many as 9% of PC cases and 14% may be amenable to DNA-damaging agents as they have “high genomic instability” [65]. It is difficult however, to translate this into widespread clinical practice because it requires biomarker driven trials targeting these rare genetic profiles and therefore enrolling large numbers of patients.

However, xenograft models have a tendency to exaggerate the efficacy of therapies under investigation. Demonstrating this point is the fact that in clinical practice, gemcitabine only demonstrates a response in 7-20% of patients and only a small survival advantage [14-16,18]; by contrast, in xenograft models gemcitabine is very effective at reducing tumour growth (Figure 1.7C). Despite this tendency to exaggerate treatment effectiveness, this is the most relevant preclinical treatment model and frequently provides evidence to support a clinical trial. This tendency to exaggerate therapeutic effect could translate to failed clinical trials. However, understanding what factors contribute to this could help improve the model, and predict behaviour in clinical settings.

Tables 1.7A and B outline the experimental parameters for these studies and show what factors potentially contribute to the overestimation of treatment efficacy and the variability across different experiments. Unlike clinical trials, xenograft studies aren't standardised in experimental design, and as such, it is difficult to compare studies that use different genetically modified mice, treatment doses, and tumour engraftment site.

The validity of xenograft models has been extensively reviewed [78-81] and some limitations have been highlighted in these publications. The most important factor for a preclinical model is the ability to accurately model human disease to predict therapeutic efficacy and reliably translate into human trials. It has been shown that cell line-derived xenografts are not predictive for response to therapy in human disease [81] and therefore should not be used as a preclinical trial, rather, they are

best suited for interrogating the pathways effected by certain treatments. By contrast, personalised PDXs are 80% predictive of response in human disease [82]. However, when PDX models are applied in unselected patients, they become less predictive of patient outcomes. The differences between the two models are highlighted in Table 1.8, where the limitations of cell lines are apparent.

The most important drawback to xenograft models, both patient-derived and cell line-derived, is the inability to model the tumour-immune interaction and test immunotherapies. To allow tumour growth animals must be immune-deficient, the more immune-compromised, the higher the engraftment rate (Tables 1.7A and B). However, the immune system is important for tumour genesis, progression and treatment resistance [83-88]. In PC this is particularly relevant, as chronic pancreatitis is associated with the development of PC, whereby chronic inflammation leads to a non-invasive precursor lesion, pancreatic intraepithelial neoplasia (PanIN), which can progress to pancreatic ductal adenocarcinoma [89-93]. PanIN has well-defined stages of progression, and these are based predominantly on histological appearance, and secondarily on the genetic alterations observed [94-96]. Genetic mutations common to PDAC are also seen in a large proportion of PanIN [11,94-97]. Options are being explored to improve the modelling of the tumour-immune interactions in xenografts. These include orthotopic engraftment in the murine pancreas, rather than sub-cutaneous or renal capsular graft sites; however, orthotopic models are more technically challenging and can reduce engraftment rate compared to more vascular and accessible sites (i.e. sub-cutaneous grafts). In addition, co-culturing cells that are thought to be important in the pathogenesis of the disease (e.g. immune cells), or resistance to therapy (e.g. fibroblasts) [98]. Another way to capture the immune system and tumour interaction in xenograft models is to reconstitute the immune system of the animal with human cells. This technique can be achieved by irradiating the animal before implanting human bone marrow or isolated T and B cells to establish a humanised immune system [99-101]. The

advantage of this type of model is that an intact immune system more accurately reflects true human disease, and it allows researchers to test immunomodulation therapies. This could allow a fully personalised model of disease, whereby a patient donates tumour samples as well as bone marrow or blood samples. The tumour samples could be grafted in a mouse with an immune system re-constituted with that same patient's immune cells. However, by re-constituting the animal's immune system the model the humanised immune system mounts a response to the animal's own tissues, i.e. graft-versus-host disease (GvHD), thus limiting the utility of these models [102,103]. There is still an experimental window for these models as GvHD develops between 2 – 5 weeks after engraftment, enabling tumour biology experiments, however treatment efficacy experiments are not feasible within this timeframe.

1.6 Targeting *KRAS* wild type tumours

In PC *KRAS* mutation is highly prevalent and often thought to be crucial for the initiation of tumourigenesis [24,95,96]. Of particular interest is the fact that in colorectal cancer and lung cancer *KRAS* mutation has been shown to reduce the efficacy of anti-EGFR therapies (e.g. erlotinib and panitumumab) [34,35,104-106]. The same may be true in PC, where *KRAS* mutation occurs in approximately 80-96% of patients [10,26,41,42,46-51,107], therefore, there may be as many as 20% of PC patients who would benefit from anti-EGFR therapy [26,36]. Interestingly, recent genomic, transcriptomic and proteomic profiling of PC has demonstrated that *KRAS* wild-type tumours indeed have distinct oncogenic drivers including additional RAS pathway genes [24]. The mechanism of action of panitumumab is depicted in Figure

1.8, highlighting how blocking this receptor inhibits the pro-tumourigenic RAS signalling pathway.

In PC, Moore, et al [17] performed a trial comparing anti-EGFR therapy (erlotinib) in combination with gemcitabine compared to standard gemcitabine monotherapy in an unselected cohort of patients. This trial demonstrated an improved median survival 6.24 compared to 5.91 months with gemcitabine alone. This might indicate that, as is the case in other malignancies [34,35,104-106], *KRAS* mutation status conveys resistance to this therapy and the difference in overall survival between the two treatments in the trial by Moore, et al would indicate that 5-20% of these patients might have benefited from the addition of erlotinib. There was no difference in objective response rates between the two treatment arms in this study, however, the effect of erlotinib alone is likely to be obscured by the combination with gemcitabine and therefore a monotherapy treatment group would be required. It is important to examine whether *KRAS* wild type is indeed a potentially targetable phenotype of PC, and therefore include the tumour mutation status in these trials.

1.8 Summary

PC is a disease that has been largely refractory to treatment despite decades of research. To achieve improvement in outcomes for patients, research needs to address the heterogeneity of the disease with personalised approaches to treatment. However, this has proved difficult to implement as single therapeutic targets occur rarely in PC and obtaining genetic material to identify these targets has been problematic. Thus it is important to look at new ways to obtain genetic material from those patients with advanced disease, and a potential avenue is validating the use of EUS FNA for this purpose. Furthermore, the lack of success of Phase II clinical trials highlights the need for more robust pre-clinical tools for examining treatment efficacy, thereby improving the rate of success when therapies make the transition from pre-clinical to clinical trials. Finally, to improve outcomes for the majority of patients, more therapeutic targets need to be identified and novel treatments trialled.

In my thesis I will focus on validating the use of EUS FNA for genetic analysis of PC; investigate the potential of personalised treatment in PC using next generation sequencing (NGS) technology; and develop a novel pre-clinical PDX model using EUS FNA to trial a targeted therapy approach.

1.9 Tables and figures

Table 1.1A: Clinical trials in PC comparing trial therapy with gemcitabine monotherapy. #Hazard ratio for gemcitabine monotherapy compared to trial

treatment for Phase III clinical trials only. *Median overall survival not reported⁶

Pooled hazard ratio for two trials, both trials were not significant on their own, but pooled analysis by results in significance.

Gem = Gemcitabine; FOLFIRI = Folinic acid, 5-Fluorouracil, irinotecan; FOLFOX = Folinic acid, 5-Fluorouracil, oxaliplatin; NR = Not reported

Treatment	Survival (Months)	Hazard Ratio [#] [95% CI]	Reference
Gem + 5-Fluorouracil	4.3 – 7.3	0.82 [0.65, 1.03]	Phase II: Berlin, et al, 2000 [108]; Roehrig, et al, 2010 [109]; Pelzer, et al, 2011 [110] Phase III: Berlin, et al, 2002 [111]
Gem + cisplatin	6.7 – 8.2	0.96 [0.70, 1.30]	Phase II: Heinemann, et al, 2000 [112]; Philip, et al, 2001 [113]; Kulke, et al, 2009 [114] Phase III: Heinemann, et al, 2006 [115]; Colucci, et al, 2010 [116]
Gem + cisplatin + epirubicin + 5-Fluorouracil	10.0 (Phase II) *Significant increase in overall survival at 2-years compared to Gem alone (11.5% vs 2.1%, $p = 0.033$ (Phase III)	NR	Phase II: Reni, et al, 2001 [117] Phase III: Reni, et al, 2005 [118]
Gem + irinotecan	5.7 – 7.1	NR	Phase II: Rocha Lima, et al, 2002 [119]; Stathopoulos, et al, 2003 [120]; Kulke, et al, 2009 [114] Phase III: Rocha Lima, et al, 2004 [121]; Stathopoulos, et al,

				2006 [122]
Gem + oxaliplatin	5.7 – 9.4	0.87 0.98]	[0.76,	Phase II: Louvet, et al, 2002 [123]; Afchain, et al, 2009 [124]; Lee, et al, 2009 [125] Phase III: Louvet, et al, 2005 [126]; Poplin, et al, 2009 [127]
Gem + pemetrexed	6.2 – 6.5	0.98 1.18]	[0.82,	Phase II: Kindler, 2002 [128] Phase III: Oettle, et al, 2005 [129]
Gem + marimastat	5.4	0.99 1.30]	[0.76,	Phase III: Bramhall, et al, 2002 [130]
Gem + capecitabine	7.1 – 9.5	0.86 0.98] ^θ	[0.75,	Phase II: Scheithauer, et al, 2003 [131] Phase III: Herrmann, et al, 2007 [132]; Cunningham, et al, 2009 [133]
Gem + tipifarnib	6.3	1.03 1.23]	[0.86,	Phase III: Van Cutsem, et al, 2004 [134]
Gem + exatecan	6.7	NR		Phase III: Abou-Alfa, et al, 2006 [135]
Gem + cetuximab	6.3 – 7.1	1.06 1.23]	[0.91,	Phase II: Xiong, et al, 2004 [136] Phase III: Philip, et al, 2010 [137]
Gem + bevacizumab	5.8 – 8.8	1.04 1.24]	[0.88,	Phase II: Kindler, et al, 2005 [138] Phase III: Kindler, et al, 2010 [139]
Gem + sorafenib	4.0 – 6.5	1.04 1.55]	[0.70,	Phase II: Kindler, et al, 2005 [140]; El-Khoueiry, et al, 2012 [141] Phase III: Goncalves, et al, 2012 [142]
Irinotecan	6.6	-		Phase II: Yi, et al, 2009 [143]
Gem + docetaxel	6.4	-		Phase II: Kulke, et al, 2009 [114]
Gem + oxaliplatin + 5-Fluorouracil	8.7	-		Phase II: Ch'ang, et al, 2009 [144]
FOLFIRI	4.2 – 5.0	-		Phase II: Yoo, et al, 2009 [145]; Zaniboni, et al, 2012 [146]
FOLFOX	3.7	-		Phase II: Yoo, et al, 2009 [145]
Paclitaxel	2.5 – 6.5	-		Phase II: Saif, et al, 2010 [147]
Gem + etoposide	7.2	-		Phase II: Melnik, et al, 2010 [148]

Gem + oxaliplatin + capecitabine	7.8	-		Phase II: Hess, et al, 2010 [149]
Gem + docetaxel + capecitabine	9.0	-		Phase II: Xenidis, et al, 2012 [150]
Gem + cisplatin + capecitabine + epirubicin	11.0	-		Phase II: Reni, et al, 2012 [151]
Gem + cisplatin + capecitabine + docetaxel	10.7	-		Phase II: Reni, et al, 2012 [151]
Gem + S1	7.9 – 13.7	0.80 [0.66, 0.96]		Phase II: Ozaka, et al, 2012 [152]; Nakai, et al, 2012 [153]; Song, et al, 2013 [154] Phase III: Ueno, et al, 2013 [155]
CO-101	5.2	-		Phase II: Poplin, et al, 2013 [156]
PEP02	5.2	-		Phase II: Ko, et al, 2013 [157]

Table 1.1B: Phase III clinical trials showing efficacy compared to gemcitabine monotherapy. [#]Hazard ratio for gemcitabine monotherapy compared to trial treatment. NA = Not applicable; FOLFIRINOX = Folinic acid, 5-Fluorouracil, irinotecan and oxaliplatin; nab-paclitaxel = nano-albumin bound paclitaxel

Treatment	Survival	Hazard Ratio[#] [95% CI]	Reference
Gemcitabine	5.65 months	NA	Burris, et al, 1997 [15]
Gemcitabine and Erlotinib	6.24 months	0.82 [0.69, 0.97]	Moore, et al, 2007 [17]
FOLFIRINOX	11.1 months	0.57 [0.45, 0.72]	Conroy, et al, 2011 [18]
Gemcitabine and nab-paclitaxel	8.1 – 9.3 months	0.72 [0.62, 0.84]	Von Hoff, et al, 2013 [16]

Table 1.2: Clinicopathological characteristics of RNAseq PC cohort for localised versus metastatic disease analysis using EUS-FNA-derived RNA.

Patient characteristics	n = 40
Gender	
Female, n (%)	24 (60%)
Age, mean (range) years	
	68.1 (47-88)
Stage, n (%)	
Localised	20 (50%)
Metastatic	20 (50%)
Treatment, n (%)	
Surgery	5 (12.5%)
FOLFIRINOX	3 (7.5%)
Gem + nab-Paclitaxel	8 (20%)
Gemcitabine	3 (7.5%)
Palliative	5 (12.5%)
Other	2 (5%)
Unknown	14 (35%)
Site, n (%)	
Head	21 (52.5%)
Uncinate	4 (10%)
Neck	7 (17.5%)
Body	7 (17.5%)
Tail	1 (2.5%)

Table 1.3: Patient characteristics from TCGA cohort, 178 patients

Characteristic	
Sex	44.9% Female
	55.1% Male
Age (Range)	65.4 (35 - 88)
Surgery performed	
- Whipple	77.35%
- Total pancreatectomy	1.60%
- Distal pancreatectomy	12.40%
- Unknown	8.65%
Duration of treatment, days	Median = 225
	Range 0-1895
Survival	
- Alive at follow up	55.40%
- Average survival of deceased patients	462 days
Recurrence (%)	33.70%
- Distant metastasis	21.30%
- Locoregional metastasis	7.90%
- New primary tumour	1.10%
- Not specified	3.40%
Tumour grade	
1	17.60%
2	53.30%
3	28.00%
4	1.10%
Positive lymph nodes, median (range)	2 (0 - 16)

0	26.50%
1	14.10%
2	14.60%
>2	44.80%
Site	
- Head	77.80%
- Body	7.00%
- Tail	7.60%
- Other	2.20%
- Unknown	5.40%

Table 1.4: Diagnostic gene signatures for PC.

Reference	Platform	Sample type	Number of genes in gene signature	Sensitivity / Specificity
Rodriguez, et al, 2016 [57]	RNAseq	EUS FNA	83	0.87 / 0.75
Bhasin, et al, 2016 [60]	Microarray	Surgical resection	5	0.95 / 0.89

Table 1.5: Potentially treatable phenotypes in PC and the prevalence of molecular targets.

Treatment	Target	Prevalence	TCGA or EUS FNA
Surgery	Localised disease	20% [5]	EUS FNA
EGFR inhibition	<i>KRAS</i> wild type	5-20% [23,41]	TCGA
DNA damaging agents	DNA repair pathways	14% [64,65]	TCGA
Trastuzumab	HER2 amplification	10 – 30% [36,158]	No CNV available
BRAF/MEK inhibition	<i>BRAF</i> mutation	1-2% [10,26,107]	TCGA
Everolimus	PI3K/AKT/mTOR pathway		TCGA
Imatinib	<i>KIT, ABL1/2, RET</i> mutation		TCGA
Sorafenib	<i>PDGFR A/B, FLT3</i> mutation	Unknown [159]	TCGA
Tamoxifen / Letrozole	Oestrogen / Progesterone receptor expression		No protein data available
Abiraterone	Androgen receptor expression		No protein data available
c-MET inhibitor	c-MET expression	Unknown [160-162]	No protein data available

CNV, copy number variant.

Table 1.6: GEMM in PC using *Kras* mutation.

Genotype	Summary	Reference
PdxCre/Ptf1a ^{Cre} ; <i>Kras</i>	Model demonstrates progression through stages of PanIN and PDAC	Hingorani, et al, 2003 [163]
Ptf1a ^{Cre} ; <i>Kras</i> ; <i>Brg1</i> ^{lox/lox}	Combination of <i>Kras</i> and loss of <i>Brg1</i> lead to IPMN development and progression to PDAC.	von Figura, et al, 2014 [164]
Ptf1a ^{Cre} ; <i>Kras</i> ; <i>Ela-Tgfa</i>	Overexpression of <i>Tgfa</i> leads to increased rate of progression from PanIN and concurrent development of IPMN before progression to PDAC.	Siveke, et al, 2007 [165]
Pdx1-Cre; <i>Kras</i> ; <i>p16/p19</i> ^{lox/lox}	Loss of <i>p16/p19</i> in the setting of <i>Kras</i> mutation lead to rapid development of PDAC, with micro-metastases and a survival of only 2 months	Bardeesy, et al, 2006 [166]
Pdx1-Cre; <i>Kras</i> ; <i>p16/p19</i> ^{+/lox}	Heterozygosity for <i>p16/p19</i> in the context of <i>Kras</i> mutation resulted in long latency and the development of distant metastases.	Bardeesy, et al, 2006 [166]
Pdx1-Cre; <i>Kras</i> ; <i>p16</i> ^{lox/lox}	<i>Kras</i> mutation and deletion of <i>p16</i> leads to rapidly progressive PDAC	Bardeesy, et al, 2006 [166]
Pdx1-Cre; <i>Kras</i> ; <i>p53</i> ^{lox/lox}	Combination of <i>Kras</i> mutation and loss of <i>p53</i> resulted in rapidly progressive PDAC	Bardeesy, et al, 2006 [166]
Pdx1-Cre; <i>Kras</i> ; <i>p53</i> ^{R172H}	The addition of <i>p53</i> mutation leads to widespread metastasis and locally invasive tumours that represent	Hingorani, et al, 2005 [167]

	human disease.	
Ptf1a ^{Cre} ; Kras; Notch2 ^{loxlox}	Ablation of <i>Notch2</i> halts progression of PanIN and results in mucinous cystic neoplasms.	Mazur, et al, 2010 [168]
Ptf1a ^{Cre} ; Kras; Smad4 ^{loxlox}	The addition of <i>Smad4</i> deficiency to <i>Kras</i> mutation leads to the development of IPMN lesions and more rapid development of PDAC than <i>Kras</i> mutation alone.	Bardeesy, et al, 2006 [169]
Ptf1a ^{Cre} ; Kras; Tgfbr2 ^{loxlox}	The combination of <i>Kras</i> mutation with <i>Tgfbr2</i> ablation increased the rate of progression to PDAC.	Ijichi, et al, 2006 [170]
Ptf1a ^{Cre} ; Kras; p53 ^{R270H} ; Brca2 ^{Tr/D11}	The addition of two mutations (<i>p53</i> and <i>Brca2</i>) dramatically increased the rate of progression to PDAC. The model is most relevant for those with familial PC, or spontaneous <i>BRCA2</i> mutations	Skoulidis, et al, 2010 [171]
PdxCre/Ptf1a ^{Cre} ; CAGs-LSL-RIK	Combination of <i>Kras</i> mutation with shRNA leads to a malleable model.	Saborowski, et al, 2014 [172]

Tables 1.7A and B: Experimental design factors and the variability amongst xenograft studies for patient-derived xenografts (A) and cell line-derived studies (B)

Table 1.7A

Patient-derived xenograft	
Characteristic	Number (n = 18)
Mouse	
Athymic nude	8
NOD/SCID	5
NOD/SCID gamma	1
Other	4
Graft site	
Subcutaneous	13
Orthotopic	4
Renal capsule	1
GEM dose (mg/kg/week)	
<50	4
50-100	5
100-200	7
>200	1
Other	1

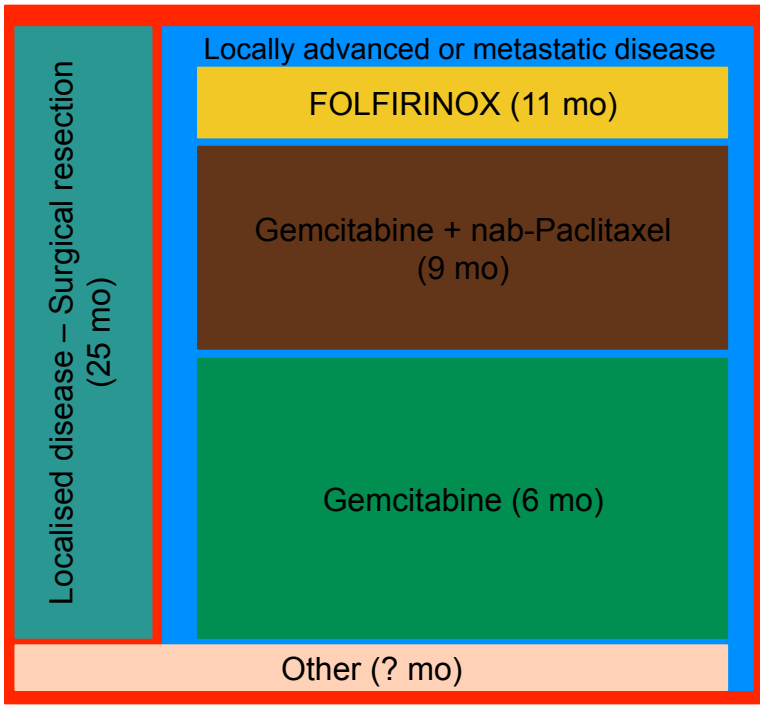
Table 1.7B

Cell lines derived xenograft	
Characteristic	Number (n = 23)
Mouse	
BALB/c nude mice	10
Athymic nude	7
SCID	3
Other	3
Graft site	
Subcutaneous	12
Orthotopic	5
Intraperitoneal	2
Intrahepatic	1
GEM dose (mg/kg/week)	
<50	3
50-100	3
100-200	10
>200	3
Other	4

Table 1.8: Differences between cell line-derived and patient-derived xenografts

Cell line-derived xenograft	Patient-derived xenograft
Homogenous cell population	Heterogeneous cell population
Minimal infiltration of murine stroma	Moderate infiltration of murine stroma
Tumour architecture lost	Tumour architecture maintained
Most cell lines are derived from aggressive disease and through passage outgrowth of most proliferative clones occurs	Allows personalised pre-clinical model, but outgrowth of most proliferative clones occurs
Short time from engraftment to result	Long time (6-12 months) from engraftment to result

Figure 1.1: Treatment options and outcomes in PC. This figure shows that number of patients who receive surgical or medical management represented by the proportional sized blocks for each treatment. The triangle on the right-hand side represents patient performance status and demonstrates how treatment choices are impacted by these patient factors. 20% of patients present with localised disease and undergo surgical resection resulting in a median survival of 25 months. 80% of patients have advanced disease at the time of diagnosis and receive medical therapies, of which, those with higher performance status are eligible for more aggressive therapy combinations FOLFIRINOX and Gemcitabine and nab-Paclitaxel, these achieve a median survival of 9-11 months. The majority will be trialed on gemcitabine monotherapy, giving a median survival of 6 months and a preferable side-effect profile. Approximately 10% of patients receive either another therapy or no therapy at all.



Performance status

Figure 1.2: Forest plot using Phase III clinical trials in PC that included a control arm of gemcitabine monotherapy for a consistent comparison. This shows the hazard ratio indicating the effect of experimental treatment compared to gemcitabine monotherapy.

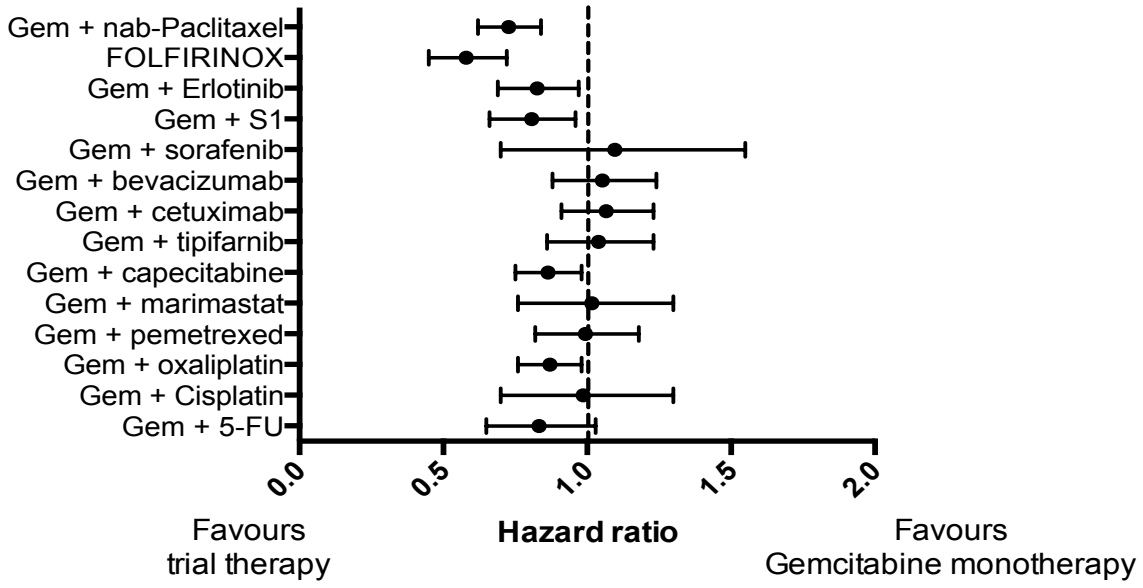


Figure 1.3: Percentage of patients who received different treatment options for pancreatic cancer. This data was derived from patients who participated in the global TCGA, n = 179

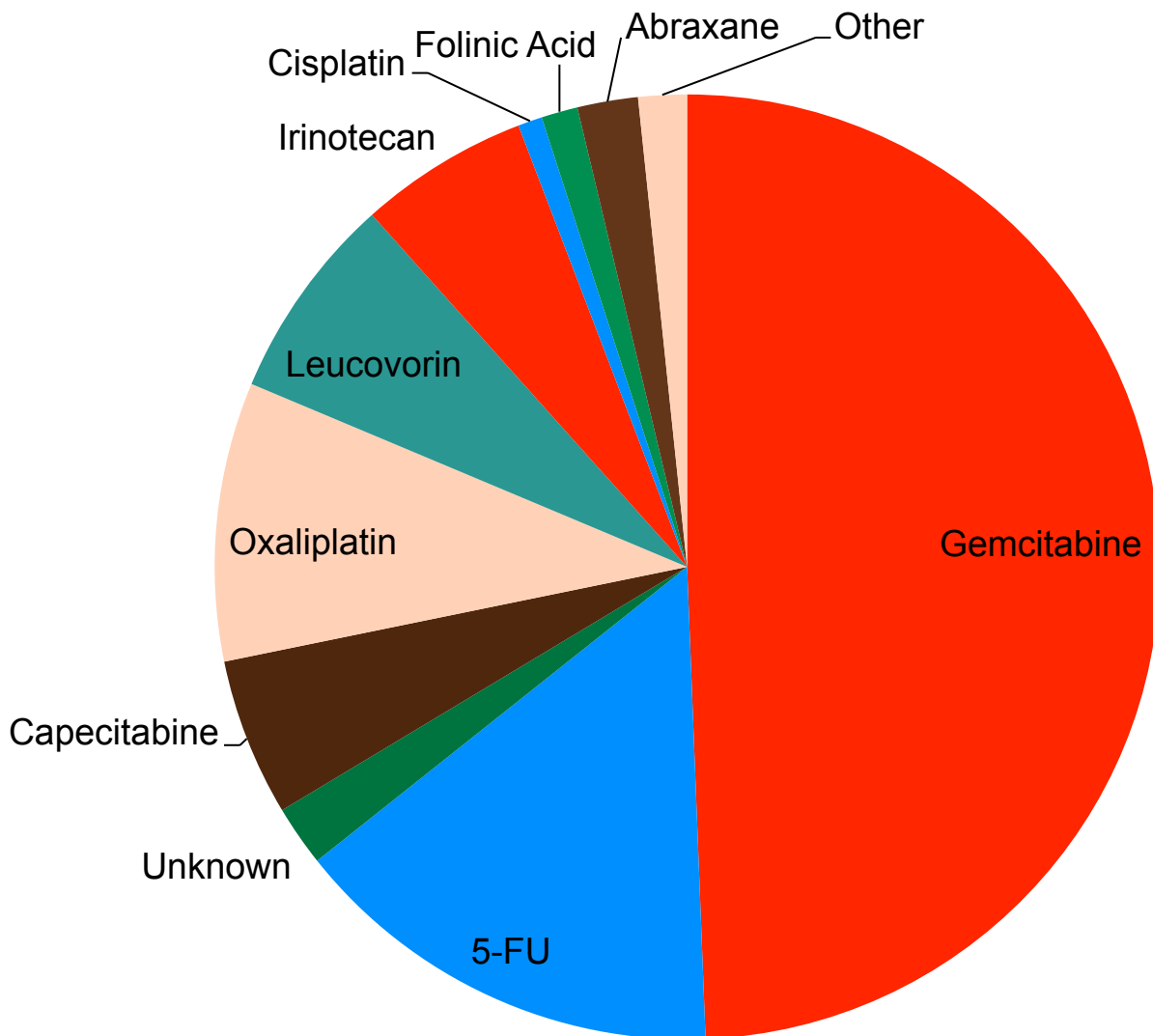


Figure 1.4: EUS FNA cytology technique. (A) Illustration indicating the positioning of the endoscope and ultrasound probe. (B) Ultrasound view of mass lesion and needle sampling the contents of the mass. (C and D) Haematoxylin and eosin staining on EUS FNA cytology specimens.

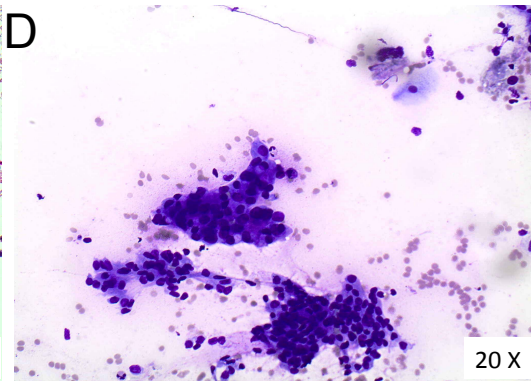
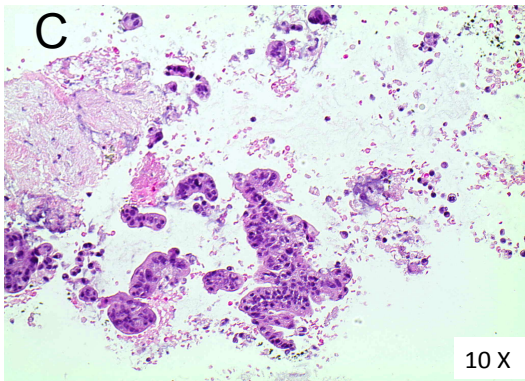
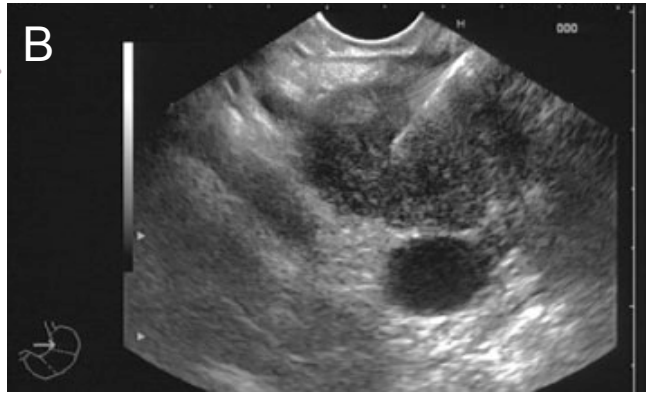
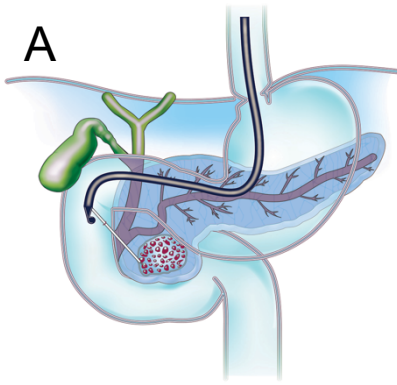
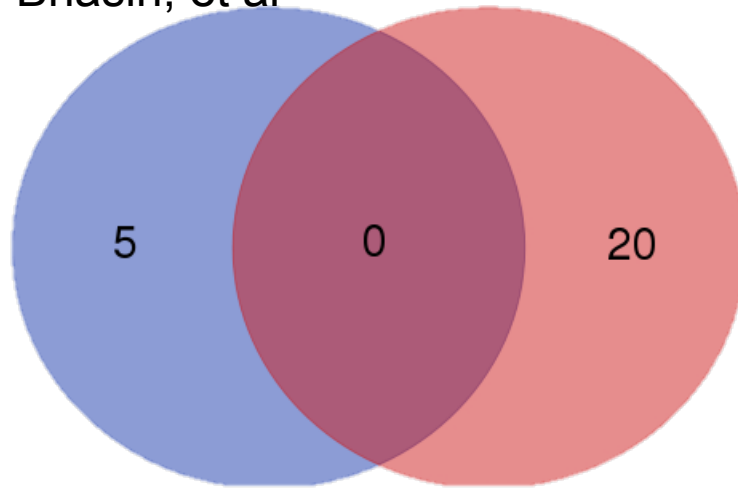


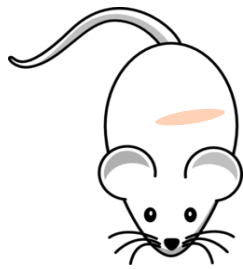
Figure 1.5: Venn diagram showing the differences between the genes up-regulated in PC in two published diagnostic gene signatures. Bhasin et al presented a 5-gene signature up-regulated in PC compared to normal pancreas; Rodriguez, et al presented an 83 gene signature of up- and down-regulated in PC, they only published 20 up-regulated genes and 20 down-regulated genes.

Bhasin, et al



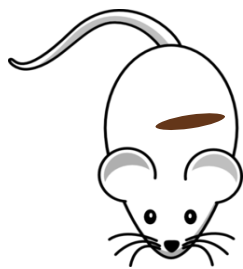
Rodriguez, et al

Figure 1.6: Flow diagram illustrating how genetically engineered mouse models progress from normal pancreas through pre-malignant conditions to PC.

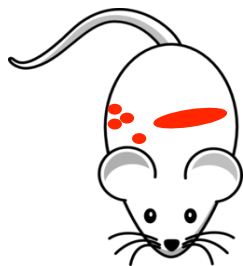


GEMM models use
PdxCre

Kras^{G12D} in
combination with
another pro-
tumourigenic change



Mice typically develop
pre-malignant lesions
(PanIN or IPMN)



Mice ultimately
develop PDAC and
sometimes metastatic
disease

Figure 1.7: Xenograft models in PC. (A) Flow diagram demonstrating the technique of cell line or patient-derived xenograft. (B) Publication rate of xenograft studies in PC (total = top, cell-line derived studies = middle, patient-derived studies = bottom) (C) Efficacy of gemcitabine monotherapy in xenograft models of PC. **** P -value <0.0001

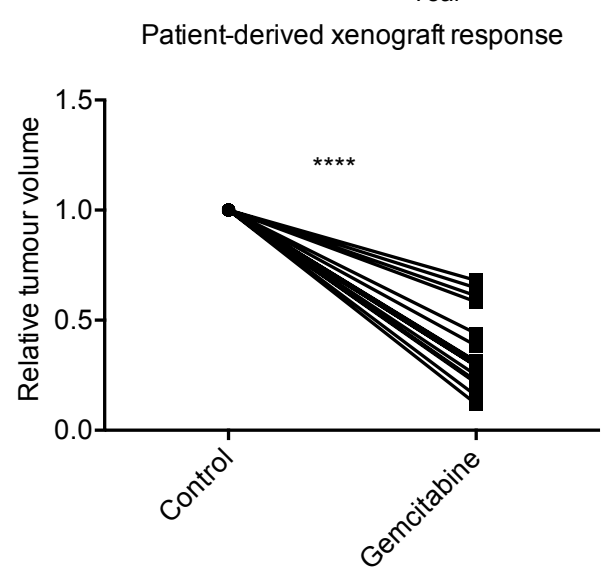
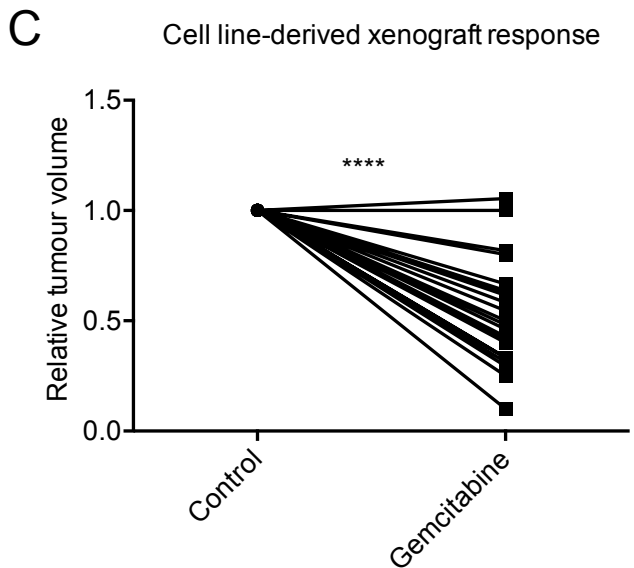
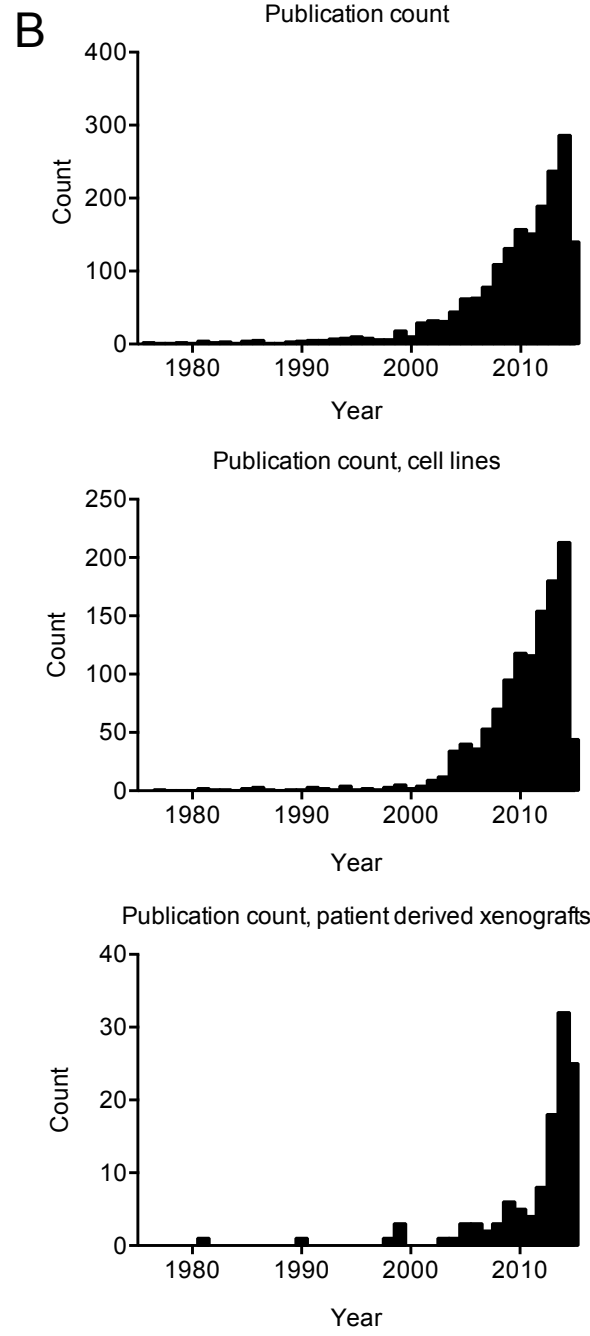
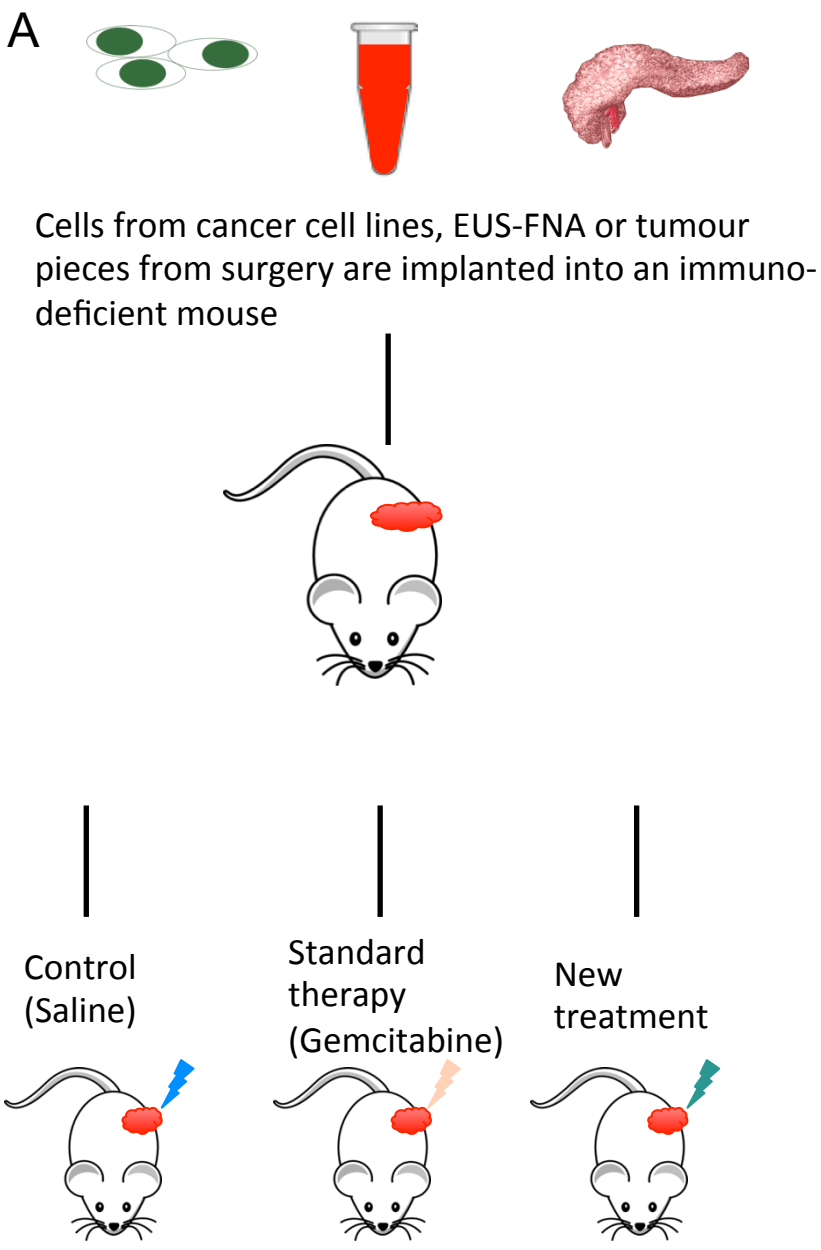
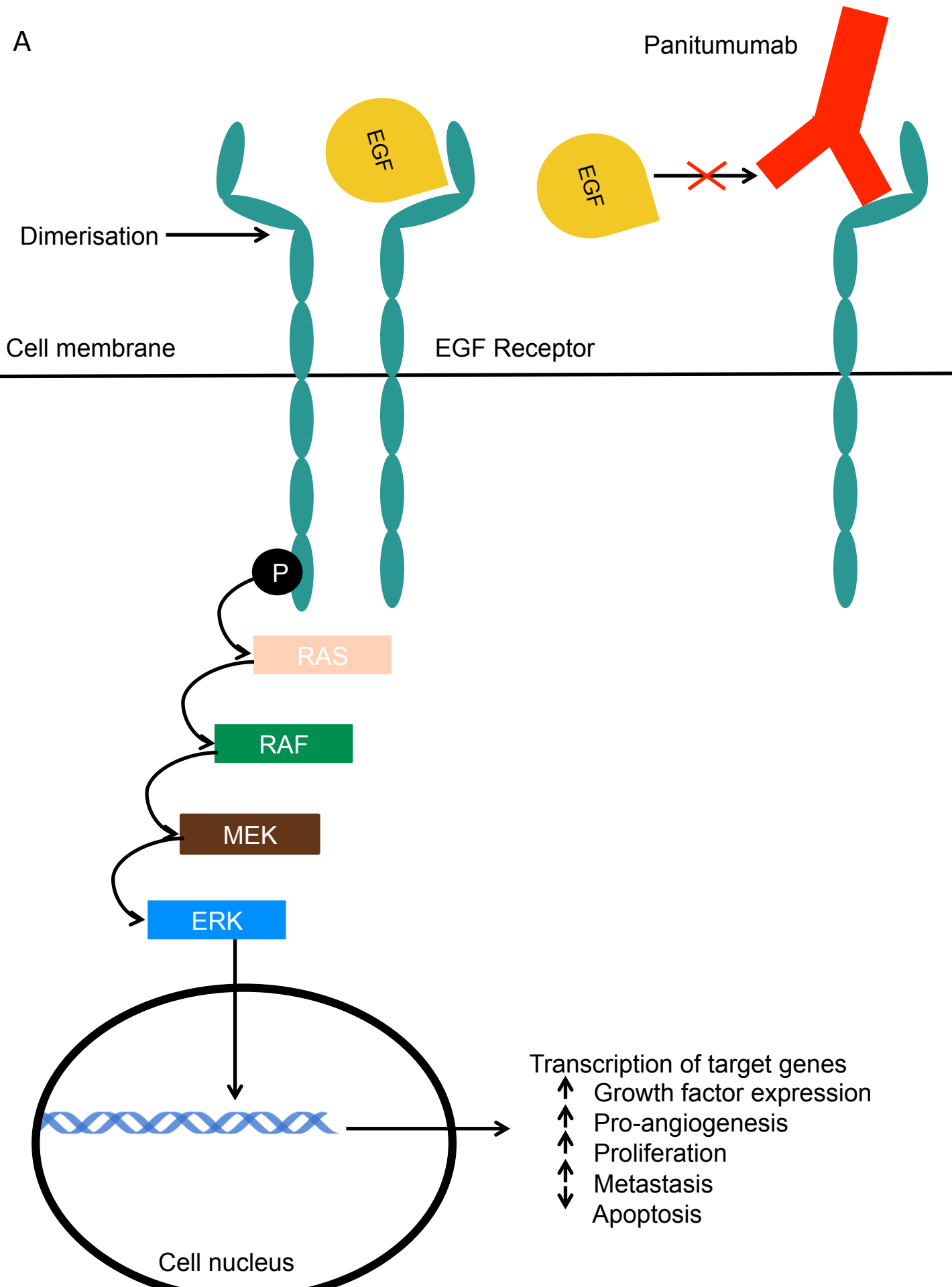


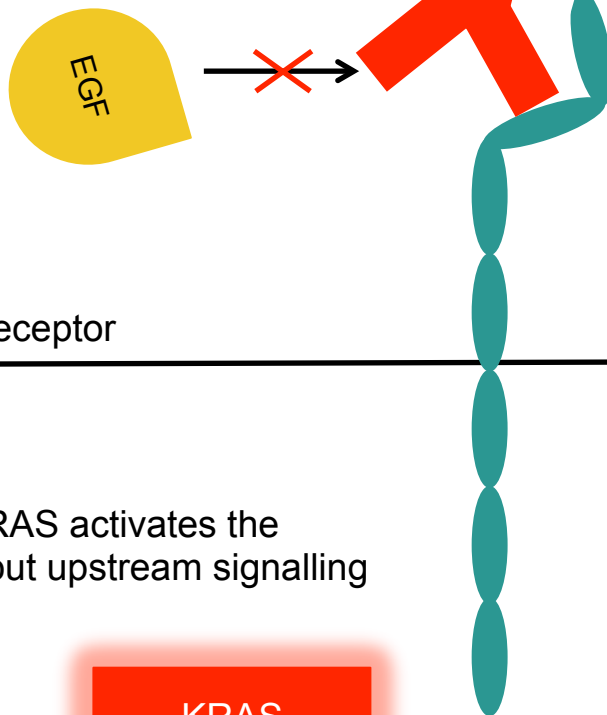
Figure 1.8: Epidermal growth factor signaling pathway and the mechanism of action of Panitumumab. Signalling cascade in *KRAS* wild-type disease (A) and *KRAS* mutant disease (B).

A

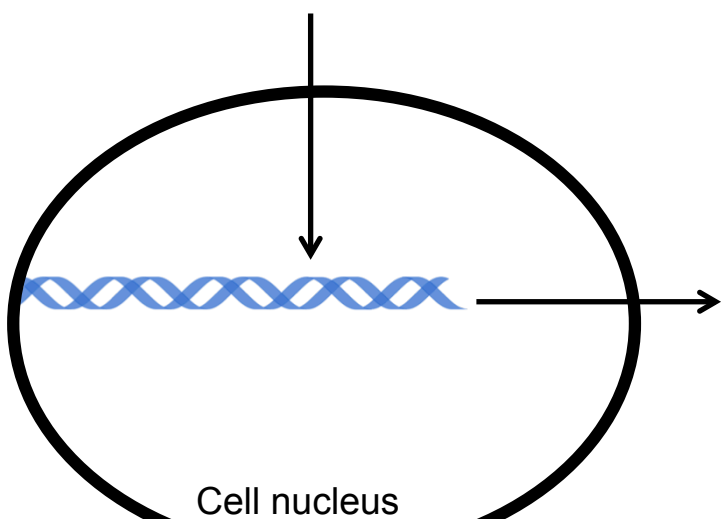
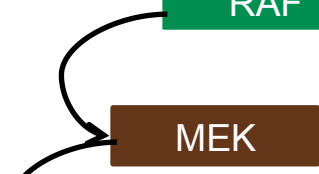
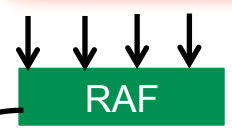
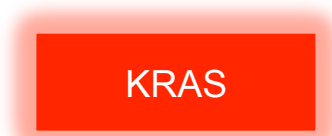


B

Panitumumab



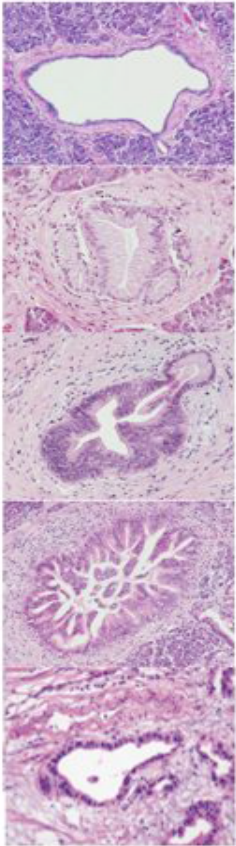
Oncogenic KRAS activates the pathway without upstream signalling



- Transcription of target genes
- ↑ Growth factor expression
 - ↑ Pro-angiogenesis
 - ↑ Proliferation
 - ↑ Metastasis
 - ↓ Apoptosis

Cell nucleus

Figure 1.9: Pancreatic cancer progression model from normal pancreatic epithelium through to intra-epithelial neoplasia and adenocarcinoma.



Normal pancreatic duct

Pan-IN 1

Pan-IN 2

Pan-IN 3

Invasive carcinoma

Chapter 2: Methods

2.1 Human specimen collection

PC samples were collected from patients undergoing EUS FNA for investigation of a pancreatic mass at Monash Medical Centre (MMC), Victoria, Australia. Initial diagnostic aspirates from the pancreatic mass were collected using 22-gauge Procore needles with 10cc of suction for immediate cytological assessment. Following confirmation of the cellular quantity and provisional diagnosis, additional 1-2 passes were taken from the same position as the diagnostic biopsies and then either snap-frozen in liquid nitrogen or placed into 0.5ml RNeasy (Qiagen), and stored at -80°C. Another method was trialled: samples were collected on wet ice, centrifuged, and cell pellets homogenised in TRIzol reagent (BioLine), and stored at -80°C.

Normal (control) pancreas was obtained by surgical resection at MMC for conditions other than PC. Surgical resection specimens of PC were obtained via a punch biopsy through the lesion after the specimen was removed. Normal duodenum and stomach tissues were obtained from patients without PC by endoscopic biopsy. Whole blood was collected from healthy age-matched volunteers in Ethylenediaminetetraacetic acid (EDTA) -coated tubes (Becton Dickinson and Company).

In addition to tissue collection, blood was collected for serum, plasma and isolation of buffy coat and these were all stored at -80°C.

Informed patient consent was obtained for each procedure, with approval from Monash Health and Monash University Human Research Ethics Committees (approval number 13058A).

2.2 Genetic work

2.2.1 Genomic DNA (gDNA) and RNA extraction

Total RNA only was extracted from snap-frozen EUS FNA samples (300 μ l), cell pellet samples and surgical resection specimens (50-100 μ g) using TRIsure reagent (Bioline). RNA and gDNA from frozen samples were simultaneously extracted along with RNA using the AllPrep DNA/RNA Universal Kit (Qiagen). The isolation of gDNA from FFPE tissue was performed on 5 x 10micron-thick sections using the ReliaPrep FFPE gDNA Miniprep System (Promega). The quality and quantity of gDNA were determined on a NanoDrop Spectrophotometer (ThermoScientific). RNA was assessed using a NanoDrop and Qubit Fluorometer (Life Technologies), and the Aligent Bioanalyzer (Aligent Technologies).

2.2.2 Gene mutation analyses

gDNA (25-50ng) was subjected to the KRAS-BRAF StripAssay (ViennaLab Diagnostics GmbH) [173]. Mutations were objectively scored using StripAssay Evaluator software. This assay detects mutations on codons 12 and 13, which account for the vast majority of *KRAS* mutations in PC [173].

2.2.3 Reverse transcription (RT)-polymerase chain reaction (PCR)

Complimentary (c) DNA was generated from 500ng of RNA (made up to a volume of 8 μ l with DEPC-treated water) using SuperScript III (Invitrogen) first strand synthesis kit. For each reaction 1 μ l of random hexamers and 1 μ l dNTP mix were added to the RNA for the final volume of 10 μ l. The samples were incubated at 65°C for 5

minutes and then chilled on ice for at least 1 minute. Meanwhile, a cDNA synthesis mix consisting of 4 μ l of 5x First-strand buffer, 4 μ l of MgCl₂, 2 μ l Dithiothreitol (DTT), 1 μ l of RNaseOut and 1 μ l of superscript III enzyme was prepared. Superscript III enzyme was substituted for DEPC treated water in the negative RT-PCR control. To each RNA sample, 10 μ l of cDNA synthesis mix was added and the samples were incubated at 25°C for 10 minutes, 50°C for 1 hour and the enzyme was heat inactivated at 85°C for 5 minutes. To ensure that the samples did not contain single stranded RNA, 1 μ l of RNase H was added to each tube and incubated at 37°C for 20 minutes. cDNA was stored at -20°C prior to quantitative-PCR (qPCR).

qPCR was performed on cDNA in triplicate over 40 cycles using the 7900HT Fast RT-PCR system (Applied Biosystems). The expression of each gene was normalised relative to *18S*, and data acquisition and analyses were performed using the Sequence Detection System Version 2.4 software (Applied Biosystems). For genes whose expression was not detected, a cycle threshold (Ct) value of 40 was assigned for data analysis. Sequences of human gene forward and reverse primers are listed in Appendix 1.

2.2.4 Transcriptome profiling

RNAseq was performed on high quality EUS FNA-derived RNA with an RNA integrity number (RIN)>4 using Ion Ampliseq™ technology (Life Technologies). Sequence reads were aligned to the Ion AmpliSeq™ Transcriptome reference file (hg19_AmpliSeq_Transcriptome_ERCC_v1.fasta) in Torrent Suite™ Software using the Ion Torrent Mapping Alignment Program (TMAP) (<https://github.com/iontorrent/TMAP>). The reference file contains the entire set of RefSeq transcripts from which all 20,802 Ion AmpliSeq™ Transcriptome panel primers were designed. Following alignment, the *ampliSeqRNA* plugin examined the

number of reads mapping to the expected amplicon ranges and assigned counts per gene for reads which align to these regions as defined in the BED file (hg19_AmpliSeq_Transcriptome_21K_v1.bed). Reads aligning to the expected amplicon locations were referred to as 'on target' reads and were reported as a percentage of total reads by the plugin.

2.2.4 *In silico* molecular analyses

Transcriptome datasets were analysed using R packages Bioconductor and limma. These were used for quality control, normalisation, hierarchical clustering analyses and differential gene expression analyses. Normalised datasets were further processed using Gene Set Enrichment Analysis (GSEA) software. The data processing pipeline is described in detail in Appendix 2.

2.3 Protein work

2.3.1 Immunohistochemistry

Unstained FFPE sections of EUS FNA, surgical specimens or xenograft tumour tissue were used for immunohistochemical staining with antibodies and antigen retrieval listed in Appendix 3.

2.3.2 Histological and cytological analyses

The adequacy of the biopsy was confirmed during the time of the EUS FNA procedure in the endoscopic suite. Cytological evaluation was performed on Diff-Quik stained and air-dried slides, as well as Papanicolaou-stained and wet-fixed smears.

EUS FNA cell block preparations were made using the clotted needle cores, which were placed, in a fine mesh cassette and then into a regular cassette for processing in histology. Haematoxylin and Eosin (H&E)-stained sections derived from these cell blocks aided accurate morphological assessment.

2.3.3 Protein lysates from tissue

Protein lysates were made from snap frozen tissue (EUS FNA, surgical specimens or xenograft tumour tissue). To each piece of tissue 500 μ L of protein lysis buffer (Appendix 4) was added. The tissue sample was homogenised, then agitated for 40 minutes, and then centrifuged for 10 minutes at 14,100G at 4°C to pellet insoluble material. To this, 20 μ l of sepharose G beads (Pharmacia Biotech) was added and the samples were placed on the wheel in the cold room for another 30 minutes. The sepharose G beads were removed by centrifugation at 3000xg for 3 minutes and the concentration of protein present was determined by performing a Lowry assay. Protein lysates were stored at -80°C for future use.

2.3.4 Lowry protein assay

Bovine serum albumin (BSA) protein standards (Sigma-Aldrich) were prepared, in duplicate, with a starting concentration of 20 μ g and serial dilutions were performed to generate a standard curve. Once 5 μ l of protein standard and samples were added to each well, 25 μ l of working reagent (20 μ l of Reagent S to 1ml of Reagent A, Biorad) was added, followed by the addition of 200 μ l of Reagent B (Biorad). The plate was gently agitated to mix the reagents and after 15 minutes the absorbance was read at 490nm using the Infinite M200 and results were analysed by the Mars software. From the standard curve, the total protein concentration was determined for each sample.

2.3.5 Western blot

Sodium dodecyl sulphate (SDS) page gels were used to fractionate cell lysates. Polyacrylamide gels were prepared at 10% with 1.5mm thickness (Appendix 4) and once polymerised, an upper gel prepared (Appendix 4) and left to polymerise with a 10- or 15- well comb in place. Aliquots of lysate was made up to uniform volumes and total protein quantity with lysate buffer and combined with Laemlli buffer (Bio-Rad). Samples were heated to 95°C for 5 minutes and immediately returned to ice. Boiled lysates were loaded into wells along with a molecular weight marker (New England Biolabs). Gels were run at 100V for approximately 2 hours at room temperature. Fractionated protein was transferred onto a nitrocellulose Hybond-C extra (GE healthcare) membrane using the Mini Trans-blot Electrophoretic Transfer Cell (Bio-Rad) in transfer buffer (Appendix 4) at 100V for 100 minutes.

Membranes were blocked in 5mL Odyssey Blocking Buffer (LI-COR) and 5µL Tween-20 (Sigma) for 1 hour at room temperature. Membranes were then probed with primary antibody (Appendix 3) diluted in blocking buffer overnight at 4°C.

After overnight incubation, membranes were washed in Tris-buffered saline (TBS) supplemented with Tween-20 (0.05%) and then the membrane was probed with the appropriate AlexaFluor (Invitrogen) secondary antibody diluted to 1:3000 in blocking buffer for 1 hour at room temperature. Membranes were washed in TBS supplemented with Tween-20 and protected from light-exposure. Membranes were scanned on an Odyssey fluorimager (LI-COR) infrared imaging system.

2.4 Animal work

2.4.1 Porcine specimen collection and FNA needle comparison

Animal pancreatic samples were obtained at three interventional gastroenterology training workshops for EUS FNA through Cook Medical, Brisbane, Australia. Ethical approval was attained under the Queensland University of Technology University Animal Ethics Committee, approval number 140000024. Under controlled settings using a variety of needles, EUS FNA was conducted by on unconscious animals (*sus scrofa domestica*). At the conclusion of the training section of the workshop, three additional passes with each needle were performed (19-gauge Ultra, 22-gauge Ultra, 25-gauge Ultra, 22-gauge EchoTip ProCore and 25-gauge EchoTip ProCore; Cook Medical). To collect these samples one operator (Dr Nam Nguyen, Royal Adelaide Hospital), performed EUS FNA for all sample replicates, where 10cc of suction was used with 10 backwards and forwards movements. The specimens were expelled with 0.5ml of saline and snap-frozen in liquid nitrogen for isolation of DNA and RNA.

2.4.2 Patient-derived xenograft and treatment

All experiments were performed following approval from the Monash University Monash Medical Centre "A" Animal Ethics Committee under project 2015/08. All mice were housed in a specific pathogen-free area at Monash Medical Centre Animal Services.

EUS FNA samples were collected on wet ice in saline; these samples were immediately transferred to a sterile petri dish where the sample was finely minced with a scalpel. The minced sample was then transferred into a falcon tube and washed with pancreatic cell culture media (Appendix 4) by thorough mixing followed

by centrifugation. This was repeated 3 times to wash the sample thoroughly. The sample was then re-suspended in 150µl of pancreatic cell culture media and 150µl of thawed Matrigel (Corning Life Sciences). Throughout this process care was taken to keep the sample at 4°C by using refrigerated centrifuges and handling the sample over ice. Samples were implanted into 4-6 week-old female NOD/SCID mice using a subcuticular injection of 150µL. Tumours were allowed to grow for 3-6 months to a maximum volume of 1000mm³ at which point the tumour was passaged into a treatment cohort of 16 mice.

To passage the tumour from the 'donor' mouse was divided into several 2mm pieces. These were then coated in Matrigel and implanted into a subcuticular pocket on the flank of the new NOD-SCID mouse. In some cases there was no need to immediately passage the tumour, in this circumstance pieces of the tumour were stored in 20% DMSO and 80% FCS and frozen at a cooling rate of ~1°C/minute using a Mr Frosty™ Freezing Container (ThermoFischer Scientific). These pieces were stored at -80°C and could then be thawed and implanted at a later date.

Mice within the treatment cohort were randomised to one of four treatment options: Saline (0.2mL i.p. twice weekly), Panitumumab (200ug, i.p. twice weekly), Gemcitabine (50mg/kg i.p. twice weekly) and a combination therapy (Panitumumab and Gemcitabine). This treatment was commenced once grafted tumours were established and reached a volume of 100mm³. Tumour volume was measured weekly with digital callipers, tumour volume calculated using the following formula: $(2 \times Width \times Length) / 2 = V \text{ mm}^3$. Treatment was continued for 28 days, upon cessation of treatment, tumours were harvested for histology, protein lysates, RNA and DNA extraction and serum was collected from the animal.

2.5 Statistical analyses and computational analysis of molecular metadata

Statistics were generated using GraphPad Prism for Windows version 5.0, and where appropriate parametric (one-way ANOVA, student t-test) or nonparametric (Kruskal Wallis, Mann-Whitney) tests were used. $P < 0.05$ was considered statistically significant. Data are expressed as the mean \pm standard error of the mean (SEM). *In silico* metadata analyses were performed using R statistical programming software packages limma and Bioconductor, both packages have in built algorithms to measure statistical significance. These algorithms calculate significance based on a P -value adjusted for multiple-comparisons using a Benjamani adjustment equation. Adjusted $P < 0.01$ were considered statistically significant.

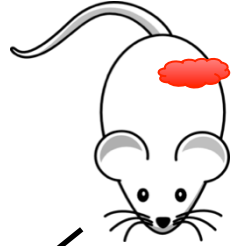
2.6 Figures

Figure 2.1: Schematic overview of study methodology from collecting patient samples, to processing for genetic extraction or xenograft and downstream data generation and analyses.

EUS-FNA



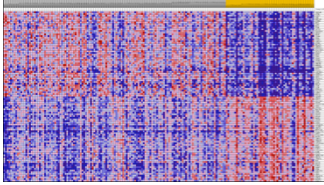
Establish a xenograft



RNA and DNA isolation



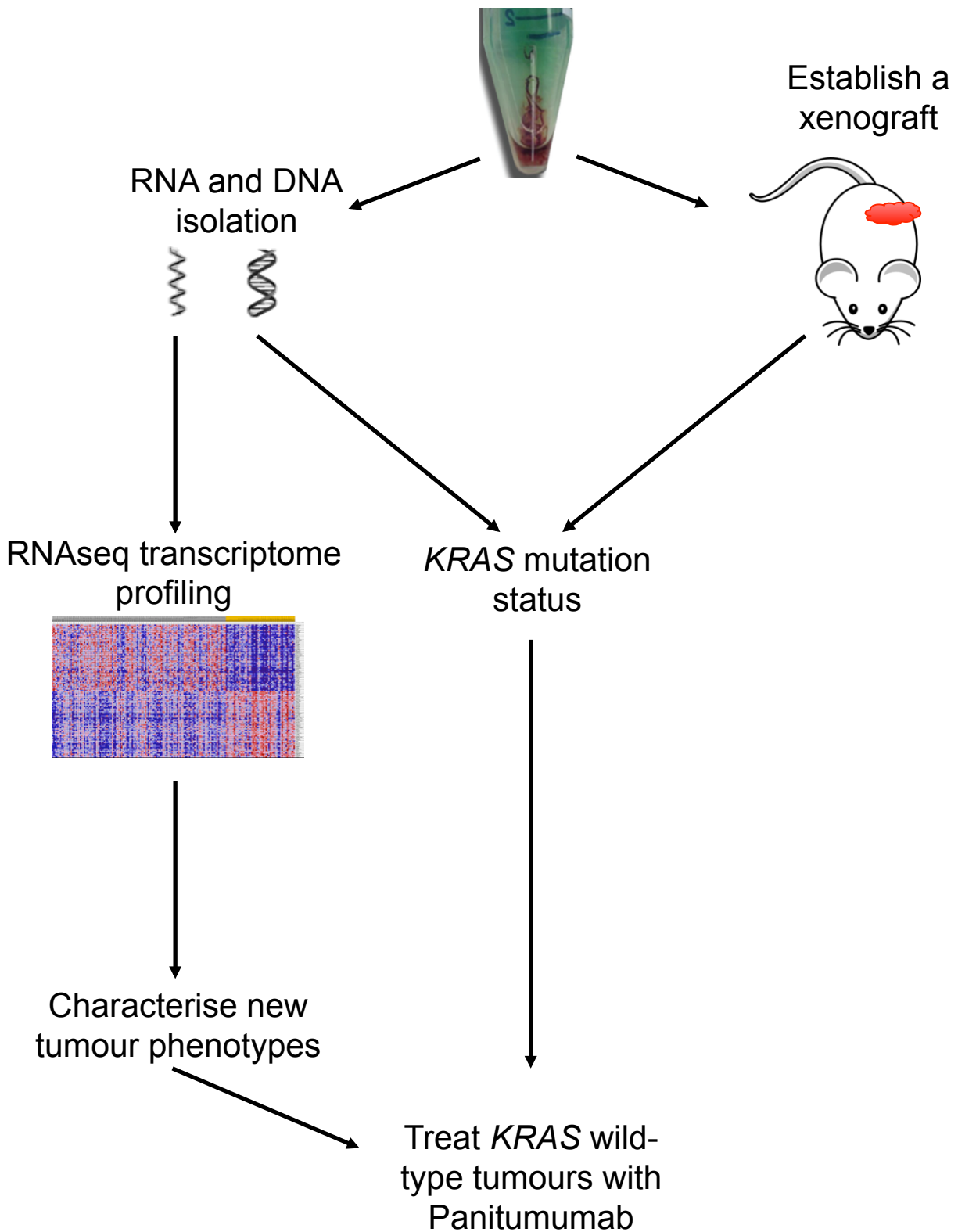
RNAseq transcriptome profiling



Characterise new tumour phenotypes

KRAS mutation status

Treat *KRAS* wild-type tumours with Panitumumab



Chapter 3: Defining the utility of EUS guided FNA for the genetic characterisation of pancreatic cancer

Although most PC patients undergo EUS FNA for cytological diagnosis, the clinical utility of EUS FNA for genetic analysis of tumours has been limited by suboptimal yields and poor quality of genetic material [41-43]. Nonetheless, the inherent advantage of EUS FNA is the ability to sample tumours from the majority of patients, including those who are ineligible for surgery [5].

Recent advances in next-generation sequencing technologies have enhanced our understanding of the inter-tumoural heterogeneity in PC and identified mutations in genes (e.g. *KRAS*) that could indicate sensitive tumour phenotypes for targeted chemotherapy [21,22]. Personalised medicine based on mutations such as *KRAS* has the potential to improve patient outcomes [28], however, a major obstacle to personalising therapy in PC has been isolating sufficient amounts of high quality gDNA and RNA for molecular profiling. As mentioned in Chapter 1, this was reported by the IMPaCT Trial [36], which aimed to screen patients for therapeutic targets within their tumour genomes. This trial failed due in part due to the reliance upon FFPE samples for gDNA extraction predominantly from surgical resections, which are only possible in 20% of PC patients [36]. Accordingly, there is an urgent and unmet need to improve methodologies for the robust isolation of high quality genetic material from the vast majority of PC patients, including those with non-resectable disease.

Here, I demonstrate that high quality genetic material can be routinely extracted from PC patient tumours using EUS FNA. My findings provide a substantial practical advance in the genetic characterisation of PC, and pave the way for future

studies aimed at generating molecular profiles to stratify patients for personalised treatment regimens.

3.1 Optimisation of genomic DNA and total RNA extraction from EUS FNA samples

Using EUS FNA for genetic profiling of PC tumours is dependent on obtaining genetic material of sufficient quantity and quality. I therefore optimised the isolation of PC tumoural gDNA/RNA by trialling a variety of strategies from a total of 66 EUS FNA samples. Methods 1 and 2 involved the extraction of total RNA only from 17 and 29 EUS FNA samples, respectively, whereas method 3 (20 EUS FNA samples) allowed for the simultaneous isolation of genomic DNA and RNA from the one sample (Figure 3.1).

In method 1, upon expulsion from the EUS FNA needle, the samples were stored on ice prior to centrifugation; the cell pellets were then snap-frozen in liquid nitrogen. In methods 2 and 3, EUS FNA samples were immediately snap-frozen in liquid nitrogen upon expulsion from the FNA needle, and later thawed and processed as 2-3 x 300 μ L aliquots using either an acid guanidinium thiocyanate-phenol-chloroform RNA extraction in tube (Trisure, Biotline) or on column (Allprep DNA/RNA, Qiagen).

Both methods 1 and 2 were comparable in terms of RNA quality (RIN for method 1 = 2.3 ± 1.8 , and for method 2 = 2.9 ± 2.1), with method 2 providing a slightly greater quantity of RNA (method 1 = $5.1 \pm 7.0 \mu\text{g}$ versus method 2 = $9.3 \pm 8.5 \mu\text{g}$) (Figure 3.2). For method 3, both the quantity and quality of RNA generated were higher than those for methods 1 and 2 ($12.9 \pm 13.2 \mu\text{g}$, and RIN = 3.2 ± 0.98), albeit not

significantly (Figure 3.2), and the mean yield of genomic DNA (gDNA) simultaneously extracted was $4.8 \pm 3.7 \mu\text{g}$.

Taken together, the above findings identify methodologies that allow for extraction of gDNA and RNA from EUS FNA biopsies of PC in sufficient quantities and quality for certain molecular assays.

3.2 Optimisation of sample collection

Having established the best protocol for RNA and gDNA extraction, I subsequently sought to simplify collection methodology by comparing the practice of snap-freezing samples and collecting samples in RNAlater (Qiagen). For this purpose two additional passes were performed from 7 patients, with both passes being taken from the same lesion using the same aspiration technique (10cc of suction, and 10 backwards and forwards motions of the needle). Both passes were expelled from the needle by stylet replacement and a flush with either 0.5mL of saline prior to snap-freezing in liquid nitrogen (first pass), or with 0.5mL of RNAlater prior to storage at room temperature for 2 hours (second pass). All samples were then used for simultaneous gDNA and total RNA isolation using the optimised method outlined previously (Method 3). As shown in Figure 3.3, storage of samples in RNAlater provided greater DNA yield, with no difference observed in RNA yield or quality, although overall the quantity of RNA produced in this set of experiments was less than previously observed, perhaps reflecting inherent variability in tumour cellularity.

3.3 High epithelial cell content of PC EUS FNA-derived samples

Histopathological examination of H&E-stained EUS FNA-derived PC specimens revealed a cellular mix comprising atypical malignant cells, benign epithelial cells and immune/inflammatory cells (Figure 3.4A). Therefore to define the cellular nature of the PC-derived EUS FNAs, I subsequently utilised RNA selected from 20 PC patients (Table 3.1) to quantify the expression levels of target genes representative of epithelial and inflammatory cells (blood), as well as pancreatic, gastric and duodenal tissue. The latter 2 tissue types were chosen since FNA needles necessarily pass through either the gastric or duodenal mucosa to sample the pancreas, and may therefore contain “contaminating” cells from these tissues. As a control for these analyses, I also compared pancreatic tissue collected by EUS FNA from patients without PC (e.g. pancreatitis) or normal pancreatic tissue obtained from surgical resection.

The qPCR analyses demonstrated that gene expression of the pan-epithelial cell markers *cytokeratin (KRT) 7* and *19* was significantly increased in RNA extracted from PC EUS FNA samples compared to normal or benign pancreatic tissue collected by either EUS FNA (pancreatitis) or resection (normal), as well as gastric, duodenal and whole blood samples (Figure 3.4 B, C), thus confirming the high epithelial content of PC EUS FNAs. As expected, gene expression levels of cell markers for the duodenum (*Villin; VIL1*) and stomach (*ATPase, H+/K+ exchanging, alpha polypeptide; ATP4A*) were highest in their respective tissue (Figure 3.4 D, E). By contrast, comparable low levels of *VIL1* gene expression were detected in EUS FNA-derived PC and normal pancreas, with lowest expression observed in resected normal pancreas, suggesting that the EUS FNA procedure itself may inadvertently collect a low level of contaminating cells of duodenal origin as a result of the needle passing through the duodenum (Figure 3.4 D). Similar and low expression levels of

ATP4A were present in all pancreatic-derived tissue samples, irrespective of whether they were collected by EUS FNA or resection (Figure 3.4 E). I also observed that expression levels of the leukocyte (immune) cell marker CD45 were among the lowest in EUS FNA-derived PC samples, with highest expression levels observed in whole blood samples (as expected) and surprisingly, resected normal pancreas tissue (Figure 3.4 F).

To further verify the high epithelial cell content of EUS FNA-derived PC biopsies, I performed immunohistochemistry on PC EUS FNA biopsy sections with antibodies directed against the epithelial cell markers, Cytokeratin 7 and 19. I note that biopsy sections used for immunohistochemistry were among serial sections of the same pancreatic mass EUS FNA that cytology was performed on to confirm the diagnosis of PC. I observed pronounced staining with both antibodies throughout EUS FNA-derived PC sections derived from the cell blocks (Figure 3.4 G, H). By contrast, very few CD45-positive immune cells were observed in the PC sections (Figure 3.4 I).

Collectively, these results validate at the protein level the qPCR gene expression data obtained on RNA from PC EUS FNA, and thus confirm that EUS FNA biopsies are predominantly pancreatic in origin with relatively high epithelial cell content.

3.4 Comparison of gDNA derived from fixed tissue and additional biopsies

All EUS FNA samples are processed into formalin-fixed paraffin embedded (FFPE) cell blocks for cytological diagnosis. Using these FFPE blocks to obtain gDNA would remove the need for an extra needle pass during EUS. To verify that an additional

pass was indeed warranted I recruited a different cohort of 20 PC patients (Table 3.2) who underwent EUS FNA to obtain tissue both for routine diagnostic purposes (2-3 passes for slides and FFPE cell block) and snap-freezing (1 additional pass), thus allowing a direct comparison of gDNA from FFPE blocks and snap-frozen additional biopsies (Figure 3.5 A). The quantity of gDNA obtained from additional biopsies was ~10-fold greater than that obtained from FFPE blocks (Figure 3.5 B). In 6 cases, the diagnostic process completely exhausted the FFPE tissue. Therefore, an additional biopsy is important to ensure an adequate amount of high quality genetic material for further analyses.

3.5 Detection of oncogenic *KRAS* mutations in gDNA derived from fixed tissue and additional biopsies

Having established that EUS FNA can provide meaningful tumour-derived genetic material, I then proceeded to use EUS FNA-derived gDNA to identify mutations. As a proof-of-principle, I therefore tested for the presence of *KRAS* mutations in EUS FNA-derived gDNA. *KRAS* mutations are of particular interest because they may predict responsiveness to EGFR inhibitors [34,44,62,63].

KRAS mutations were detected in 80% (16/20) of patients using DNA extracted from additional biopsies, while the frequency of *KRAS* mutation detection in the same patients was significantly lower at 45% (9/20, $p < 0.05$) when using gDNA extracted from FFPE blocks (Figure 3.5 C). Therefore, these data suggest the importance of an additional biopsy to ensure adequate quality and quantity of genetic material for further analyses. In one patient a *KRAS* mutation was identified from examination of the cell block material but was not found in the matching snap frozen

additional biopsy, resulting in an overall frequency of KRAS mutation in 85% of patients.

3.6 Genetic yield with different EUS FNA needles

In optimising the EUS FNA procedure on pancreatic tissue for the extraction of genetic material the type of needle employed is a variable that hasn't been explored before. Although numerous studies have examined the diagnostic yield of different EUS FNA needles, the amount of genetic material obtained has not been quantified [52,174-181]. I therefore addressed this issue in a novel way by comparing the quantity and quality of gDNA/RNA obtained using five different needles under controlled conditions in a porcine animal model. My results indicate that gDNA/RNA yields decrease with decreasing calibre of needle, irrespective of needle tip design (Procore versus Ultra: Figure 3.6).

3.7 Discussion

This is the first study to quantify the epithelial content of EUS FNA samples and thereby validate the potential use of EUS FNA to provide material for the genetic characterisation of PC. I have shown that collecting an additional EUS FNA biopsy solely for isolating gDNA/RNA provides genetic material sufficient in quality and quantity for in-depth genetic analysis. Importantly, this technique can be applied to nearly all PC patients who are ineligible for surgical resection.

By using EUS FNA-derived gDNA to assess the mutation status of *KRAS*, I revealed that 85% of patients had *KRAS* mutations, which reflects the frequency observed in resection specimens in the literature 80-96% [24,42]. However, 85% is indeed lower than more recent studies using more in depth sequencing technology, which may be a result of the difference in sensitivity of different detection methods. As mentioned in Chapter 2, the strip-assay used here only detects *KRAS* mutations at codon 12 and 13, thereby failing to detect those tumours with mutations of *KRAS* at different loci (such as codons 60, 61, and more rarely 59, 117 and 146).

Importantly, the method of snap-freezing an additional biopsy solely for obtaining genetic material was more sensitive in detecting *KRAS* mutations compared to retrieving gDNA from FFPE blocks (80% vs 45%). However, there was one instance where *KRAS* mutation was not identified in the additional biopsy, but was in the FFPE block. Notably, the FFPE specimen is derived from 2-4 EUS FNA passes, whereas additional biopsies are from only 1 pass. This discrepancy may be the result of not adequately sampling the tumour in every pass. Nevertheless, these data substantiate the necessity of an additional biopsy for gDNA/RNA isolation to enhance the detection of candidate genes. It is possible that the failure to detect a

KRAS mutation may reflect sampling error rather than true absence of the mutation. This could be addressed by using a larger gene panel including the other common mutations seen in PC, in particular *TP53*, *SMAD4* and *CDKN2A*, we know from previous work using whole-exome sequencing surgical resection specimens suggests that 95% of PC would have at least one of these mutations [10].

To optimise specimen collection I examined the effect of needle choice on the amount of genetic material retrieved by EUS FNA. This is the first study that attempts to quantify the genetic material provided by different needles. Interestingly, the amount of genetic material increased with increasing needle calibre despite reports that diagnostic rates did not differ between different needle gauges [52,174-181]. It is well known that conventional 19-gauge needles can be difficult to use in the duodenum due to the angulation of the scope. However, it is almost always possible to use a 22-gauge needle in this position. Therefore my results show that these needles may be more effective than 25-gauge needles in obtaining genetic material. Notably, the Procore needle design did not provide any advantage over the standard FNA needle, consistent with a recent meta-analysis which did not show a significant effect of needle design on diagnostic yield [182]. However, it is important to note that this study was conducted on normal porcine pancreas in a controlled environment with a single operator; this was chosen to eliminate potential confounding factors that contribute to sample yield; therefore, these findings could be further substantiated in future studies in human patients.

In summary, I have shown that EUS FNA can provide sufficient genetic material for the genetic characterisation of the majority of PC patients, and thus guide future personalised chemotherapy trials. In the next chapter I will explore the genetic landscape of PC using NGS from a large global cohort of PC and a smaller cohort of cancers sourced through the Monash biobank.

3.8 Tables and figures

Table 3.1: 20 PC patients used for gene expression analysis

Patient characteristics	Patient number
Gender	
Female, n (%)	7 (35%)
Male, n (%)	13 (65%)
Age, mean (range) years	67.8 (47-91)
Stage, n (%)	
Localised	6 (30%)
Locally advanced	5 (25%)
Metastasis	9 (45%)
Treatment, n (%)	
Surgery	6 (30%)
Gemcitabine + nab-Paclitaxel	5 (25%)
FOLFIRINOX	1 (5%)
Radiotherapy	1 (5%)
Other palliative chemotherapy	4 (20%)
Nil	3 (15%)

Table 3.2 20 PC patients used for KRAS mutation detection in matched FFPE and additional biopsy samples

Patient characteristics	Patient number
Gender	
Female (%)	5 (25%)
Male (%)	15 (75%)
Age, mean (range) years	66.3 (42-84)
Stage, n (%)	
Localised	3 (15%)
Locally advanced	7 (35%)
Metastasis	10 (50%)
Treatment, n (%)	
Surgery	4 (20%)
Gemcitabine + nab-Paclitaxel	9 (45%)
FOLFIRINOX	2 (10%)
Nil	3 (15%)
Other palliative chemotherapy	2 (10%)

Figure 3.1: Comparison of DNA / RNA isolation methods for EUS-FNA samples. Flow diagram of study. Two different sample preparation methods were optimized to generate maximal nucleic acid yields; EUS-FNA samples were either pelleted prior to RNA extraction (n=17), or were snap-frozen into aliquots prior to either RNA only (n=29) or RNA and genomic DNA (n=20) extraction.

A

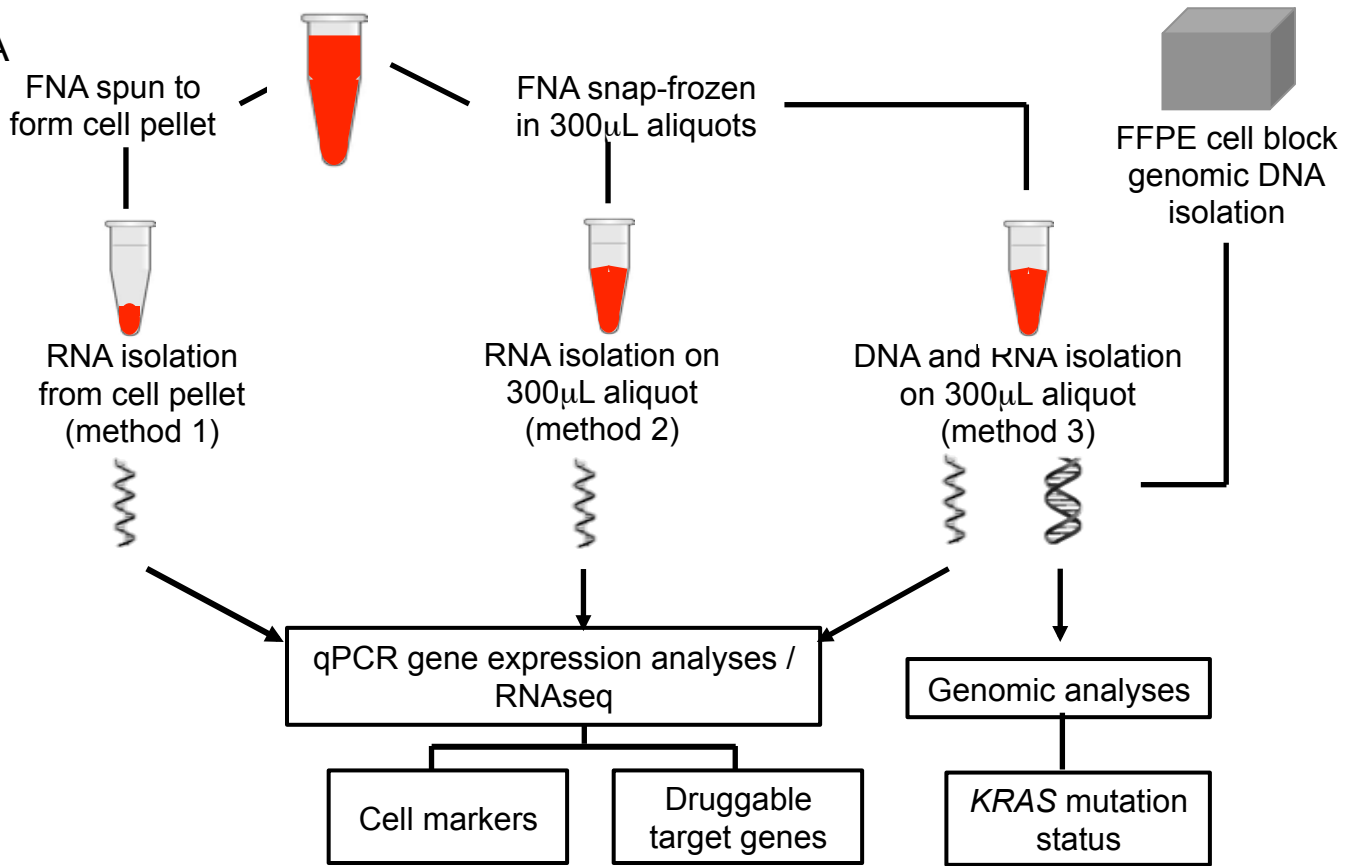


Figure 3.2: RNA yield for each isolation method. (A) RNA yields (mg) and (B) RNA integrity number (RIN) for each method.

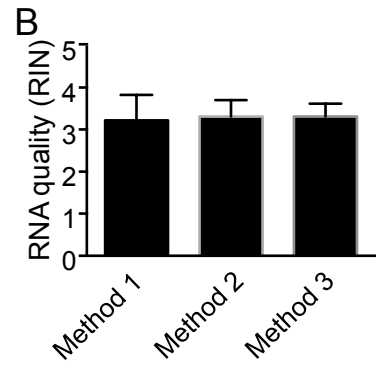
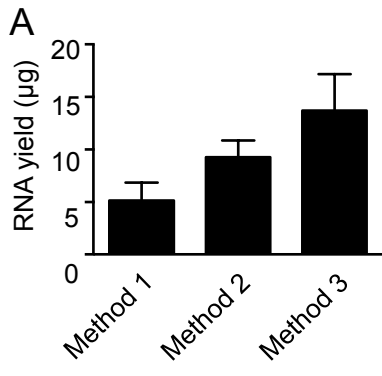


Figure 3.3: RNA yield for each collection method. Snap-frozen compared to RNAlater: Effect of sample collection method on genetic material yields. (A) RNA yield, (B) DNA yield, and (C) RNA quality for different collections.

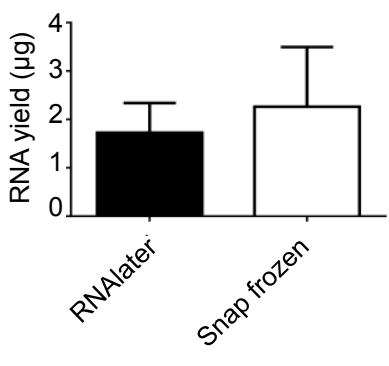
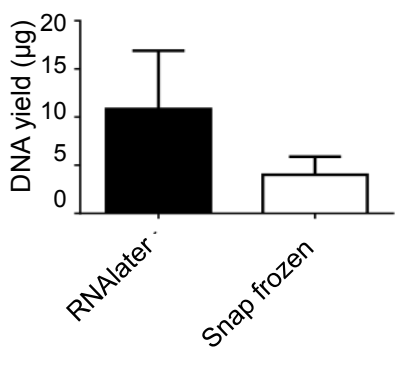
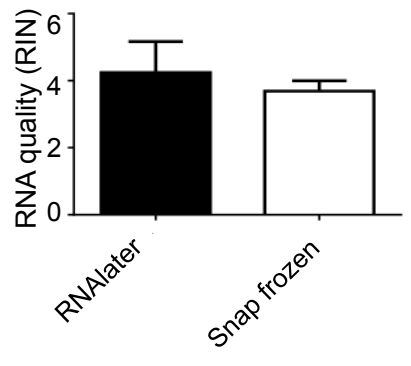
A**B****C**

Figure 3.4: Gene expression analyses of the high epithelial cell content, of pancreatic origin, in EUS-FNA-derived PDAC samples. (A) Representative EUS-FNA-derived PDAC cross-section stained with H&E. MEC, malignant epithelial cells; BEC, benign epithelial cells; IC, inflammatory cells. Scale bar, 100 μ m. (B-F) qPCR of the indicated cell marker genes on RNA from EUS-FNA-derived PDAC (PDAC^{FNA}; n=20) and normal pancreas (N^{FNA}; n=3) biopsies, resected normal pancreas (N^{Resect}; n=5), stomach (Stom^{Resect}; n=4) and duodenum (Duod^{Resect}; n=4) biopsies, and whole blood (n=5) samples. (G-I) Immunohistochemistry of PC EUS-FNA cell block stained with Cytokeratin 7 (G), 19 (H) and CD45 (I). Relative expression derived from Delta Ct normalized against 18S, and are presented as the mean \pm SEM. ***P*<0.01; ****P*<0.001; *****P*<0.0001.

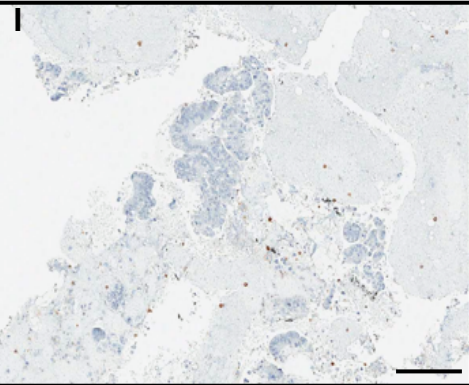
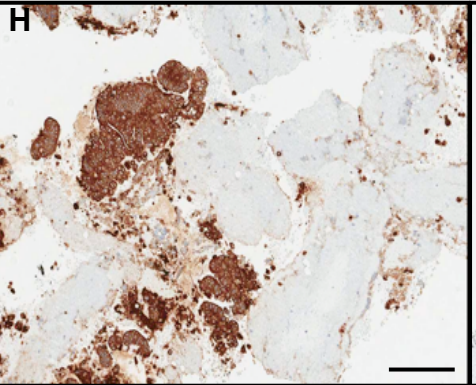
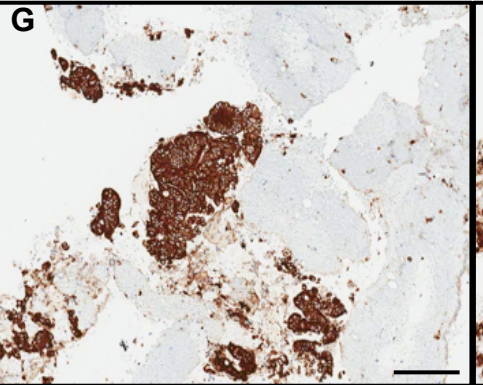
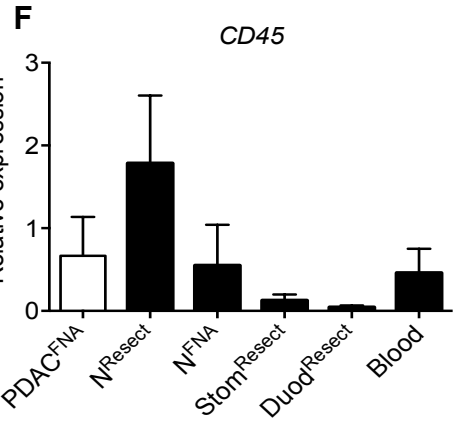
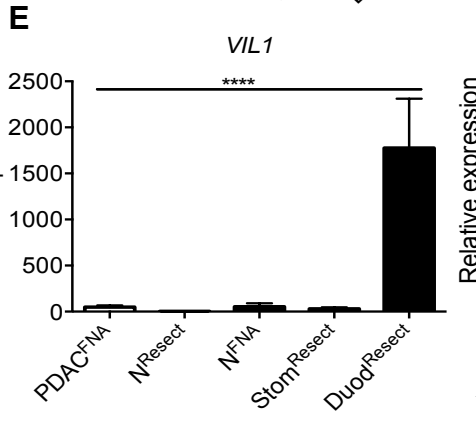
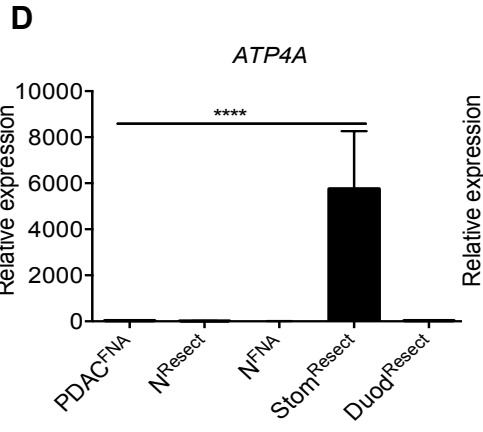
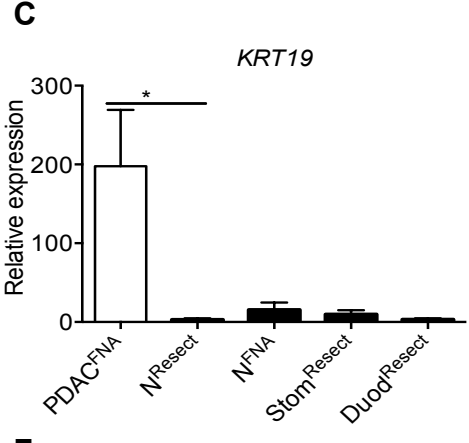
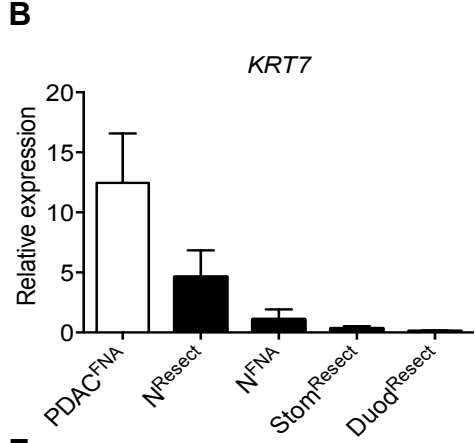
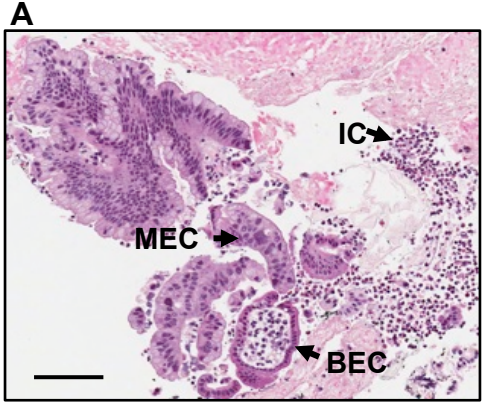
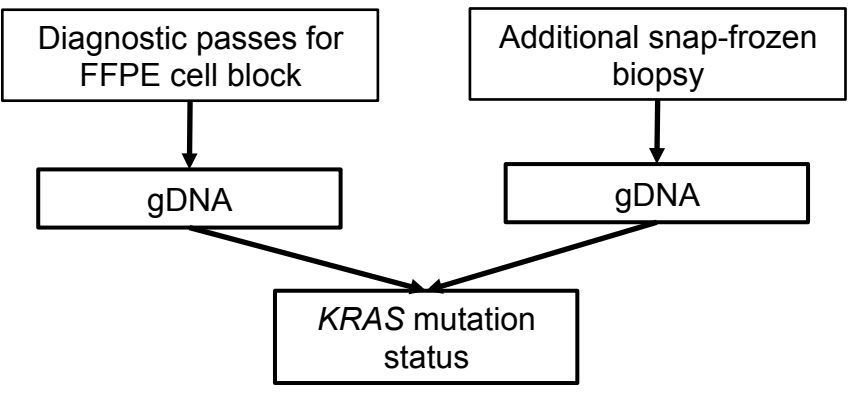
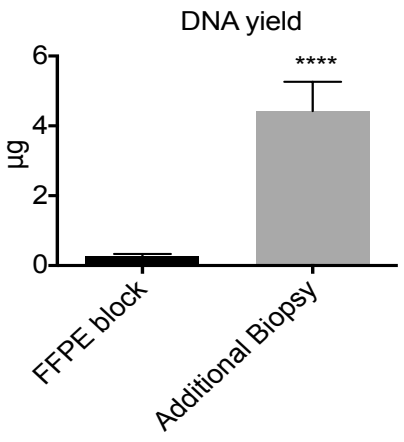


Figure 3.5: Detection of *KRAS* mutation in FFPE and additional biopsies. (A) Flow diagram depicting the method of obtaining genomic DNA from EUS-FNA-derived patient tumour samples. (B) DNA yield for different tissue processing methods. (C) Frequency of *KRAS* mutation detected in matched patient samples using different tissue methods for obtaining genomic DNA. $N = 20$ patients with matched additional biopsy and FFPE cell block, $**P < 0.01$; $****P < 0.0001$.

A



B



C

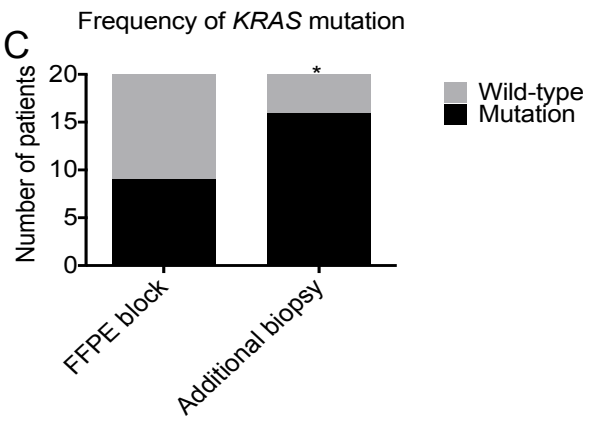
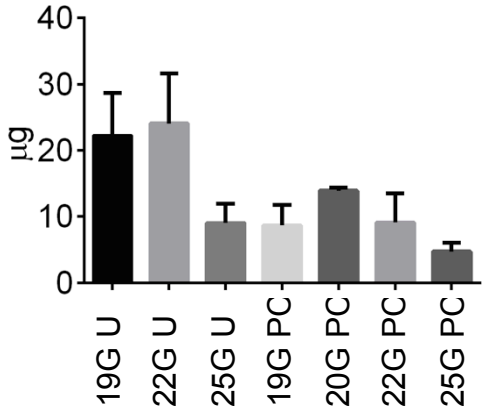
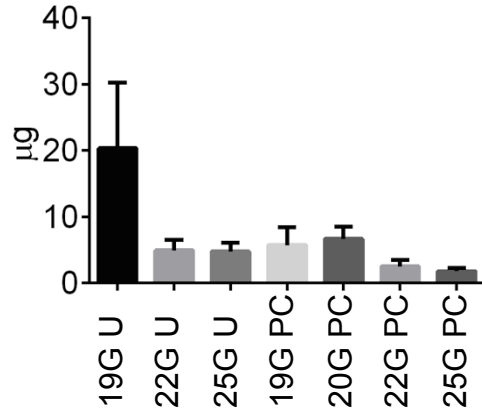


Figure 3.6: EUS FNA needle comparisons. Three different gauges of needle were used: 19-gauge, 22-gauge and 25-gauge. Two different needle designs were used: Ultra (U) and Procore (PC). (A) RNA yield for each needle design. (B) DNA yield for each needle design. (C, D) RNA and DNA yield for 19-gauge U and PC needles. (E, F) RNA and DNA yield for 22-gauge U and PC needles. (G, H) RNA and DNA yield for 25-gauge U and PC needles. * $P < 0.05$

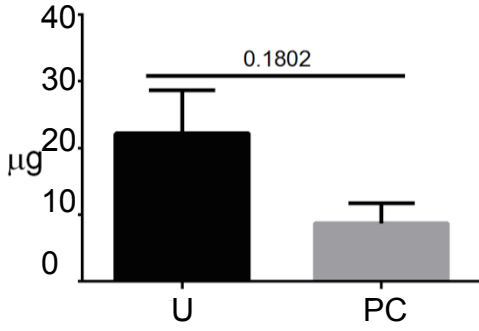
RNA yield



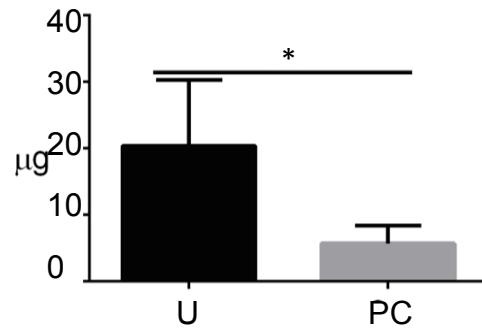
DNA yield



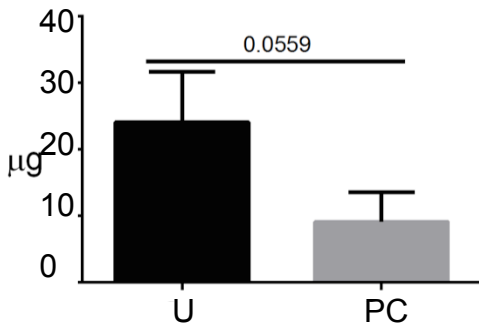
19G RNA yield



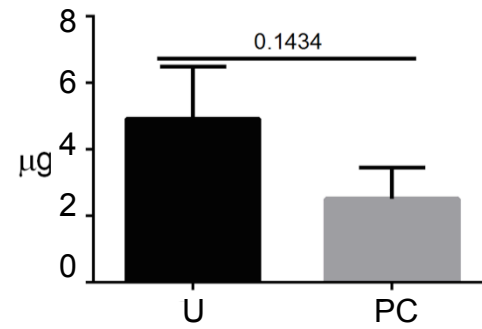
19G DNA yield



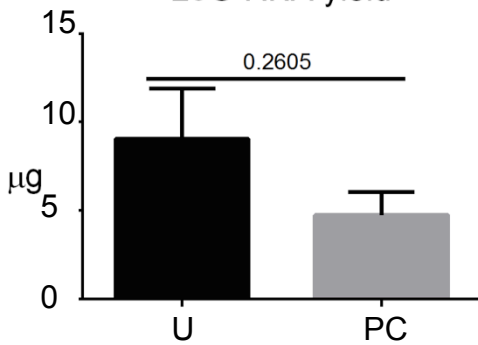
22G RNA yield



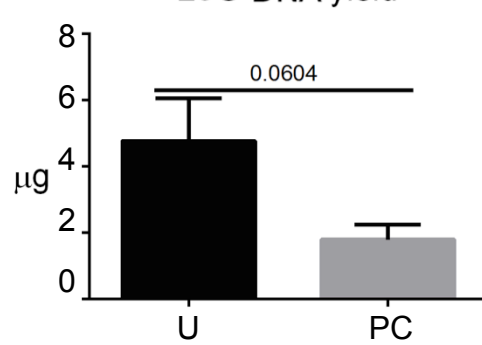
22G DNA yield



25G RNA yield



25G DNA yield



Chapter 4: Transcriptome profile of pancreatic cancer using EUS FNA

Personalised therapy relies on understanding the molecular subtypes of PC that can be targeted with existing and novel therapeutics; In this Chapter I validate methods to investigate the molecular profile of PC and identify potential tumour phenotypes that may respond to targeted therapies. To this end, recent studies using next generation sequencing (NGS) technology have focused on the molecular underpinnings of tumourigenesis in PC, as well as investigating tumour phenotypes potentially amenable to specific treatment, and thus have vastly improved our understanding of the molecular landscape of PC [21-23,27]. However, such findings are yet to translate into improvements in patient outcomes due to the inherent difficulties in designing and implementing a clinical trial of personalised therapy.

As mentioned in Chapter 1, Chantrill, et al [36] have recently reported on the failings of a current attempt to run a personalised therapeutic trial. The authors describe difficulty in recruiting sufficient patient numbers, as many molecular targets identified occurred only in small percentages of patients. Another factor that contributed to the failure of this trial was the inability to obtain genetic material from metastatic disease, because only patients with localised disease are eligible for surgical resection, and surgery was the primary means of obtaining material for this trial.

The greatest potential for the in-depth genetic analysis of PC is providing clinicians with the ability to guide treatment selection for individual patients based on the molecular profile of their tumour. To this end, a known molecular target that is a viable candidate for personalised medicine for PC is *KRAS* wild type disease. *KRAS* is particularly important in PC as mutation occurs in approximately 80-96% of

patients [10,26,107,23,24]; indeed my data presented in Chapter 3 reflected this occurring in 85% of the cohort. As mentioned in Chapter 1, *KRAS* mutation is thought to be an early oncogenic event in PC and has been associated with poorer prognosis [96,95]; most importantly for personalising cancer therapy, *KRAS* wild type tumours may respond to specific therapy with anti-EGFR agents [26,34-36,104-106]

In this Chapter I have included datasets that utilise EUS FNA-derived RNA, and datasets that used surgical resection specimens, namely The Cancer Genome Atlas (TCGA), and Gene Expression Omnibus (GEO). Using these transcriptomic datasets I explore the potential for NGS to inform diagnosis, identify targetable phenotypes and characterise distinct phenotypes of PC.

One potential application of NGS is to identify diagnostic gene signatures to aid in differentiating inconclusive histological or cytological diagnostic samples. Here I focus on two recently published gene signatures to demonstrate their accuracy in independent transcriptome datasets. Rodriguez, et al [57] use EUS FNA-derived RNA to profile the transcriptome of PC and pancreatitis. This study identified a gene expression signature of 83 genes that differentiated benign (pancreatitis) from malignant (PC) samples at a sensitivity and specificity of 0.87 and 0.75, respectively. Bhasin et al [60] also sought to identify a gene signature to distinguish between benign and malignant samples; this study included 12 microarray datasets to identify a 5-gene signature with 0.95 and 0.89 sensitivity and specificity, respectively. Here, I explore the accuracy of this gene signature in multiple external cohorts of PC from publically available datasets and my own transcriptome experiment.

The next potential use for NGS that I explore is the potential to personalise patient therapy based on the molecular biology of their tumour; I identify known targets that have been successfully treated in other malignancies and assess whether these targets are indeed viable in PC as well. Importantly, by using the methods optimised and validated in Chapter 3, I show transcriptome profiling on EUS FNA-derived PC RNA. As such, I am able to contrast the transcriptome profiles of

metastatic disease and localised disease for the first time, as this has previously been impossible for all studies using surgically derived samples. Importantly, localised tumours, which occur in 20% of cases, can be surgically resected, and they are currently the most treatable subtype of PC as surgical resection is associated with a median overall survival of 27 months, more than double that of all medical treatments. However, it remains unclear whether there are differences between localised and metastatic PC at a molecular level.

Overall, this Chapter expands the utility of EUS FNA-derived genetic material and demonstrates the potential applications for metadata derived from NGS experiments.

4.1 EUS-FNA-derived RNA quality control for RNAseq

Transcriptome profiling by RNAseq was performed for 40 PC patients and 5 normal pancreas control samples (Table 4.1). As EUS FNA-derived genetic material has only recently been used for NGS [57], it is important to first demonstrate the validity of EUS FNA-derived RNA. Therefore, I present the relevant RNAseq quality control data, which confirms that a high proportion of sequence reads successfully mapped to the reference genome (Figure 4.1A and Table 4.2). In addition, the dataset shows a relatively uniform number of read counts per gene and in each sample library, indicating equivalent sequencing efficiency across all samples and multiple experiments (Figure 4.1B and D). Principal component analysis (PCA; Figure 4.1C) was used to identify three outlier samples; these were removed from subsequent analyses. Together, these data demonstrate EUS FNA-derived RNA is high quality and can be used for high quality NGS datasets.

4.2 Transcriptome profile of PC to inform diagnosis

Sample libraries that satisfied the quality control measures were included in the subsequent analyses. Libraries were normalised using the R software packages Bioconductor and limma (described in detail in Appendix 2). Normalised read counts were grouped based on whether the sample was a normal pancreas sample or PC tumour sample, and these were then contrasted to compare the gene expression levels in both tissue types. This revealed 2443 genes that were significantly differentially expressed (Figure 4.2A, B), confirming that, at a molecular level, PC is distinct from normal pancreatic tissue. Importantly, the heat map (Figure 4.2A) demonstrates a high degree of heterogeneity in the tumour samples compared to the uniform gene expression seen in the 5 normal samples. Of note, one PC sample had a transcriptional profile that was typical of normal pancreas, although the cytological diagnosis of this specimen indicated PC.

Given the dramatic differences between normal pancreas and PC samples, I explored the utility of the transcriptome profile to inform diagnosis. I identified two previous studies that derived PC specific diagnostic gene signatures: Bhasin et al [60] and Rodriguez et al [57]. For these analyses I used multiple datasets, namely the EUS FNA-derived RNA from the Monash cohort, as well as TCGA and GEO transcriptomic datasets (Table 4.3). Using GSEA I measured the enrichment for PC and non-malignant controls against both diagnostic gene sets (Table 4.4). Figure 4.3 shows the gene expression for each diagnostic gene signature across all datasets, displaying the difference between normal pancreas and PC tumour tissue. Despite these gene lists being specific for PC, there is wide variability in gene expression levels amongst the tumour samples in these cohorts (Figure 4.3). This observation is validated by the associated GSEA results, where only two of four datasets significantly enriched against the Bhasin et al gene signature (Figure 4.4).

Furthermore, only one dataset significantly enriched against the up-regulated gene list derived from the Rodriguez et al gene signature (Figure 4.5); however, this result was offset by the tumour samples also positively enriching against the genes that were reported to be down-regulated in PC from the Rodriguez et al gene signature.

Together, these analyses further highlight the wide inter-tumoural heterogeneity of PC and the caution that needs to be taken into account when considering such diagnostic gene signatures for potential clinical utility on individual patients.

4.3 Molecular profiling to guide treatment selection in PC

Although inter-tumoural heterogeneity is an undesirable trait for developing specific diagnostic biomarkers and gene signatures, this may explain the heterogeneous response to treatment seen in PC and may in fact lend itself to identifying treatable phenotypes of disease. Molecular targets with established treatments that have been successfully used in other malignancies have the potential to immediately translate into clinical success [67]. I therefore performed a meta-analysis to identify current targets for personalised medicine in PC: electronic searches were performed using Ovid Medline, PubMed and Embase to identify potentially treatable PC phenotypes by combining the terms “pancreatic adenocarcinoma”, “molecular targeted therapy” and “chemotherapy”. All retrieved articles were reviewed to compile a list of all mutations targetable with currently available treatments (Table 4.5). The incidence of each of these phenotypes in PC was then obtained by analysis of the COSMIC database and TCGA dataset (Figure 4.6, Table 4.5; [5,10,26,36,41,64,65,107,158-162]). However some of these potential targets are of very low prevalence (e.g. PDGFR A/B mutations which occurs in <2% of PC cases) and others depend upon

the analysis of gene expression or protein expression levels for which the diagnostic threshold is not clearly defined (e.g. c-MET expression and the use of cabozantinib; [160-162]).

The five most prevalent and potentially treatable phenotypes of PC identified were as follows; localised PC treated with resection; *KRAS* wild type treated with anti-EGFR inhibitors [34,44,62]; DNA repair pathway mutations (*BRCA1/2*, *ATM*, *PALB2*) treated with DNA-damaging agents [64]; *HER2*-amplification treated with trastuzumab [29,30]; and *BRAF* mutant PC treated with BRAF and MEK inhibitors [31,33] (Table 4.5). To identify the most attractive candidate for “targeted therapy” I compared the frequency, clinical phenotype and transcriptional profile in each of these PC phenotypes using TCGA clinical and NGS datasets (Figure 4.6).

Resection for localised tumours remains the most effective treatment for PC, and approximately 20% of patients with PC have localised tumours [5,13]. However, a fundamental unanswered question likely to have profound implications with respect to selection of patients for surgical resection is whether localised PC possesses a different molecular and genetic phenotype to metastatic PC. To address this question, I performed transcriptome profiling on EUS FNA specimens from 20 localised and 20 metastatic PC by RNASeq (Table 4.1). Somewhat surprisingly, there was a marked homogeneity between the gene expression profiles of localised and metastatic tumours overall, with no significantly differentially expressed genes identified in the entire transcriptome of either disease stage (Figure 4.7A, B). These observations were also confirmed upon GSEA, which indicated that no gene sets were significantly enriched ($P < 0.01$; false-discovery rate (FDR) $q < 0.25$). These results therefore suggest that despite wide inter-tumoural heterogeneity, the molecular (i.e. gene expression) profile of localised and metastatic PC tumours is comparable, thus providing a potential explanation for the poor outcomes of patients with localised disease following pancreatic resection.

I next performed *in silico* analysis on genomic, transcriptomic and clinical data in the TCGA database derived from surgical resection specimens (i.e. patients with localised disease only) to explore the other 4 potentially treatable phenotypes of PC based on the above-mentioned non-surgical treatment regimes. To identify whether the mutational status of tumours for these potentially responsive PC phenotypes correlated with a specific molecular (i.e. gene expression) signature, I compared matched TCGA genomic and transcriptomic datasets from 166 PC patients with localised disease. The genetic (i.e. mutational status) analysis identified 38 cases with *KRAS* wild type tumours, 17 cases with DNA repair pathway mutations (*BRCA1/2*, *PALPB*, *ATM*), and 4 cases with *BRAF* mutation (Table 4.5 and Figure 4.6). I note that there was no copy number variant TCGA data available for *HER2*, which prevented assessment of *HER2* amplification in PC patients. Also, the low number (i.e. 4/166) of *BRAF* mutant tumours precluded any statistically meaningful analyses of this treatable phenotype.

Assessment of the transcriptome data for patients with *KRAS* wild type tumours demonstrated clustering to one side of the hierarchical analysis heat map (Figure 4.8). In addition, differential gene expression analysis between *KRAS* wild type and mutant tumours revealed 391 genes that achieved significance ($|\text{Log}_2\text{FC}| > 1$ and $P < 0.01$; Figure 4.9). Furthermore, comparing these transcriptome profiles against published gene sets using GSEA software revealed 5 gene sets (Computational gene sets, Cancer Modules 35, 110, 160, 184 and 221) that were significantly enriched in *KRAS* wild type PC and 2 gene sets (miR-518 B/C and Kegg pathway glycosaminoglycan-biosynthesis) that were significantly enriched in *KRAS* mutant PC (Table 4.6 and Figure 4.10; $P < 0.01$ and FDR $q < 0.25$).

Conversely, the molecular analysis of tumours potentially sensitive to DNA-damaging agents (i.e. tumours with DNA-repair pathway mutations) indicated there was no clustering of cases or any genes significantly differentially expressed (Figure 4.8).

Finally I contrasted various clinicopathological disease criteria, including overall survival, disease stage and site of disease in the *KRAS* wild type and mutant PC, as well as tumours that possess DNA repair pathway mutations (Table 4.7 and 4.8). I show that patients with *KRAS* mutant tumours are more likely to be of a higher grade and have shorter overall survival versus patients with wild type *KRAS* (Table 4.7, and Figure 4.11A). *KRAS* mutation status did not correlate with other baseline patient characteristics such as age, sex, tumour stage or site. In addition, there was no difference in the clinical phenotype based on the presence of absence of DNA repair pathway mutations, which is consistent with the results observed in these transcriptomic studies (Figure 4.11B, and Table 4.8).

Collectively, these analyses suggest that *KRAS* wild type tumours are the most prevalent and have the most distinctive transcriptome profile of these treatable phenotypes.

4.4 Discussion

Expanding on Chapter 3, where I demonstrate that EUS FNA-derived RNA is indeed a valid readout for PC gene expression, in Chapter 4 I show further applications of this RNA using NGS technology and *in silico* analyses. There has only been one other report of RNAseq being performed on EUS FNA-derived RNA in the literature, and in this study Rodriguez and colleagues attempt to generate a diagnostic gene signature using EUS FNA-derived RNA from both benign and malignant samples [57]. In this Chapter I seek to validate Rodriguez and colleagues' diagnostic signature and to apply transcriptomic and exomic datasets to better characterise molecular targets for personalised medicine.

As mentioned previously, genetic studies to date have largely focused on surgically-derived tissue, and therefore these have excluded the majority of patients, as 80% of cases present with locally advanced or metastatic disease. Another advantage of EUS FNA is that it enables the acquisition of genetic material early in the clinical course of the disease. Therefore a potential application is the use of this genetic material to inform diagnosis, or improve the diagnostic accuracy of EUS FNA cytology by combining genetic data. Indeed, initial analyses reveal the vast differences in gene expression profiles of PC and normal pancreas tissue. However, examining these PC cohorts reveal vast inter-tumoural heterogeneity and diagnostic gene signatures did not improve the accuracy of EUS FNA, compared to cytology alone (Figures 4.3 – 4.5). An important consideration in these comparisons of various PC cohorts is that all experiments were performed separately, and Rodriguez and colleagues used RNAseq, whereas Bhasin and colleagues used microarray datasets, as such further increasing the number of patient samples and experimental datasets may identify true differences in PC gene expression and therefore provide a more robust gene signature with diagnostic relevance. Conversely, this finding may reflect that PC is vastly heterogeneous and molecular analyses are just as likely to identify these inter-tumoural differences, as they are to distinguish differences between malignant and non-malignant processes, as such a diagnostic gene signature is always going to have low specificity.

Overall, efforts to use molecular analyses for diagnostics have failed to show meaningful improvement in diagnostic accuracy; whether these analyses focus on gene expression signatures [57,60], supported by the analyses in this Chapter, or the detection of known oncogenes, such as *KRAS*, as mentioned in Chapter 1 [41,42,46-51]. Given the added cost and complexity of running sequencing experiments for negligible gains, this is an area unlikely to lead to significant clinical applications.

The use of EUS FNA in these analyses facilitates the first experiment to contrast the transcriptome profile of localised and metastatic PC. Surprisingly, no

significant differences at the molecular level (i.e. gene expression) were identified between these two patient cohorts, suggesting that although patients with localised or metastatic disease have markedly different clinical phenotypes, at a molecular level they are remarkably similar. Importantly, this finding is consistent with two previous studies that attempted to address this issue with a different approach involving patients who underwent pancreatic resection for their cancer. Recent publications contrast the genetic profile of matched primary and metastatic PC lesions using autopsy specimens [66,183]. Moffitt, et al [66] used transcriptome profiling of tumour samples and adjacent normal tissue to perform a “virtual microdissection”, which demonstrated that the transcriptome profiles between primary and secondary sites of the same tumour are indeed very similar [66]. In addition, Yachida et al [183] demonstrated that there is high mutational concordance between primary and secondary lesions. Overall, these findings support my data and the notion that there is no great molecular difference between metastatic or localised PC, and further suggest it is unlikely that a specific molecular biomarker for a localised tumour phenotype exists. These findings suggest that it is unlikely that a molecular event occurs that drives metastasis, rather all tumours have the necessary molecular changes to potentiate metastatic spread early and the difference between localised and metastatic disease is merely the time of presentation in reference to the clinical course, or natural history of the disease. It also suggests that using molecular-based approaches to predict the metastatic potential of individual tumours, or the presence of micro-metastases or disease recurrence after pancreatic resection may be problematic.

Although there were no differences at a molecular level between localised and metastatic PC, there is potential for molecular analyses to reveal other treatable phenotypes of PC and, as is the case for other malignancies, some genetic variations may produce distinct tumour phenotypes that are responsive to specific therapy. Here I perform a meta-analysis to identify such targets that may be

applicable to PC. Of these potential targets I have identified three phenotypes of PC that occur in at least 10% of patients in the Monash or TCGA cohorts. I excluded uncommon phenotypes (<10%) because the low number of patients with targets makes differential gene expression analyses statistically powerless, although these targets may indeed be amenable to targeted therapies.

Using these datasets to contrast patients “with target” and “without target” in terms of clinical phenotype and transcriptome profile reveals that *KRAS* mutation status has a substantial impact on these parameters. This suggests *KRAS* mutation, thought to be an early oncogenic mutation, drives PC in a different direction compared to *KRAS* wild type tumours. Indeed, the recent publication from The Cancer Genome Atlas Research Network indicates that in the absence of oncogenic *KRAS* mutation, tumours have distinct oncogenic drivers, including different *RAS* gene pathway genes, *GNAS*, *BRAF* and *CTNNB1* [24] Although there is no clinical trial indicating that in PC *KRAS* wild type tumours will respond to targeted therapy, this distinct phenotype described here suggests that the two tumour subtypes indeed behave differently and therefore may respond to therapy in different ways. Furthermore, anti-EGFR agents have been successful, albeit with a very small treatment effect, in PC in unselected patients [17]. Given the survival benefit seen in colorectal cancer [34,104-106], it is reasonable to hypothesise a similar benefit may be seen in PC when these treatments are used in a targeted fashion.

Interestingly, despite there being no significant differences at both molecular and clinical levels between patients with tumours that had a mutation in one of the DNA repair pathway genes and those that didn't (Figures 4.8, 4.11, and Table 4.8), there has been a case report that shows one patient with *PALB2* mutation was an exceptionally good responder to mitomycin-C (DNA damaging agent) [64]. The authors of this report suggested that the use of DNA damaging agents for patients with a similar genetic profile is warranted.

It is interesting to note that because other molecular targets are exceedingly rare, this may explain the lack of clinical efficacy demonstrated for various agents used in clinical trials. As mentioned in Chapter 1, although several agents have been trialled in Phase II and III clinical trials, very few have demonstrated improved efficacy compared to gemcitabine. This may be because trials have been performed in unselected patients, when in fact only small subsets of the population of PC patients will respond to specific agents, and my analyses show that targets frequently occur in less than 1-2% of patients. Through my meta-analysis I have identified several candidates for personalised medicine that could potentially be trialled using existing therapies. Together with my molecular analyses, these data support the further investigation of rare genetic targets in personalised therapy trials to demonstrate efficacy for specific agents in these subsets of PC patients. However, these trials would require large numbers of patients to be enrolled and this has been shown to be exceedingly difficult in a recent trial for personalised therapy in PC [67].

Overall, these analyses are amongst the first comprehensive interrogation of EUS FNA-derived PC RNA for personalised therapy. Furthermore, I am the first to demonstrate that localised and metastatic PC are largely the same at a gene expression level, despite having such distinct clinical phenotypes. The next step on from these *in silico* analyses is to demonstrate treatment efficacy when using a personalised approach to treatment specifically against the molecular targets identified here.

4.5 Tables and figures

Table 4.1: Clinicopathological characteristics of RNAseq PC cohort for localised versus metastatic disease analysis using EUS-FNA-derived RNA.

Patient characteristics	n = 40
Gender	
Female, n (%)	24 (60%)
Age, mean (range) years	
	68.1 (47-88)
Stage, n (%)	
Localised	20 (50%)
Metastatic	20 (50%)
Treatment, n (%)	
Surgery	5 (12.5%)
FOLFIRINOX	3 (7.5%)
Gem + nab-Paclitaxel	8 (20%)
Gemcitabine	3 (7.5%)
Palliative	5 (12.5%)
Other	2 (5%)
Unknown	14 (35%)
Site, n (%)	
Head	21 (52.5%)
Uncinate	4 (10%)
Neck	7 (17.5%)
Body	7 (17.5%)
Tail	1 (2.5%)

Table 4.2: Quality control for RNAseq, library total and mapped reads

Sample	Input Reads	Mapped Reads
PC1	7294680	99.30%
PC2	6800852	99.55%
PC3	8810674	99.29%
PC4	8079082	99.51%
PC5	3541408	99.12%
PC6	11007972	99.30%
PC7	10512689	99.36%
PC8	8439726	99.31%
PC9	9928997	99.76%
PC10	9972198	99.75%
PC11	9364446	99.70%
PC12	9879865	99.76%
PC13	4572749	99.63%
PC14	13862302	99.70%
PC15	10930830	99.68%
PC16	7580333	99.76%
PC17	16685130	99.62%
PC18	10285237	99.63%
PC19	10313367	99.70%
PC20	9893210	99.71%
PC21	5302098	99.56%
PC22	7802876	99.76%
PC23	8480305	99.70%
PC24	14855965	99.73%

PC25*	7294680	99.30%
PC26*	6800852	99.55%
PC27*	8810674	99.29%
PC28	5,561,478	94.63
PC29	5,226,219	93.26
PC30	50,605,645	93.22
PC31	4,135,206	90.66
PC32	6,799,034	92.16
PC33	4,967,267	91
PC34	6,040,146	90.45
PC35	4,955,012	91.39
PC36	11,861,735	92.92
PC37	8,298,222	93.09
PC38	15,682,808	92.62
PC39	13,817,811	90.14
PC40	15,255,731	89.29
PC41	9,453,017	90.99
PC42	7,267,470	92.21
PC43	6,627,342	92.6
N1	8079082	99.51%
N2	3541408	99.12%
N3	11007972	99.30%
N4	10512689	99.36%
N5	8439726	99.31%

Asterisk (*) indicates samples that were removed from further analysis because they failed quality control (Principal component analysis).

Table 4.3 Clinicopathological characteristics of The Cancer Genome Atlas (TCGA) PC cohort

Characteristic	
Sex	44.9% Female
	55.1% Male
Age (Range)	65.4 (35 - 88)
Surgery performed	
Whipple	77.35%
Total pancreatectomy	1.60%
Distal pancreatectomy	12.40%
- Unknown	8.65%
Duration of treatment (days)	Median = 225
	Range 0-1895
Survival	
Alive at follow up	55.40%
Average survival of deceased patients	462 days
Recurrence (%)	33.70%
Distant metastasis	21.30%
Locoregional metastasis	7.90%
New primary tumour	1.10%
Not specified	3.40%
Tumour grade	
1	17.60%
2	53.30%
3	28.00%

4	1.10%
Positive lymph nodes, median (range)	2 (0 - 16)
0	26.50%
1	14.10%
2	14.60%
>2	44.80%
Site	
Head	77.80%
Body	7.00%
Tail	7.60%
Other	2.20%
Unknown	5.40%

Table 4.4: Published diagnostic gene signatures for PC

Reference	Platform	Sample type	Number of genes in gene signature	Sensitivity / Specificity
Rodriguez et al, 2016 [57]	RNAseq	EUS FNA	83	0.87 / 0.75
Bhasin et al, 2016 [60]	Microarray	Surgical resection	5	0.95 / 0.89

Table 4.5: Treatable molecular targets in PC identified through meta-analysis

Treatment	Target	Prevalence	TCGA or EUS-FNA
Surgery	Localised disease	20% [5]	EUS-FNA
Panitumumab	<i>KRAS</i> wild type	5-20% [23,24,41]	TCGA
DNA damaging agents	DNA repair pathways	14% [64,65]	TCGA
Trastuzumab	HER2 amplification	10 – 30% [36,158]	No CNV available
BRAF and MEK inhibition	<i>BRAF</i> mutation	1-2% [10,26,107]	TCGA
Everolimus	PI3K/AKT/mTOR pathway		TCGA
Imatinib	<i>KIT, ABL1/2, RET</i> mutation		TCGA
Sorafenib	<i>PDGFR A/B, FLT3</i> mutation	[159]	TCGA
Tamoxifen / Letrozole	Oestrogen / Progesterone receptor expression		Requires protein expression data
Abiraterone	Androgen receptor expression		Requires protein expression data
c-MET inhibitor (Cabozantinib)	c-MET expression	Unknown [160-162]	Requires protein expression data

4.6: Significantly enriched gene sets for KRAS wild type tumours

Gene set	Functional annotations	Clinical annotations
Cancer module 35	Transfer RNA ligase activity Amino acid activation Catalytic activity	Renal cell carcinoma (RCC) Haematological malignancy (cell line) Macrophage / Monocyte Atypical teratoid / rhabdoid tumour
Cancer module 110	Transfer RNA ligase activity Amino acid activation Nucleic acid binding Protein synthesis	RCC Lymphoma Atypical teratoid / rhabdoid tumour
Cancer module 160	Transfer RNA synthesis Transfer RNA ligase activity Amino acid activation Kinase activity	RCC Lymphoma
Cancer module 184	Fatty acid and lipid degradation / metabolism Propanoate metabolism	Liver cancer Hepatitis Colon cancer Lung cancer Normal tissue (Liver)
Cancer module 221	Fatty acid and lipid degradation / metabolism Propanoate metabolism	Liver cancer Hepatitis Colon cancer Lung cancer Normal tissue (Liver)

Table 4.7. Clinicopathological characteristics of TCGA PC cohort contrasting patient tumours with wild type and mutant KRAS.

Characteristic	KRAS wild type	KRAS mutant	P-value
Sex (Female)	44%	45%	0.921
Age, mean (Range)	63.3 (39 - 84)	65.2 (35 - 88)	0.361
5-year survival	12.50%	9.40%	0.58
Median survival (Days)	551	445	0.016
Response (%)			0.061
Progressive Disease	14.71	28.67	
Stable Disease	5.88	4.20	
Complete response	14.71	26.57	
Unknown	64.71	40.56	
Tumour grade (%)			0.0009
G1	39.39	12.75	
G2	51.52	53.69	
G3	9.09	32.21	
G4	0.00	1.34	
Lymph node staging (%)			0.145
N0	40.63	27.70	
N1	59.38	72.30	
TNM Staging (%)			0.641
Stage IA	6.25	2.65	
Stage IB	9.38	7.95	
Stage IIA	21.88	15.23	
Stage IIB	59.38	68.21	
Stage III or IV	3.13	5.96	

Tumour site (%)			0.401
Pancreatic Head	73.53	80.14	
Pancreatic Body	14.71	8.51	
Pancreatic Tail	5.88	9.22	
Other	5.88	2.13	

Statistical significance tested using Fischer-exact test and Chi-square test.

Table 4.8. Clinicopathological characteristics of TCGA cohort contrasting patients with tumours with DNA-repair pathway mutations.

Characteristic	DNA-repair mutant	DNA-repair wild type	P-value
Sex (Female)	31.6%	46.4%	0.2190
Age (Range)	64.9 (43 - 81)	64.9 (35 - 88)	0.9925
5-year survival	0%	11.3%	0.2884
Median survival (Days)	511	666	0.1486
Response (%)			0.2556
Progressive Disease	44.4	23.9	
Stable Disease	5.6	4.4	
Complete response	22.2	24.5	
Unknown	27.8	47.2	
Tumour grade (%)			0.7979
G1	10.5	18.4	
G2	57.9	52.8	
G3	31.6	27.6	
G4	0.00	1.27	
Lymph node staging (%)			0.4354
N0	42.1	27.9	
N1	57.9	72.1	
TNM Staging (%)			0.4886
Stage IA	3.0	5.3	
Stage IB	7.3	15.8	
Stage IIA	15.9	21.1	
Stage IIB	67.7	57.9	
Stage III or IV	6.1	0.0	

Tumour site (%)			0.4787
Pancreatic Head	57.9	81.6	
Pancreatic Body	10.5	6.7	
Pancreatic Tail	10.5	7.4	
Other	21.1	4.3	

Statistical significance tested using Fischer-exact test and Chi-square test.

Figure 4.1: Quality control assessment of EUS-FNA-derived RNA from Monash Biobank cohort. (A) Percentage of aligned bases and base length of each read. (B) Density of raw read counts per sample. (C) Principal component analysis. (D) Raw read counts per sample.

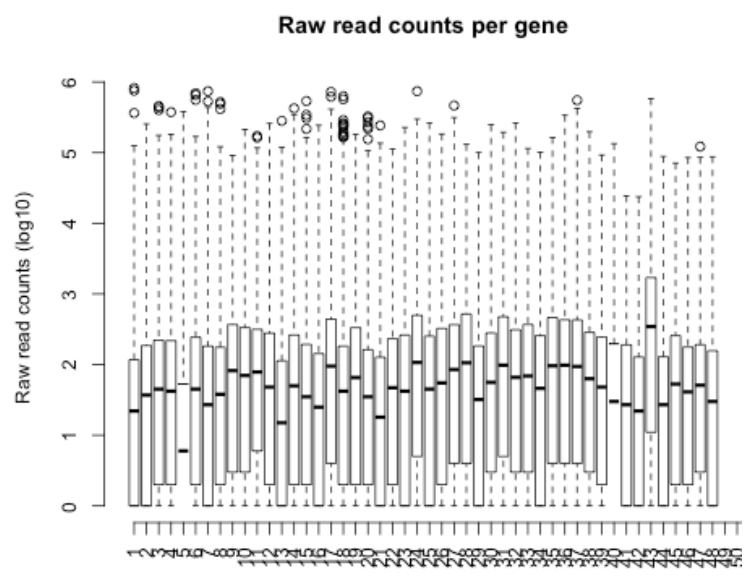
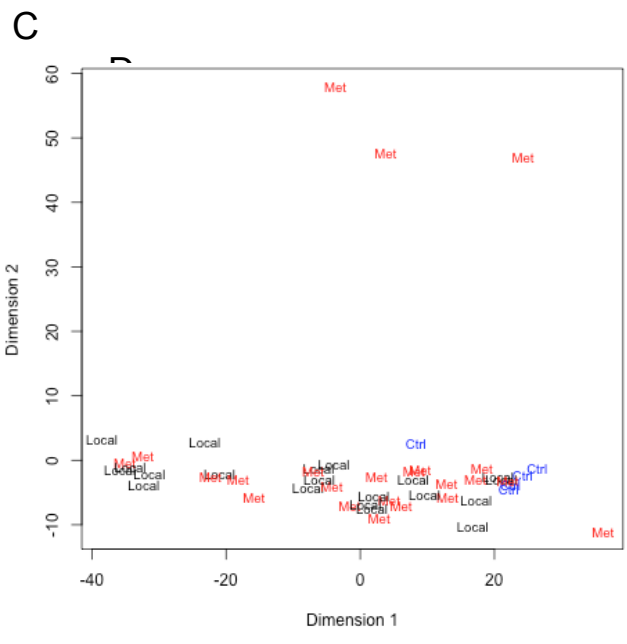
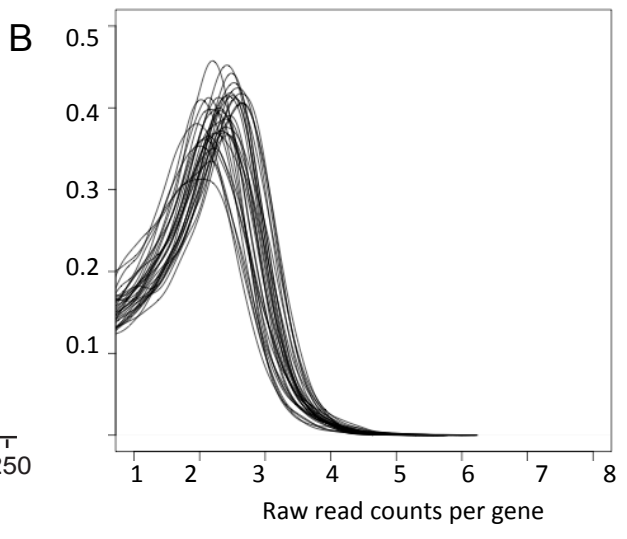
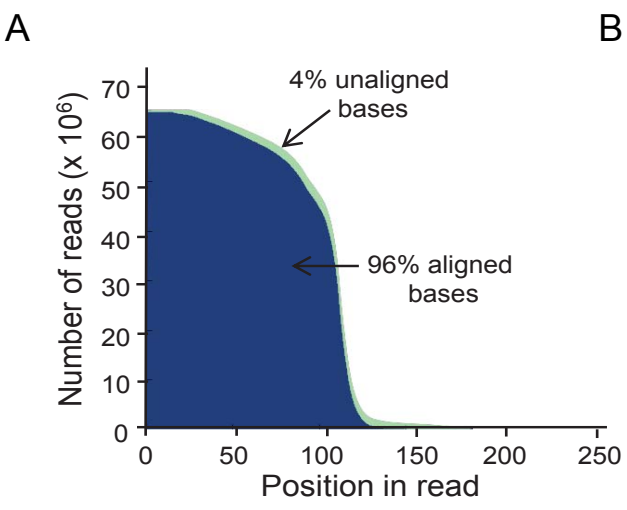


Figure 4.2: RNAseq contrasting the transcriptome of PC (N = 40) and normal pancreas (N = 5). (A) Heatmap demonstrating distinct transcriptome profiles of PC and normal pancreas. (B) Volcano plot showing 2443 significantly differentially expressed genes; Green dot = $|\text{Log}_2\text{FC}| > 1$ and $P < 0.01$, red dot = $P < 0.05$.

A PCFNA Norm^{Resect} **B**

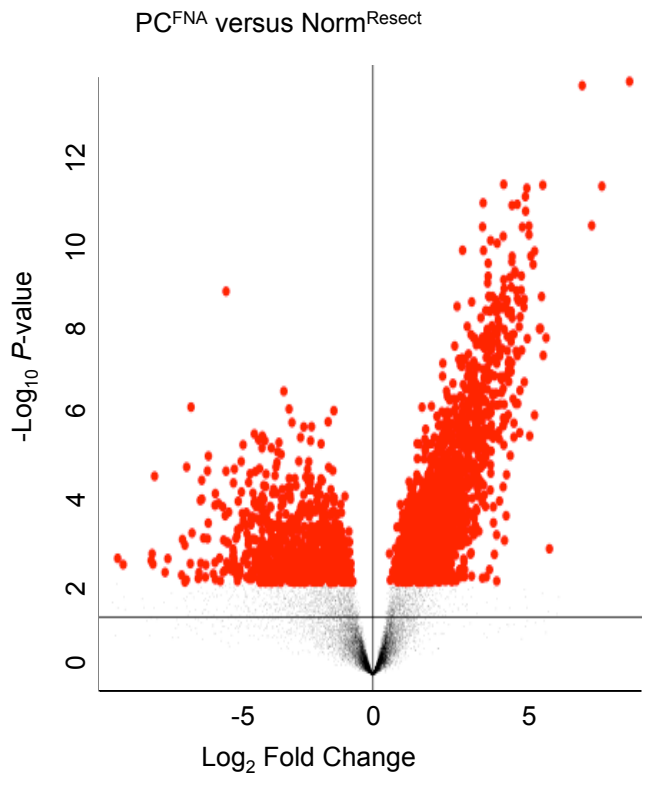
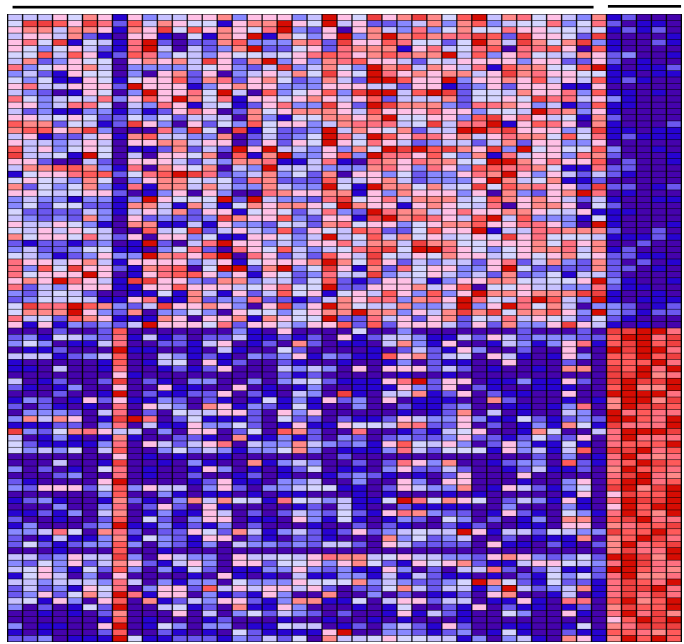


Figure 4.3: Heatmap indicating the gene expression of genes in two diagnostic gene lists (Rodriguez and Bhasin, Table 4.2) for independent transcriptome profile datasets. Rodriguez gene list is divided into genes that were reported to be up-regulated in PC (top) and genes that were down-regulated in PC (middle); Bhasin gene list consisted of 5 genes all reported to be up-regulated in PC (bottom). (A) TCGA, (B) Monash, (C – F) Gene expression omnibus datasets.

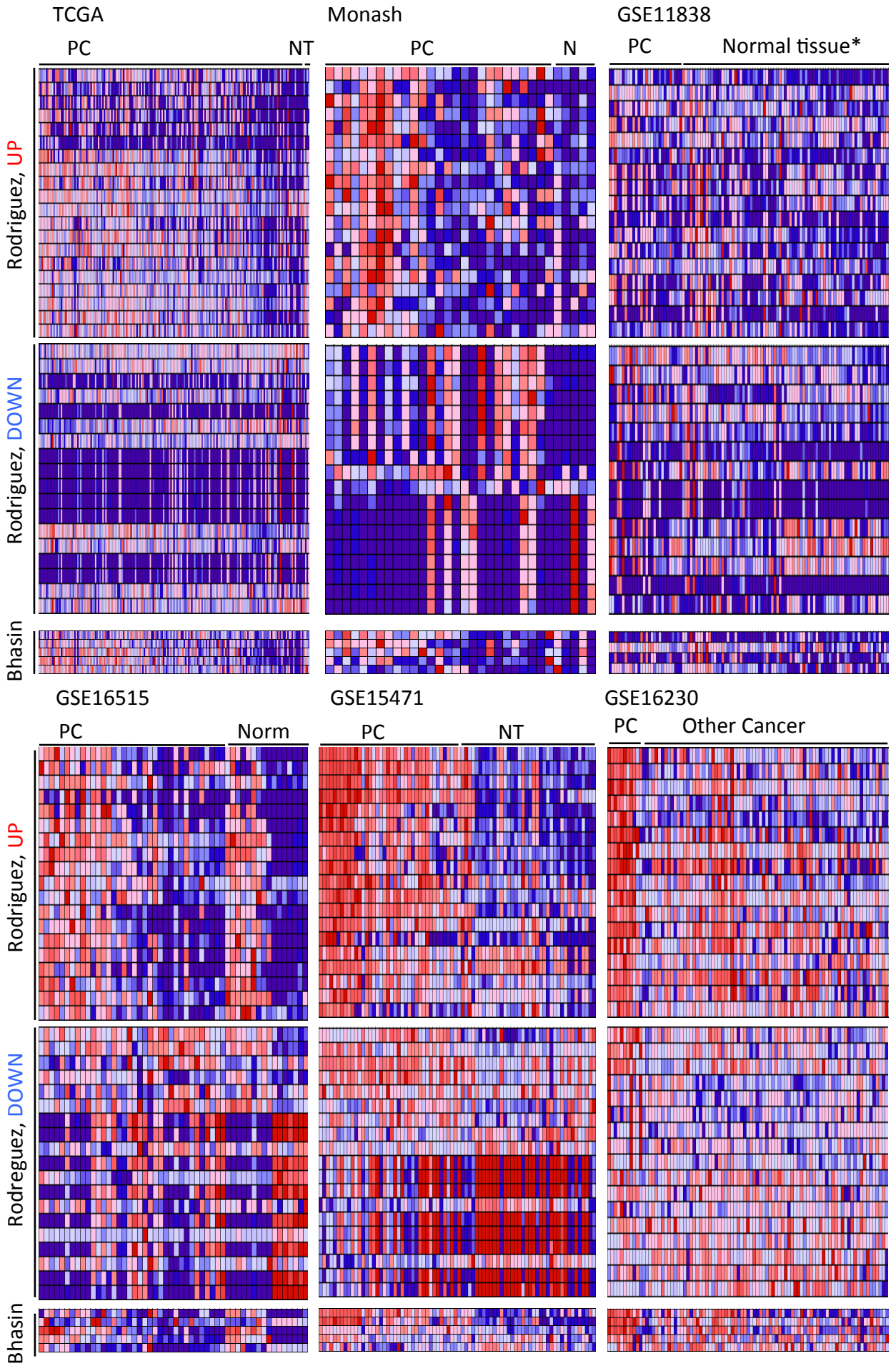
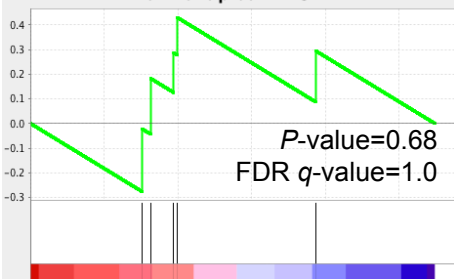


Figure 4.4: Gene set enrichment results for Bhasin, et al gene list. (A) TCGA, (B) Monash, (C – F) Gene expression omnibus datasets.

TCGA

Enrichment plot: BHASIN



Tumour correlated

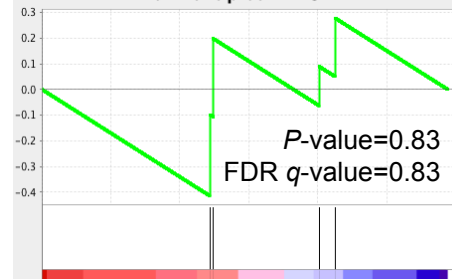
Monash

Enrichment plot: BHASIN



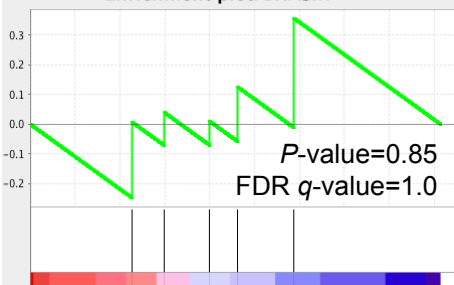
GSE11838

Enrichment plot: BHASIN



GSE16515

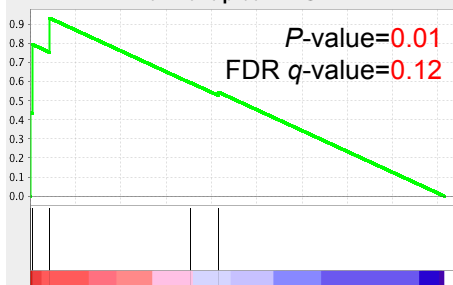
Enrichment plot: BHASIN



Tumour correlated

GSE15471

Enrichment plot: BHASIN



GSE16230

Enrichment plot: BHASIN

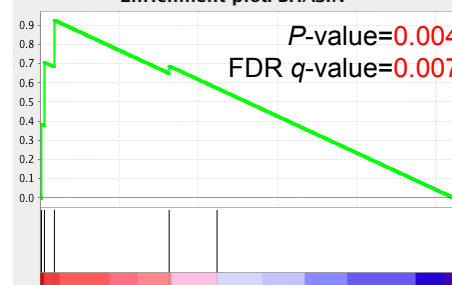
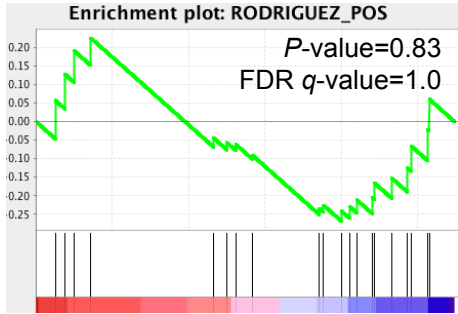
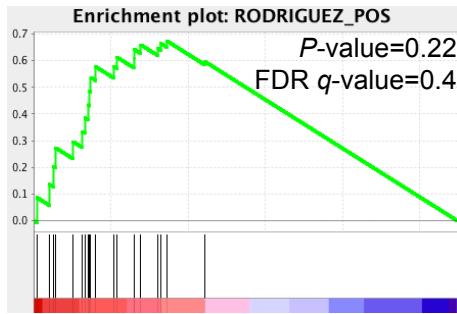


Figure 4.5: Gene set enrichment results for Rodriguez, et al gene lists of up- (top) and down-regulated genes (bottom). (A) TCGA, (B) Monash, (C – F) Gene expression omnibus datasets.

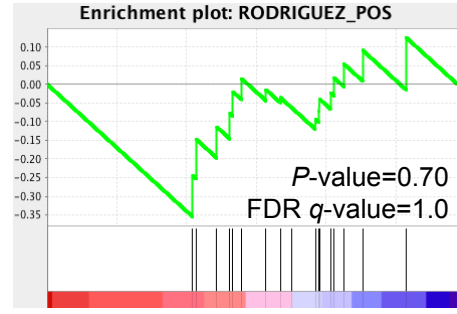
TCGA



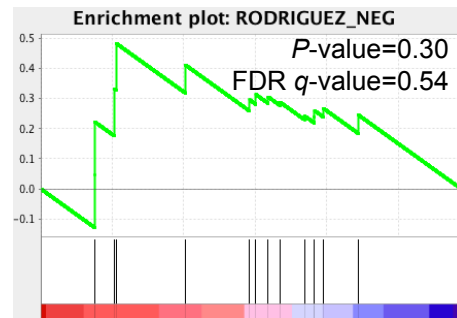
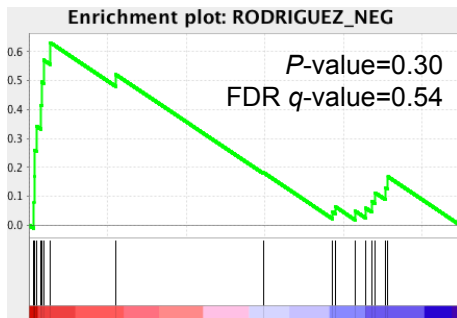
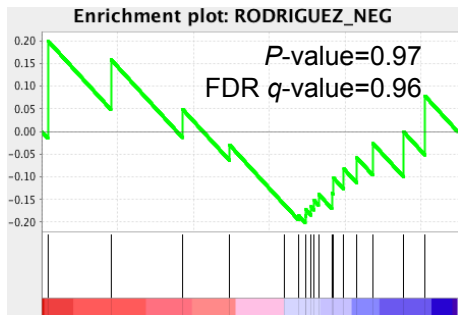
Monash



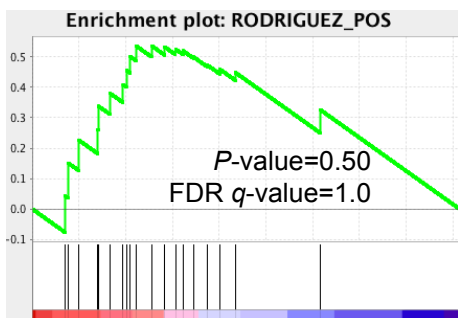
GSE11838



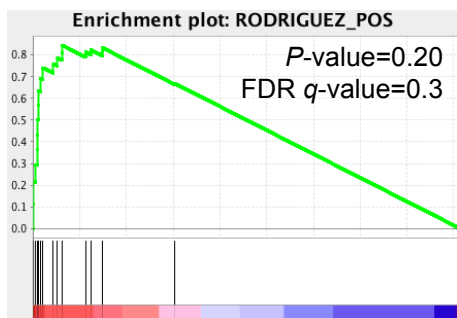
Tumour correlated



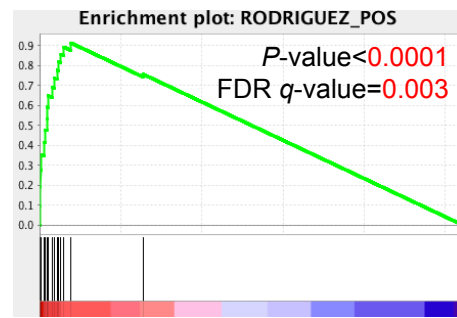
GSE16515



GSE15471



GSE16230



Tumour correlated

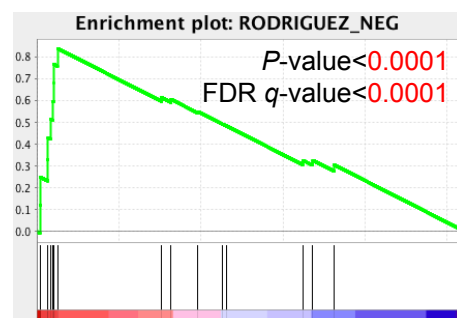
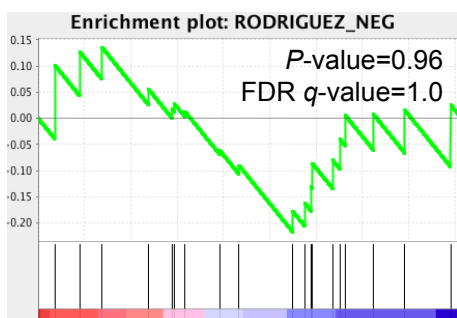
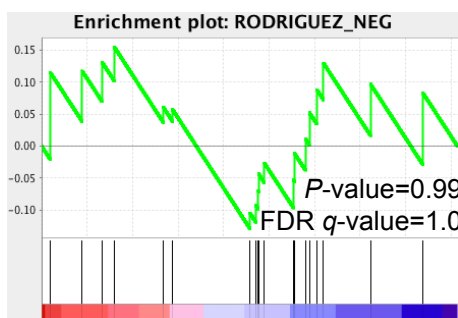


Figure 4.6: Incidence of mutations potentially targetable with existing chemotherapy agents in TCGA. Red indicates mutation present and blue indicates wild-type for each gene.

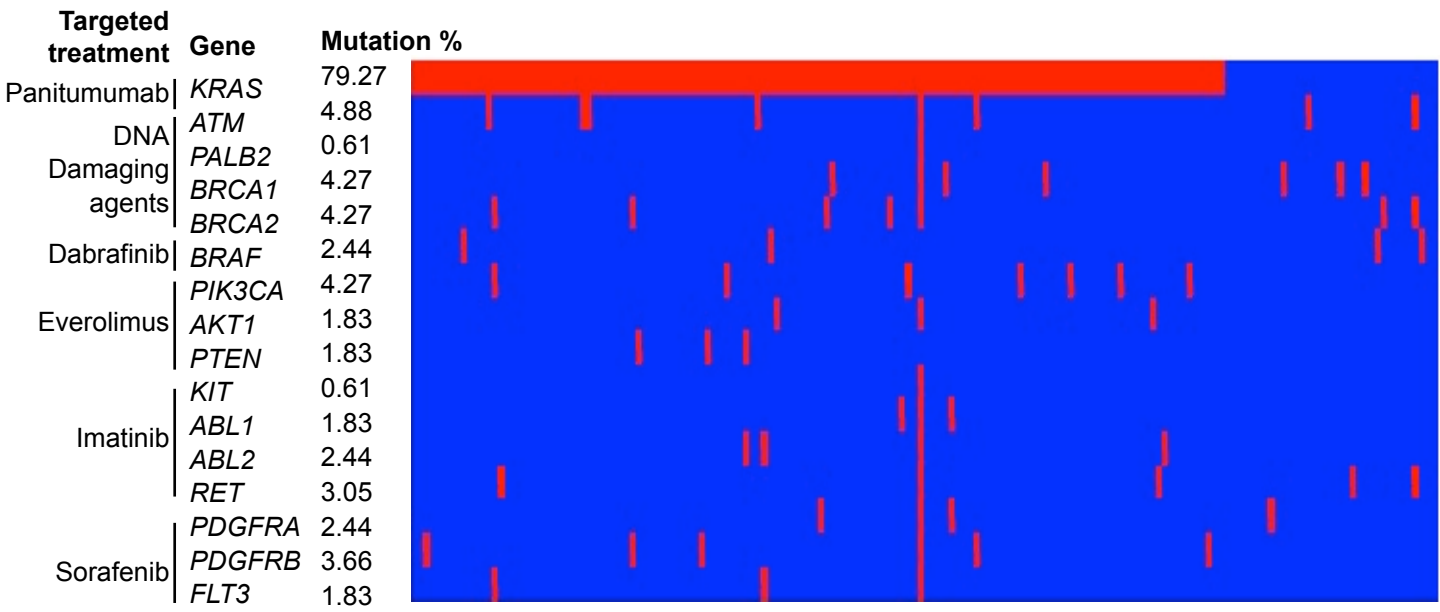


Figure 4.7: Transcriptome profile contrasting localised and metastatic PC. (A) Unsupervised hierarchical clustering of the two phenotypes. (B) Volcano plot showing zero genes were significantly differentially expressed between the two phenotypes.

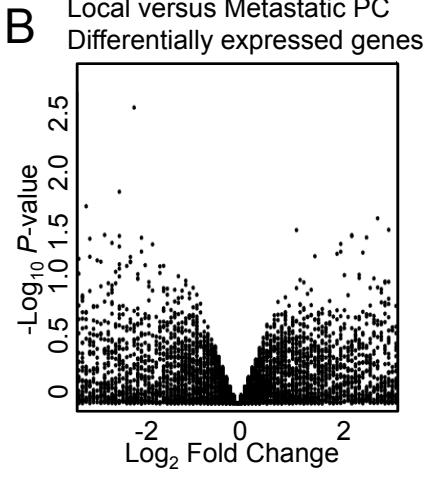
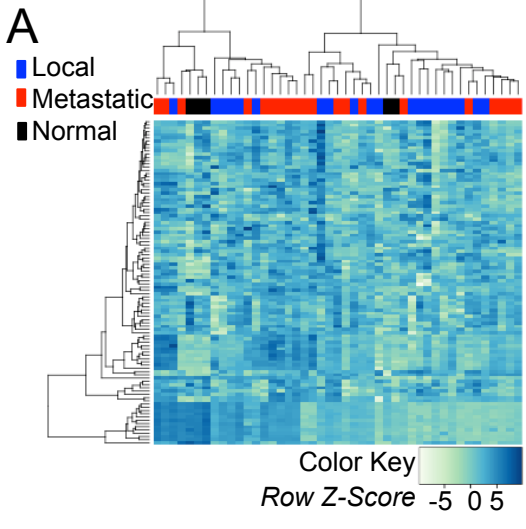
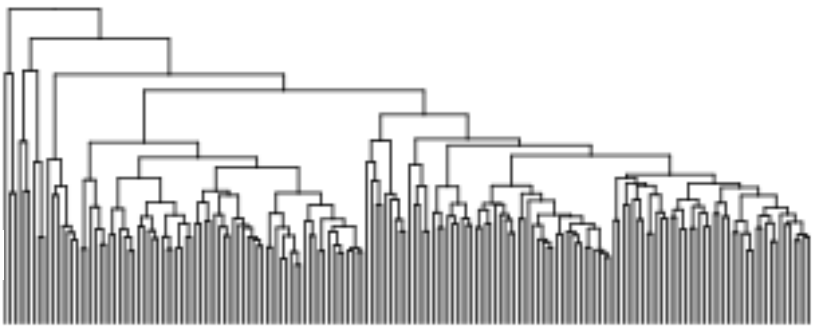


Figure 4.8: Heatmap of TCGA data demonstrating unsupervised hierarchical clustering of *KRAS* wild-type tumours and tumours with DNA repair pathway mutations.

Color Key
Row Z-Score -5 0 5

Treatable
Not treatable



KRAS
DNA repair genes

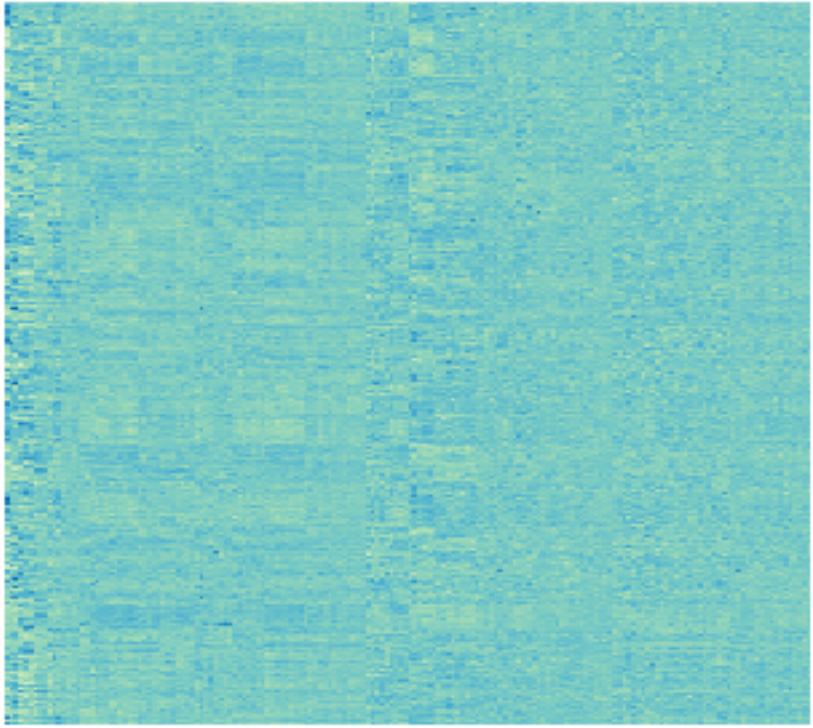
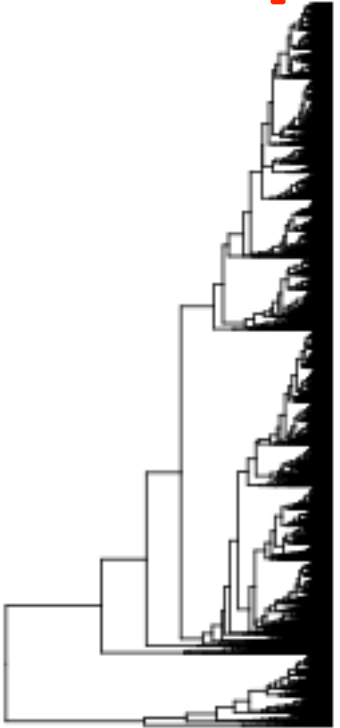
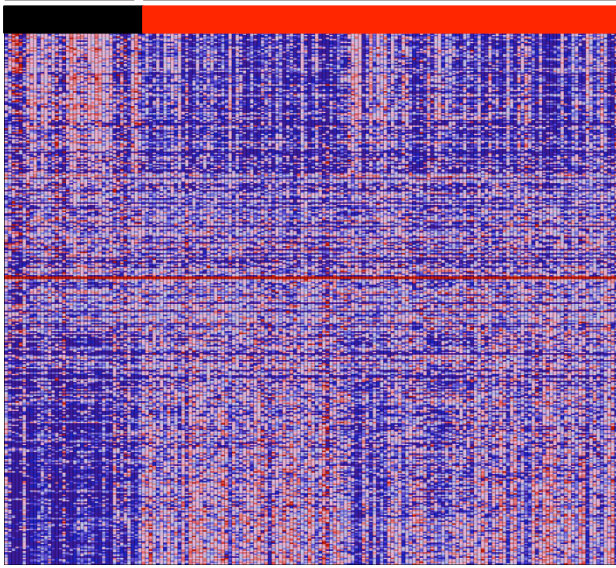


Figure 4.9: Transcriptome profile of *KRAS* wild-type and mutant tumours. (A) Heatmap showing contrasting wild-type and mutant samples. (B) Volcano plot demonstrating 391 significantly differentially expressed genes (Red; $|\text{Log}_2\text{FC}| > 1$ and $P < 0.01$)

A*KRAS* WT*KRAS* MUT**B***KRAS* WT versus MUT

Differentially expressed genes

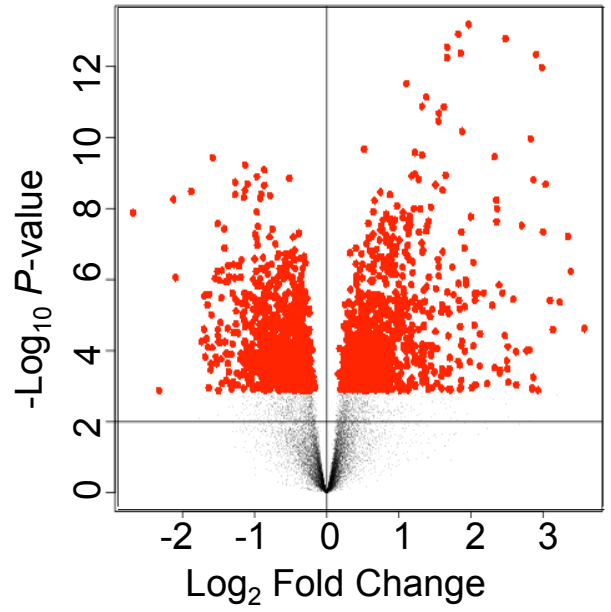
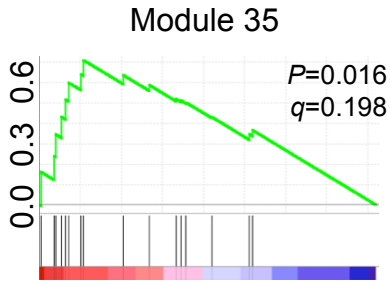
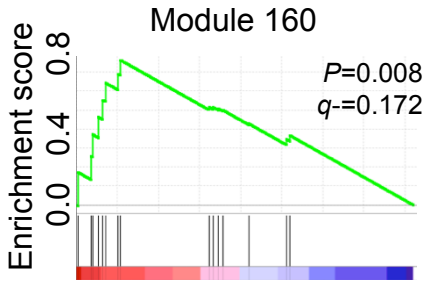
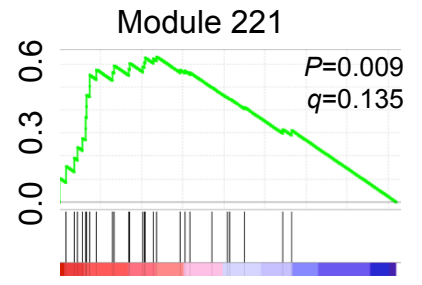
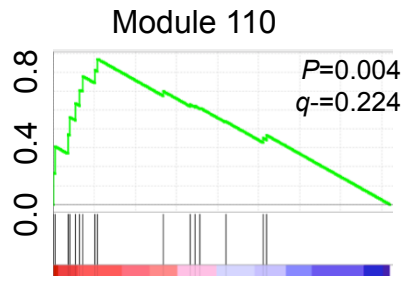
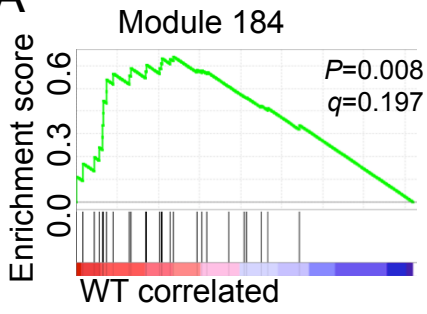
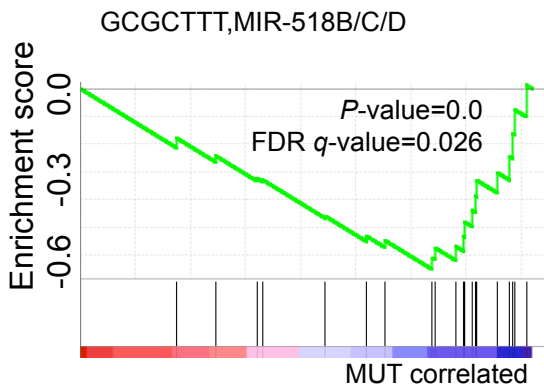


Figure 4.10: Gene set enrichment analysis for *KRAS* wild-type and mutant tumours in TCGA dataset. (A) 5 gene sets significantly enriched in the *KRAS* mutant tumours. (B) 2 gene sets significantly enriched in the wild-type tumours.

A**B**

KEGG GLYCOSAMINOGLYCAN BIOSYNTHESIS
CHONDROITIN SULFATE

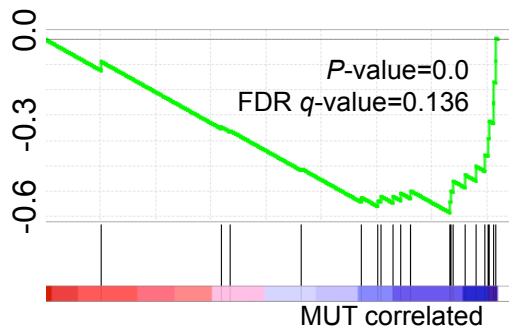


Figure 4.11: Transcriptome profile of tumours with and without a DNA repair pathway mutation (*BRCA1/2*, *PALB2*, *ATM*). Volcano plot demonstrating no significantly differentially expressed genes (Red; $|\text{Log}_2\text{FC}| > 1$ and $P < 0.01$)

DNA-repair MUT versus WT
Differentially expressed genes

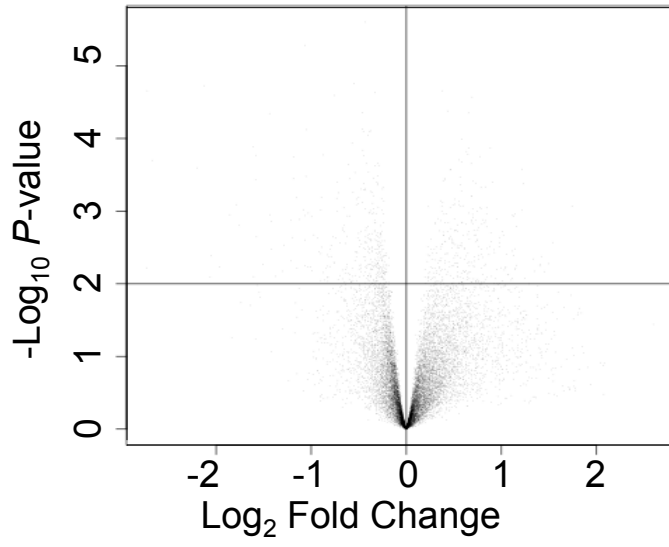
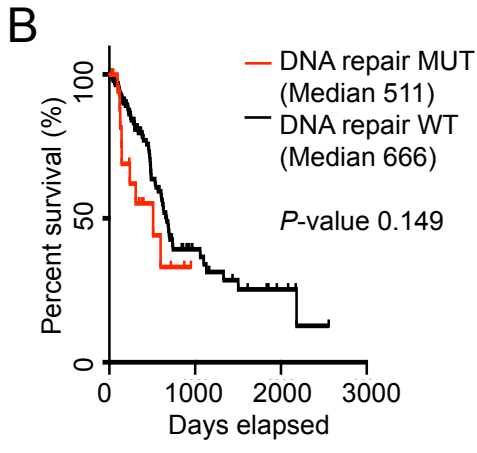
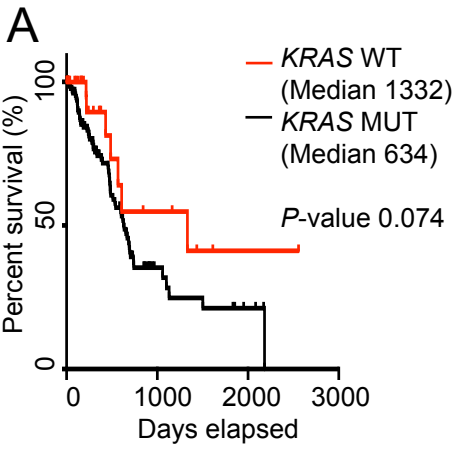


Figure 4.12: Overall survival of TCGA cohort, with and without molecular targets. (A) Kaplan-Meier analysis of *KRAS* wild-type compared to *KRAS* mutant tumours. (B) Kaplan-Meier analysis of patients with tumours positive for DNA repair pathway mutations, and those without a mutation.



Chapter 5: Using a novel patient-derived xenograft model to demonstrate efficacy of panitumumab in *KRAS* wild type tumours

One of the most important changes in oncology in recent times has been the acknowledgement of inter-tumoural heterogeneity, and the subsequent embrace of personalised therapies, however, clinical trials testing personalised treatments have proved difficult in PC. As demonstrated in Chapter 4, trials are limited by the low prevalence of potential targets for personalised medicine in patient tumours, as well as the previous inability to obtain genetic material early in the clinical course of disease, a result of the reliance on surgical specimens for this purpose. The second barrier has largely been overcome with the use of EUS FNA-derived genetic material, validated in Chapters 3 and 4. EUS FNA not only allows access to genetic material at the time of diagnosis, but also enables clinicians to include patients with metastatic disease. However, the paucity of patients with known targets remains problematic. A preclinical disease model addresses this problem, allowing for trials of personalised medicine against specific targets, without the need to recruit large numbers of patients. As discussed in Chapter 1, PDX models are well suited to study treatment efficacy for personalised medicine as they retain the genetic characteristics and histological architecture of the original tumour and allow expansion into large cohorts of identical tumours [65,184,185]. Therefore, here I demonstrate the utility of EUS FNA as a source of PC tissue for PDX generation.

With the knowledge that *KRAS* wild type tumours as a distinct, and relatively common tumour phenotype, I present the efficacy of the anti-EGFR therapeutic, panitumumab, in *KRAS* wild type and mutant PDXs. As mentioned in previous

chapters, *KRAS* wild type tumours may be amenable to anti-EGFR therapies such as panitumumab, as is the case with colorectal and lung cancers, and is thought to be due to the oncogenic mutation of *KRAS* causing aberrant signalling downstream of EGFR [34,35,104-106]. Therefore, in *KRAS* wild type disease, EGFR signalling can be blocked and therefore halt tumour growth signals driven by EGFR. However, in tumours where there is a *KRAS* mutation, these signals will persist regardless of the status of the upstream EGFR, which manifests clinically as resistance to anti-EGFR therapies.

5.1 Establishing a patient-derived xenograft using EUS FNA samples of PC

I used EUS FNA samples from 2 patients with confirmed PC and implanted these into NOD-SCID mice (Table 5.1). As shown in Figure 5.1A, haematoxylin and eosin staining of grafted tumours revealed these are highly cellular, with high mitoses and large, atypical nuclei. Immunostaining for epithelial cells using a pan-Cytokeratin antibody demonstrated that these are indeed epithelial cells, in keeping with PC (Figure 5.1B). Staining with an anti-human nuclei antibody demonstrated that these cells are of human origin and not an endogenous mouse tumour (Figure 5.1C). Finally, CD45 staining for immune cells was used to exclude lymphoma, which is known to commonly mistakenly grow in PDX models of gastrointestinal cancer (Figure 5.1D).

Together, these results demonstrate that my EUS FNA-derived PDX model reliably replicated human PC in terms of histological architecture and cytological cell content.

5.2 *KRAS* genotyping of PDX tumours

The great advantage of PDX as a pre-clinical disease model is the ability to trial personalised therapies against different phenotypes of PC. Therefore it is imperative that the grafted tumour possesses the same genetic profile as the original patient tumour. One of the PDX models was *KRAS* wild type, while the other PDX had a p.Gly12Val; c.35G>T mutation of the *KRAS* gene (Table 5.1). Importantly, these were consistent with the mutation status in gDNA isolated from original patient tumours and the grafted tumours.

5.3 Treatment with Panitumumab

To establish the effectiveness of anti-EGFR therapy in these two PC phenotypes (*KRAS* wild type and mutant), I expanded both PDXs into a larger cohort of mice. Each cohort consisted of 16 mice, and these were divided into four treatment groups: saline, gemcitabine monotherapy (chosen as a representative first-line chemotherapy agent used in PC), panitumumab monotherapy, and a combination of gemcitabine and panitumumab. The *KRAS* wild type tumours treated with saline all grew to a maximum volume (1000mm³) before the treatment course was completed, ranging from 14 – 21 days, with an average final tumour weight of 1.07 ± 0.08g. Notably, compared to saline treated controls, *KRAS* wild type tumours treated with panitumumab were significantly smaller in volume (day 14, $P < 0.05$, day 21 $P < 0.0001$) and final weight (0.19 ± 0.05g; $P < 0.0001$) over the experimental treatment period (Figures 5.2, 5.3). Similarly, gemcitabine treatment also significantly impaired tumour growth compared to control saline-treated PDXs, however this anti-tumour activity was less pronounced compared to panitumumab (day 14 and 21, $P < 0.05$;

day 28, $P < 0.01$). Combination therapy had similar effects on tumour growth as panitumumab monotherapy (Figures 5.2 and 5.3).

Conversely, in *KRAS* mutant tumours, panitumumab alone had no effect on tumour growth, which was comparable to the unimpaired exponential growth seen in saline-treated xenografts (Figures 5.2 and 5.3). Similar to *KRAS* wild type tumours, gemcitabine alone or in combination with panitumumab had a pronounced inhibitory effect on the growth rate of *KRAS* mutant tumours (Figures 5.2, 5.3), thus ruling out any synergistic effects between these drugs on PC tumours irrespective of their *KRAS* mutation status.

5.4 Changes in cell proliferation and cell death on treatment

To examine the treatment effects on cell proliferation, I performed immunostaining for the cell proliferation marker PCNA. PCNA staining was significantly reduced in panitumumab-treated *KRAS* wild type compared to saline treated controls, but no change was observed in the treated animals with *KRAS* mutant tumours (Figure 5.4A, B). This result is in concordance with the effect of the treatment on tumour growth seen in Figures 5.2 and 5.3.

I also measured changes to cell death rates for each treatment group using the apoptotic TUNEL assay. Somewhat surprisingly, tumours treated with saline had substantially increased rates of cell death despite faster growth rates (Figure 5.5A, B). The central part of the tumour is highly necrotic, with high cell death rates and large amounts of cellular debris, whereas the edge of the tumour has low rates of cell death, resulting in more positive staining in the larger saline tumours, with a more prominent necrotic core. This result is somewhat surprising given the higher growth

rate of tumours treated with saline compared to panitumumab for *KRAS* wild type disease.

5.5 Changes in EGFR signalling pathway activation

In light of these observations, I next assessed the impact of panitumumab treatment on the EGFR signalling pathway by performing Western blot analyses. As shown in Figures 5.6A, B, compared to saline treatment, panitumumab treatment alone resulted in reduced levels of phosphorylated (p) EGFR in both *KRAS* wild type and mutant tumours, albeit only statistically significant in the former. These data are consistent with the mode of action of panitumumab, which directly blocks the activation of the EGFR irrespective of the *KRAS* mutation status, and this manifests as a decrease in pEGFR. Interestingly, activation of the ERK1/2 MAPK pathway, which is associated with cellular proliferation, is significantly reduced in *KRAS* wild type tumours treated with panitumumab compared to saline (Figures 5.6A, B), which is consistent with the lower proliferative potential of these tumours observed on PCNA staining (Figures 5.4). By contrast, no changes were observed in the activation status of the cell survival pathway mediator, AKT (Figures 5.6A, B). Once again this is consistent with cell survival data shown in Figure 5.5, however, as mentioned previously, these data may be confounded by the presence of a necrotic core in saline treated tumours with rapid tumour growth rates.

Collectively, these *in vivo* data demonstrate that panitumumab is a highly effective agent for the treatment of *KRAS* wild type, but not mutant, tumours in this PDX model of PC. Furthermore, the reduced growth of these *KRAS* wild type tumours treated with panitumumab is consistent with the suppression of ERK MAPK signalling and tumour cell proliferation measured in these protein expression data.

5.6 Discussion

Overall, these data demonstrate that EGFR is a viable target for the subset of PC patients with *KRAS* wild type disease. In addition, these results also validate a novel pre-clinical disease model, a model that has the ability to test numerous therapies, and capture inter-tumoural heterogeneity specific to individual patients. Therefore this study also serves as a proof-of-principal experiment for future studies using a similar pipeline from phenotype discovery and characterisation, to treatment efficacy experiments *in vivo*. Therefore, this model is well suited to test therapies against targets for personalised medicine mentioned in Chapters 1 and 4, such as TLR2, the DNA-repair pathway and potentially rare targets such as *BRAF* mutations.

The most striking finding in this Chapter is the responsiveness of *KRAS* wild type tumours to panitumumab, when used as a monotherapy and in combination with cytotoxic agent, gemcitabine. Most importantly, I demonstrate that this treatment is having on target effects by showing reduction in the phosphorylation of EGFR and downstream signalling molecules, the effect of which leads to a reduction in cell proliferation and ultimately tumour growth. In addition, these experiments are performed on NOD-SCID mice, which are immune-compromised to facilitate tumour growth; therefore, the effect of these therapies are most likely directly on the tumour epithelium, rather than relying on an intact immune system.

Overall, although this experiment is only the result of one patient per *KRAS* mutation status, nonetheless the combination of these demonstrated on target effects and the fact that these results are congruent with what has been observed in other epithelial tumours, namely colorectal and lung cancers [34,35,104-106], is compelling evidence for targeted EGFR therapy in wild type *KRAS* PC. Of course, it is important

to note that in lung cancer it has recently emerged that there are problems with *KRAS* wild type tumours developing resistance to anti-EGFR therapies after several months. To combat resistance in non-small cell lung cancer, newer agents are used in combination, these are 3rd and 4th generation EGFR-inhibitors, in some cases these are used after resistance develops, in others these are used first-line as part of a combination therapy [186].

It is important to acknowledge the potential for this to occur in PC, therefore it is likely that panitumumab will be used in combination with cytotoxic agents or other anti-EGFR agents, with the aim to eliminate panitumumab resistant cells. In addition, although resistance may become an issue in PC in the future, the current survival outcomes in PC are such that developing resistance after a number of months may in fact still be an improved outcome for the majority of patients.

The evidence supporting a biomarker driven clinical trial targeting *KRAS* wild-type PC is mounting, recently Schultheis, et al [187] demonstrate that the addition of nimotuzumab (an anti-EGFR monoclonal antibody) to gemcitabine improved overall survival and progression free survival in patients with advanced (unresectable, locally advanced or metastatic) PC by 2.6 months ($P = 0.034$). The authors also tested for *KRAS* mutation status and show the effect on survival was greater in *KRAS* wild-type patients, where overall survival was extended to 11.6 months compared to 5.6 months ($P = 0.03$).

Once again, the advantage of using EUS FNA-derived tissue for xenograft development vastly increases the number of patients eligible for such studies. Unlike surgical resection specimens, which are routinely grafted into xenograft cohorts at large cancer centres in the United States, EUS FNA allows for patients who would otherwise be ineligible for these studies to be included. This makes the potential for xenografts to be developed for approximately four-fold more patients, which dramatically increases the power of these studies to identify rare tumour phenotypes.

It is also important to note, that PC often progresses before a PDX model can yield results on treatment efficacy, which may take up to six months. Therefore, once grafted, PDX models may not be useful for the donor, but for future patients, who have similar genetic profiles with specific targets. For example, both patients in this study died before the results of the panitumumab treatment experiment were complete. However, these results may lead to a clinical trial, where all patients are tested for *KRAS* mutation, and wild type patients will be enrolled in a panitumumab trial.

Therefore, a drawback of this model is the long time between engraftment and a treatment efficacy result. One methodology that can overcome this problem is organoid culture; where a patient sample can be grown *in vitro* in a three dimensional culture [188]. This culture can be more rapidly expanded and treated *in vitro* or implanted into an immune-compromised mouse for *in vivo* testing in an organoid-derived xenograft model. This culture involves stimulating all cells from the sample to grow, most importantly the stem cells, which then creates a microenvironment and tissue architecture representative of what is seen in human disease [188]. However, to stimulate stem cell differentiation the growth medium required must be rich in factors important for this process in the organ of origin, in this case human foregut differentiation. This medium has been estimated to cost \$7.50 per millilitre [189], which is prohibitive for many centres performing pre-clinical research, however, this may be feasible, once organoids have been validated for translational research and therefore provide clinical benefit.

In addition, although PDX models have indeed been demonstrated to predict oncological outcomes reliably [65,184,185], there are some inherent limitations to these models [190,191]. PDX models require expansion via passaging tumours through generations of animals, during this time it has been noted that there is some “genetic drift”, whereby the grafted tumour accumulates copy number alterations (CNA) due to the selection of specific clonal populations pre-existing in the tumour.

Therefore, after a number of passages and generations of PDX, the grafted tumour may resemble a clone of the original tumour that is not actually the dominant clone in human disease [190,191]. Therefore, PDX treatment experiments need to be performed as close to the original generation as possible, limiting the number of passages between the first engraftment and treatment.

Another interesting finding in this Chapter is the responsiveness both tumours demonstrate when treated with gemcitabine monotherapy, which does not reflect the behaviour of PC in human disease. This highlights a tendency of PDX models to over-estimate treatment efficacy, as human disease treated with gemcitabine has been shown to get a response in only 10% of patients and extend median survival to six months [14,15]. As mentioned in Chapter 1, there are inherent limitations with PDX models that cannot have a functioning immune system, lest they develop severe GvHD. With certain cytotoxic agents this is of minimal significance, however the EGFR pathway has been shown to be closely linked with the immune system and therefore therapies targeting this pathway may be impacted [192]. The role of EGFR in the immune system is multi-faceted and as such, EGFR-antagonists in clinical practice have significant off target adverse effects, but more importantly for this discussion, EGFR-antagonists may have different efficacy in cancer therapy with a functioning immune system and within the individualised immune profile of each patient. Once again, although this contributes to the *in vivo* efficacy of both panitumumab and gemcitabine, the use of positive treatment controls and untreated replicates for each PDX model helps interpret these results. This is why gemcitabine is an important control in PC PDX experiments; it acts as a standard therapy to measure experimental treatments against. As such, the effect that the model is having on treatment efficacy can be roughly estimated by observing the difference between saline treated and gemcitabine treated tumours. Importantly, in my experiment the panitumumab was significantly more effective than gemcitabine alone in *KRAS* wild type tumours.

In this Chapter I have presented a novel target for PC in *KRAS* wild type disease, which responds exceptionally well to panitumumab treatment. This treatment could be used in a clinical trial in the future as part of a combination therapy with gemcitabine, or as a second or line agent it might be used as a monotherapy. Furthermore, I have validated novel pre-clinical disease model that accurately replicates human disease at a histological and a molecular level, and this can be used to trial emerging therapies for PC and rapidly translate into clinical trials.

5.7 Tables and figures

Table 5.1. Clinicopathological characteristics for two PC patients used for patient-derived xenografts.

Characteristic	KRAS wild type	KRAS mutant
Sex	Male	Female
Age (Range)	47	52
Survival (Months)	13	5
First line treatment	FOLFIRINOX	Gem + nab-Paclitaxel
Response to initial treatment	Partial response	Progressive disease
Ca 19-9 (At diagnosis)	127	1762
TNM Staging	IV (Liver metastases)	IV (Peritoneal metastases)
Site	Pancreatic neck	Pancreatic head
Pancreatitis history	YES	YES
KRAS mutation status	No mutation	p.Gly12Val; c.35G>T

Figure 5.1: Representative immunostaining images on two PDX (one *KRAS* wild-type and one *KRAS* mutant) displaying H & E stain (A), pan-cytokeratin stain (B), anti-human nuclei stain (C), and CD45 stain (D). Scale bars = 50 μ m

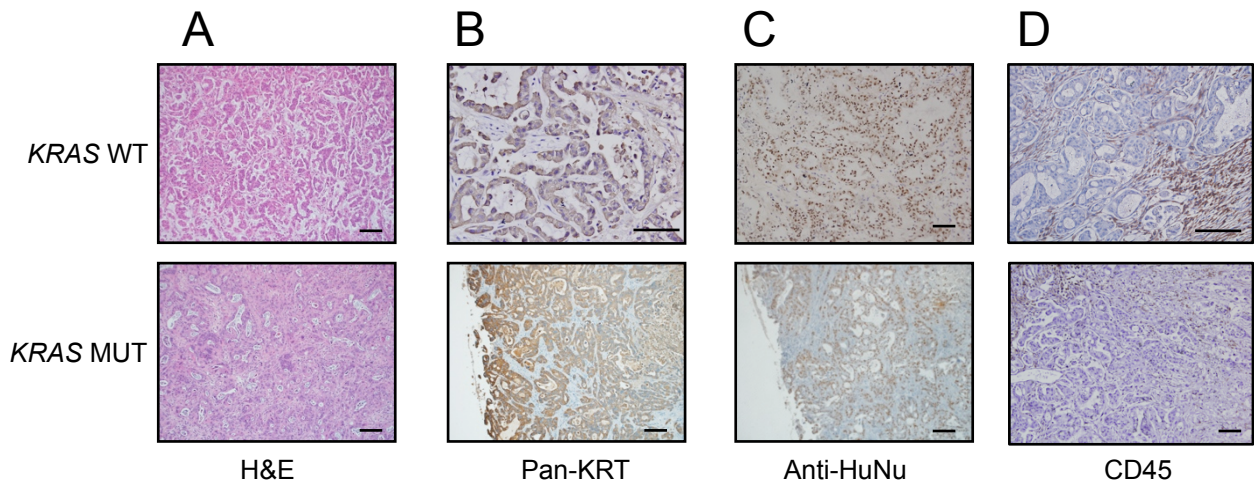


Figure 5.2: Differential responsiveness of EUS FNA-derived *KRAS* wild-type (WT) and *KRAS* mutant (MUT) PDXs to anti-EGFR therapy. Treatment of *KRAS* WT (A) and MUT (B) PDXs with panitumumab (Pan), gemcitabine (Gem) and combination therapy (Pan + Gem), along with saline (Sal). Shown are tumour volumes measured weekly throughout the treatment schedule. $n = 4$ mice per treatment group. Data are expressed as the mean \pm SEM. Statistical significance presented for panel (A) *KRAS* WT: $**P < 0.01$ and $***P < 0.001$ Sal-treated versus Pan-treated tumour groups, and $\#P < 0.05$ and $##P < 0.01$ Gem-treated versus Pan-treated tumour groups, at the corresponding time points. Panel (B) *KRAS* MUT: $*P < 0.05$ Sal-treated versus Gem-treated tumour groups, and $\#P < 0.05$ and $##P < 0.01$ Pan-treated versus Gem-treated tumour groups, at the corresponding time points. Panel (C), $*P < 0.05$, $***P < 0.001$, and $****P < 0.0001$.

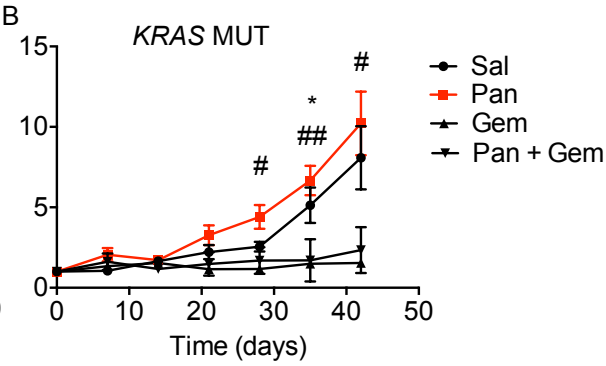
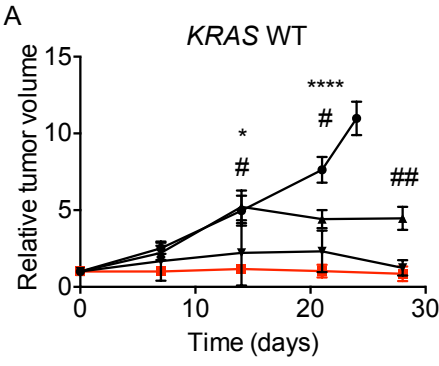


Figure 5.3: Differential responsiveness of EUS-FNA-derived *KRAS* wild-type and *KRAS* mutant PDXs to anti-EGFR therapy. Treatment of *KRAS* WT (A) and MUT (B) PDXs with panitumumab (Pan), gemcitabine (Gem) and combination therapy (Pan + Gem), along with saline (Sal). Shown are tumour weights and photographs of tumour size. n = 4 mice per treatment group. Data are expressed as the mean \pm SEM, * P <0.05, *** P <0.001, and **** P <0.0001.

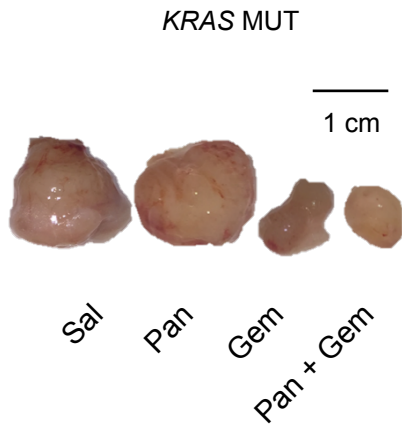
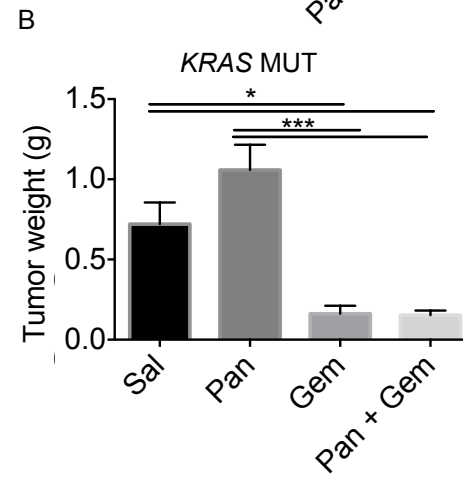
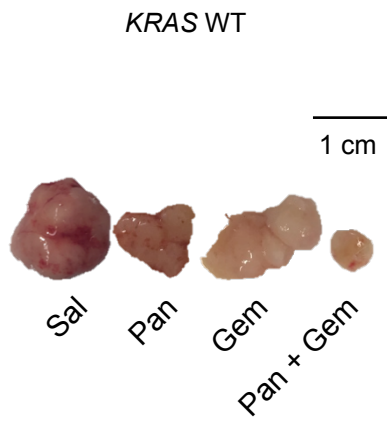
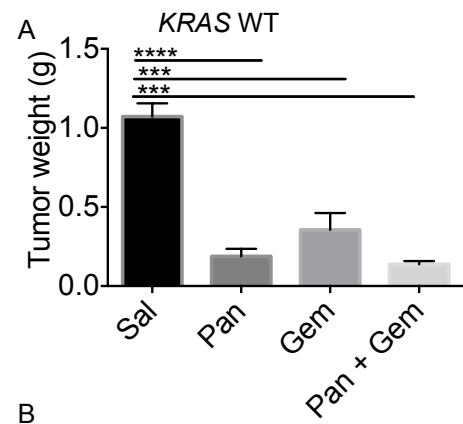


Figure 5.4: Reduced cellular proliferation in panitumumab-treated *KRAS* wild-type PDX tumours. (A, B) Representative immunostaining for PCNA with associated quantified data for (A) *KRAS* wild-type (WT) tumours and (B) *KRAS* mutant (MUT) tumours treated with saline (Sal) or panitumumab (Pan). Scale bars, 100 μ m. In (A), arrows point to positively-stained cells. Data are presented as mean \pm SEM from n = 4 samples/group. *** P <0.001.

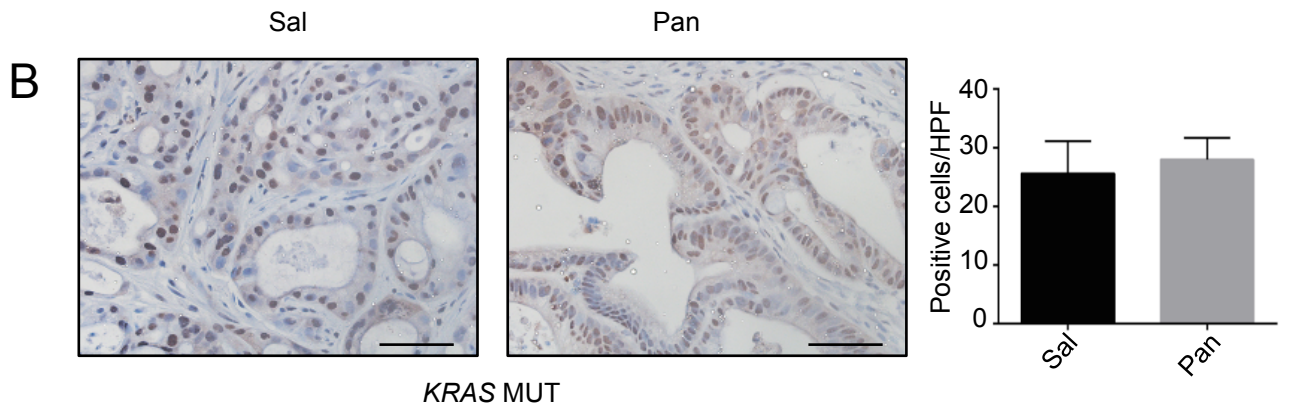
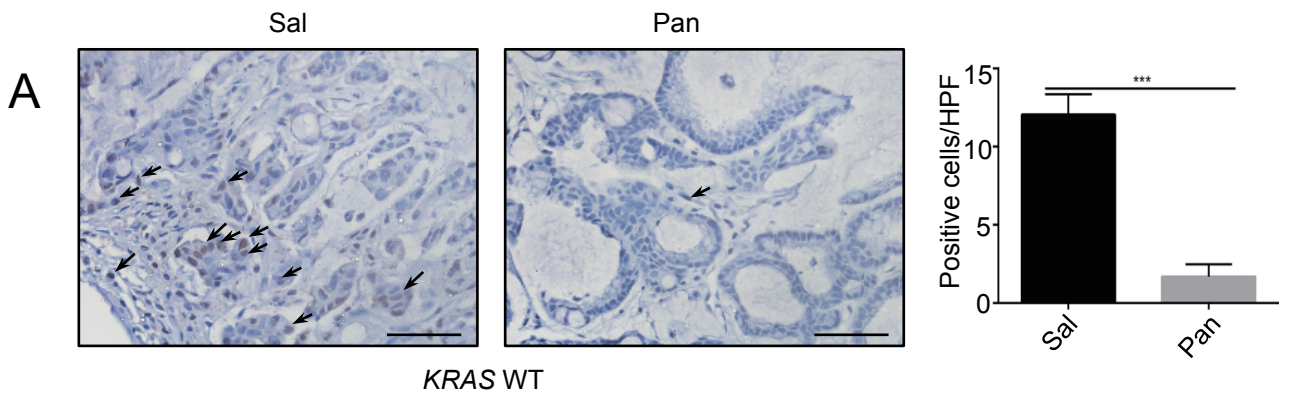


Figure 5.5: TUNEL staining for treated PDX tumours.(A, B) Representative immunostaining for TUNEL with associated quantified data for (A) *KRAS* wild-type (WT) tumours and (B) *KRAS* mutant (MUT) tumours treated with saline (Sal) or panitumumab (Pan). Scale bars, 100µm. In (A), arrows point to positively-stained cells. Data are presented as mean ± SEM from n = 4 samples/group. ** $P < 0.01$.

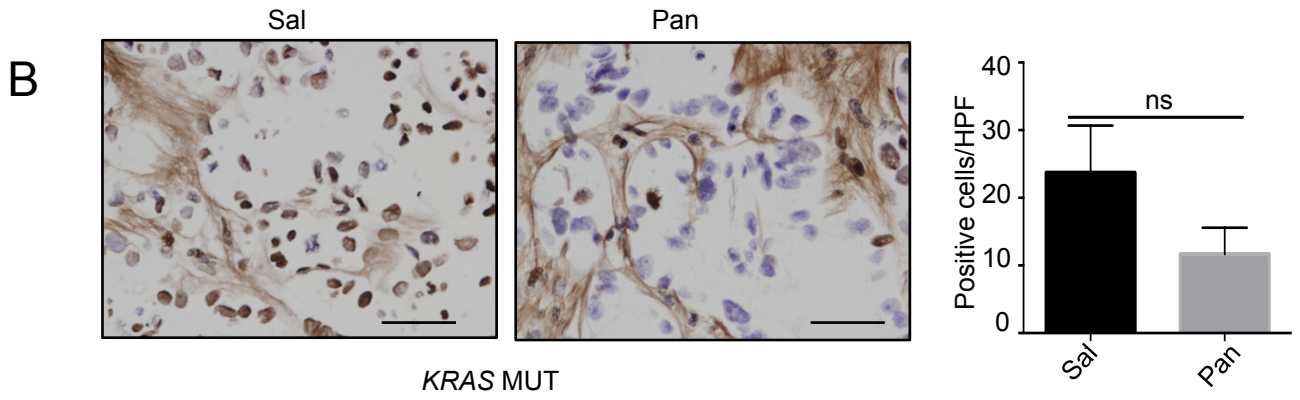
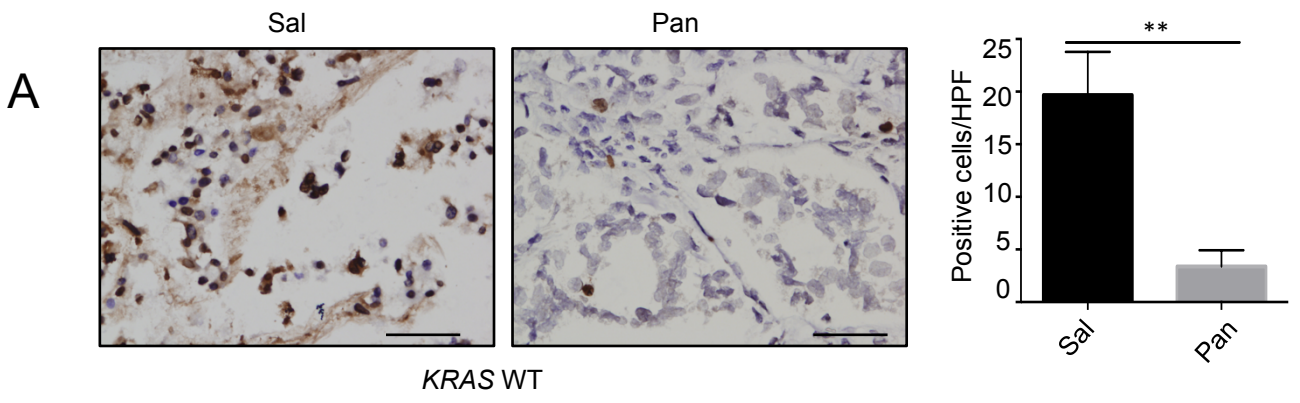
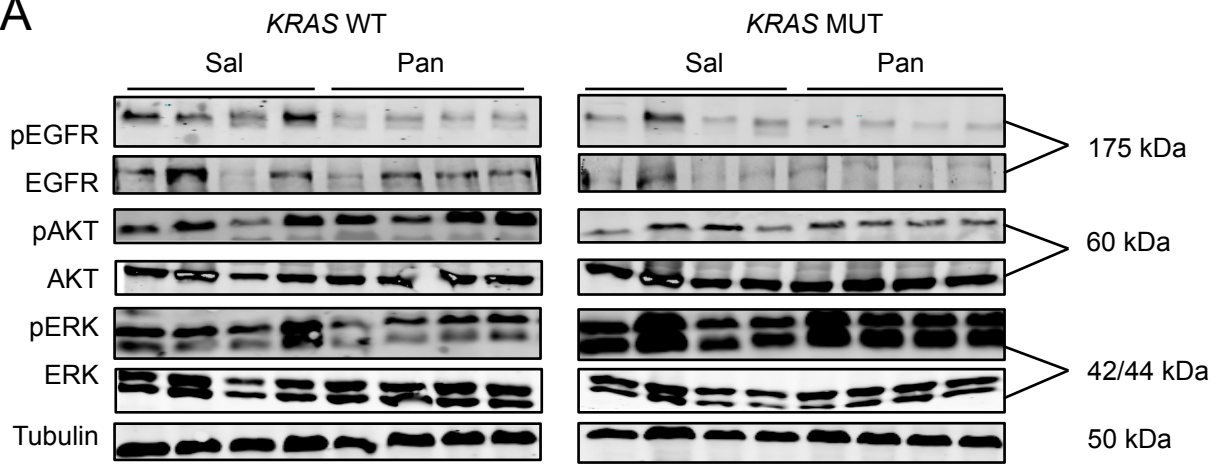
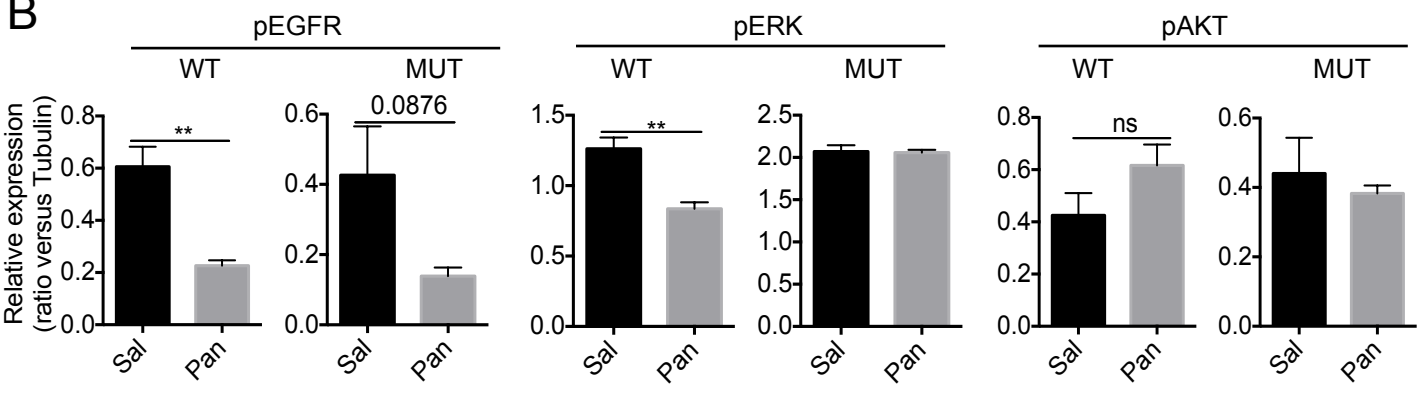


Figure 5.6: Western blots with the indicated antibodies for EGFR signaling pathways in protein lysates from treated tumours (A). Each lane represents a single xenograft tumour. (B) Semi-quantitative densitometry analyses of the blots shown in (A). Data presented as mean \pm SEM from n = 4 samples/group; ** P <0.01.

A**B**

Chapter 6

6.1 Summary

The aims of this thesis were to validate the use of EUS FNA-derived material for genetic studies and subsequently to explore its application to precision medicine for PC patients.

In Chapter 3, I successfully demonstrated that EUS FNA can provide a reliable source of high quality gDNA and RNA, and that this genetic material is indeed of tumoural origin. This addresses concerns over the potential for cell contaminants within EUS FNA samples [36,41-45] and allows future genetic studies to include patients who are ineligible for surgery and therefore have been excluded from such studies until now [5,13]. Importantly, as this is one of the first studies to use EUS FNA-derived RNA, I presented various approaches to optimise the process of extracting genetic material from these samples.

In Chapter 4 I used EUS FNA-derived genetic material to explore targets in personalised medicine for PC. This chapter presents the first comparison of primary PC tumours from patients with localised and metastatic disease, and surprisingly, showed no difference in transcriptome profile of these two clinical phenotypes. Using TCGA datasets (clinical, exomic and transcriptomic data) to explore the prevalence of personalised therapy targets, and the differences between patients with and without these targets, I was able to show that *KRAS* wild type disease is indeed a distinct phenotype of PC, in terms of transcriptome profile and clinical features.

In Chapter 5, I further expand the use of EUS FNA samples to generate a PDX, a pre-clinical model that is well suited to study personalised medicine. This provides a pre-clinical disease model that reflects the individual characteristics of the

patient from which the PDX was generated. Using this model I tested the efficacy of panitumumab, an anti-EGFR therapy, in a *KRAS* wild type PDX and in a *KRAS* mutant PDX. This demonstrated that the *KRAS* wild type had an exceptional response to panitumumab, whereas the mutant had no response. This result provides strong supporting evidence for the use of panitumumab in a clinical trial for patients with *KRAS* wild type disease.

Overall, my thesis presented a pre-clinical research methodology that allows for the identification of potential genetic targets using *in silico* analyses and then to measure the treatment efficacy of targeting these phenotypes in a personalised pre-clinical disease model. Indeed, my studies have shown that one such target for personalised medicine is *KRAS* wild type disease, and that this should be further investigated in clinical trials.

6.2 EUS FNA in molecular medicine

The majority of patients with PC will not be candidates for surgical resection and EUS FNA will often be the only means of obtaining tissue to establish a pathological diagnosis. My thesis serves to highlight the potential role of EUS FNA in personalising therapy. I show that EUS FNA is viable as a source of tissue for isolating genetic material to detect targets, and therefore direct precision medicine. Also, EUS FNA-derived tissue can be used to generate PDX to demonstrate treatment efficacy for novel targeted therapies. Although EUS FNA has been used to provide tissue for the genetic analysis for PC and other cancers, the clinical utility of this technique has been hampered by concerns about low tissue quantities leading to a suboptimal yield of genetic material, as well as sample contamination with non-malignant cells [36,41-45]. Nonetheless, the inherent advantage of EUS FNA is the ability to sample locally advanced and metastatic tumours, which are unsuitable for

surgical resection, giving clinicians the ability to obtain tissue, which would be otherwise unavailable [5].

Data from Chapter 3 shows that EUS FNA samples are highly epithelial, with minimal contaminating cell types, and indeed EUS FNA-derived DNA reliably detects oncogenic *KRAS* mutations. However, the potential of EUS FNA sampling to obtain insufficient cellular material remains a concern, and in diagnostic studies, the sensitivity of EUS FNA is 85% [52,174-181]. Therefore, the use of EUS FNA to obtain tissue for personalised medicine could mean that up to 15% of patients will not have an adequate sample to enable personalised medicine. However, there are ways to maximise the diagnostic yield of EUS FNA: increasing the number of “passes” (times the needle is inserted into the lesion and cells aspirated); the use of onsite cytology to confirm sample cellularity; and having an experienced operator [52]. Furthermore, it is possible that the genetic material obtained from procedures that did not provide a cytological diagnosis might be sufficient, in the future, to provide a genetic diagnosis of cancer. This could further improve the sensitivity of this technique and avoid the need for repeat procedures to establish the diagnosis. However, EUS FNA, unlike surgery, can be more readily repeated for re-biopsy, and in some cases this may be warranted to ensure personalised therapy is available. Finally, data presented in Chapter 3 shows that the use of a large calibre needle could increase genetic yield, although these needles are often more difficult to manipulate during endoscopy especially in the duodenum, and therefore may not be appropriate in all cases.

As mentioned in Chapter 1, several studies have attempted to combine genetic analyses (*KRAS* mutation) and cytology to improve diagnostic accuracy of EUS FNA [41,42,46-51]. These studies show a slight advantage when combining *KRAS* mutation detection with cytology; however, this advantage was not substantial enough to translate into clinical practice. Importantly, these studies, with my own data presented in Chapter 3, demonstrate that *KRAS* mutation is reliably detected in EUS

FNA-derived gDNA, and therefore, this is an accurate means of obtaining tumoural gDNA.

Together, this shows that EUS FNA can indeed be used to direct therapy based on individual tumour molecular profiles, as EUS FNA can reliably detect mutations (such as *KRAS*) and measure gene expression.

6.3 Pre-clinical disease models for personalised medicine in PC

In Chapter 5 of my thesis I further expand the utility of EUS FNA to perform both molecular analyses and establish a PDX from EUS FNA-derived tissue. As discussed in Chapter 1, there are distinct advantages to using PDX models for personalised therapy experiments, such as capturing inter-tumoural heterogeneity and performing personalised therapy trials for individual tumours. Once again, for PC it is important that PDX are able to be generated from EUS FNA samples, rather than relying on surgical resection specimens, which would severely limit the ability to capture patients with rare disease variants (such as *BRAF* mutation, which occurred in 4/166 TCGA patients). However, an unexplored area that remains is the use of organoid culture which could be employed to screen drugs in a high throughput preclinical setting to predict responsiveness of tumours with a particular molecular profile for personalised therapy trials in PC. This would also allow the capture and modelling of disease variants and the demonstration of treatment efficacy for personalised therapies in all disease phenotypes.

Organoid culture is a model in which cells are isolated from human (or murine) organs and placed in an environment that provides the conditions whereby cells can self-organise into structures (organoids) that closely models their native state [80] (Figure 6.1). This allows replication and growth of stem cells and differentiated cells to create a heterogeneous mix of cells that resemble that seen in normal (or neoplastic)

tissues. Cells are embedded in an extracellular matrix and supplemented with conditioned media containing growth factors specific to that seen in the pancreas. This stimulates stem cells to differentiate into pancreatic cells and the already differentiated cells to proliferate, whereby neoplastic cells proliferate more rapidly than normal cells [188]. Organoids have also proved suitable for xenograft implantation, which allows for treatment experiments and cell growth assays to occur *in vitro* and *in vivo* for each tumour [80,188]. In addition, organoids may address a key shortcoming of PDX models, which is the time taken between obtaining the biopsy and developing a useable model system. Generating a PDX takes months for the graft to take, then further months to passage the grafted tumour into a treatment cohort (at least 10 mice), then a minimum of 2 months for the treatment experiment itself. In PC, the majority of patients with disease that is not amenable to surgical resection may well have expired as a result of disease progression by this time, and therefore, the results of these experiments are likely to be relevant only to subsequent patients who have tumours with similar molecular profiles (e.g. *KRAS* wild type tumours). However, using personalised models has the potential to allow these results to inform treatment of the patient, if the time from biopsy to result can be reduced. Organoid culture is much faster and with cultures being passaged approximately weekly, a cohort of organoids for therapeutic testing may be achievable in a much shorter timeframe.

One limitation of organoids is that the media required for culture is designed to stimulate stem cell differentiation and proliferation and this is expensive. Using the methods described by the Clevers laboratory [193], the cost of the media will be above \$7.00 per millilitre [194]. Another limitation is that organoids do not allow for the investigation of the role of the immune system in PC, in the same way that PDX require immune-compromised mice to facilitate tumour engraftment. Furthermore, there are currently only a limited number of reports demonstrating the feasibility of this technique using EUS FNA as the source material [80,188], therefore, successful

engraftment rate, tumour histological architecture and response to therapy are not validated yet.

Overall, both the PDX disease model and organoid culture of PC have the potential to further expand the use of EUS FNA to characterise both treatable tumour phenotypes of PC and to test the treatment efficacy for novel personalised therapeutics. However, the main limitation of both models is the absence of a functioning immune system, therefore future studies may include the use humanised mouse models that can reconstitute the immune system. These models use immune-compromised mice (e.g. NSG mice) and irradiation to completely eliminate the endogenous immune system before implanting human bone marrow-derived macrophages or isolated CD34+ T-cells to re-constitute the immune system with human cells [99-101]. These *in vivo* technologies have been utilised to study the pathophysiology of malignancy and therapeutic trials [100,195], as well as examining the role of the immune system in organ transplantation (xenotransplantation) [196,197]. The advantage of this type of model is that an intact immune system more accurately reflects the true human disease, but it also allows researchers to test immunomodulating therapies.

In addition, this has the potential to allow a fully personalised model of disease, where a patient could donate tumour samples as well as bone marrow that could be used to re-constitute the animal's immune system with the same patient's immune cells. The tumour would then grow in an environment that closely matches to that seen in the patient. This might more accurately predict responsiveness to therapy, especially for immunomodulating therapies.

6.4 *KRAS* wild type disease and panitumumab treatment

Using the PDX model and a pre-clinical trial of personalised therapy, I presented data in Chapters 4 and 5 to suggest that *KRAS* wild type is a phenotype of PC that can be treated with anti-EGFR therapy. As mentioned previously, *KRAS* wild type disease has been successfully targeted in other malignancies, and as such, this is an appealing target for PC. A new clinical trial has been started as a result of my work; whereby patients are being screened for *KRAS* wild type tumours using EUS FNA-derived DNA, so that those with *KRAS* wild type disease can be selected for treatment with panitumumab as second-line therapy.

In addition, a recently published trial using another EGFR antagonist, nimotuzumab, in combination with gemcitabine retrospectively examined *KRAS* mutation status for enrolled patients [187]. Schultheis, et al show that *KRAS* wild-type patients who received combination therapy responded significantly better compared to those with *KRAS* mutant tumours, overall survival was 11.6 months compared to 5.6 months respectively.

These trials reinforce that personalised therapy is an important endeavour, especially for PC, where treatment is currently failing to make substantial improvements in patient outcomes for the majority of patients. However, as mentioned in Chapter 1, personalised therapy trials in PC are extremely difficult; hampered by the fact that most targets occur at a low prevalence and patient survival is usually extremely short. The advantages of this trial are the simplicity of only investigating one target (*KRAS* wild type disease) and the use of EUS FNA to increase the number of patients that can be screened. One of the potential disadvantages of targeting *KRAS* wild type disease, is that one is looking for the absence of a mutation, which means that sampling error (failing to obtain true tumour genetic material) could lead to false negative results. To address this, a panel of known oncogenic mutations will be tested

alongside *KRAS*. Only those *KRAS* wild type patients with other oncogenic mutations will be deemed to have *KRAS* wild type disease.

Overall, although my results demonstrate that *KRAS* wild type disease is a viable potential target for personalising cancer therapy, there are limitations with the pre-clinical model used. The fact that my pre-clinical experiments only involved one *KRAS* wild type PDX and one mutant PDX mean that these results need to be further substantiated either in clinical trials or by increasing the patient numbers in pre-clinical PDX experiments. In addition, in Chapter 1, I alluded to the fact that PDX models have a tendency to over-estimate treatment effects, which is made evident by the data presented in Chapter 5, where I show that both the *KRAS* wild type and mutant xenografts responded to gemcitabine, whilst in clinical practice, although gemcitabine can extend median survival to 6-7 months (from 3-6 months), it rarely induces remission [5,13-15]. Improving the accuracy of *in vivo* models by using organoids and humanised mice, as discussed previously, may enhance the ability to model the tumour microenvironment by culturing the non-tumour cells via stem cell propagation and re-constituting a human immune system.

Taken together, my thesis has provided the foundation to establish a clinical trial examining the efficacy of panitumumab in *KRAS* wild type PC. Whether this treatment strategy will be effective in the clinic, however, remains to be demonstrated.

6.5 Novel targets for personalised therapy

As mentioned in Chapter 4, there are several potential tumour phenotypes that have been effectively treated with targeted chemotherapy in other malignancies, and these may be amenable to targeted therapy in PC patients. Using my model in combination with the methods described and validated in Chapters 3 and 4 would enable the detailed characterisation of such phenotypes in PC and allow for pre-

clinical trials of targeted therapy, along the lines of my results suggesting that panitumumab is effective in *KRAS* wild type disease. Using these methods and newly established infrastructure at Monash Health (Monash Surgical Oncology Biobank), we could now potentially offer molecular profiling to all patients undergoing EUS FNA for suspected PC. This could enable us to detect those patients with tumours that have a particular target of interest (e.g. *BRAF* mutation) and to demonstrate, in a preclinical model, if such personalised therapy is likely to be effective. This can then be rapidly translated into a clinical trial, as demonstrated by initiation of the aforementioned “Panitumumab in *KRAS* wild type pancreatic cancer trial” currently underway at Monash Health.

Furthermore, the ability to capture all patients who undergo EUS FNA compared the minority of patients who undergo pancreatic resection, enhances efforts such as these biobanks and the national and global efforts to capture clinical and molecular data from PC.

Within these datasets, identifying new targets is not restricted to those that have been successfully treated in other malignancies, and as such, work has begun to characterise novel targets in PC for personalised therapy. Indeed, our model has garnered interest for the testing of novel targets from overseas academic and industry collaborators, with potential targets for cancer therapy in the preclinical testing phases as described below.

My results validate techniques that can be used as the foundation for an exciting area of novel biomarker discovery, as well as treatment efficacy experiments using *in vivo* testing.

6.6 Targeting inflammation in PC

Of particular interest to our laboratory is the role of the immune system and dysregulated inflammation in tumourigenesis and response (or resistance) to anti-cancer treatments. The association between inflammation and cancer is well founded [84,87,198]; although this is particularly relevant in PC, where chronic inflammation leads to a non-invasive precursor lesion, PanIN, which can progress to PDAC [89-93]. PanIN has well-defined stages of progression (Figure 6.2), and these are based predominantly on histological appearance, and secondarily on the genetic alterations observed [94-96]. At a 'Pancreatic Cancer Think Tank' in 1999 a classification for these precursor lesions was defined, and Hruban et al published a progression model of PDAC. This model outlines how normal pancreatic epithelial DNA undergoes activating point mutations in oncogenes (e.g. *KRAS*) and inactivating mutations in tumour suppressor genes (e.g. *TP53*) to promote the progression to PanIN and ultimately invasive PDAC [95,96]. Although the link between the immune system, chronic inflammation and PC is established, this is something that has not been exploited for therapeutic purposes. There is some potential for specific pathways to be targeted with therapies that may improve outcomes for patients.

One target of promise has recently emerged in toll-like receptor (TLR) 2. TLR2 is a pattern recognition receptor which acts as a critical sensor of the innate immune system to trigger the inflammatory response to cell damage products, extracellular matrix, inflammatory mediators and oxidised lipids [199]. The diverse nature of ligands recognised by TLR2 is facilitated by its formation of heterodimers with TLR1 or TLR6 [199]. TLR2 signalling involves both the adaptor proteins Myeloid differentiation primary response gene 88 (MyD88) and Mal (also called TIRAP), which lead to the activation of nuclear factor kappa B (NF- κ B), phosphoinositide-3-kinase (PI3K)/Akt, as

well as p38, extracellular-regulated kinase (ERK) and c-Jun N-terminal kinase (JNK) mitogen-activated protein kinase (MAPK) pathways [199] (Figure 6.3).

In 2010 Morse, et al [200] investigated the gene and protein expression of cell surface targets, to identify novel therapeutic targets in PC. Comparing normal pancreas and PC tumour samples, the authors identified markers that were frequently expressed on tumour samples, but not expressed in normal tissue. TLR2 was identified as a marker that was absent from the cell surface of normal pancreas epithelium and expressed in tumour samples. Using tissue microarray the authors showed TLR2 is expressed in 98% of PC tumour samples and highly expressed in 70% of these (N = 42), whereas high expression was only observed in 2% of normal pancreas (N = 16). Together, this shows that TLR2 is a potential tumour specific biomarker in the pancreas, however, the expression of TLR2 on normal immune cells, other tissue types, prohibit the use of this clinically and increase the potential for “off-target” effects for any TLR2 targeting therapies.

As a therapeutic target TLR2 remains viable since our laboratory has shown that TLR2 blockade can suppress gastric cancer cell growth (see below). [201,202].

To date, limited studies have attempted to enhance the anti-tumour immune response initiated by TLR2 using TLR2-agonists. One such study used an orthotopic xenograft model using the cell line Panc 02 implanted into C57 Black 6 mice treated with macrophage activating lipopeptide (MALP) 2 [203]. This resulted in an increase in T lymphocyte and natural killer cell infiltration of the tumour, and prolonged survival when compared to untreated mice and mice treated with gemcitabine monotherapy. However, the effect on tumour burden and growth was not well documented as this study focused on survival as the primary endpoint. Tumours were measured *in situ* via trans abdominal ultrasound, and upon reaching 6mm in the longest dimension the animals were sacrificed. Therefore, the animals with shorter survival indeed had faster growing tumours, but it is not clear what the pattern of growth was or if other survival factors impacted on these data. However, the histology presented in this study

suggests that TLR2 agonists can improve the host anti-tumour immune response and therefore may be an effective immune-modulating therapy to treat the PC. Unfortunately, these experiments cannot be replicated using human cell lines or the current PDX model as they require an immune-competent host, however, as mentioned previously, humanised models may help overcome this limitation.

Subsequently a small Phase I/II clinical trial was performed on 10 patients who underwent incomplete pancreatic resection for tumours that were not fully resectable [204]. MALP 2 was injected intra-tumourally at the time of surgery and patients were treated with ongoing adjuvant gemcitabine. These 10 patients had a median survival of 9.3 months, which in 2007 was remarkably high compared to available medical treatments. However, it is unclear how a “de-bulking” procedure, such as incomplete pancreatic resection, impacts survival. In addition, these patients received a range of different treatments before enrolling in the trial: 4 patients had received no treatment; 2 had undergone intra-operative radiotherapy; 2 had undergone intra- and pre-operative radiotherapy, 2 had undergone intraoperative radiotherapy and pre-operative radio-chemotherapy; and 2 received chemotherapy then radiotherapy pre-operatively and intraoperative radiotherapy. Furthermore, post-operatively (i.e. during the trial) patients were treated with gemcitabine with or without radiotherapy. Together, this makes it impossible to determine the factors that influence patient outcomes, especially overall survival, which ranged from 1.6 months to 38 months. Moreover, there was no attempt to investigate tumoural factors (e.g. TLR2 expression) that may influence individual patient response.

Interestingly, in some cancers TLR2 may in fact act to facilitate tumour growth [205,206], and as such, attempts to inhibit TLR2 signalling, rather than augment it, may be beneficial to patient outcomes. On this latter point, it is noteworthy that the humanised anti-TLR2 mAb, OPN-305, has recently been assessed for its safety and tolerability in a phase I trial on healthy individuals [207]. Our laboratory has

demonstrated successful inhibition of TLR2 using OPN-305 and as a result a reduction in tumour growth in human gastric cell line-derived xenografts [201].

The specific over expression of TLR2 in PC tumour tissue, but the absence of TLR in normal pancreas and the *in vivo* data on cell-line derived xenografts suggest TLR2 may play a role in PC. However, it remains unclear whether TLR2 is beneficial and important for mounting an anti-tumour response from the host immune system, or, whether TLR2 is in fact in promoting a pro-tumourigenic microenvironment through aberrant over-activity. My pre-clinical disease model is well suited to capture patients with tumours that have high and low TLR2 expression levels and treat these tumours with TLR2 antagonists, such as OPN-305 and TLR2 agonists, such as MALP 2. This experiment, in combination with *in silico* analyses shown in Chapter 4 would allow the complete molecular characterisation of a tumour phenotype dependent on TLR2 signalling as well as provide data on treatment efficacy. Ultimately, this highlights the potential to use these experimental methods I have validated to explore new targets and expand the number of potentially treatable phenotypes in PC.

6.7 Conclusion

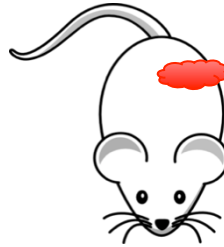
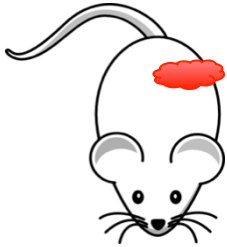
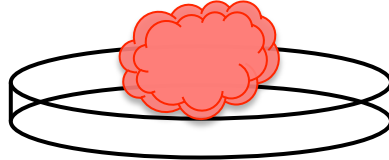
In conclusion, my studies have validated the use of EUS FNA to obtain tissue samples that are suitable for molecular characterisation of tumours and to develop a novel pre-clinical disease model for PC. Importantly my studies provide a substantial advance in the field of personalised therapy for PC, where advanced disease stage at presentation, short survival, and wide inter-tumoural heterogeneity has hampered efforts to implement personalised therapy clinical trials. Furthermore, these methods provide a reproducible experimental prototype, whereby therapeutic targets can be identified in the molecular profile of pancreatic tumours and treatment efficacy can be established using *in vivo* trials. The results of these experiments have already yielded

a clinical trial of personalised medicine in PC, which serves to highlight the potential of pre-clinical trials of personalised therapy to rapidly translate into clinical results.

Figure 6.1: A flow diagram demonstrating the potential utility of personalised pre-clinical disease models that capture inter-tumoural heterogeneity. EUS FNA or surgical resection specimens can be used for patient-derived xenograft or organoid culture, these methods allow for *in vivo* (or *in vitro*, if organoid is not grafted) testing of various treatments available to the patient, then the most efficacious of these can be used for the patient.



EUS-FNA or tumour pieces from surgery can be used for xenograft or organoid culture



A personalised *in vivo* trial of available treatments can be applied to each patient's tumour

Treatment A

Treatment B

Treatment C

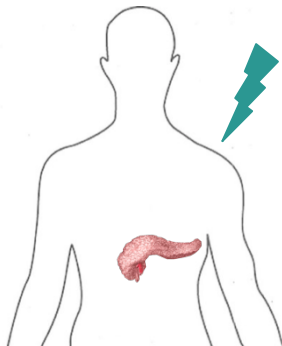
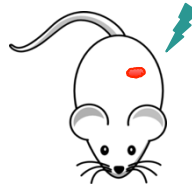
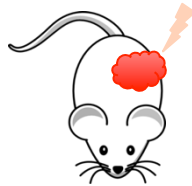
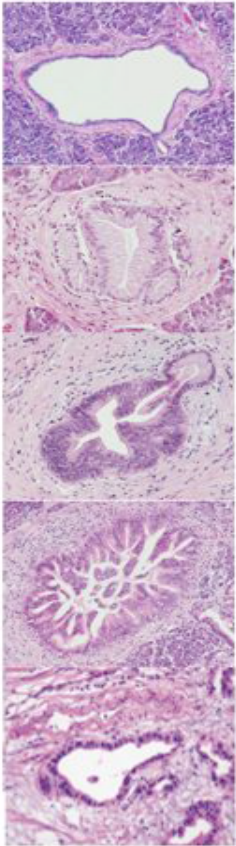


Figure 6.2: Pancreatic cancer progression model from normal pancreatic epithelium through to intra-epithelial neoplasia and adenocarcinoma.



Normal pancreatic duct

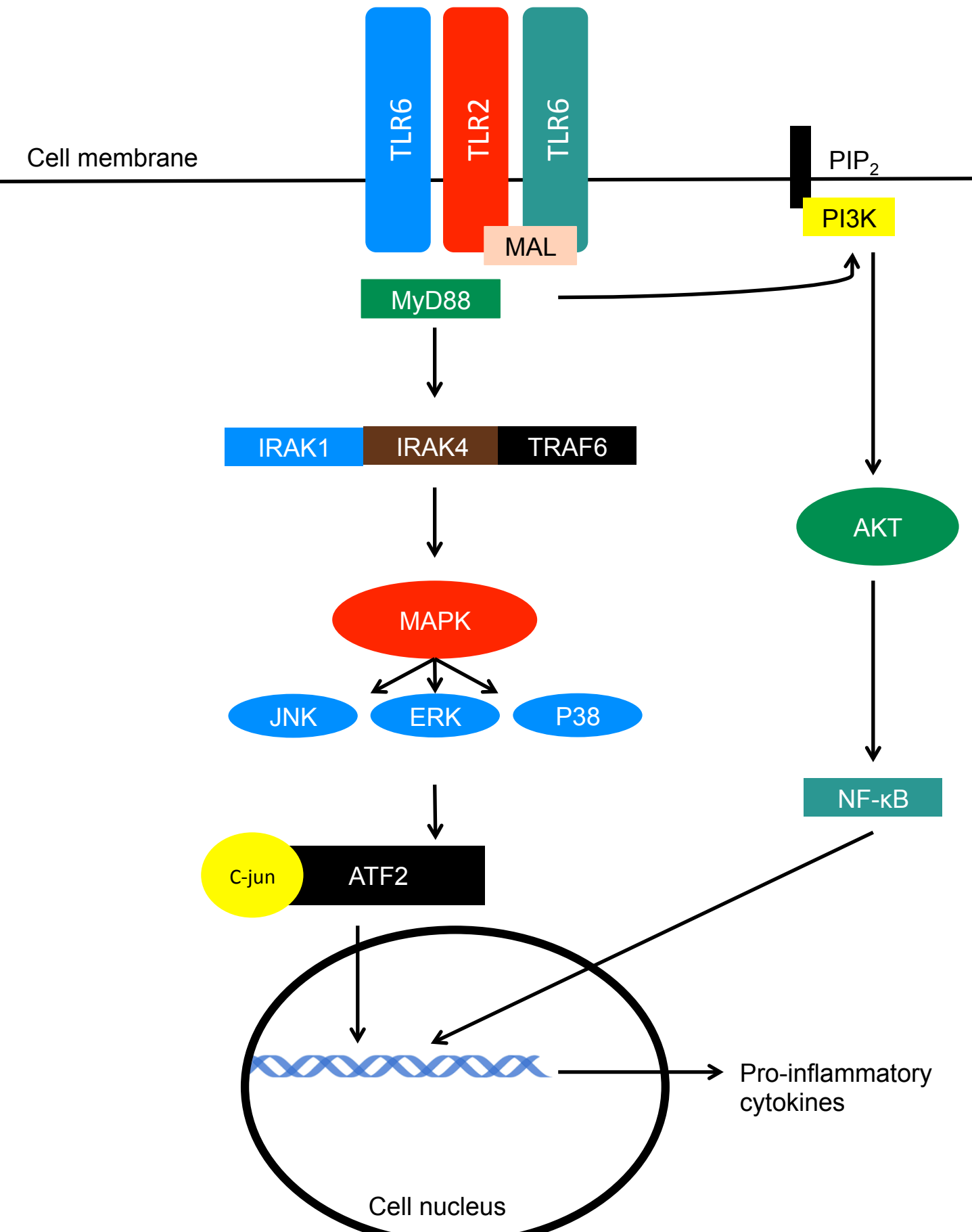
Pan-IN 1

Pan-IN 2

Pan-IN 3

Invasive carcinoma

Figure 6.3: TLR2 signalling pathway via MyD88 activates multiple signalling molecules including JNK, ERK, NF- κ B, p38, MAPK, and PI3K/MAPK axis. TLR = Toll-like receptor, PIP = , PI3K = , IRAK = , TRAF = , MAPK = , , AKT = , JNK = , ERK = , NF- κ B = , ATF =



Appendix

Appendix 1: RT-qPCR Primers

Gene	Summary	Primer sequence
KRT7 KRT19	These genes encode cytoke- ratin 7 and 19 that are highly expressed in pancreatic ductal epithelial cells.	KRT7: Forward primer 5' AGGAGAGCGAGCAGATCAAG 3' Reverse primer 5' CAATCTGGGCCTCAAAGATG 3' KRT19: Forward primer 5' AGCAGGTCCGAGGTTACTGA 3' Reverse primer 5' GCTCACTATCAGCTCGCACA 3'
CD45	This gene encodes a leukocyte marker that is highly expressed on hematopoietic-derived immune cells.	Forward primer 5' CTGACATCATCACCTAGCAG 3' Reverse primer 5' TGCTGTAGTCAATCCAGTGG 3'
VIL1	This gene encodes Villin, and is highly expressed in duodenal epithelial cells.	Forward primer 5' GTGGACGGAGAGAATGAATTG 3' Reverse primer 5' CCTTTCCACACGTAGATCTT 3'
ATP4A(B)	This gene encodes one protein subunit of the membrane transporter H ⁺ /K ⁺ ATPase found in the gastric mucosa.	Forward primer 5' TTCGCCCTGTGCCTCTATGT 3' Reverse primer 5' TGTGAGGTCTGCCAGGTT 3'
18S	Housekeeping gene	Forward primer 5' CGGCTACCACATCCAAGGAA3' Reverse primer 5' GCTGGAATTACCGCGGCT 3'
IL-6	Gene encoding cytokine	<i>IL-6</i> Forward primer 5' CTCCAGGAGCCCAGCTCTGA3' Reverse primer 5' CCCAGGGAGAAGGCAACTG 3'

STAT3	Gene encoding transcription factor in IL-6 / STAT3 pathway	Forward primer 5' GGAGGAGGCATTTCGGAAAG 3' Reverse primer 5' TCGTTGGTGTACACAGAT 3'
SOCS3	Negative regulator of STAT3 signalling	Forward primer 5' GGCCACTCTTTCAGCATCTC 3' Reverse primer 5' ATCGTACTGGTCCAGGAACTC 3'
IL-6 Receptor	IL-6 receptor in IL-6 / STAT3 signalling axis	Forward primer 5' AAAGCTGGGCAGGTTGGTG 3' Reverse primer 5' AGCTTGTGCAGAGGTGTTGAG 3'
A disintegrin and metalloproteinase (ADAM) 10	Encodes molecule responsible for cleaving the IL-6 receptor	Forward primer 5' AGCAACATCTGGGGACAAAC 3' Reverse primer 5' CTTCCCTCTGGTTGATTTGC 3'
ADAM17	Encodes molecule responsible for cleaving the IL-6 receptor	Forward primer 5' GAAGTGCCAGGAGGCGATTA 3' Reverse primer 5' CGGGCACTCACTGCTATTACC 3'
Glycoprotein (GP) 130	Glycoprotein responsible for signal transduction in IL-6 / STAT3 signalling axis (also known as <i>IL-6 signal transducer</i>)	Forward primer 5' CTGTATCACAGACTGGCAACAAG 3' Reverse primer 5' GCATTTGCTCTCTGCTAAGTTCC 3'
IL-11	STAT3 target gene and encoding a cytokine that induces STAT3 signalling	Forward primer 5' TGAAGACTCGGCTGTGACC3' Reverse primer 5' CCTCACGGAAGGACTGTCTC 3'
Serum amyloid A1 (SAA1)	STAT3 target gene	Forward primer 5' CTGCAGAAGTGATCAGCG 3' Reverse primer 5' ATTGTGTACCCTCTCCCC 3'
Toll-like receptor (TLR) 2	Pattern-recognition receptor that is a target gene of STAT3 signalling	Forward primer 5' GCCTCTCCAAGGAAGAATCC 3' Reverse primer 5' TCCTGTTGTTGGACAGGTCA 3'

Human equilibrative nucleoside transporter (hENT) 1	This encodes the nucleoside transporter located on the cell membrane responsible for transporting chemotherapy gemcitabine into the cell	Forward primer 5' TCCTGTTGTTGGACAGGTCA 3' Reverse primer 5' CAGGCAGTCCTTCTGTCCAT 3'
Secreted protein and rich in cysteine (SPARC)	Encodes extracellular matrix protein implicated in sensitivity to chemotherapy nab-paclitaxel	Forward primer 5' CAAGAAGCCCTGCCTGATGAG 3' Reverse primer 5' GGGTCCTGGCACACGCACAT 3'
Epidermal growth factor receptor (EGFR)	Growth factor implicated in oncogenesis that has the potential to be inhibited with antibody treatment (e.g. Erlotinib)	Forward primer 5' GTGGTCCTTGGGAATTTGG 3' Reverse primer 5' GGAATTCGCTCCACTGTGTT 3'

Appendix 2: R code for RNAseq data analyses

Published using knitr, figures and analyses have been excluded to avoid redundancy.

This code is specific to my machine and unique file paths, in addition, some files are formatted outside “R” and then introduced into the “R” environment, therefore the code may require changes to suit different datasets.

RNAseq_process

william

14 November 2016

RNAseq_QC.TCGA.r

Script to run basic QC plots on RNAseq data (from raw read counts)

Source the input parameters from config file so that script does not need to be modified

Use MDS function for PCA plot

NOTE: need latest R version (2.15.3+) and DESeq library

```
install.packages('rmarkdown')
```

load libraries that will be required along the script

```
library(DESeq2) library(DESeq) library(RColorBrewer) library("gplots")
```

Get experimental design and read count table

```
expmtdes <- read.table("/Users/william/Dropbox/Monash_24_ed.txt",header=T,row.names=1,sep="") raw_counts <- read.table("/Users/william/Dropbox/Monash_24_raw_counts.txt", header = TRUE, sep = "")
```

current row names are in column 1

Make sure all row names are unique and then move them out of column 1

```
nams <- raw_counts[,1] row.names(raw_counts) <- make.names(nams, unique = TRUE) raw_counts <- raw_counts[,-1] raw_counts_mat = as.matrix(as.data.frame(lapply(raw_counts, as.numeric))) ## object <- new("ExpressionSet", exprs=as.matrix(counts( cdsFull, normalized=TRUE )))
```

TCGA data is in a separate file for each patient sample. I use a "for loop" to read the table from each file within the TCGA folder

Get raw read counts for all samples from TCGA data

If you are using existing datasets, then skip this step

```
listOfFiles <- list.files(path = READCOUNTSDIR, pattern = "*.rsem.genes.results") for (f in 1:length(listOfFiles)){ file <- listOfFiles[f] uuid <- strsplit(file,"\\.\\.\\.")[1][3] data <- read.table(file.path(READCOUNTSDIR,file), header = TRUE, row.names=1, sep="") if(f == 1){ counts <- as.data.frame(data) raw_count <- rownames(counts) <- rownames(data) colnames(counts) <- uuid }else{ counts <- cbind(counts,data) raw_count <- colnames(counts)[ncol(counts)] <- uuid } } dim(counts) #[1] 20531 183
```

transform raw counts (numeric) into integer for later

```
raw_counts <- round(raw_counts, digits = 0) dim(raw_counts)
```

Remove outlier samples, if any listed in config file

OUTLIERS needs to be defined in QC as a list of Sample ID that should be excluded

Then run this "if" statement

```
if (length(OUTLIERS)>0){ counts <- counts[,-which(colnames(counts) %in% OUTLIERS)] expmtdes <- expmtdes[-which(expmtdes$SampleID %in% OUTLIERS),] }
```

Get the number of samples and factor other variables, for plotting purposes

```
group <- expmtdes$Tumor.Stage
```

create the output directory in your file system

```
system(paste("mkdir", OUTPUTDIR, sep=" "))
```

save raw read counts in text file defined in config file

define output as "READCOUNTSFILE" e.g. file = /directory/filename.txt

```
write.table(raw_counts, file=READCOUNTSFILE, row.names=T, quote=F, sep="")
```

BASIC PLOTS

box plots

Ensure all file names are changed as appropriate, otherwise new analyses will replace old files

```
png(file=file.path(OUTPUTDIR, "test_boxplot.png")) par(mar=c(10, 4, 4, 2)) boxplot(raw_counts, main="Raw read counts per gene", xlab="", ylab="Raw read counts", axes=FALSE) axis(2) axis(1, at=c(1:nbsamples), labels=samples, las=2) dev.off()
```

```
png(file=file.path(OUTPUTDIR, "test_boxplot.log10.png")) par(mar=c(10, 4, 4, 2)) boxplot(log(raw_counts, 10), main="Raw read counts per gene", xlab="", ylab="Raw read counts (log10)", axes=FALSE) axis(2) axis(1, at=c(1:nbsamples), labels=samples, las=2) dev.off()
```

with group for labels

```
png(file=file.path(OUTPUTDIR, "test_boxplot.annot.png")) par(mar=c(10, 4, 4, 2)) boxplot(raw_counts, main="Raw read counts per sample", xlab="", ylab="Raw read counts", axes=FALSE) axis(2) axis(1, at=c(1:32), labels=group, las=2) dev.off()
```

```
png(file=file.path(OUTPUTDIR, "test_boxplot.log10.annot.png")) par(mar=c(10, 4, 4, 2)) boxplot(log(raw_counts, 10), main="Raw read counts per sample", xlab="", ylab="Raw read counts (log10)", axes=FALSE) axis(2) axis(1, at=c(1:32), labels=group, las=2) dev.off()
```

distribution

Kernel Density Plot

```
png(file=file.path(OUTPUTDIR, "test_density.png")) d <- density(log(raw_counts[,1], 10)) plot(d, xlim=c(1,8), ylim=c(0,0.5), main="Distribution of raw read counts per gene") for (s in 2:32){ d <- density(log(raw_counts[,s], 10)) lines(d) } dev.off()
```

QC with DESeq

Instantiate a CountDataSet, which is the central data structure in the DESeq package

```
cdsFull = newCountDataSet( raw_counts, group ) cdsFull head(counts(cdsFull))
```

Normalisation

```
cdsFull = estimateSizeFactors( cdsFull ) #sizeFactors( cdsFull ) head( counts( cdsFull, normalized=TRUE ) ) write.table(counts( cdsFull, normalized=TRUE ), file=file.path(OUTPUTDIR, "test_Normalised_readcounts.txt"), row.names=T, quote=F, sep="") ## Data quality assessment by sample clustering and visualisation #Data quality assessment and quality control (i. e. the removal of insufficiently good data) are essential steps of any #data analysis. They should typically be performed very early in the analysis of a new data set, preceding or in parallel to the differential expression testing. #We define the term quality as fitness for purpose. Our purpose is the detection of differentially expressed genes, #and we are looking in particular for samples whose experimental treatment suffered from an anomaly that renders #the data points obtained from these particular samples detrimental to our purpose.
```

1. Heatmap of the count table

```
cdsFullBlind = estimateDispersions( cdsFull, method = "blind" ) #sizeFactors( cdsFullBlind )
```

```
png(file="DispEsts.png")
```

```
plotDispEsts( cdsFullBlind )
```

```
dev.off()
```

VST transformation

```
vsdFull = varianceStabilizingTransformation( cdsFullBlind )
```

heatmap for the 100 most highly expressed genes

```
select = order(rowMeans(counts( cdsFull, normalized=TRUE )), decreasing=TRUE)[1:100] hmcCol = colorRampPalette(brewer.pal(9, "GnBu"))(100)
## add a coloured banner # Install a colour palette that looks fab install.packages("wesanderson") library(wesanderson) col.samples <-
palette(wes_palette(n=3, name = "Royal1", type = "discrete"))[group] ## with transformed counts
png(file=file.path(OUTPUTDIR,"test1_Monash_heatmap100.png")) heatmap(exprs(vsdFull[select,]), col = hmcCol, margin=c(10, 6), ColSideColors =
col.samples) dev.off()
```

re plot the heatmap

```
png(file=file.path("/Users/william/Desktop/output",paste("HeatMap_SMAD4_100highestexprgenes.col","png",sep="."))) heatmap.2(exprs(object)
[select,], col=hmcCol, scale="row", margins=c(15,1), key=TRUE, symkey=FALSE, density.info="none", trace="none", cexCol=1.0,labRow=NA,
ColSideColors = col.samples) dev.off()
```

2. Heatmap of the sample-to-sample distances

#Another use of variance stabilized data is sample clustering. Here, we apply the dist function to the transpose of the

#transformed count matrix to get sample-to-sample distances.

```
dists = dist( t( exprs(vsdFull) ) )
```

#A heatmap of this distance matrix gives us an overview over similarities and dissimilarities between samples:

```
mat = as.matrix( dists )
```

```
rownames(mat) = colnames(mat) =
with(pData(cdsFullBlind), group)
```

```
png(file=file.path(OUTPUTDIR,"SampleToSample.png"))
```

```
heatmap(mat, col = rev(hmcCol), margin=c(13, 13))
```

```
dev.off()
```

The clustering correctly reflects our experimental design, i.e., samples are more similar when they have the same treatment or the same library type. (To avoid potential circularities in this conclusion, it was important to re-estimate

the dispersions with method="blind" in the calculation for cdsFullBlind above, as only then, the variance stabilizing transformation is not informed about the design, and we

can be sure that it is not biased towards a result supporting

the design.)

3. Principal component plot of the samples

```
png(file=file.path(OUTPUTDIR,"PCA.png"))
```

```
plotPCA(vsdFull)
```

```
dev.off()
```

PCA

select data for the 1000 most highly expressed genes

```
select = order(rowMeans(exprs(vsdFull)), decreasing=TRUE)[1:1000] highexprgenes <- exprs(vsdFull)[select,] colnames(highexprgenes)<- samples
## transpose the data to have variables (genes) as columns data_for_PCA <- t(highexprgenes) dim(data_for_PCA)
```

calculate MDS

```
mds <- cmdscale(dist(data_for_PCA), k=3, eig=TRUE) # Performs MDS analysis ## get the proportion of explained variance eigenvalues <- mds
eig/sum(mds$eig)
```

```
png(file=file.path(OUTPUTDIR,"test_Proportion_Explained_Variance.png")) barplot(eigenvalues[1:10], main = "", xlab = "Number of dimensions",
ylab = "Proportion of explained variance", col = "steelblue") dev.off()
```

```
png(file=file.path(OUTPUTDIR,"test_PCA_Dim1vsDim2.png")) plot(mds$points[, 1], -mds$points[,2], type="n", xlab="Dimension 1",
ylab="Dimension 2", main="") text(mds$points[, 1], -mds$points[,2], rownames(mds$points), cex=0.8) dev.off()
```

PCA labelled and coloured for every column in experiment design file

```
for (a in 1:ncol(expmtdes)){ annot <- colnames(expmtdes)[a] rownames(data_for_PCA) <- expmtdes[,annot] mds <- cmdscale(dist(data_for_PCA))
# Performs MDS analysis
```

```
## Lets see how many groups we have we have and create color palette samples.group <- rownames(data_for_PCA) annot.classes <-
unique(samples.group) col.samples <- c(rep("black",length(samples.group))) if(length(annot.classes) <= 8){ for (i in 1:length(annot.classes)){
col.samples[which(samples.group==annot.classes[i])] <- palette()[i] } }
```

```
png(file=file.path(OUTPUTDIR,paste("PCA_Dim1vsDim2.",annot, ".png", sep="")) plot(mds[,1], -mds[,2], type="n", xlab="Dimension 1",
ylab="Dimension 2", main="") text(mds[,1], -mds[,2], rownames(mds), cex=0.8, col=col.samples) dev.off() }
```

OPTION: Box plots for genes of interest

```
if(length(GENESTOLOT)>=1){ # subset of normalised data only for these genes of interest cdsGenesNorm <- counts( cdsFull, normalized=TRUE
)[which(featureNames(cdsFull) %in% GENESTOLOT),] dim(cdsGenesNorm) ## box plots ## pdf(file="genes_boxplot.pdf") par(mfrow=c(3,2)) for
(g in 1:length(GENESTOLOT)){ counts<-as.numeric(counts[g,]) datatoplot<-data.frame(counts,group) boxplot(datatoplot
counts datatoplotgroup, main=paste("Normalized read counts per sample group for gene:",GENESTOLOT[g],sep=""), varwidth=TRUE,
xlab="", ylab="Normalized read counts",axes=TRUE, cex.axis=0.7) } dev.off() }
```

Differential gene expression analysis

limma_voom.r

This script runs Differential Expression analysis with limma-voom for RNAseq data, from raw read counts.

load libraries that will be required along the script

```
library(limma) library(edgeR)
```

make sure the experiment design table follow the same order

```
rownames(expmtdes) <- expmtdes$SampleIDexperiment_design.ord <- expmtdes[colnames(raw_counts),] experiment_design.ord <-
expmtdes[colnames(raw_counts),] experiment_design.ord ## Filter out unexpressed genes ## Keep genes with least 1 count-per-million reads
(cpm) in at least 15 samples isexpr <- rowSums(cpm(raw_counts)>0) >= 15 table(isexpr) raw_counts_exp <- raw_counts[isexpr,] isexpr[1:5]
```

```
dim(raw_counts_exp) counts[1:3,1:3] genes <- rownames(raw_counts_exp)
```

Apply TMM normalisation

```
dge <- DGEList(counts=raw_counts_exp)
```

Calculate normalization factors

```
dge <- calcNormFactors(dge)
```

Create design matrix for limma

```
group <- factor(expmtdes$Tumor.Stage) design <- model.matrix(~0+group) colnames(design)<- gsub("group","",colnames(design)) design # Ctrl  
Local Met # 0 1 0 # 0 1 0 # 0 0 1 # 0 0 1 # 0 0 1 # 0 1 0 # 0 1 0 # 0 1 0 # 1 0 0 # 1 0 0 # 0 1 0 # 0 1 0 # 0 0 1 # 0 0 1 # 0 0 1 # 0 1 0 # 1 0 0 # 1 0 0  
# 0 1 0 # 0 1 0 # 0 0 1 # 0 0 1 # 0 0 1 # 0 0 1 # 0 1 0 # 0 0 1 # 0 1 0 # 0 0 1 # 0 0 1 # 0 0 1 # 0 0 1 # 1 0 0
```

Normalise read counts with voom

```
y <- voom(dge,design,plot=TRUE) y$genes <- genes
```

Fit linear model with limma and testing for DE with eBayes

```
fit <- lmFit(raw_counts, design)
```

Define the comparisons to be made, based on design

NOTE: Need to update this line manually to compare different groups

```
cont.matrix <- makeContrasts(Local - Met, levels=design)
```

Add the contrast matrix to the fit

```
fit <- contrasts.fit(fit, cont.matrix)
```

Run the statistical test

```
fit <- eBayes(fit) options(digits=3) dim(fit) mycoefs=colnames(fit$coefficients) mycoefs # Define P-value cut-off PVAL <- 0.01
```

Output the statistics for all comparisons and all pvalues

Check all output file names and destinations, if this analysis is run more than once, files with the same name will be deleted and replaced with the new analysis

RUN ALL OF THIS SECTION TOGETHER

NOTE: This is a bad example because there were zero genes differentially expressed between local and metastatic disease

```
for (p in 1:length(PVAL)){ pval <- PVAL[p] DEgenesSummary <- data.frame()
```

```
for (c in 1:length(mycoefs)){ mycoef=mycoefs[c] mycoef
```

```

## write full table
res <- topTable(fit,coef=mycoef,n=dim(fit)[1])
write.table(res,file=file.path(OUTPUTDIR,paste("Test_FNA",mycoef,".txt",sep="")),row.names=F,quote=F,sep="\t")

## write DE genes at pvalue < pval only
respval <- topTable(fit,coef=mycoef,n=dim(fit)[1],p.val=pval)
DEgenesSummary[c,1] <- nrow(respval)
print(paste("Test_FNA",mycoef," at pval ",pval, ": ", dim(respval)[1],sep=""))
write.table(respval,file=file.path(OUTPUTDIR,paste("Test_FNA",mycoef,"_pval",pval,".txt",sep="")),row.names=F,quote=F,sep="\t")

## with logFC > 1 only
if(nrow(respval)>0){
  for (fc in 1:3){
    respvalFC<-respval[which(abs(respval$logFC)>fc),]
    print(paste("Test_FNA",mycoef, " at pval ",pval, " with FC>",fc,": ", dim(respvalFC)[1],sep=""))

write.table(respvalFC,file=file.path(OUTPUTDIR,paste("Test_FNA",mycoef,"_pval",pval,"_logFC",fc,".txt",sep="")),row.names=F,quote=F,sep="\t")
    DEgenesSummary[c,fc+1] <- nrow(respvalFC)
  }
}
## Plot volcano plot
png(file=file.path(OUTPUTDIR,paste("Test_FNA",mycoef,"png",sep=".")))
with(res, plot(logFC, -log10(P.Value), pch=20, main="Volcano plot", xlim=c(-2,2)))

# Add colored points: red if padj<0.01, orange if log2FC>1, green if both
with(subset(res, adj.P.Val<.01 ), points(logFC, -log10(adj.P.Val), pch=20, col="red"))
with(subset(res, adj.P.Val<.01 & abs(logFC)>1), points(logFC, -log10(adj.P.Val), pch=20, col="green"))
dev.off()

```

```

}
rownames(DEgenesSummary) <- mycoefs colnames(DEgenesSummary) <- c("all logFC","logFC > 1","logFC > 2","logFC > 3")
write.table(DEgenesSummary,file=file.path(OUTPUTDIR,paste("Test_FNA",mycoef,"at_pval_",pval,".summary.txt",sep="")),row.names=TRUE,col.names=TRUE,qu
}

```

END

```
save.image(file=RDATAFILE)
```

Appendix 3: Antibodies

Antibody	Concentration (Use)	Species	Company
Actin	1:1000 (WB)	Mouse	Sigma- Aldrich
Tubulin	1:1000 (WB)	Rat	Abcam
Phosphorylated-STAT3	1:1000 (WB) 1:400 (IHC) Citrate antigen retrieval	Rabbit	CST
Total-STAT3	1:1000 (WB)	Mouse	CST
IL-6 Receptor	1:1000 (WB)	Mouse	R & D Systems
Anti-Human Nuclear	1:20 (IHC) Proteinase K antigen retrieval	Mouse	Merck- Millipore
Pan-Cytokeratin	1:50 (IHC) Citrate antigen retrieval	Mouse	Abcam
Cytokeratin 7	(IHC) Citrate antigen retrieval	Mouse	Dako
Cytokeratin 19	(IHC) Citrate antigen retrieval	Mouse	Roche
CD45	(IHC) Citrate antigen retrieval	Rabbit	CST
TUNEL	Kit instructions (IHC)	Apop-tag Peroxidase In Situ Apoptosis Detection kit	Merck- Millipore
PCNA	1:500 (IHC)	CST	CST
pEGFR	1:1000 (IHC)	Rabbit	R & D Systems
EGFR	1:1000 (WB)	Rabbit	
pERK	1:1000 (WB)	Rabbit	CST
ERK	1:1000 (WB)	Rabbit	Santa Cruz
pAKT	1:1000 (WB)	Rabbit	CST
AKT	1:1000 (WB)	Rabbit	CST

Appendix 4: Buffers and solutions

Solution	
SDS-Page running buffer (10x solution)	250mM Tris-HCl, 1920mM Glycine, 1% Sodium Dodecyl Sulphate (SDS), diluted in milli-Q H ₂ O, pH 8.3
SDS-Page transfer buffer (10x solution, diluted in 2 parts methanol and 7 parts milli-Q H ₂ O)	250mM Tris-HCl, 1920mM Glycine, diluted in milli-Q H ₂ O
Western blot wash buffer	20mM Tris, 150mM NaCl, 0.1% Tween 20
Immunohistochemistry wash buffer	1.4 mM NaCl, 0.3 mM KCl, 1 mM Na ₂ HPO ₄ .12H ₂ O, 0.18 mM KH ₂ HPO ₄ , pH 7.4
Citrate buffer (antigen retrieval)	10 mM Sodium Citrate, pH 6.0
Proteinase K solution (Antigen retrieval)	1 part Proteinase K solution, 19 parts buffer Buffer: 50 mM Tris, 1 mM EDTA, 0.5% Triton X-100, pH 8.0 Proteinase K solution: Proteinase K 400 ug/mL, 1 part TE buffer, 1 part glycerol
Protein lysis buffer	150mM NaCl, 1% Triton X-100, 50mM Tris, pH 8.0, made up to 100mL with H ₂ O
Lower gel (western blot)	3.95 mL H ₂ O, 3.35 mL Acrylamide (30%), 2.5 mL 1.5 M Tris (pH 8.8), 100 µl SDS (10%), 100 µl ammonium persulphate (APS; 10%), 4 µl Tetramethylethylenediamine (TEMED). Volumes for 1 gel
Upper gel (western blot)	2.05 mL H ₂ O, 0.5 mL Acrylamide (30%), 375 µl 0.5 M Tris (pH 6.6), 30 µl SDS (10%), 30 µl APS (10%), 3 µl TEMED. Volumes for 1 gel

Appendix 4: Manufacturers

Axygen	Union City, California, USA
Bioline	London, England
Invitrogen	Melbourne, Australia
Life Technologies	Carlsbad, California, USA
Promega	Madison, Wisconsin, USA
Qiagen	Hilden, Germany
Roche	Mannheim, Germany
Sigma	Saint Louis, USA
Thermo Scientific	Waltham, Massachusetts, USA

Appendix 5 - Journal article:

Berry, W., et al. Endoscopic ultrasound-guided fine-needle aspirate-derived preclinical pancreatic cancer models reveal panitumumab sensitivity in KRAS wild-type tumors. *International journal of cancer* (2017).

Endoscopic ultrasound-guided fine-needle aspirate-derived preclinical pancreatic cancer models reveal panitumumab sensitivity in *KRAS* wild-type tumors

William Berry^{1,2}, Elizabeth Algar^{3,4}, Beena Kumar⁵, Christopher Desmond⁶, Michael Swan⁶,
Brendan J. Jenkins ^{1,2*} and Daniel Croagh^{7*}

¹Centre for Innate Immunity and Infectious Diseases, Hudson Institute of Medical Research, Clayton, VIC 3168, Australia

²Department of Molecular Translational Science, School of Clinical Sciences, Monash University, Clayton, VIC 3168, Australia

³Genetics and Molecular Pathology Laboratory, Monash Health, Clayton, VIC 3168, Australia

⁴Centre for Cancer Research, Hudson Institute of Medical Research, Monash University, Clayton, VIC 3168, Australia

⁵Department of Anatomical Pathology, Monash Health, Clayton, VIC 3168, Australia

⁶Department of Gastroenterology, Monash Health, Clayton, VIC 3168, Australia

⁷Department of Surgery (School of Clinical Sciences at Monash Health), Monash University, Clayton, VIC 3800, Australia

Pancreatic cancer (PC) is largely refractory to existing therapies used in unselected patient trials, thus emphasizing the pressing need for new approaches for patient selection in personalized medicine. *KRAS* mutations occur in 90% of PC patients and confer resistance to epidermal growth factor receptor (EGFR) inhibitors (e.g., panitumumab), suggesting that *KRAS* wild-type PC patients may benefit from targeted panitumumab therapy. Here, we use tumor tissue procured by endoscopic ultrasound-guided fine-needle aspirate (EUS-FNA) to compare the *in vivo* sensitivity in patient-derived xenografts (PDXs) of *KRAS* wild-type and mutant PC tumors to panitumumab, and to profile the molecular signature of these tumors in patients with metastatic or localized disease. Specifically, RNASeq of EUS-FNA-derived tumor RNA from localized ($n = 20$) and metastatic ($n = 20$) PC cases revealed a comparable transcriptome profile. Screening the *KRAS* mutation status of tumor genomic DNA obtained from EUS-FNAs stratified PC patients into either *KRAS* wild-type or mutant cohorts, and the engraftment of representative *KRAS* wild-type and mutant EUS-FNA tumor samples into NOD/SCID mice revealed that the growth of *KRAS* wild-type, but not mutant, PDXs was selectively suppressed with panitumumab. Furthermore, *in silico* transcriptome interrogation of The Cancer Genome Atlas (TCGA)-derived *KRAS* wild-type ($n = 38$) and mutant ($n = 132$) PC tumors revealed 391 differentially expressed genes. Taken together, our study validates EUS-FNA for the application of a novel translational pipeline comprising *KRAS* mutation screening and PDXs, applicable to all PC patients, to evaluate personalized anti-EGFR therapy in patients with *KRAS* wild-type tumors.

Pancreatic cancer (PC) is the fourth most common cause of cancer-related death worldwide, and has a poor 5–7% five-year overall survival rate which has remained relatively constant over the last few decades.¹ Most PC patients require a tissue diagnosis, and endoscopic ultrasound-guided fine-needle aspiration (EUS-FNA) is now the most widely used technique to obtain tissue for the diagnosis of PC prior to commencement of palliative or neoadjuvant chemotherapy.^{2,3} Although EUS-FNA

Key words: EUS-FNA, pancreatic cancer, patient-derived xenograft, *KRAS*, panitumumab, RNASeq

Additional Supporting Information may be found in the online version of this article.

*B.J.J. and D.C. contributed equally to this work

Disclosures: No conflicts of interest, financial or otherwise, are declared by all other authors

Author Contributions: W.B. performed experiments, analyzed and interpreted the data, and co-wrote the manuscript. E.A. performed *KRAS* genotyping, and edited the manuscript. B.K. performed histological analyses and immunohistochemistry. C.D., M.S. and D.C. provided clinical samples. D.C. and B.J.J. designed the research study, analyzed and interpreted data, and wrote the manuscript. All authors read the manuscript.

Grant sponsors: CASS Foundation, Life Technologies Ion AmpliSeqTM Transcriptome Grant Program, and Victorian Government of Australia (Operational Infrastructure Support Program); **Grant sponsor:** Government of Australia (Australian Postgraduate Award; W.B.);

Grant sponsor: NHMRC Senior Medical Research Fellowship (B.J.J.)

DOI: 10.1002/ijc.30648

History: Received 3 Oct 2016; Accepted 7 Feb 2017; Online 15 Feb 2017

Correspondence to: Brendan J. Jenkins, Centre for Innate Immunity and Infectious Diseases, Hudson Institute of Medical Research, 

What's new?

While pancreatic cancer is a genetically heterogeneous disease, 90% of patients exhibit mutations in *KRAS*. Most patients also respond poorly to generalized treatments, suggesting that patient outcomes may depend on genetic profiling and personalized therapeutic approaches. A potential role for those approaches was explored here, using tumor tissue procured from patients via endoscopic ultrasound-guided fine-needle aspirate (EUS-FNA). Patient-derived xenografts were developed and screened for *KRAS* mutation status and sensitivity to panitumumab. Only *KRAS* wild-type EUS-FNA patient-derived xenografts were sensitive to the drug. Genetic profiling coupled with EUS-FNA, an existing clinical tool, is suited for rapid translation into clinical trials.

can cause potential complications including pancreatitis, bleeding, infection and perforation,³ these are quite infrequent (0.3–2.2%), and its accuracy of ~85% compares favourably with other biopsy techniques,² thus ideally placing it to provide material for the genetic characterization of PC. While EUS-FNA has been used to provide tissue for genetic analysis of PC, the clinical utility of this information has been limited largely due to low tissue quantities leading to suboptimal yields of genetic material, and sample contamination with non-malignant cells.⁴ Nonetheless, the inherent advantage of EUS-FNA is the ability to sample tumors from patients who are ineligible for surgical resection, which in the context of PC is ~80%, thus providing clinicians the ability to obtain tissue which would otherwise be unavailable.⁵

Recent advances in next-generation sequencing (NGS) technologies have enhanced our understanding of the high degree of inter-tumoral heterogeneity among PC patients. For instance, genome-wide association studies on large cohorts (>5,000) of PC patients and control individuals have identified numerous PC susceptibility loci containing genes which have previously been implicated in oncogenesis (e.g., *BCAR1*, *KLF14*, *PDX1*, *TERT*).⁶ More recently, whole-exome sequencing of resected tumor tissue from a smaller cohort of 109 PC patients reported that ~5% of cases contained 24 significantly mutated genes, some of which not only provided prognostic value in terms of disease pathology or patient survival (e.g., *KRAS*, *RBM10*), but also identified patients who may respond to targeted therapies (e.g., *BRAF*, *PIK3CA*).⁷ Notably, the high genetic diversity of PC tumors provides a rational explanation for the relatively slow progress in the development of novel and effective chemotherapies for PC, especially since all new treatments have previously been evaluated on unselected PC patient populations.^{8–12} Accordingly, personalized therapeutic approaches based on the genetic profile of individual tumors in PC provide the opportunity to vastly improve patient outcomes.^{8,9} In PC, *KRAS* mutations are of particular interest because they are observed in ~90% of patients, and based on other cancers such as non-small cell lung cancer and colorectal cancer, the mutation status of *KRAS* may predict responsiveness to epidermal growth factor receptor (EGFR) inhibitors.^{13–15}

A major obstacle to personalized therapy for PC has been the difficulty in isolating high quality tumor-derived genetic

material (genomic DNA and/or RNA) in sufficient quantities for subsequent molecular profiling. Indeed, this has been recently reported by the Individualized Molecular Pancreatic Cancer Therapy (IMPACT) Trial which was designed to identify subsets of patients with advanced metastatic disease who could be targeted, based on mutations within their tumor genome, with currently-available therapies.⁹ An additional limitation of the IMPACT study was the heavy reliance upon tissue primarily from archival formalin-fixed, paraffin-embedded (FFPE) samples for genomic DNA extraction, most of which were derived from surgical resections which are possible in only 20% of PC patients presenting with localized disease.⁹ Accordingly, there is an urgent and unmet clinical need to improve methodologies for the robust isolation of high quality genetic material in a timely manner from the vast majority of PC patients.

Here, we systematically address current issues with tumor sampling, as well as specimen collection and processing, and demonstrate that EUS-FNA can be a reliable source of high quality genetic material for the molecular profiling of both localized and metastatic PC. Moreover, transcriptome profiling of EUS-FNA, along with interrogation of TCGA datasets (from surgical resection), for PC identified potentially targetable phenotypes for localized and metastatic disease, as evidenced by the responsiveness of *KRAS* wild-type tumors from an EUS-FNA-derived PDX model to the EGFR inhibitor, panitumumab. Collectively, our findings pave the way for future studies aimed at both improving our understanding of advanced (i.e., metastatic) PC, and also generating molecular profiles to stratify patients for personalized treatment regimens.

Material and Methods**Human specimen collection**

PC samples were collected from patients undergoing EUS-FNA for investigation of a pancreatic mass at Monash Health (MH) Victoria, Australia. For each patient, initial diagnostic aspirates from the pancreatic mass were collected using 22-Gauge procure needles (Cook Medical) with 10 ml of suction for immediate cytological assessment. After confirmation of cellular quantity, an additional aspirate was taken from the same position and snap-frozen in liquid nitrogen. Normal pancreas was obtained by surgical resection, performed at MH, for conditions other than PC. Duodenum and stomach

tissues were obtained from patients without PC by routine endoscopic biopsy and snap-frozen. All tissue samples were stored at -80°C .

Whole blood was collected from healthy volunteers in EDTA-coated tubes (Becton Dickinson and Company).

Written and informed patient consent was obtained for each procedure, with approval from MH and Monash University Human Research Ethics Committees (approval number 13058A).

RNA and genomic DNA extraction

Total RNA and genomic DNA (gDNA) were simultaneously extracted from snap-frozen EUS-FNA samples by homogenization in Buffer RLT Plus (Qiagen AllPrep DNA/RNA Universal Kit) as per the manufacturer's protocol. Isolation of gDNA from formalin-fixed, paraffin-embedded (FFPE) tissue was performed on 5×10 μm -thick sections using the ReliaPrep FFPE gDNA Miniprep System (Promega). The quality and quantity of gDNA and RNA were determined using the Nanodrop Spectrophotometer (ThermoScientific), and Qubit Fluorometer (Life Technologies).

Gene expression analyses

cDNA was synthesized from 0.5 μg RNA using SuperScript III (Invitrogen), and subsequent real-time quantitative polymerase chain reaction (qPCR) was performed using the 7900HT Fast RT-PCR system (Applied Biosystems). The expression of target genes was normalized relative to 18S rRNA, and data acquisition and analyses were performed using the Sequence Detection System Version 2.4 software (Applied Biosystems). Sequences of human gene forward and reverse primers are listed in Supporting Information Table 1. Gene expression is represented as relative expression, derived from the difference between the Ct values of the target gene and the housekeeper gene, 18S rRNA.

Transcriptome profiling

EUS-FNA-derived RNA samples from PC ($n = 40$) and normal pancreas samples ($n = 5$) were sequenced using AmpliSeq kit and Ion Proton sequencing technology, and libraries generated. Sequence reads were aligned to the Ion AmpliSeq™ Transcriptome reference file (hg19_AmpliSeq_Transcriptome_ERCC_v1.fasta) in Torrent Suite™ Software using the Ion Torrent Mapping Alignment Program (TMAP; <https://github.com/iontorrent/TMAP>). The reference file contains the entire set of RefSeq transcripts from which all 20,802 Ion AmpliSeq™ Transcriptome panel primers were designed. After alignment, the *ampliSeqRNA* plugin examined the number of reads mapping to the expected amplicon ranges and assigned counts per gene for reads which align to these regions as defined in the BED file (hg19_AmpliSeq_Transcriptome_21K_v1.bed). Reads aligning to the expected amplicon locations were referred to as “on target” reads and were reported as a percentage of total reads by the plugin.

Gene mutation analyses

gDNA (25–50 ng) was subjected to the KRAS-BRAF Strip Assay (ViennaLab Diagnostics GmbH), and mutations were objectively scored using Strip Assay Evaluator software.

Identification and selection of treatable PC phenotypes

Electronic searches were performed using Ovid Medline, Pubmed and Embase to identify potentially treatable PC phenotypes by combining the terms “pancreatic adenocarcinoma,” “molecularly targeted therapy” and “chemotherapy.” All retrieved articles were reviewed to compile a list of all mutations targetable with currently available treatments. The incidence of each of these phenotypes in PC was then obtained by analysis of the OMICS database.

In silico analyses

Transcriptome analysis of our EUS-FNA samples and TCGA data sets (<http://cancergenome.nih.gov/>) was performed using R packages: DESeq2, Bioconductor and Limma for quality control, normalization and differential gene expression analysis. Clinical data and mutation status from DNaseq datasets were compiled and analyzed by contrasting the transcriptome profile, histological and clinical information for tumors with or without *KRAS* and DNA-repair pathway mutations (*BRCA1/2*, *PALB2* and *ATM*) from TCGA data sets.

Cytology and histological analyses

Cytological evaluation was performed on Diff-Quik stained and air-dried slides, Papanicolaou-stained and wet-fixed smears. EUS-FNA cell block preparations were made using clotted needle cores which were placed in a fine mesh cassette and then into a regular cassette for processing in histology, thus mimicking a mini biopsy for diagnostic staining.

Immunohistochemistry

EUS-FNA cell block sections were used for immunohistochemical staining with antibodies against Cytokeratin 7 (Dako), Cytokeratin 19 (Ventana Medical Systems/Roche) and CD45 (Ventana Medical Systems, Inc./Roche). Slides were stained using the Ventana BenchMark ULTRA Automated IHC slide staining system (Roche), and the Ventana ultraView Universal DAB Detection kit (Roche) with amplification step was used for visualization of the staining reaction. Hematoxylin was used as the counterstain.

EUS-FNA PDX tumor sections were stained with antibodies against pan-Cytokeratin (Santa Cruz), CD45 (BD Biosciences), Human Nuclei (Merck-Millipore), Proliferating Cell Nuclear Antigen (PCNA, Cell Signaling Technologies), and the ApopTag Peroxidase In Situ Apoptosis Detection Kit (Merck-Millipore). The Avidin/Biotin complex formation kit ABC Vectastain (Vector Labs), and DAB chromogen (Biocare Medical) staining, were also used. Sections were counterstained with Hematoxylin. Staining was quantified by counting positive cells per 20 high-powered fields (HPF).

Western blotting

Protein lysates from PDX tumors were prepared by homogenizing tumor tissue pieces in 1 mL of lysis buffer (50 mM Tris, 150 mM NaCl, 1% (v/v) Triton X-100, 1 mM EDTA, (v/v) NaF, 1% (v/v) NaVO₄, 1% (v/v) and 1 tablet of protease inhibitor (EDTA-free)). Lysates were examined by Western blot with primary antibodies against total and phosphorylated (p) EGFR (R&D Systems), total and pAKT (Cell Signaling Technologies), total and pERK1/2 (Santa Cruz, and Cell Signaling Technologies), and α -tubulin (Abcam). Membranes were exposed to IRDye[®] Secondary Antibodies diluted in Odyssey[®] Blocking Buffer, and then scanned on an Odyssey fluorimager (LI-COR) infrared imaging system.

Patient-derived xenografts

EUS-FNA samples were collected in saline, finely minced, washed and re-suspended in ice-cold 150 μ L Dulbecco's Modified Eagles Media (DMEM) and 150 μ L Matrigel (Corning Life Sciences). Samples were implanted into each of 2 female NOD/SCID mice (Animal Resource Centre, Western Australia) using a subcuticular injection (150 μ L). Tumors grew for 3–6 months to a maximum volume of 1,000 mm³, at which point tumors were excised for subsequent passaging (up to 4 times prior to expansion in experimental treatment cohorts).

To passage, tumors from “donor” mice were minced into 2 mm pieces and then coated in Matrigel, followed by implantation into a subcuticular pocket on the flank of a female NOD/SCID mouse.

For experimental treatment cohorts, female NOD/SCID mice were randomized into one of four treatment groups ($n = 4$ mice/group): saline (0.2 mL intraperitoneal (i.p.) injection twice weekly), panitumumab alone (Amgen; 200 μ g, i.p. twice weekly), gemcitabine alone (Accord; 50 mg/kg i.p. twice weekly), and a combination of panitumumab and gemcitabine. Mice were administered with reagents once grafted tumors were established and reached a volume of \sim 100 mm³. Tumor volume was measured weekly with digital callipers, and calculated $(2 \times \text{Width} \times \text{Length})/2 = V_{\text{mm}^3}$ until the end of the treatment course.

All experiments were performed on mice housed in a specific pathogen-free environment with approval from the Monash University Animal Ethics Committee (MMCA 2015/08).

Statistical analyses

Statistical analysis was performed using GraphPad Prism for Windows version 5.0, and where appropriate parametric (one-way ANOVA) or nonparametric (Kruskal–Wallis, Mann–Whitney) tests were used. For clinical characteristics, χ^2 or Fischer exact tests were used to compare groups of patients from TCGA datasets based on phenotype. $p < 0.05$ was considered to be statistically significant. Data are expressed as the mean \pm standard error of the mean (SEM).

Results

Optimization of genomic DNA and total RNA extraction from EUS-FNA samples

The potential of EUS-FNA for personalizing cancer therapy is dependent on the quality and quantity of genetic material that can be isolated from EUS-FNA-acquired biopsies. We therefore optimized the isolation of PC tumor gDNA and RNA by trialling a variety of strategies from 66 EUS-FNA samples (Supporting Information Fig. 1a). Ultimately, we demonstrated that maximal yields were obtained from one EUS-FNA pass when snap-frozen in liquid nitrogen, and then homogenized and divided into smaller aliquots prior to processing (Supporting Information Figs. 1b–1d). Using this strategy, both RNA and DNA were simultaneously isolated with an average yield of 12.9 ± 3.2 μ g and 4.8 ± 3.7 μ g, respectively (Method 3; Supporting Information Figs. 1b and 1d). Yields of gDNA were approximately 10-fold higher when an additional EUS-FNA pass was performed, thus demonstrating utility in overcoming sampling deficiencies.

High epithelial cell content of PC EUS-FNA-derived samples

As previous studies utilizing EUS-FNA biopsies have documented issues with suboptimal content of tumor (*i.e.*, epithelial) cells, as well as contamination with non-malignant cells,⁹ we investigated the cellular content of EUS-FNA-derived PC specimens. Histopathological examination of H&E-stained EUS-FNA PC biopsy sections revealed a mix of malignant epithelial, benign epithelial and immune/inflammatory cells (Fig. 1a). The high epithelial content of EUS-FNA samples was verified by immunostaining for Cytokeratin 7 and 19, demonstrating pronounced numbers of cells positive for either marker throughout EUS-FNA-derived PC sections (Figs. 1b and 1c). In contrast, very few CD45-positive immune cells were observed in PC sections (Fig. 1d).

We further assessed the epithelial (*i.e.*, tumor cell) content of EUS-FNA samples by performing qPCR to compare the expression levels of target genes representative of epithelial and immune (blood) cells, as well as pancreatic, gastric and duodenal tissue, in EUS-FNA-derived RNA selected from 20 PC patients (Supporting Information Table 2). The latter two tissue types were chosen since FNA needles pass through either the gastric or duodenal mucosa when sampling the pancreas, and may therefore contain “contaminating” cells from these tissues. Gene expression of the epithelial cell markers *Cytokeratin (KRT) 7* and *19* was equal or higher in RNA extracted from PC EUS-FNAs compared to normal pancreatic tissue collected by either resection or EUS-FNA, as well as gastric, duodenal and whole blood samples, thus confirming the high epithelial content of PC EUS-FNAs (Figs. 1e and 1f). In contrast, mRNAs for cell markers of the duodenum (*Villin*; *VIL1*) and stomach (*ATPase*, *H+/K+ exchanging, alpha polypeptide*; *ATP4A*) were detected at low levels in both EUS-FNA-derived PC and normal pancreas (Figs. 1g and 1h). We also observed that expression levels of

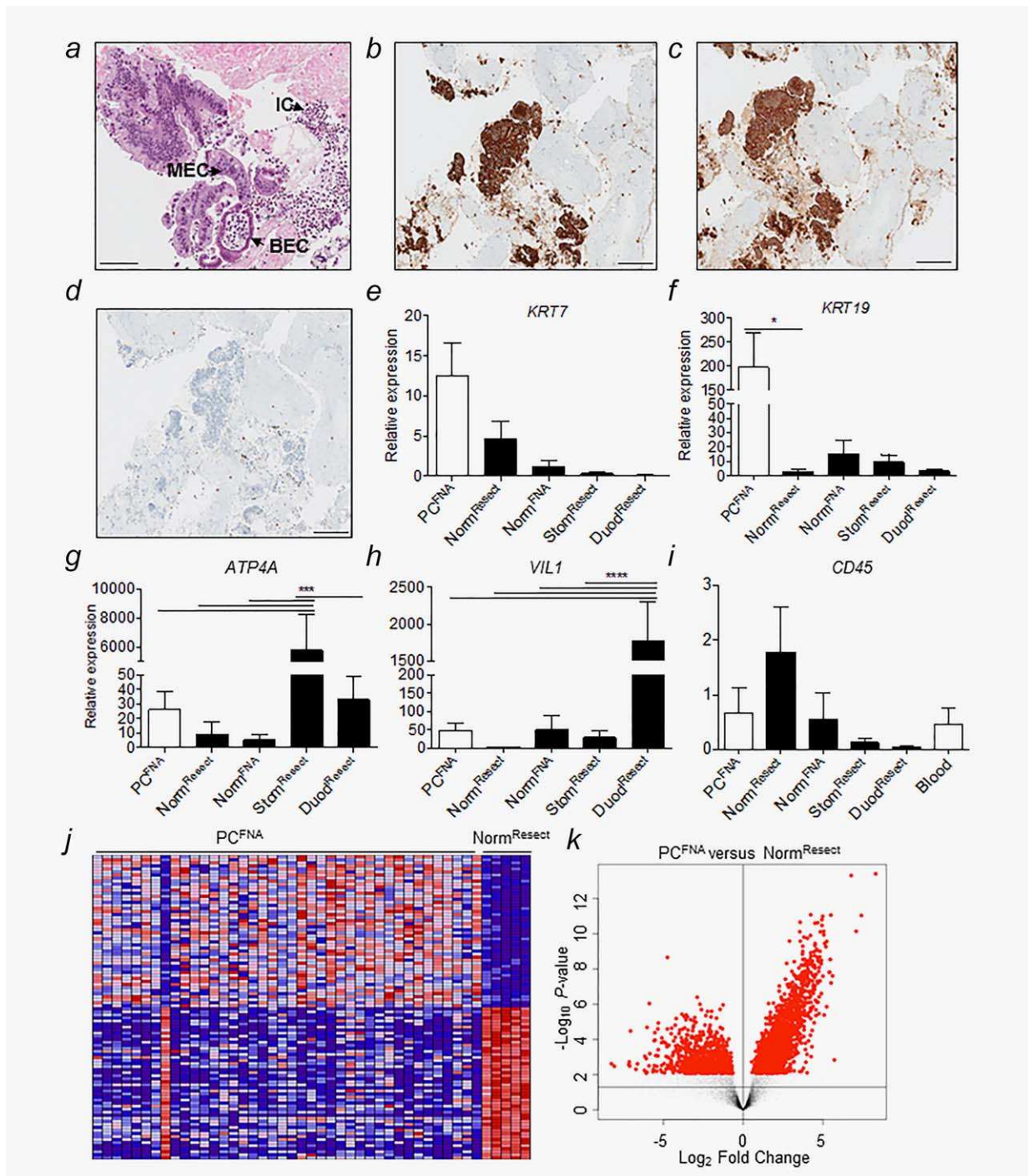


Figure 1. Gene expression analyses of the high epithelial cell content, of pancreatic origin, in EUS-FNA-derived PC samples. (a) Representative EUS-FNA-derived PC cross-section stained with H&E. MEC, malignant epithelial cells; BEC, benign epithelial cells; IC, inflammatory cells. Scale bar, 100 μ m. (b–d) Immunohistochemistry of PC EUS-FNA cell blocks stained with Cytokeratin 7 (B), Cytokeratin 19 (c) and CD45 (D). Scale bars, 100 μ m. (e–i) qPCR of the indicated cell marker genes on RNA from EUS-FNA-derived PC (PC^{FNA}; $n = 20$; Supporting Information Table 2) and normal pancreas (Norm^{FNA}; $n = 3$) biopsies, resected normal pancreas (Norm^{Resect}; $n = 5$), stomach (Stom^{Resect}; $n = 4$) and duodenum (Duod^{Resect}; $n = 4$) biopsies, and whole blood ($n = 5$) samples. Data are relative expression derived from Delta Ct normalized against 18S, and are presented as the mean \pm SEM. * $p < 0.05$; *** $p < 0.001$; **** $p < 0.0001$. (j, k) RNAseq of 40 PC tumor samples and 5 normal pancreas samples (Supporting Information Table 4) with heat map (j) and volcano plot (k) demonstrating the number of significantly, differentially expressed genes. In (k), black data points represent genes not significantly, differentially expressed between the two groups (Norm^{Resect} and PC), and red data points represent genes that achieve significance in terms of gene expression levels between two groups ($p < 0.05$, $|\text{Log}_2\text{FC}| > 1$). Statistical significance was assessed using one-way ANOVA for panels e–i, and using in-built statistical tests within the R package Bioconductor to adjust for false-discovery rates for panel k.

Table 1. Treatable phenotypes of PC

Treatment	Target	Prevalence	TCGA or EUS-FNA
Surgery	Localized disease	20% ⁴	EUS-FNA
Panitumumab	<i>KRAS</i> wild-type	20% ⁴	TCGA
DNA damaging agents	DNA repair pathways	14% ^{16,32}	TCGA
Trastuzumab	HER2 amplification	10–30% ^{9,33}	No CNV available
BRAF and MEK inhibition	<i>BRAF</i> mutation	< 2% ^{8,34,35}	TCGA
Everolimus	PI3K/AKT/mTOR pathway	Unknown expression cut-off ³⁶	NA
Imatinib	<i>KIT</i> , <i>ABL1/2</i> , <i>RET</i> mutation	< 2% ^{37,38}	TCGA
Sorafenib	<i>PDGFR A/B</i> , <i>FLT3</i> mutation	< 2% ³⁹	TCGA
Tamoxifen/Letrozole	Oestrogen/Progesterone receptor expression	Unknown expression cut-off ^{40,41}	Requires protein expression data
Abiraterone	Androgen receptor expression	Unknown expression cut-off ⁴²	Requires protein expression data
c-MET inhibitor (Cabozantinib)	c-MET expression	Unknown expression cut-off Unknown ^{43–45}	Requires protein expression data

CNV, copy number variant.

the leukocyte (immune) cell marker *CD45* were among the lowest in EUS-FNA-derived PC samples, with highest expression levels observed in whole blood samples (as expected) and surprisingly, in resected normal pancreas (Fig. 1I).

To confirm the presence of malignant cells in EUS-FNA samples, we used mutated *KRAS* as a specific marker for PC. *KRAS* mutations were detected in 80% (16/20) of patients (Supporting Information Table 3). Notably, the *KRAS* mutation frequency in the same patients was significantly lower at 45% (9/20, $p < 0.05$) when using gDNA extracted from FFPE blocks (Supporting Information Table 3). We also observed in one of 20 PC patients, mutated *KRAS* in FFPE-derived DNA but not from EUS-FNA-derived DNA specimen. Despite this discrepancy, these data support the requirement for an additional EUS-FNA biopsy for DNA (and/or RNA) isolation in order to enhance sensitivity for *KRAS* mutation detection.

To demonstrate the utility of EUS-FNA-derived RNA for transcriptome profiling, we performed RNASeq on tumor samples from 40 PC patients, and on five normal pancreatic specimens. These analyses revealed 2,148 genes that were significantly, differentially expressed between the two groups (Figs. 1j and 1k). Importantly, the heat map (Fig. 1j) demonstrated a higher degree of heterogeneity in tumor samples compared to the uniform gene expression seen in the five normal samples. Of note, 1/40 PC sample had a transcriptional profile that appeared typical of normal pancreas (Fig. 1j). Since cytological diagnosis confirmed PC, and *KRAS* mutation was detected in the sample used for RNASeq, thus confirming the presence of malignant cells, we speculate that this specimen reflects inter-tumoral heterogeneity.⁶

Collectively, these data indicate the successful procurement of tumor tissue by EUS-FNA with minimal contamination of immune and non-pancreatic epithelial cells. In addition, the

high epithelial (tumor) cell content of EUS-FNA-derived PC suggests the suitability of EUS-FNA for both DNA and RNA-based molecular profiling in PC.

Genetic analysis and transcriptional profiling to guide treatment selection in PC

The greatest potential for the in-depth genetic analysis of EUS-FNA specimens lies in its ability to guide personalized treatment selection for virtually all PC patients. Review of the literature reveals that there are many potential treatable PC phenotypes (Table 1), although some are of very low prevalence (e.g., *PDGFR A/B* mutations which occurs in <2%) and others depend upon the analysis of gene or protein expression levels for which the diagnostic threshold is not clearly defined (e.g., c-MET expression and the use of Cabozantinib). The five most prevalent and potentially treatable phenotypes of PC identified were; Localized PC treated with resection; *KRAS* wild-type treated with anti-EGFR inhibitors^{13–15}; DNA repair pathway mutations (*BRCA1/2*, *ATM*, *PALB2*) treated with DNA-damaging agents¹⁶; *HER2*-amplification treated with trastuzumab^{17,18}; and *BRAF* mutant PC treated with BRAF and MEK inhibitors^{19,20} (Table 1 and Supporting Information Fig. 2). Among these, resection for localized tumors remains the most effective treatment for PC.^{5,21}

A fundamental unanswered question likely to have profound implications with respect to selection of patients for surgical resection is whether localized PC possesses a different molecular and genetic phenotype to metastatic PC. To address this question, we performed transcriptome profiling on EUS-FNA specimens from 20 localized and 20 metastatic PC by RNASeq (Supporting Information Table 4). Somewhat surprisingly, there was a marked homogeneity between the gene expression profiles of localized and metastatic tumors overall, with no significantly, differentially expressed genes

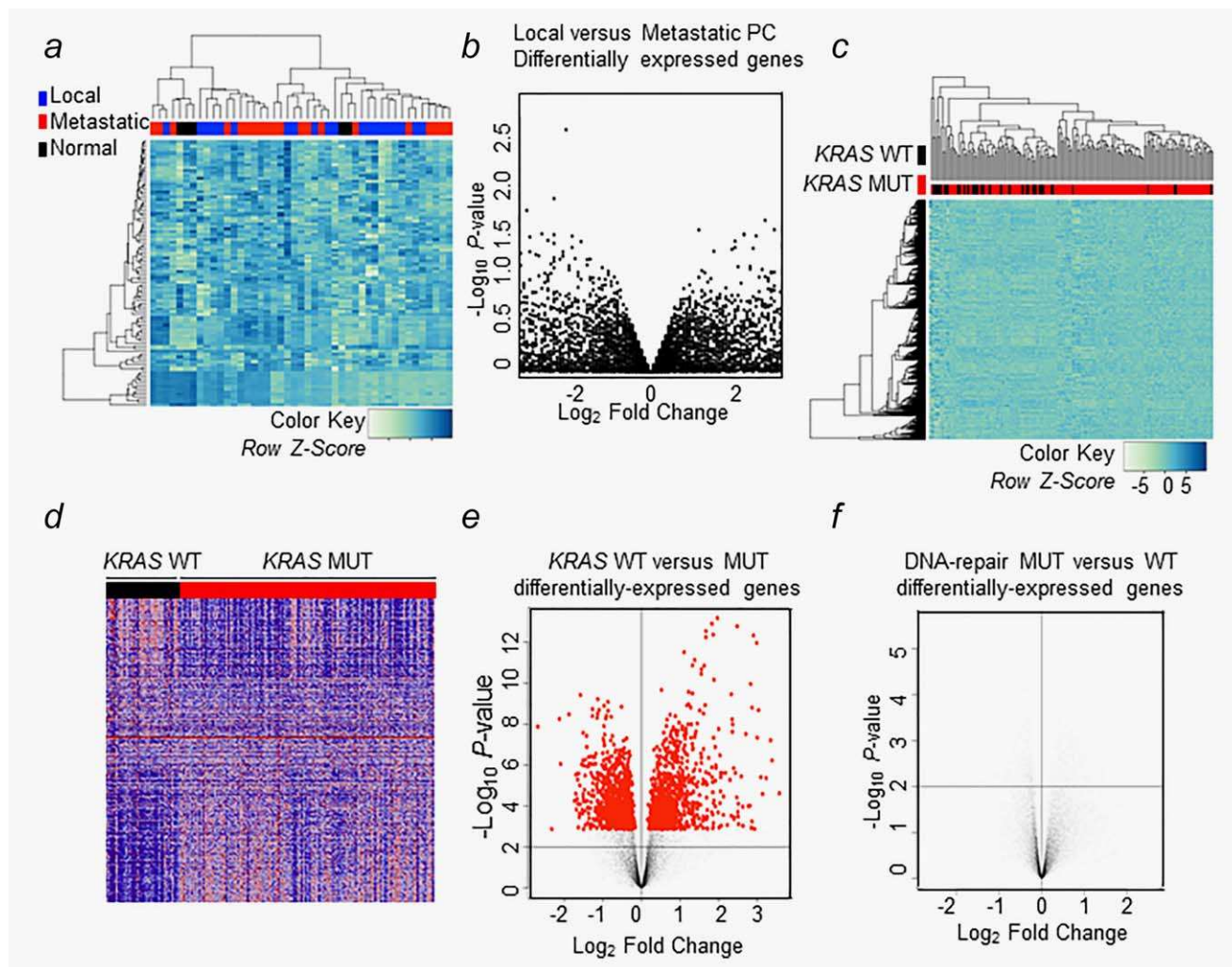


Figure 2. Characterizing treatable phenotypes of PC. Differential gene expression analysis contrasting localized and metastatic PC. (a) Heat map demonstrating gene expression profile of localized ($n = 20$) and metastatic ($n = 20$) EUS-FNA-derived tumors (Supporting Information Table 4), and associated hierarchical clustering. (b) Volcano plot depicting differential gene expression between localized and metastatic tumors from (a). (c–e) For TCGA PC cohort ($n = 170$; Supporting Information Table 5) *KRAS* wild-type (WT) and *KRAS* mutant (MUT) transcriptome profile with (c) a heat map of hierarchical clustering for *KRAS* WT versus *KRAS* MUT, (d) a heat map of 391 differentially-expressed genes, and (e) Volcano plot demonstrating 391 differentially-expressed genes ($|\text{Log}_2\text{FC}| > 1$, $p < 0.01$). (f) Volcano plot showing differential gene expression analysis contrasting PC tumors with DNA repair pathway mutations and those without; no genes reached statistical significance. For panels (b), (e) and (f), black data points represent genes not significantly differentially expressed between the two groups, and red data points represent genes that achieve significance in terms of gene expression levels between two groups ($p < 0.05$, $|\text{Log}_2\text{FC}| > 1$). Statistical significance was assessed using in-built statistical tests within the R package Bioconductor to adjust for false-discovery rates. Panels a and b refer to the RNASeq PC cohort (Supporting Information Table 4), and c–f refer to TCGA cohort (Supporting Information Tables 5 and 7).

identified in the entire transcriptome of either disease stage (Figs. 2a and 2b). These observations were also confirmed upon gene set enrichment analyses (GSEA), which indicated that no gene sets were significantly enriched ($p < 0.01$; false-discovery rate (FDR) $q < 0.25$). These results therefore suggest that despite wide inter-tumoral heterogeneity, the molecular (*i.e.*, gene expression) profile of localized and metastatic PC tumors is comparable, thus providing a potential explanation for the poor outcomes of patients with localized disease after pancreatic resection.

To identify whether the mutational status of tumors for these potentially treatable PC phenotypes correlated with a specific molecular (*i.e.*, gene expression) signature, we next performed *in silico* comparative analyses on matched TCGA genomic and transcriptomic datasets from 170 PC patients with localized disease (*i.e.*, surgical resection specimens; Supporting Information Table 5). The genetic (*i.e.*, mutational status) analysis identified 38 cases with *KRAS* wild-type tumors, 17 cases with DNA repair pathway mutations (*BRCA1/2*, *PALPB*, *ATM*), and four cases with *BRAF* mutation (Table 1, and

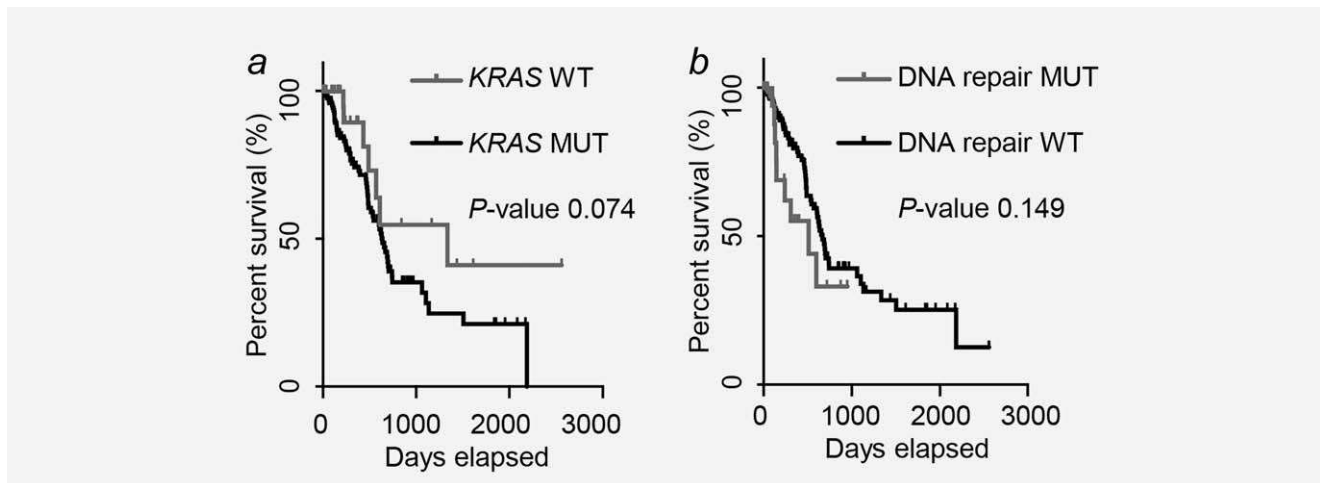


Figure 3. Kaplan–Meier survival analysis for (a) *KRAS* wild-type (WT; $n = 38$) and *KRAS* mutant (MUT; $n = 132$) tumors, and (b) DNA repair pathway mutant (MUT; $n = 17$) and wild-type (WT; $n = 153$) tumors in TCGA PC cohort (Supporting Information Tables 6 and 7).

Supporting Information Fig. 2). We note that there was no copy number variant TCGA data available for *HER2*, which prevented assessment of *HER2* amplification in PC patients. Also, the low number (4/170) of *BRAF* mutant tumors precluded any statistically-meaningful analysis of this treatable phenotype.

Assessment of the transcriptome data for patients with *KRAS* wild-type tumors demonstrated clustering to one side of the hierarchical analysis heat map (Fig. 2c). Also, differential gene expression analysis between *KRAS* wild-type and mutant tumors revealed 391 genes that achieved significance ($p < 0.01$, $|\text{Log}_2\text{FC}| > 1$; Figs. 2d and 2e). Furthermore, comparing these transcriptome profiles against published gene sets using GSEA software revealed five gene sets (Computational gene sets, Cancer Modules 35, 110, 160, 184 and 221) that were significantly enriched in *KRAS* wild-type PC and two gene sets (miR-518 B/C and Kegg pathway glycosaminoglycan-biosynthesis) that were significantly enriched in *KRAS* mutant PC (Supporting Information Table 6, Supporting Information Fig. 3; $p < 0.01$ and $\text{FDR } q < 0.25$). Conversely, the comparison of tumors with and without DNA repair pathway mutations (*BRCA1/2*, *PALPB*, *ATM*) indicated there was no clustering of cases nor any genes that were significantly, differentially expressed (Fig. 1f, and Supporting Information Fig. 2).

Finally, we measured the frequencies of various clinicopathological disease criteria, including overall survival, disease stage and site of disease using Fischer-Exact or χ^2 tests to compare the phenotypes of the *KRAS* wild-type and mutant PC, and to compare the phenotypes in presence or absence of DNA repair pathway mutations (*BRCA1/2*, *PALPB*, *ATM*). Among the criteria assessed, patients with *KRAS* mutant tumors were of a higher grade ($p = 0.0009$) and have shorter survival ($p = 0.016$) versus patients with wild-type *KRAS* (Fig. 3a, and Supporting Information Table 5). In contrast, there was no difference in the clinical phenotype based on the presence or absence of DNA repair mutations (Fig. 3b, and Supporting Information Table 7).

Collectively, these analyses suggest that among the treatable phenotypes in PC, *KRAS* wild-type tumors are the most prevalent and have the most distinctive transcriptome profile and clinical phenotype.

Establishment of PDX models for PC using EUS-FNA to evaluate the treatment responsiveness of *KRAS* wild-type versus mutant tumors

To evaluate the responsiveness of *KRAS* wild-type and mutant tumors to the anti-EGFR inhibitor panitumumab, we established a preclinical PDX model from two PC patients, one *KRAS* wild-type and the other *KRAS* mutant, using EUS-FNA tumor samples (Fig. 4a, and Supporting Information Table 8). We subsequently divided both PDX PC models into four different treatment cohorts: saline, gemcitabine alone (chosen as a representative first-line chemotherapy agent used in PC), panitumumab alone, and a combination of gemcitabine and panitumumab. The *KRAS* wild-type tumors treated with saline all grew to a maximum volume (1,000 mm³) before the treatment course was completed, ranging from 14–21 days, with an average final tumor weight of 1.07 ± 0.08 g. Notably, compared to saline-treated controls, *KRAS* wild-type tumors treated with panitumumab were significantly smaller in volume (Day 14, $p < 0.05$; Day 21, $p < 0.0001$) and final weight (0.19 ± 0.05 g; $p < 0.0001$) over the 28 day experimental treatment period (Figs. 4b and 4c). Similarly, gemcitabine treatment also significantly impaired tumor growth compared to control saline-treated xenografts, however this anti-tumor activity was less pronounced compared to panitumumab (Day 14 and 21, $p < 0.05$; Day 28, $p < 0.01$). Combination therapy had similar effects on tumor growth as panitumumab monotherapy (Figs. 4b and 4c).

Conversely, in *KRAS* mutant tumors, panitumumab alone had no effect on tumor growth, which was comparable to the unimpaired exponential growth seen in saline-treated xenografts (Figs. 4b and 4c). Similar to *KRAS* wild-type tumors, gemcitabine

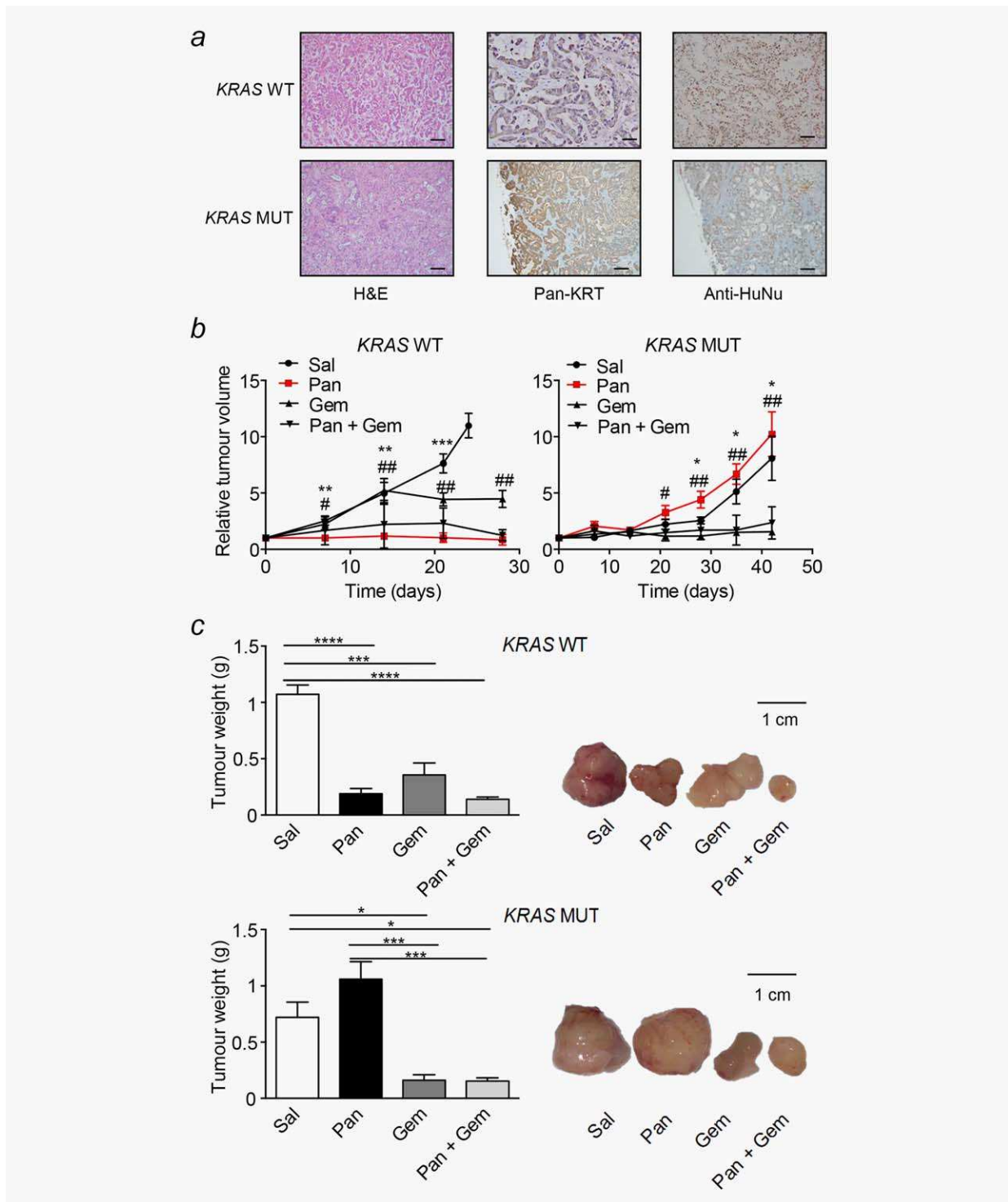


Figure 4. Differential responsiveness of EUS-FNA-derived *KRAS* wild-type and *KRAS* mutant PDXs to anti-EGFR therapy. (a) PDX histology for both *KRAS* wild-type (WT) and *KRAS* mutant (MUT) tumors stained with H&E, as well as pan-Cytokeratin (KRT) and anti-human nuclei (HuNu) antibodies. Scale bars, 50 μ m. (b, c) Treatment of *KRAS* WT and MUT PDXs with panitumumab (Pan), gemcitabine (Gem) and combination therapy (Pan + Gem), along with saline (Sal). Shown are (b) tumor volumes assessed at the indicated times, and (c) tumor weights and photographs of tumor size. $n = 4$ mice per treatment group. Data are expressed as the mean \pm SEM. Panel (b) *KRAS* WT: $**p < 0.01$ and $***p < 0.001$ Sal-treated versus Pan-treated tumor groups, and $\#p < 0.05$ and $##p < 0.01$ Gem-treated versus Pan-treated tumor groups, at the corresponding time points. Panel (b) *KRAS* MUT: $*p < 0.05$ Sal-treated versus Gem-treated tumor groups, and $\#p < 0.05$ and $##p < 0.01$ Pan-treated versus Gem-treated tumor groups, at the corresponding time points. Panel (c), $*p < 0.05$, $***p < 0.001$, and $****p < 0.0001$. Statistical significance was assessed using parametric (one-way ANOVA) or nonparametric (Kruskal-Wallis, Mann-Whitney) tests where appropriate.

alone or in combination with panitumumab had a pronounced inhibitory effect on the growth rate of *KRAS* mutant tumors (Figs. 4*b* and 4*c*), thus ruling out any synergistic effects between these drugs on PC tumors irrespective of their *KRAS* mutation status.

The differential responsiveness of PC *KRAS* wild-type and mutant tumors to panitumumab was associated with changes in tumor cell proliferation, since immunostaining with the cell proliferation marker PCNA was significantly reduced in panitumumab-treated *KRAS* wild-type, but not mutant, PC tumors compared to the corresponding saline-treated control xenografts (Figs. 5*a* and 5*b*). In light of these observations, we next assessed the signalling pathways impacted by the preferential sensitivity of PC *KRAS* wild-type tumors to panitumumab by performing Western blots for proteins related to the EGFR pathway. As shown in Figures 5*c* and 5*d*, compared to saline treatment, panitumumab treatment alone resulted in reduced levels of phosphorylated (p) EGFR in both *KRAS* wild-type and mutant tumors, albeit only significant in the former, which further supports the mode of action of panitumumab to directly block the activation of the EGFR irrespective of the *KRAS* mutation status in PC. Interestingly, activation of the ERK1/2 MAPK pathway, which is associated with cellular proliferation, was significantly reduced only in *KRAS* wild-type tumors treated with panitumumab compared to saline (Figs. 5*c* and 5*d*), which is consistent with the lower proliferative potential of these tumors (Figs. 5*a* and 5*b*). By contrast, no changes were observed in the activation status of the cell survival pathway mediator, AKT (Figs. 5*c* and 5*d*).

Collectively, these *in vivo* data demonstrate that panitumumab is a highly effective agent for the selective treatment of *KRAS* wild-type, but not mutant, tumors in PC. Furthermore, the reduced growth of these PC tumors to panitumumab is associated with the suppression of ERK MAPK signalling and tumor cell proliferation.

Discussion

It is becoming increasingly likely that future advances in PC therapy will rely on treatments tailored to each patient's individual tumor. In this respect, previous genetic characterization of PC has largely relied upon tissue obtained from resection specimens, which are only available in the minority of patients. Therefore, EUS-FNA could overcome this problem since it can be performed in virtually all PC patients. Here, we have sought to validate this by demonstrating the clinical potential for EUS-FNA to provide meaningful genetic information on nearly all patients with PC. EUS-FNA has been widely used to detect mutations in *KRAS*,⁴ but we demonstrate that an additional biopsy is more effective than using FFPE cell blocks, which have been primarily used as the source of genetic material (*i.e.*, genomic DNA) in the past. Therefore, we propose that the acquisition of an additional biopsy during the EUS-FNA procedure is necessary in order to reach sufficient sensitivity if we are to use

mutational status of particular genes to direct therapy. In addition, as *KRAS* mutations are rarely seen in non-neoplastic, solid pancreatic lesions,^{4,8} the ability to detect *KRAS* mutations in EUS-FNA-derived DNA indicates that neoplastic tissue is present in sufficient quantities to obtain meaningful molecular information.

More recently, the transcriptome profile of EUS-FNA-derived RNA for PC has been reported.²² Our study used RNASeq to profile malignant and benign samples in order to generate a diagnostic gene signature, intended for lesions that cannot be diagnosed with cytology alone. However, the sensitivity and specificity of this approach did not improve on cytology alone, suggesting that it is unlikely to be applied in the clinic for diagnostic purposes. Another recent study used EUS-FNA-derived DNA from PC patients to compare the allelic frequency and mutation status of 160 cancer-related genes in EUS-FNA-derived and surgically-derived DNA.²³ In keeping with our findings, our study reported high concordance of mutation status results and similar allelic frequency between both sampling techniques. To further substantiate the tumoral component of EUS-FNA-derived genetic material we have shown here that there is a strong epithelial gene signature, and *KRAS* mutation is detectable in the majority of PC patients. Therefore, these findings support EUS-FNA as a viable technique for obtaining PC tumoral genetic material of sufficient quantity and quality for next-generation sequencing, and thus underpins the advancement of personalized medicine through identification of signatures comprising aberrantly-expressed and/or mutated genes in all PC patients.

Consistent with the known inter-tumoral heterogeneity of PC,⁶ the transcriptome profile of 1/40 EUS-FNA-derived PC samples resembled that of normal pancreas, despite this sample being positive for mutant *KRAS* and cytological analysis verifying adenocarcinoma. Such an example of natural inter-tumoral heterogeneity is also supported by TCGA cohorts stratified into *KRAS* wild-type and mutant, where, for example, the transcription profile of *KRAS* wild-type tumors did not all cluster together (Fig. 2*c*). Furthermore, the heat map (Fig. 2*d*) reveals individual *KRAS* wild-type tumors with a gene expression pattern similar to that seen in *KRAS* mutant tumors (and vice versa).

Since genetic studies to date have largely focused on surgically-derived tissue, thus excluding the majority of patients who present with advanced metastatic disease, an advantage of our current study utilizing EUS-FNA is the ability to contrast the transcriptome profile of localized and metastatic PC. Surprisingly, no significant differences at the molecular level (*i.e.*, gene expression) were identified between these two patient cohorts, therefore indicating that although patients with localized or metastatic disease have markedly different clinical phenotypes, at the molecular level they are remarkably comparable. Importantly, this finding is consistent with two previous studies that attempted to address this issue with a different approach involving patients who underwent pancreatic resection for their cancer and later acquired tissue

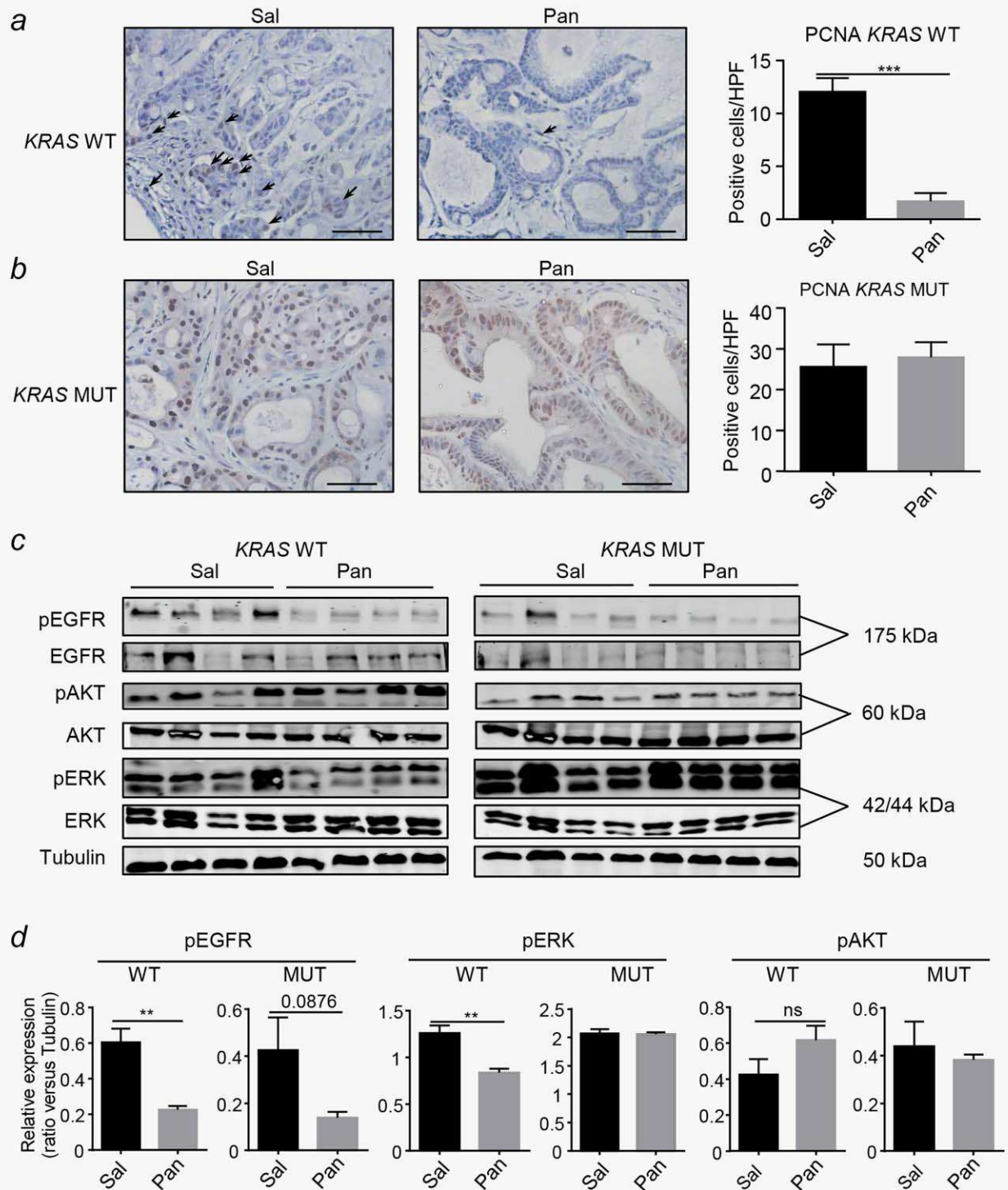


Figure 5. Reduced cellular proliferation in panitumumab-treated *KRAS* wild-type PDX tumors. (a, b) Representative immunostaining for PCNA with associated quantified data for (a) *KRAS* wild-type tumors and (b) *KRAS* mutant tumors treated with saline (Sal) or panitumumab (Pan). Scale bars, 100 μ m. In (a), arrows point to positively-stained cells. Data are presented as mean \pm SEM from $n = 4$ samples/group. $***p < 0.001$. (c) Western blots with the indicated antibodies for EGFR signaling pathways in protein lysates from treated tumors. Each lane represents a single xenograft tumor. (d) Semi-quantitative densitometry analyses of the blots shown in (c). Data presented as mean \pm SEM from $n = 4$ samples/group; $**p < 0.01$. Statistical significance was assessed using one-way ANOVA. [Color figure can be viewed at wileyonlinelibrary.com]

from secondary lesions post-mortem.^{24,25} Transcriptome profiling of tumor samples and adjacent normal tissue has also been used to perform a “virtual microdissection,” which demonstrated that the transcriptome profiles between primary and secondary sites of the same tumor are indeed very similar.²⁵ Also, a high mutational concordance between primary and secondary lesions has been reported.²⁴ Overall, these findings support our data and the notion that there is no molecular difference between metastatic or localized PC, and further suggest it is unlikely that a molecular biomarker for a localized tumor phenotype exists.

Another novel aspect of our current study was the use of TCGA to characterize the most prevalent treatable cancer phenotype, *KRAS* wild-type tumors, in PC, and thus build on previous studies demonstrating that *KRAS* wild-type acts as a biomarker for anti-EGFR treatment in colorectal and lung cancers.^{13,26–29} Indeed, stratifying PC patients according to *KRAS* mutation status revealed, for the first time, large differences in the transcriptome profile. In addition, the differential gene expression profile of *KRAS* wild-type PC tumors corresponded to a different clinical phenotype, characterized by lower tumor grade and longer overall survival. Furthermore, using our PDX PC models derived from EUS-FNA samples, we demonstrate that *KRAS* wild-type tumors were sensitive to the EGFR inhibitor panitumumab, unlike *KRAS* mutant tumors, and the anti-tumor activity of panitumumab was associated with a lower proliferative index and ERK MAPK activation in treated tumors.

Interestingly, Moore, *et al.*³⁰ have previously shown in a trial of another anti-EGFR agent, erlotinib, on unselected

patients that overall survival was increased. However, this difference was only 6.24 months compared to 5.91 months and therefore the treatment has not been widely adopted in clinical practice. It is possible that the relative ineffectiveness of this trial indicates that anti-EGFR therapies (such as erlotinib and panitumumab) need to be applied in a personalized approach, and will not work in all patients. A recent publication has presented data also suggesting that *KRAS* wild-type tumors are more responsive to panitumumab than *KRAS* mutant tumors in a PC PDX model.³¹ Together with our current findings, this provides a strong argument for the use of EUS-FNA to stratify the *KRAS* status of PC for eligibility for panitumumab treatment, and therefore paves the way to replicate these findings in preclinical studies and subsequently in a clinical trial setting.

In summary, we have shown that EUS-FNA can provide a useable source of genetic material to profile the genetic and molecular landscape of individual PC tumors, which in concert with matched PDXs can be used to evaluate the efficacy of personalized anti-cancer treatments. Such a translational pipeline provides the overwhelming majority of patients with PC the potential to participate in and benefit from both preclinical xenograft studies and clinical trials of personalized medicine in the future.

Acknowledgements

The authors would like to recognize the contribution of the research groups involved in the pancreatic cancer arm of The Cancer Genome Atlas (TCGA). We would also like to thank all patients who donated specimens to the Monash Biobank and TCGA.

References

- Hidalgo M. Pancreatic cancer. *N Engl J Med* 2010;362:1605–17.
- Matsuyama M, Ishii H, Kuraoka K, et al. Ultrasound-guided vs endoscopic ultrasound-guided fine-needle aspiration for pancreatic cancer diagnosis. *World J Gastroenterol* 2013;19:2368–73.
- Jani BS, Rzouq F, Saligram S, et al. Endoscopic ultrasound-guided fine-needle aspiration of pancreatic lesions: a systematic review of technical and procedural variables. *N Am J Med Sci* 2016;8:1–11.
- Fuccio L, Hassan C, Laterza L, et al. The role of K-ras gene mutation analysis in EUS-guided FNA cytology specimens for the differential diagnosis of pancreatic solid masses: a meta-analysis of prospective studies. *Gastrointest Endosc* 2013;78:596–608.
- Wade TP, Halaby IA, Stapleton DR, et al. Population-based analysis of treatment of pancreatic cancer and Whipple resection: department of defense hospitals, 1989–1994. *Surgery* 1996;120:680–7.
- Wolpin BM, Rizatto C, Kraft P, et al. Genome-wide association study identifies multiple susceptibility loci for pancreatic cancer. *Nat Genet* 2014;46:994–1000.
- Witkiewicz AK, McMillan EA, Balaji U, et al. Whole-exome sequencing of pancreatic cancer defines genetic diversity and therapeutic targets. *Nat Commun* 2015;6:6744–54.
- Biankin AV, Waddell N, Kassahn KS, et al. Pancreatic cancer genomes reveal aberrations in axon guidance pathway genes. *Nature* 2012;491:399–405.
- Chantrill LA, Nagrial AM, Watson C, et al. Precision medicine for advanced pancreas cancer: the individualized molecular pancreatic cancer therapy (IMPACT) trial. *Clin Cancer Res* 2015;21:2029–37.
- Jones S, Zhang X, Parsons DW, et al. Core signaling pathways in human pancreatic cancers revealed by global genomic analyses. *Science* 2008;321:1801–6.
- Conroy T, Desseigne F, Ychou M, et al. FOLFIRINOX versus gemcitabine for metastatic pancreatic cancer. *N Engl J Med* 2011;364:1817–25.
- Von Hoff DD, Ervin T, Arena FP, et al. Increased survival in pancreatic cancer with nab-paclitaxel plus gemcitabine. *N Engl J Med* 2013;369:1691–703.
- Amado RG, Wolf M, Peeters M, et al. Wild-type *KRAS* is required for panitumumab efficacy in patients with metastatic colorectal cancer. *J Clin Oncol* 2008;26:1626–34.
- Boeck S, Jung A, Laubender RP, et al. EGFR pathway biomarkers in erlotinib-treated patients with advanced pancreatic cancer: translational results from the randomised, crossover phase 3 trial AIO-PK0104. *Br J Cancer* 2013;108:469–76.
- Costa DB, Nguyen KS, Cho BC, et al. Effects of erlotinib in EGFR mutated non-small cell lung cancers with resistance to gefitinib. *Clin Cancer Res* 2008;14:7060–7.
- Villarroel MC, Rajeshkumar NV, Garrido-Laguna I, et al. Personalizing cancer treatment in the age of global genomic analyses: PALB2 gene mutations and the response to DNA damaging agents in pancreatic cancer. *Mol Cancer Ther* 2011;10:3–8.
- Perez EA, Romond EH, Suman VJ, et al. Four-year follow-up of trastuzumab plus adjuvant chemotherapy for operable human epidermal growth factor receptor 2-positive breast cancer: joint analysis of data from NCCTG N9831 and NSABP B-31. *J Clin Oncol* 2011;29:3366–73.
- Slamon DJ, Leyland-Jones B, Shak S, et al. Use of chemotherapy plus a monoclonal antibody against HER2 for metastatic breast cancer that overexpresses HER2. *N Engl J Med* 2001;344:783–92.
- Chapman PB, Hauschild A, Robert C, et al. Improved survival with vemurafenib in melanoma with BRAF V600E mutation. *N Engl J Med* 2011;364:2507–16.
- Johnson AS, Crandall H, Dahlman K, et al. Preliminary results from a prospective trial of

- preoperative combined BRAF and MEK-targeted therapy in advanced BRAF mutation-positive melanoma. *J Am Coll Surg* 2015;220:581–93.
21. Krska Z, Šváb J, Hoskovec D, et al. Pancreatic cancer diagnostics and treatment—current state. *Prague Med Rep* 2015;116:253–67.
 22. Rodriguez SA, Impney SD, Pelz C, et al. RNA sequencing distinguishes benign from malignant pancreatic lesions sampled by EUS-guided FNA. *Gastrointest Endosc* 2016;84:252–8.
 23. Gleeson FC, Kerr SE, Kipp BR, et al. Targeted next generation sequencing of endoscopic ultrasound acquired cytology from ampullary and pancreatic adenocarcinoma has the potential to aid patient stratification for optimal therapy selection. *Oncotarget* 2016;7:54526
 24. Yachida S, Jones S, Bozic I, et al. Distant metastasis occurs late during the genetic evolution of pancreatic cancer. *Nature* 2010;467:1114–7.
 25. Moffitt RA, Marayati R, Flate EL, et al. Virtual microdissection identifies distinct tumor- and stroma-specific subtypes of pancreatic ductal adenocarcinoma. *Nat Genet* 2015;47:1168–78.
 26. Brugger W, Triller N, Blasinska-Morawiec M, et al. Prospective molecular marker analyses of EGFR and KRAS from a randomized, placebo-controlled study of erlotinib maintenance therapy in advanced non-small-cell lung cancer. *J Clin Oncol* 2011;29:4113–20.
 27. Douillard JY, Oliner KS, Siena S, et al. *Panitumumab-FOLFOX4 treatment and RAS mutations in colorectal cancer*. *N Engl J Med* 2013;369:1023–34.
 28. Lievre A, Bachet JB, Le Corre D, et al. *KRAS mutation status is predictive of response to cetuximab therapy in colorectal cancer*. *Cancer Res* 2006;66:3992–5.
 29. Van Cutsem E, Köhne CH, Hitre E, et al. Cetuximab and chemotherapy as initial treatment for metastatic colorectal cancer. *N Engl J Med* 2009;360:1408–17.
 30. Moore MJ, Goldstein D, Hamm J, et al. Erlotinib plus gemcitabine compared with gemcitabine alone in patients with advanced pancreatic cancer: a phase III trial of the National Cancer Institute of Canada Clinical Trials Group. *J Clin Oncol* 2007;25:1960–6.
 31. Lindberg JM, Newhook TE, Adair SJ, et al. Cotreatment with panitumumab and trastuzumab augments response to the MEK inhibitor trametinib in a patient-derived xenograft model of pancreatic cancer. *Neoplasia* 2014;16:562–71.
 32. Waddell N, Pajic M, Patch AM, et al. Whole genomes redefine the mutational landscape of pancreatic cancer. *Nature* 2015;518:495–501.
 33. Saxby AJ, Nielsen A, Scarlett CJ, et al. Assessment of HER-2 status in pancreatic adenocarcinoma: correlation of immunohistochemistry, quantitative real-time RT-PCR, and FISH with aneuploidy and survival. *Am J Surg Pathol* 2005;29:1125–34.
 34. Chang DK, Grimmond SM, Biankin AV. Pancreatic cancer genomics. *Curr Opin Genet Dev* 2014;24C:74–81.
 35. Forbes SA, Beare D, Gunasekaran P, et al. COSMIC: exploring the world's knowledge of somatic mutations in human cancer. *Nucleic Acids Res* 2015;43:D805–11.
 36. Kordes S, Klumpen H, Weterman MJ, et al. Phase II study of capecitabine and the oral mTOR inhibitor everolimus in patients with advanced pancreatic cancer. *Cancer Chemother Pharmacol* 2015;75:1135–41.
 37. Ali Y, Lin Y, Gharibo MM, et al. Phase I and pharmacokinetic study of imatinib mesylate (Gleevec) and gemcitabine in patients with refractory solid tumors. *Clin Cancer Res* 2007;13:5876–82.
 38. Al-Batran SE, Atmaca A, Schleyer E, et al. Imatinib mesylate for targeting the platelet-derived growth factor beta receptor in combination with fluorouracil and leucovorin in patients with refractory pancreatic, bile duct, colorectal, or gastric cancer—a dose-escalation Phase I trial. *Cancer* 2007;109:1897–904.
 39. Cardin DB, Goff L, Li CI, et al. Phase II trial of sorafenib and erlotinib in advanced pancreatic cancer. *Cancer Med* 2014;3:572–9.
 40. Bakkevold KE, Pettersen A, Arnesjø B, et al. Tamoxifen therapy in unresectable adenocarcinoma of the pancreas and the papilla of Vater. *Br J Surg* 1990;77:725–30.
 41. Check JH, Dix E, Cohen R, et al. Efficacy of the progesterone receptor antagonist mifepristone for palliative therapy of patients with a variety of advanced cancer types. *Anticancer Res* 2010;30:623–8.
 42. Negi SS, Agarwal A, Chaudhary A, Flutamide in unresectable pancreatic adenocarcinoma: a randomized, double-blind, placebo-controlled trial. *Invest New Drugs* 2006;24:189–4.
 43. Hage C, Rausch V, Giese N, et al. The novel c-Met inhibitor cabozantinib overcomes gemcitabine resistance and stem cell signaling in pancreatic cancer. *Cell Death Dis* 2013;4:e627.
 44. Jin H, Yang R, Zheng Z, et al. MetMab, the one-armed 5D5 anti-c-Met antibody, inhibits orthotopic pancreatic tumor growth and improves survival. *Cancer Res* 2008;68:4360–8.
 45. Delitto D, Vertes-George E, Hughes SJ, et al. c-Met signaling in the development of tumorigenesis and chemoresistance: potential applications in pancreatic cancer. *World J Gastroenterol* 2014;20:8458–70.

Appendix 6 - Book chapter: Methods in molecular biology:
Inflammation and cancer. **Berry, W.**, Croagh, D. Chapter: Utility of
endoscopic ultrasound-guided fine-needle aspiration for preclinical
evaluation of therapies in cancer

Utility of endoscopic ultrasound-guided fine-needle aspiration for preclinical evaluation of therapies in cancer

William Berry, Daniel Croagh

Abstract

Personalising cancer therapy is a way of improving treatment efficacy, by selecting specific treatments for patients with certain molecular changes to their tumour. This requires both molecular material to detect these targets and a preclinical disease model to demonstrate treatment efficacy. In pancreatic cancer this is problematic, as most patients present with advanced disease and are therefore ineligible for surgery. As a result, biological material derived from such patients has been excluded from all preclinical studies in personalised medicine. This chapter presents methodology to achieve both of the above-mentioned requirements using endoscopic ultrasound-guided fine-needle aspiration, which can be offered to nearly all patients with early or advanced disease.

Keywords: RNAseq, RNA, xenograft, target therapy, personalised therapy, NOD-SCID mice, EUS-FNA, pancreatic cancer, oncology

1 Introduction

Pancreatic cancer (PC) is a highly lethal malignancy, and often patients will present late, with advanced disease. As such, only very few patients are eligible for surgical resection, and the overall five-year survival remains low at 5%. PC and other malignancies are beginning to look towards personalised therapy, whereby treatments are designed to specifically target mutations unique to individual tumours. In terms of establishing viable therapeutic targets in a pre-clinical setting, two main points need to be addressed: 1) obtain genetic material from the tumour to detect molecular target; 2) demonstrate efficacy for targeted therapy against specific tumour phenotype. In PC, this presents a problem, as genetic material is often obtained from

surgery, however, surgery is only offered to 20% of patients. Tissue can also be obtained from percutaneous biopsy of liver metastases but this is often of small volume and quality and thus the majority of patients are not potential candidates for personalised therapy [1].

Endoscopic ultrasound-guided fine-needle aspirate (EUS-FNA) is a minimally invasive biopsy technique that is an important means of obtaining tissue in PC. It is the predominant method of obtaining tissue from patients with locally advanced PC [1] and with the increasing utilization of neoadjuvant chemotherapy it is likely that EUS-FNA will also be increasingly utilised in patients with resectable PC. This emphasizes the importance of maximizing the potential utility of this technique to guide personalised therapy in PC. However, to date there has been minimal use of EUS-FNA to characterize the genetic profile of PC.

Although DNA has been isolated from these samples in numerous studies [2-9], RNA has only been reported in two studies [10,11]. Both of these studies performed RNAseq, a highly sensitive sequencing technology to analyse the entire transcriptome. To address this issue, this chapter presents methodology for utilizing EUS-FNA for molecular characterisation of PC based on the isolation of DNA and RNA from EUS-FNA samples.

Any novel personalised therapies will need to be assessed in preclinical models to establish their potential efficacy, prior to embarking on clinical trials. Patient-derived xenografts represent an excellent *in vivo* model for this purpose [12]. Patient-derived xenograft studies involve the growth of a cancer cells in an immune-deficient mouse, whereby the cancer cells for the xenografts are derived directly from the patient. Xenografted tumours have been shown to retain the characteristics of the original patient tumour in terms of histological architecture and molecular profiles [13-15], which makes xenograft models an ideal tool to demonstrate a biological response to personalised therapies designed to target specific tumour molecular profiles [16]. However, patient-derived xenograft models in PC have been largely restricted to utilizing surgical resection specimens that are only available in

approximately 20% of patients. Importantly, there have only been 2 reports of the use of EUS-FNA samples to create patient-derived xenograft models [10,17]. Here we present the methodology for using EUS-FNA to develop patient-derived xenograft models in PC and thus allow preclinical trials of targeted therapy in this setting.

2 Materials

2.1 Human specimen collection

1. EUS-FNA needle used by Endoscopist to collect tissue for diagnostic, molecular and xenograft purposes. (see **Note 1**)
2. Microscope, glass slides and *Diff-Quik* stain, used by cytopathologist to confirm adequate cellularity and provide a provisional diagnosis.
3. 1 x 2mL plastic collection tube with lockable lid labeled with de-identified sample code to collect research sample for molecular studies.
4. 1 x specimen jar with 5mL cell culture medium for collecting research sample for xenograft studies.
5. 2mL sterile 0.9% saline, used to flush the EUS-FNA needle.
6. Liquid nitrogen in insulated container for snap freezing sample for molecular analyses.
7. Wet ice in insulated container for transporting sample for xenografting.

2.2 Molecular analyses

1. *Qiagen Universal Allprep kit*. (see **Note 2**)
2. Supplement *Allprep* lysis buffer with 5% beta-mercaptoethanol.

2.3 Xenograft

1. Cell culture sterile fume hood.
2. Wet ice for transporting samples at ~4°C.
3. Sterile cell culture petri-dish and scalpel for preparing the sample.
4. 100µm cell strainer.

5. 15mL and 50mL conical centrifuge tubes for washing and re-suspending the sample.
6. Centrifuge.
7. 1:1 ratio (v/v) of 300µL of *Matrigel* diluted in cell culture medium. (see **Note 3**)
8. 4 x 1mL syringe (for xenograft and analgesic drug delivery).
9. 2 x 27 gauge needles (for xenograft and analgesic drug delivery).
10. 2 x 6 week-old female (preferred for housing logistics) NOD-SCID or NOD-SCID Gamma mice (Non-obese diabetic, severe combined immune deficiency).
11. Isoflurane for light anesthesia with anesthetic chamber.
12. Heat mat and sterile sheet for operating field.
13. Caprofen and bupivacaine for peri-operative analgesia for the mice.
14. Recovery cage.
15. Cell culture medium (serum free): RPMI (Roswell Park Memorial Institute) medium supplemented with 1% Penicillin-Streptomycin, 1% L-Glutamine, 1% HEPES (4-(2-hydroxyethyl)-1-piperazineethanesulfonic acid), 1% Non-essential amino acids. Store at 4°C. (see **Note 4**)

2.4 Passage of xenografts

1. Donor NOD-SCID mouse with grafted tumour.
2. Recipient NOD-SCID mice (up to n = 8 per 1000mm³ tumour).
3. Sterile cell culture petri dish.
4. Thawed 1:1 (v/v) *Matrigel* diluted with cell culture medium.
5. Wet ice in insulated container.
6. Specimen pot with formalin.
7. 1 x 2mL plastic collection tube with lockable lid.
8. Liquid nitrogen in insulated container.
9. Isoflurane and anesthesia induction chamber, with nose cone and maintenance flow (or injectable anesthesia equipment).
10. Hair clippers.
11. Antiseptic solution (betadine or 80% ethanol).
12. Surgical kit (with dissection scissors, forceps and scalpel).

13. Suturing material or surgical staples for wound closure.
14. Heat mat and sterile sheet for surgical field.
15. Caprofen and bupivacaine for peri-operative analgesia for the mice.
16. 3 x 1mL syringes for local anaesthesia, analgesia and blood collection.
17. 3 x 27 gauge needles for local anaesthesia, analgesia and blood collection.
18. Recovery cage.

3 Methods

3.1 Human specimen collection

1. PC samples were collected from patients undergoing EUS FNA for investigation of a pancreatic mass. Initial diagnostic aspirates from the pancreatic mass were collected using 22-gauge *Procore* needles with 10cc of suction for immediate cytological assessment (see **Note 1**).
2. Cytopathologist confirms the cellular quantity and provides a provisional diagnosis based on the initial passes and diagnostic material is obtained for the cell block, which is then processed according to local pathology service protocol.
3. Additional 1-2 passes were taken from the same position as the diagnostic passes and then either snap-frozen in liquid nitrogen or placed into 5mL of cell culture medium pot to be kept on wet ice (see **Note 5**).
4. To expel samples from the needle stylus replacement was followed by 1mL flush with 0.9% saline and 5mL of air (see **Note 6**).

3.2 Molecular analyses

1. Snap frozen EUS-FNA samples are transferred into double the recommended volume of lysis buffer provided in the *Allprep* kit. (see **Notes 2 and 7**)
2. Samples are homogenised and then processed according to the manufacturer's instructions. (see **Note 8**)

3.3 Xenograft

1. EUS-FNA samples appear as a “worm” of tissue, which is carefully transferred to a sterile petri dish in a cell culture hood.
2. The sample (worm) is minced with a scalpel blade.
3. This slurry of sample and 5mL cell culture medium is then passed through the 100 μ m cell strainer into a 50mL conical centrifuge tube. This is done with a 1mL pipette and then gently pressed through the 100 μ m strainer with the flat plunger end of a 2-5ml sterile syringe.
4. Once the majority of the slurry has been strained, invert the strainer and “back-wash” with cell culture medium into the same conical centrifuge tube (see **Note 9**).
5. Centrifuge the slurry at 800g for 5 minutes (at 4°C if possible).
6. Remove supernatant.
7. Re-suspend pellet in 5mL cell culture medium.
8. Centrifuge the slurry at 800g for 5 minutes (at 4°C if possible) to wash sample.
9. Re-suspend pellet in 5mL cell culture medium.
10. Centrifuge the slurry 800g for another 5 minutes (at 4°C if possible) for final wash.
11. Re-suspend pellet in 300 μ L 1:1 (v/v) of *Matrigel* and cell culture medium (see **Note 3** and **4**).
12. Mix gently by slowly pipetting up and down 10 times.
13. Draw up 150 μ L of slurry into 2 x 1mL syringes and carefully place on ice (see **Note 10**).
14. Maintaining sterility and sample temperature ~4°C, by keeping all samples on wet ice in a closed container, transport all materials to animal housing facility (see **Note 11**).
15. Prepare heat mat, sterile field and a spare recovery cage for mice to rise from sedation.
16. Prepare isoflurane anesthesia chamber.
17. Induce isoflurane anesthesia by placing mouse in induction chamber, then move mouse into position for maintenance dose

- (onto nose cone with low flow isoflurane) (see **Notes 12, 13 and 14**).
18. Check for adequate sedation using toe or tail pinch and corneal reflex.
 19. Once the animal is sedated inject a small volume (10-50 μ L) of bupivacaine into the site of the graft (flank) intradermally (see **Note 15**).
 20. Inject 150 μ L of sample slurry into the flank subcutaneously.
 21. Inject 50 μ L of caprofen into another site subcutaneously (see **Notes 12 and 16**).
 22. Cease isoflurane flow and administer oxygen or room air until animal wakes.
 23. Place animal into recovery cage and monitor.
 24. Repeat above steps with second animal.
 25. Monitor both animals until effects of anesthesia have worn off.
 26. Return 24 hours later to administer second dose of caprofen subcutaneously.
 27. Monitor mice twice weekly for tumour growth using palpation and digital calipers (see **Notes 17 and 18**).

3.4 Passage of xenografts

1. Prepare surgical equipment and surgical field in animal house fume hood (see **Note 11**).
2. Euthanize donor mouse using carbon dioxide induced asphyxiation (see **Note 12**).
3. Collect blood for serum if desired via cardiac puncture of venipuncture using a 1mL syringe and 27 gauge needle.
4. Make a midline incision in the skin on the abdomen of the mouse using surgical scissors and expand this up the midline of the mouse, taking care to only cut the skin and not pierce the abdominal wall.
5. Expose the tumour by creating a large mobile skin flap with the tumour still attached to the skin, but dissected away from the abdominal wall.

6. Dissect away tumour using blunt dissection.
7. Take photos of the tumour with a ruler or measuring device and weigh the tumour.
8. Cut the tumour into quarters.
9. Place one quarter into specimen pot with 5mL formalin for histology (see **Note 19**).
10. Place one quarter into a plastic 2mL capped tube and then into liquid nitrogen for subsequent molecular analyses.
11. The remaining half (i.e. two quarters) will be used for passaging.
12. In the sterile petri dish, use the scalpel to shave off 2mm pieces of the fleshy outer layer of the tumour (see **Note 20**).
13. Place these into the diluted *Matrigel* and leave on wet ice
14. Anaesthetize one recipient mouse using inhaled isoflurane (see **Notes 12 and 13**).
15. Shave the flank of the mouse where the graft will be implanted.
16. Clean the graft site with antiseptic solution (betadine or 80% ethanol).
17. Make a 2mm incision in the flank of the animal using surgical scissors.
18. Using blunt dissection create a larger subcutaneous pocket.
19. Carefully implant 2 x 2mm slices of grafted tumour coated with diluted *Matrigel* into the pocket.
20. Oppose wound edges with forceps and close wound with either sutures or surgical staples.
21. Inject 50 μ L bupivacaine intradermally into the wound and surrounding skin (see **Note 15**).
22. Inject 50 μ L caprofen subcutaneously in a site separate to graft site (see **Notes 12 and 16**).
23. Monitor animal until complete recovery from anesthesia.
24. Return in 24 hours for a second dose of 50 μ L caprofen injected subcutaneously.
25. Repeat this process with all remaining recipient mice
26. Monitor tumour growth in new cohort of mice twice weekly with palpation and digital calipers (see **Notes 17, 18 and 21**).

4 Notes

1. Collection needle will be determined by Endoscopist.
2. It is likely that the RNA or DNA extraction kit is immaterial, however, it is important to use more than the recommended volume of lysis buffer as the amount of sample and type of tissue can result in low or degraded yields if the lysis buffer volume is inadequate.
3. Matrigel needs to be stored at -80°C and thawed at 4°C overnight to become a viscous liquid. At room temperature this will set and become solid, therefore care must be taken to ensure Matrigel is kept on ice at 4°C and needles, syringes and cell culture medium that will come into contact with Matrigel should be kept on ice also.
4. Additional growth factors can be added to supplement cell growth and facilitate grafting, however many of these are already present in *Matrigel*.
5. Number of passes and amount of material available to researchers will be determined by the Endoscopist, local ethical research governance and patient factors.
6. Caution should be taken when expelling samples from needles as this requires handling of the sharp needle. In addition, the flushing of saline and air can result in a splash, eye protection should be worn and care taken to avoid the sample splashing out of the collection tube or pot.
7. Ensure lysis buffer is supplemented with beta-mercaptoethanol to stabilize RNA throughout the process.
8. Make sure extraction process is performed in an RNAase free environment and performed in an efficient manner, as contamination and prolonged time at room temperature can lead to RNA degradation.
9. The purpose of the cell strainer is not to create a single-cell suspension, but to finely break up sample into small enough pieces so that the slurry that can be injected. As such, the “back-wash”

step is used to capture any cells that didn't pass through the strainer, but they are still able to be used.

10. It is important that these needles remain sterile and that the contents are not accidentally expelled when they are placed on ice.
11. NOD-SCID and NOD-SCID Gamma mice are severely immunocompromised. Animal housing facility needs to maintain diligent pathogen free environment and all animal handling needs to be performed in a sterile fume hood with sterile surgical gown and gloves.
12. Anesthesia, analgesia and euthanasia protocols should be used in accordance with the local practices of the animal facility, the training of the researcher and the approval of relevant ethical governing bodies.
13. When administering general anesthesia or sedation to animals it is best if two researchers are present, one to monitor the animal's breathing and conscious state, while the other researcher performs the xenograft.
14. High flow oxygen aids recovery and minimizes sedation time, the availability of high flow oxygen on inhaled anesthetic machines is also an important tool to prevent overdose as rapid reversal can be achieved.
15. Bupivacaine is a local anesthetic agent that works for 4-8 hours and provides relief as there is a significant stretch of the skin at the site of injection.
16. Caprofen is a non-steroidal anti-inflammatory drug that acts systemically to minimize inflammation, this should be administered at the time of injection and 24 hours later to prevent pain and excessive inflammation.
17. Once tumours reach a maximum size (defined as an ethical end point in ethics approval document), then tumours must be passaged or cryopreserved and the animal humanely sacrificed.
18. Tumour volume calculated using the following formula: $(2 \times \text{Width} \times \text{Length}) / 2 = V \text{ mm}^3$.

19. Histology staining should be performed at each passage to confirm cell type and tumour architecture. Xenografts of upper gastrointestinal tumours can commonly grow lymphoma, rather than the desired adenocarcinoma, therefore immunostaining for epithelial markers should be performed.
20. It is important to only use the fleshy outer layers of the tumour, as the hard inner layer is fibrotic and paucicellular, as can be seen on the histology studies of the formalin fixed samples. In addition, some larger tumours will have a liquefied core, this is necrosis and therefore not viable grafting tissue.
21. Tumours tend to grow much faster in subsequent passages, therefore care should be taken to monitor these tumours closely.

References

1. Wade TP, Halaby IA, Stapleton DR, Virgo KS, Johnson FE (1996) Population-based analysis of treatment of pancreatic cancer and Whipple resection: Department of Defense hospitals, 1989-1994. *Surgery* 120 (4):680-685; discussion 686-687
2. Fuccio L, Hassan C, Laterza L, Correale L, Pagano N, Bocus P, Fabbri C, Maimone A, Cennamo V, Repici A, Costamagna G, Bazzoli F, Larghi A (2013) The role of K-ras gene mutation analysis in EUS-guided FNA cytology specimens for the differential diagnosis of pancreatic solid masses: a meta-analysis of prospective studies. *Gastrointestinal endoscopy* 78 (4):596-608. doi:10.1016/j.gie.2013.04.162
3. Bournet B, Souque A, Senesse P, Assenat E, Barthet M, Lesavre N, Aubert A, O'Toole D, Hammel P, Levy P, Ruszniewski P, Bouisson M, Escourrou J, Cordelier P, Buscail L (2009) Endoscopic ultrasound-guided fine-needle aspiration biopsy coupled with KRAS mutation assay to distinguish pancreatic cancer from pseudotumoral chronic pancreatitis. *Endoscopy* 41 (6):552-557. doi:10.1055/s-0029-1214717
4. Maluf-Filho F, Kumar A, Gerhardt R, Kubrusly M, Sakai P, Hondo F, Matuguma SE, Artifon E, Monteiro da Cunha JE, Cesar Machado MC, Ishioka S, Forero E (2007) Kras mutation analysis of fine needle aspirate under EUS guidance facilitates risk stratification of patients with pancreatic mass. *Journal of clinical gastroenterology* 41 (10):906-910. doi:10.1097/MCG.0b013e31805905e9
5. Pellise M, Castells A, Gines A, Sole M, Mora J, Castellvi-Bel S, Rodriguez-Moranta F, Fernandez-Esparrach G, Llach J, Bordas JM, Navarro S, Pique JM (2003) Clinical usefulness of KRAS mutational

- analysis in the diagnosis of pancreatic adenocarcinoma by means of endosonography-guided fine-needle aspiration biopsy. *Alimentary pharmacology & therapeutics* 17 (10):1299-1307
6. Tada M, Komatsu Y, Kawabe T, Sasahira N, Isayama H, Toda N, Shiratori Y, Omata M (2002) Quantitative analysis of K-ras gene mutation in pancreatic tissue obtained by endoscopic ultrasonography-guided fine needle aspiration: clinical utility for diagnosis of pancreatic tumor. *Am J Gastroenterol* 97 (9):2263-2270. doi:10.1111/j.1572-0241.2002.05980.x
 7. Takahashi K, Yamao K, Okubo K, Sawaki A, Mizuno N, Ashida R, Koshikawa T, Ueyama Y, Kasugai K, Hase S, Kakumu S (2005) Differential diagnosis of pancreatic cancer and focal pancreatitis by using EUS-guided FNA. *Gastrointestinal endoscopy* 61 (1):76-79
 8. Wang X, Gao J, Ren Y, Gu J, Du Y, Chen J, Jin Z, Zhan X, Li Z, Huang H, Lv S, Gong Y (2011) Detection of KRAS gene mutations in endoscopic ultrasound-guided fine-needle aspiration biopsy for improving pancreatic cancer diagnosis. *Am J Gastroenterol* 106 (12):2104-2111. doi:10.1038/ajg.2011.281
 9. Ogura T, Yamao K, Hara K, Mizuno N, Hijioka S, Imaoka H, Sawaki A, Niwa Y, Tajika M, Kondo S, Tanaka T, Shimizu Y, Bhatia V, Higuchi K, Hosoda W, Yatabe Y (2013) Prognostic value of K-ras mutation status and subtypes in endoscopic ultrasound-guided fine-needle aspiration specimens from patients with unresectable pancreatic cancer. *Journal of gastroenterology* 48 (5):640-646. doi:10.1007/s00535-012-0664-2
 10. Berry W, Algar E, Kumar B, Desmond C, Swan M, Jenkins BJ, Croagh D (2017) Endoscopic ultrasound-guided fine-needle aspirate-derived preclinical pancreatic cancer models reveal panitumumab sensitivity in KRAS wild-type tumors. *International journal of cancer Journal international du cancer*. doi:10.1002/ijc.30648
 11. Rodriguez SA, Impey SD, Pelz C, Enestvedt B, Bakis G, Owens M, Morgan TK (2016) RNA sequencing distinguishes benign from malignant pancreatic lesions sampled by EUS-guided FNA. *Gastrointestinal endoscopy*. doi:10.1016/j.gie.2016.01.042
 12. Morton CL, Houghton PJ (2007) Establishment of human tumor xenografts in immunodeficient mice. *Nature protocols* 2 (2):247-250. doi:10.1038/nprot.2007.25
 13. Daniel VC, Marchionni L, Hierman JS, Rhodes JT, Devereux WL, Rudin CM, Yung R, Parmigiani G, Dorsch M, Peacock CD, Watkins DN (2009) A primary xenograft model of small-cell lung cancer reveals irreversible changes in gene expression imposed by culture in vitro. *Cancer Res* 69 (8):3364-3373. doi:10.1158/0008-5472.CAN-08-4210
 14. Fichtner I, Rolff J, Soong R, Hoffmann J, Hammer S, Sommer A, Becker M, Merk J (2008) Establishment of patient-derived non-small cell lung cancer xenografts as models for the identification of predictive biomarkers. *Clinical cancer research : an official journal of the American Association for Cancer Research* 14 (20):6456-6468. doi:10.1158/1078-0432.CCR-08-0138
 15. Whiteford CC, Bilke S, Greer BT, Chen Q, Braunschweig TA, Cenacchi N, Wei JS, Smith MA, Houghton P, Morton C, Reynolds CP, Lock R, Gorlick R, Khanna C, Thiele CJ, Takikita M, Catchpole D, Hewitt SM,

- Khan J (2007) Credentialing preclinical pediatric xenograft models using gene expression and tissue microarray analysis. *Cancer Res* 67 (1):32-40. doi:10.1158/0008-5472.CAN-06-0610
16. Rangarajan A, Weinberg RA (2003) Opinion: Comparative biology of mouse versus human cells: modelling human cancer in mice. *Nat Rev Cancer* 3 (12):952-959. doi:10.1038/nrc1235
 17. Jang SY, Bae HI, Lee IK, Park HK, Cho CM (2015) Successful Xenograft of Endoscopic Ultrasound-Guided Fine-Needle Aspiration Specimen from Human Extrahepatic Cholangiocarcinoma into an Immunodeficient Mouse. *Gut Liver* 9 (6):805-808. doi:10.5009/gnl14279

Appendix 7 – Professional development

Training Title	Graduate Education Hours
Excellence in Research & Teaching (26)	73.50
Cutting Edge Research Technologies in Biomedical Sciences - Research Technology Platforms (Advanced) - Monash Bioinformatics Platform (Programming in R)	10.00
Cutting Edge Research Technologies in Biomedical Sciences - Research Technology Platforms (Advanced) - Data Workshop - Histology Platform	2.00
Cutting Edge Research Technologies in Biomedical Sciences - Research Technology Platforms (Introductory) - Animal Models and Drug Development	1.00
Cutting Edge Research Technologies in Biomedical Sciences - Research Technology Platforms (Introductory) - Drug Discovery	1.00
Cutting Edge Research Technologies in Biomedical Sciences - Research Technology Platforms (Introductory) - Gene characterisation - Research Technologies	1.00
Cutting Edge Research Technologies in Biomedical Sciences - Research Technology Platforms (Introductory) - Imaging - Research Technologies	1.00
Cutting Edge Research Technologies in Biomedical Sciences - Research Technology Platforms (Introductory) - Informatics and Applied Maths - Research Technologies	1.00

Cutting Edge Research Technologies in Biomedical Sciences - Research Technology Platforms (Introductory) - Microscope and Data Management - Research Technologies	1.00
Cutting Edge Research Technologies in Biomedical Sciences - Research Technology Platforms (Introductory) - Overview - Research Technologies	1.00
Cutting Edge Research Technologies in Biomedical Sciences - Research Technology Platforms (Introductory) - Rapid Fabrication - Research Technologies	1.00
Foundations for Teaching Associates (Online)	3.00
Maximise Your Motivation: Why Human Needs are Key	7.00
MGE Online: Excel 2016 - Advanced Formulas and Functions	6.50
MGE Online: Learn NVivo - The Basics	1.50
MGE Online: Learning Python	2.50
MGE Online: Learning R	2.50
MGE Online: R Statistics Essential Training	6.00
MGE Online: SPSS Statistics Essential Training	5.00
MGE Online: Word 2013 - Creating Long Documents	3.50
MS Word 2013 - Level 2 (19/7/16)	3.00
Ph.D. Completion Masterclass (2/6/16)	3.00
Questionnaire Design (18/05/16)	2.00
Research Platforms: Software packages for statistics	2.00
Research Platforms: What statistical methods should you be using?	2.00
Structural Biology - Research Technologies - level 1 COMPULSORY	1.00
Turbocharge Your Writing (30/5/16)	3.00

Professionalism, Career & Innovation (19)	74.50
Communicating the Impact of your Research – The Use of Media (1/6/16)	3.00
Entrepreneurship and Commercialisation Series - Lecture 4 (22/4/16)	2.00
Getting published: how to write a good journal article (9/5/16)	3.00
Introduction to Management (ONLINE Foundation Unit)	7.00
Introduction to Project Management ONLINE	7.00
MGE Online: Professional Skills for Research Leaders	
MGE Online: Professional skills for research leaders - Communicating your research	3.50
MGE Online: Professional skills for research leaders - Developing and consolidating your research career	3.00
MGE Online: Professional skills for research leaders - Funding your research	2.00
MGE Online: Professional skills for research leaders - Introduction	1.50
MGE Online: Professional skills for research leaders - Managing a research team	3.00
MGE Online: Professional skills for research leaders - Research collaboration	2.50
MGE Online: Unleash your teamwork	1.50
MGE: Presenting Your Research with Impact	4.00
Nailing Grants, papers, prizes, and awards: How to write yourself to success (18/5/16)	10.00
Networking: (ONLINE Foundation Unit) The essential guide to connecting and building your profile.	7.00

Networking: The essential guide to connecting and building your profile (19/5/16)	6.50
Project Management Support Webinar 2	1.00
Working with teams ONLINE	7.00
Total hours	148

References

1. Jemal A., Siegel R., Ward E., Murray T., Xu J., Smigal C. *et al.* (2006) Cancer statistics, 2006. *CA Cancer J Clin* 56 (2):106-130
2. Hidalgo Manuel (2010) Pancreatic Cancer. *New England Journal of Medicine* 362 (17):1605-1617. doi:doi:10.1056/NEJMra0901557
3. Cascinu S., Jelic S., Group Esmo Guidelines Working (2009) Pancreatic cancer: ESMO clinical recommendations for diagnosis, treatment and follow-up. *Annals of Oncology* 20 Suppl 4:37-40
4. Jemal Ahmedin, Bray Freddie, Center Melissa M., Ferlay Jacques, Ward Elizabeth, Forman David (2011) Global cancer statistics. *CA Cancer J Clin* 61 (2):69-90. doi:10.3322/caac.20107
5. Wade T. P., Halaby I. A., Stapleton D. R., Virgo K. S., Johnson F. E. (1996) Population-based analysis of treatment of pancreatic cancer and Whipple resection: Department of Defense hospitals, 1989-1994. *Surgery* 120 (4):680-685; discussion 686-687
6. Lynch S. M., Vrieling A., Lubin J. H., Kraft P., Mendelsohn J. B., Hartge P. *et al.* (2009) Cigarette smoking and pancreatic cancer: a pooled analysis from the pancreatic cancer cohort consortium. *American Journal of Epidemiology* 170 (4):403-413
7. Jiao L., Silverman D. T., Schairer C., Thiebaut A. C., Hollenbeck A. R., Leitzmann M. F. *et al.* (2009) Alcohol use and risk of pancreatic cancer: the NIH-AARP Diet and Health Study. *American Journal of Epidemiology* 169 (9):1043-1051
8. Klein A. P., Brune K. A., Petersen G. M., Goggins M., Tersmette A. C., Offerhaus G. J. *et al.* (2004) Prospective risk of pancreatic cancer in familial pancreatic cancer kindreds. *Cancer Research* 64 (7):2634-2638
9. Shi C., Hruban R. H., Klein A. P. (2009) Familial pancreatic cancer. *Archives of Pathology & Laboratory Medicine* 133 (3):365-374
10. Biankin A. V., Waddell N., Kassahn K. S., Gingras M. C., Muthuswamy L. B., Johns A. L. *et al.* (2012) Pancreatic cancer genomes reveal aberrations in axon guidance pathway genes. *Nature* 491 (7424):399-405. doi:10.1038/nature11547
11. Maitra A., Hruban R. H. (2008) Pancreatic cancer. *Annual Review Of Pathology* 3:157-188
12. Whipple A. O., Parsons W. B., Mullins C. R. (1935) Treatment of Carcinoma of the Ampulla of Vater. *Ann Surg* 102 (4):763-779
13. Krska Z., Svab J., Hoskovec D., Ulrych J. (2015) Pancreatic Cancer Diagnostics and Treatment - Current State. *Prague Med Rep* 116 (4):253-267. doi:10.14712/23362936.2015.65

14. Burris H., Storniolo A. M. (1997) Assessing clinical benefit in the treatment of pancreas cancer: gemcitabine compared to 5-fluorouracil. *European Journal of Cancer* 33 Suppl 1:S18-22
15. Burris H. A., 3rd, Moore M. J., Andersen J., Green M. R., Rothenberg M. L., Modiano M. R. *et al.* (1997) Improvements in survival and clinical benefit with gemcitabine as first-line therapy for patients with advanced pancreas cancer: a randomized trial. *J Clin Oncol* 15 (6):2403-2413
16. Von Hoff D. D., Ervin T., Arena F. P., Chiorean E. G., Infante J., Moore M. *et al.* (2013) Increased survival in pancreatic cancer with nab-paclitaxel plus gemcitabine. *N Engl J Med* 369 (18):1691-1703. doi:10.1056/NEJMoa1304369
17. Moore M. J., Goldstein D., Hamm J., Figer A., Hecht J. R., Gallinger S. *et al.* (2007) Erlotinib plus gemcitabine compared with gemcitabine alone in patients with advanced pancreatic cancer: a phase III trial of the National Cancer Institute of Canada Clinical Trials Group. *J Clin Oncol* 25 (15):1960-1966. doi:10.1200/JCO.2006.07.9525
18. Conroy T., Desseigne F., Ychou M., Bouche O., Guimbaud R., Becouarn Y. *et al.* (2011) FOLFIRINOX versus gemcitabine for metastatic pancreatic cancer. *N Engl J Med* 364 (19):1817-1825. doi:10.1056/NEJMoa1011923
19. Chan K., Shah K., Lien K., Coyle D., Lam H., Ko Y. J. (2014) A Bayesian meta-analysis of multiple treatment comparisons of systemic regimens for advanced pancreatic cancer. *PLoS One* 9 (10):e108749. doi:10.1371/journal.pone.0108749
20. Neoptolemos J. P., Palmer D. H., Ghaneh P., Psarelli E. E., Valle J. W., Halloran C. M. *et al.* (2017) Comparison of adjuvant gemcitabine and capecitabine with gemcitabine monotherapy in patients with resected pancreatic cancer (ESPAC-4): a multicentre, open-label, randomised, phase 3 trial. *Lancet* 389 (10073):1011-1024. doi:10.1016/S0140-6736(16)32409-6
21. Wolpin BM, Rizzato C, Kraft P, Kooperberg C, Petersen GM, Wang Z, *et al.* (2014) Genome-wide association study identifies multiple susceptibility loci for pancreatic cancer. *Nat Genet* 46:994-1000
22. Witkiewicz AK, McMillan EA, Balaji U, Baek G, Lin WC, Mansour J, Mollaee M, Wagner KU, Koduru P, Yopp A, Choti MA, Yeo CJ, McCue P, White MA, Knudsen ES. (2015) Whole-exome sequencing of pancreatic cancer defines genetic diversity and therapeutic targets. *Nat Commun* 6:6744-6754
23. Bailey P., Chang D. K., Nones K., Johns A. L., Patch A. M., Gingras M. C. *et al.* (2016) Genomic analyses identify molecular subtypes of pancreatic cancer. *Nature* 531 (7592):47-52. doi:10.1038/nature16965
24. Cancer Genome Atlas Research Network. Electronic address andrew.aguirre@dfci.harvard.edu, Cancer Genome Atlas Research Network (2017) Integrated Genomic Characterization of Pancreatic Ductal Adenocarcinoma. *Cancer Cell* 32 (2):185-203 e113. doi:10.1016/j.ccell.2017.07.007
25. Biankin A. V., Hudson T. J. (2011) Somatic variation and cancer: therapies lost in the mix. *Human Genetics* 130 (1):79-91

26. Chang D. K., Grimmond S. M., Biankin A. V. (2014) Pancreatic cancer genomics. *Curr Opin Genet Dev* 24C:74-81. doi:10.1016/j.gde.2013.12.001
27. Jones S., Zhang X., Parsons D. W., Lin J. C., Leary R. J., Angenendt P. *et al.* (2008) Core signaling pathways in human pancreatic cancers revealed by global genomic analyses. *Science* 321 (5897):1801-1806
28. Graham J. S., Jamieson N. B., Rulach R., Grimmond S. M., Chang D. K., Biankin A. V. (2014) Pancreatic cancer genomics: where can the science take us? *Clin Genet.* doi:10.1111/cge.12536
29. Perez E. A., Romond E. H., Suman V. J., Jeong J. H., Davidson N. E., Geyer C. E., Jr. *et al.* (2011) Four-year follow-up of trastuzumab plus adjuvant chemotherapy for operable human epidermal growth factor receptor 2-positive breast cancer: joint analysis of data from NCCTG N9831 and NSABP B-31. *J Clin Oncol* 29 (25):3366-3373. doi:10.1200/JCO.2011.35.0868
30. Slamon D. J., Leyland-Jones B., Shak S., Fuchs H., Paton V., Bajamonde A. *et al.* (2001) Use of chemotherapy plus a monoclonal antibody against HER2 for metastatic breast cancer that overexpresses HER2. *New England Journal of Medicine* 344 (11):783-792
31. Chapman P. B., Hauschild A., Robert C., Haanen J. B., Ascierto P., Larkin J. *et al.* (2011) Improved survival with vemurafenib in melanoma with BRAF V600E mutation. *N Engl J Med* 364 (26):2507-2516. doi:10.1056/NEJMoa1103782
32. Falchook G. S., Long G. V., Kurzrock R., Kim K. B., Arkenau T. H., Brown M. P. *et al.* (2012) Dabrafenib in patients with melanoma, untreated brain metastases, and other solid tumours: a phase 1 dose-escalation trial. *Lancet* 379 (9829):1893-1901. doi:10.1016/S0140-6736(12)60398-5
33. Johnson A. S., Crandall H., Dahlman K., Kelley M. C. (2015) Preliminary Results from a Prospective Trial of Preoperative Combined BRAF and MEK-Targeted Therapy in Advanced BRAF Mutation-Positive Melanoma. *J Am Coll Surg* 220 (4):581-593. doi:10.1016/j.jamcollsurg.2014.12.057
34. Amado R. G., Wolf M., Peeters M., Van Cutsem E., Siena S., Freeman D. J. *et al.* (2008) Wild-type KRAS is required for panitumumab efficacy in patients with metastatic colorectal cancer. *J Clin Oncol* 26 (10):1626-1634. doi:10.1200/JCO.2007.14.7116
35. Brugger W., Triller N., Blasinska-Morawiec M., Curescu S., Sakalauskas R., Manikhas G. M. *et al.* (2011) Prospective molecular marker analyses of EGFR and KRAS from a randomized, placebo-controlled study of erlotinib maintenance therapy in advanced non-small-cell lung cancer. *J Clin Oncol* 29 (31):4113-4120. doi:10.1200/JCO.2010.31.8162
36. Chantrill L. A., Nagrial A. M., Watson C., Johns A. L., Martyn-Smith M., Simpson S. *et al.* (2015) Precision Medicine for Advanced Pancreas Cancer: The Individualized Molecular Pancreatic Cancer Therapy (IMPaCT) Trial. *Clin Cancer Res* 21 (9):2029-2037. doi:10.1158/1078-0432.CCR-15-0426
37. Vogelstein B., Papadopoulos N., Velculescu V. E., Zhou S., Diaz L. A., Jr., Kinzler K. W. (2013) Cancer genome landscapes. *Science* 339 (6127):1546-1558

38. Crnogorac-Jurcevic T., Efthimiou E., Capelli P., Blaveri E., Baron A., Terris B. *et al.* (2001) Gene expression profiles of pancreatic cancer and stromal desmoplasia. *Oncogene* 20 (50):7437-7446
39. Symmans W. F., Ayers M., Clark E. A., Stec J., Hess K. R., Sneige N. *et al.* (2003) Total RNA yield and microarray gene expression profiles from fine-needle aspiration biopsy and core-needle biopsy samples of breast carcinoma. *Cancer* 97 (12):2960-2971. doi:10.1002/cncr.11435
40. Wakatsuki T., Irisawa A., Bhutani M. S., Hikichi T., Shibukawa G., Takagi T. *et al.* (2005) Comparative study of diagnostic value of cytologic sampling by endoscopic ultrasonography-guided fine-needle aspiration and that by endoscopic retrograde pancreatography for the management of pancreatic mass without biliary stricture. *Journal of Gastroenterology & Hepatology* 20 (11):1707-1711
41. Fuccio L., Hassan C., Laterza L., Correale L., Pagano N., Bocus P. *et al.* (2013) The role of K-ras gene mutation analysis in EUS-guided FNA cytology specimens for the differential diagnosis of pancreatic solid masses: a meta-analysis of prospective studies. *Gastrointest Endosc* 78 (4):596-608. doi:10.1016/j.gie.2013.04.162
42. Ogura T., Yamao K., Hara K., Mizuno N., Hijioka S., Imaoka H. *et al.* (2013) Prognostic value of K-ras mutation status and subtypes in endoscopic ultrasound-guided fine-needle aspiration specimens from patients with unresectable pancreatic cancer. *J Gastroenterol* 48 (5):640-646. doi:10.1007/s00535-012-0664-2
43. Shin S. H., Kim S. C., Hong S. M., Kim Y. H., Song K. B., Park K. M. *et al.* (2013) Genetic alterations of K-ras, p53, c-erbB-2, and DPC4 in pancreatic ductal adenocarcinoma and their correlation with patient survival. *Pancreas* 42 (2):216-222. doi:10.1097/MPA.0b013e31825b6ab0
44. Boeck S., Jung A., Laubender R. P., Neumann J., Egg R., Goritschan C. *et al.* (2013) EGFR pathway biomarkers in erlotinib-treated patients with advanced pancreatic cancer: translational results from the randomised, crossover phase 3 trial AIO-PK0104. *British Journal of Cancer* 108 (2):469-476. doi:10.1038/bjc.2012.495
45. Willems S Van Deurzen C, Van Diest PJ. (2012) Diagnosis of breast lesions: fineneedle aspiration cytology or core needle biopsy? A review. *Clin Pathol* 65:287–292.
46. Bournet B., Souque A., Senesse P., Assenat E., Barthet M., Lesavre N. *et al.* (2009) Endoscopic ultrasound-guided fine-needle aspiration biopsy coupled with KRAS mutation assay to distinguish pancreatic cancer from pseudotumoral chronic pancreatitis. *Endoscopy* 41 (6):552-557. doi:10.1055/s-0029-1214717
47. Maluf-Filho F., Kumar A., Gerhardt R., Kubrusly M., Sakai P., Hondo F. *et al.* (2007) Kras mutation analysis of fine needle aspirate under EUS guidance facilitates risk stratification of patients with pancreatic mass. *J Clin Gastroenterol* 41 (10):906-910. doi:10.1097/MCG.0b013e31805905e9
48. Pellise M., Castells A., Gines A., Sole M., Mora J., Castellvi-Bel S. *et al.* (2003) Clinical usefulness of KRAS mutational analysis in the diagnosis of pancreatic adenocarcinoma by means of endosonography-guided fine-needle aspiration biopsy. *Aliment Pharmacol Ther* 17 (10):1299-1307

49. Tada M., Komatsu Y., Kawabe T., Sasahira N., Isayama H., Toda N. *et al.* (2002) Quantitative analysis of K-ras gene mutation in pancreatic tissue obtained by endoscopic ultrasonography-guided fine needle aspiration: clinical utility for diagnosis of pancreatic tumor. *American Journal of Gastroenterology* 97 (9):2263-2270. doi:10.1111/j.1572-0241.2002.05980.x
50. Takahashi K., Yamao K., Okubo K., Sawaki A., Mizuno N., Ashida R. *et al.* (2005) Differential diagnosis of pancreatic cancer and focal pancreatitis by using EUS-guided FNA. *Gastrointest Endosc* 61 (1):76-79
51. Wang X., Gao J., Ren Y., Gu J., Du Y., Chen J. *et al.* (2011) Detection of KRAS gene mutations in endoscopic ultrasound-guided fine-needle aspiration biopsy for improving pancreatic cancer diagnosis. *American Journal of Gastroenterology* 106 (12):2104-2111. doi:10.1038/ajg.2011.281
52. Hewitt M. J., McPhail M. J., Possamai L., Dhar A., Vlavianos P., Monahan K. J. (2012) EUS-guided FNA for diagnosis of solid pancreatic neoplasms: a meta-analysis. *Gastrointest Endosc* 75 (2):319-331. doi:10.1016/j.gie.2011.08.049
53. Schwartz M. R. (2004) Endoscopic ultrasound-guided fine-needle aspiration. *Cancer* 102 (4):203-206. doi:10.1002/cncr.20486
54. Gillis A., Cipollone I., Cousins G., Conlon K. (2015) Does EUS-FNA molecular analysis carry additional value when compared to cytology in the diagnosis of pancreatic cystic neoplasm? A systematic review. *HPB (Oxford)* 17 (5):377-386. doi:10.1111/hpb.12364
55. Thosani N., Thosani S., Qiao W., Fleming J. B., Bhutani M. S., Guha S. (2010) Role of EUS-FNA-based cytology in the diagnosis of mucinous pancreatic cystic lesions: a systematic review and meta-analysis. *Dig Dis Sci* 55 (10):2756-2766. doi:10.1007/s10620-010-1361-8
56. LA van der Waaij, HM van Dullemen, RJ Porte (2005) Cyst fluid analysis in the differential diagnosis of pancreatic cystic lesions: a pooled analysis. *Gastrointest Endosc* 62 (3):383 - 389
57. Rodriguez S. A., Impey S. D., Pelz C., Enestvedt B., Bakis G., Owens M. *et al.* (2016) RNA sequencing distinguishes benign from malignant pancreatic lesions sampled by EUS-guided FNA. *Gastrointest Endosc*. doi:10.1016/j.gie.2016.01.042
58. Garuti Anna, Rocco Ilaria, Cirmena Gabriella, Chiaramondia Maurizio, Baccini Paola, Calabrese Massimo *et al.* (2014) Quantitative Real Time PCR assessment of hormonal receptors and HER2 status on fine-needle aspiration pre-operative specimens from a prospectively accrued cohort of women with suspect breast malignant lesions. *Gynecologic Oncology* 132 (2):389-396. doi:<http://dx.doi.org/10.1016/j.ygyno.2013.11.020>
59. De Rienzo A., Dong L., Yeap B. Y., Jensen R. V., Richards W. G., Gordon G. J. *et al.* (2011) Fine-needle aspiration biopsies for gene expression ratio-based diagnostic and prognostic tests in malignant pleural mesothelioma. *Clin Cancer Res* 17 (2):310-316. doi:10.1158/1078-0432.CCR-10-0806
60. Bhasin M. K., Ndebele K., Bucur O., Yee E. U., Otu H. H., Plati J. *et al.* (2016) Meta-analysis of transcriptome data identifies a novel 5-gene pancreatic adenocarcinoma classifier. *Oncotarget*. doi:10.18632/oncotarget.8139

61. Gleeson F. C., Kerr S. E., Kipp B. R., Voss J. S., Minot D. M., Tu Z. J. *et al.* (2016) Targeted next generation sequencing of endoscopic ultrasound acquired cytology from ampullary and pancreatic adenocarcinoma has the potential to aid patient stratification for optimal therapy selection. *Oncotarget*. doi:10.18632/oncotarget.9440
62. Costa D. B., Nguyen K. S., Cho B. C., Sequist L. V., Jackman D. M., Riely G. J. *et al.* (2008) Effects of erlotinib in EGFR mutated non-small cell lung cancers with resistance to gefitinib. *Clin Cancer Res* 14 (21):7060-7067. doi:10.1158/1078-0432.CCR-08-1455
63. Normanno N., Tejpar S., Morgillo F., De Luca A., Van Cutsem E., Ciardiello F. (2009) Implications for KRAS status and EGFR-targeted therapies in metastatic CRC. *Nat Rev Clin Oncol* 6 (9):519-527. doi:10.1038/nrclinonc.2009.111
64. Villarroel M. C., Rajeshkumar N. V., Garrido-Laguna I., De Jesus-Acosta A., Jones S., Maitra A. *et al.* (2011) Personalizing cancer treatment in the age of global genomic analyses: PALB2 gene mutations and the response to DNA damaging agents in pancreatic cancer. *Mol Cancer Ther* 10 (1):3-8. doi:10.1158/1535-7163.MCT-10-0893
65. Waddell N., Pajic M., Patch A. M., Chang D. K., Kassahn K. S., Bailey P. *et al.* (2015) Whole genomes redefine the mutational landscape of pancreatic cancer. *Nature* 518 (7540):495-501. doi:10.1038/nature14169
66. Moffitt R. A., Marayati R., Flate E. L., Volmar K. E., Loeza S. G., Hoadley K. A. *et al.* (2015) Virtual microdissection identifies distinct tumor- and stroma-specific subtypes of pancreatic ductal adenocarcinoma. *Nat Genet* 47 (10):1168-1178. doi:10.1038/ng.3398
67. Chantrill L. A. (2013) The IMPACT trial: Individualised Molecular Pancreatic Cancer Therapy . A randomised open label phase II study of standard first line treatment or personalised treatment in patients with recurrent or metastatic pancreatic cancer. AGITG,
68. Daniel V. C., Marchionni L., Hierman J. S., Rhodes J. T., Devereux W. L., Rudin C. M. *et al.* (2009) A primary xenograft model of small-cell lung cancer reveals irreversible changes in gene expression imposed by culture in vitro. *Cancer Research* 69 (8):3364-3373. doi:10.1158/0008-5472.CAN-08-4210
69. Fichtner I., Rolff J., Soong R., Hoffmann J., Hammer S., Sommer A. *et al.* (2008) Establishment of patient-derived non-small cell lung cancer xenografts as models for the identification of predictive biomarkers. *Clin Cancer Res* 14 (20):6456-6468. doi:10.1158/1078-0432.CCR-08-0138
70. Rangarajan A., Weinberg R. A. (2003) Opinion: Comparative biology of mouse versus human cells: modelling human cancer in mice. *Nature Reviews Cancer* 3 (12):952-959. doi:10.1038/nrc1235
71. Bissery M. C., Vrignaud P., Lavelle F., Chabot G. G. (1996) Experimental antitumor activity and pharmacokinetics of the camptothecin analog irinotecan (CPT-11) in mice. *Anticancer Drugs* 7 (4):437-460
72. Rubio-Viqueira B., Jimeno A., Cusatis G., Zhang X., Iacobuzio-Donahue C., Karikari C. *et al.* (2006) An in vivo platform for translational drug development in

pancreatic cancer. *Clin Cancer Res* 12 (15):4652-4661. doi:10.1158/1078-0432.CCR-06-0113

73. Zhang F., Ma J., Wu J., Ye L., Cai H., Xia B. *et al.* (2009) PALB2 links BRCA1 and BRCA2 in the DNA-damage response. *Curr Biol* 19 (6):524-529. doi:10.1016/j.cub.2009.02.018

74. Audeh M. W., Carmichael J., Penson R. T., Friedlander M., Powell B., Bell-McGuinn K. M. *et al.* (2010) Oral poly(ADP-ribose) polymerase inhibitor olaparib in patients with BRCA1 or BRCA2 mutations and recurrent ovarian cancer: a proof-of-concept trial. *Lancet* 376 (9737):245-251. doi:10.1016/S0140-6736(10)60893-8

75. Tutt Andrew, Robson Mark, Garber Judy E., Domchek Susan M., Audeh M. William, Weitzel Jeffrey N. *et al.* (2010) Oral poly(ADP-ribose) polymerase inhibitor olaparib in patients with BRCA1 or BRCA2 mutations and advanced breast cancer: a proof-of-concept trial. *The Lancet* 376 (9737):235-244

76. Yuan S. S., Lee S. Y., Chen G., Song M., Tomlinson G. E., Lee E. Y. (1999) BRCA2 is required for ionizing radiation-induced assembly of Rad51 complex in vivo. *Cancer Research* 59 (15):3547-3551

77. Fong P. C., Boss D. S., Yap T. A., Tutt A., Wu P., Mergui-Roelvink M. *et al.* (2009) Inhibition of poly(ADP-ribose) polymerase in tumors from BRCA mutation carriers. *New England Journal of Medicine* 361 (2):123-134

78. Voskoglou-Nomikos T., Pater J. L., Seymour L. (2003) Clinical predictive value of the in vitro cell line, human xenograft, and mouse allograft preclinical cancer models. *Clin Cancer Res* 9 (11):4227-4239

79. Tentler J. J., Tan A. C., Weekes C. D., Jimeno A., Leong S., Pitts T. M. *et al.* (2012) Patient-derived tumour xenografts as models for oncology drug development. *Nat Rev Clin Oncol* 9 (6):338-350. doi:10.1038/nrclinonc.2012.61

80. Hwang C. I., Boj S. F., Clevers H., Tuveson D. A. (2016) Preclinical models of pancreatic ductal adenocarcinoma. *J Pathol* 238 (2):197-204. doi:10.1002/path.4651

81. Peterson J. K., Houghton P. J. (2004) Integrating pharmacology and in vivo cancer models in preclinical and clinical drug development. *European Journal of Cancer* 40 (6):837-844. doi:10.1016/j.ejca.2004.01.003

82. Aparicio S., Hidalgo M., Kung A. L. (2015) Examining the utility of patient-derived xenograft mouse models. *Nature Reviews Cancer* 15 (5):311-316. doi:10.1038/nrc3944

83. Balkwill F., Charles K. A., Mantovani A. (2005) Smoldering and polarized inflammation in the initiation and promotion of malignant disease. *Cancer Cell* 7 (3):211-217

84. Balkwill Fran, Mantovani Alberto (2001) Inflammation and cancer: back to Virchow? *The Lancet* 357 (9255):539-545. doi:10.1016/s0140-6736(00)04046-0

85. Hanahan D., Weinberg R. A. (2000) The hallmarks of cancer. *Cell* 100 (1):57-70

86. Coussens L. M., Werb Z. (2001) Inflammatory cells and cancer: think different! *Journal of Experimental Medicine* 193 (6):F23-26

87. Candido J., Hagemann T. (2013) Cancer-related inflammation. *J Clin Immunol* 33 Suppl 1:S79-84. doi:10.1007/s10875-012-9847-0
88. Mantovani A., Allavena P., Sica A., Balkwill F. (2008) Cancer-related inflammation. *Nature* 454 (7203):436-444
89. Cylwik B., Nowak H. F., Puchalski Z., Barczyk J. (1985) Chronische Pankreatitis als prädisponierender Faktor in der Entwicklung des Pankreaskrebses (Chronic pancreatitis as a predisposing factor in the development of pancreatic cancer. Histological and histochemical studies.). *Zentralblatt für Allgemeine Pathologie und Pathologische Anatomie* 130 (3):217-224
90. Guerra C., Schuhmacher A. J., Canamero M., Grippo P. J., Verdaguer L., Perez-Gallego L. *et al.* (2007) Chronic pancreatitis is essential for induction of pancreatic ductal adenocarcinoma by K-Ras oncogenes in adult mice. *Cancer Cell* 11 (3):291-302
91. Lowenfels A. B., Maisonneuve P., Cavallini G., Ammann R. W., Lankisch P. G., Andersen J. R. *et al.* (1993) Pancreatitis and the risk of pancreatic cancer. International Pancreatitis Study Group. *New England Journal of Medicine* 328 (20):1433-1437
92. Malka D., Hammel P., Maire F., Rufat P., Madeira I., Pessione F. *et al.* (2002) Risk of pancreatic adenocarcinoma in chronic pancreatitis. *Gut* 51 (6):849-852
93. Steele C. W., Jamieson N. B., Evans T. R., McKay C. J., Sansom O. J., Morton J. P. *et al.* (2013) Exploiting inflammation for therapeutic gain in pancreatic cancer. *British Journal of Cancer* 108 (5):997-1003. doi:10.1038/bjc.2013.24
94. Hruban R. H., Wilentz R. E., Kern S. E. (2000) Genetic progression in the pancreatic ducts. *American Journal of Pathology* 156 (6):1821-1825
95. Hruban R. H., Maitra A., Goggins M. (2008) Update on pancreatic intraepithelial neoplasia. *Int J Clin Exp Pathol* 1 (4):306-316
96. Hruban R. H., Goggins M., Parsons J., Kern S. E. (2000) Progression model for pancreatic cancer. *Clinical Cancer Research* 6 (8):2969-2972
97. Tuveson D. A., Hingorani S. R. (2005) Ductal pancreatic cancer in humans and mice. *Cold Spring Harbor Symposia on Quantitative Biology* 70:65-72
98. Miki Y., Ono K., Hata S., Suzuki T., Kumamoto H., Sasano H. (2012) The advantages of co-culture over mono cell culture in simulating in vivo environment. *J Steroid Biochem Mol Biol* 131 (3-5):68-75. doi:10.1016/j.jsbmb.2011.12.004
99. Gong Z., Xu H., Su Y., Wu W., Hao L., Han C. (2015) Establishment of a Novel Bladder Cancer Xenograft Model in Humanized Immunodeficient Mice. *Cell Physiol Biochem* 37 (4):1355-1368. doi:10.1159/000430401
100. Rongvaux A., Willinger T., Martinek J., Strowig T., Gearty S. V., Teichmann L. L. *et al.* (2014) Development and function of human innate immune cells in a humanized mouse model. *Nat Biotechnol* 32 (4):364-372. doi:10.1038/nbt.2858

101. Shultz L. D., Lyons B. L., Burzenski L. M., Gott B., Chen X., Chaleff S. *et al.* (2005) Human lymphoid and myeloid cell development in NOD/LtSz-scid IL2R gamma null mice engrafted with mobilized human hemopoietic stem cells. *Journal of Immunology* 174 (10):6477-6489
102. Holzapfel B. M., Wagner F., Thibaudeau L., Levesque J. P., Hutmacher D. W. (2015) Concise review: humanized models of tumor immunology in the 21st century: convergence of cancer research and tissue engineering. *Stem Cells* 33 (6):1696-1704. doi:10.1002/stem.1978
103. King M. A., Covassin L., Brehm M. A., Racki W., Pearson T., Leif J. *et al.* (2009) Human peripheral blood leucocyte non-obese diabetic-severe combined immunodeficiency interleukin-2 receptor gamma chain gene mouse model of xenogeneic graft-versus-host-like disease and the role of host major histocompatibility complex. *Clin Exp Immunol* 157 (1):104-118. doi:10.1111/j.1365-2249.2009.03933.x
104. Douillard J. Y., Oliner K. S., Siena S., Tabernero J., Burkes R., Barugel M. *et al.* (2013) Panitumumab-FOLFOX4 treatment and RAS mutations in colorectal cancer. *N Engl J Med* 369 (11):1023-1034. doi:10.1056/NEJMoa1305275
105. Lievre A., Bachet J. B., Le Corre D., Boige V., Landi B., Emile J. F. *et al.* (2006) KRAS mutation status is predictive of response to cetuximab therapy in colorectal cancer. *Cancer Research* 66 (8):3992-3995. doi:10.1158/0008-5472.CAN-06-0191
106. Van Cutsem E., Kohne C. H., Hitre E., Zaluski J., Chang Chien C. R., Makhson A. *et al.* (2009) Cetuximab and chemotherapy as initial treatment for metastatic colorectal cancer. *N Engl J Med* 360 (14):1408-1417. doi:10.1056/NEJMoa0805019
107. Forbes S. A., Beare D., Gunasekaran P., Leung K., Bindal N., Boutselakis H. *et al.* (2015) COSMIC: exploring the world's knowledge of somatic mutations in human cancer. *Nucleic Acids Res* 43 (Database issue):D805-811. doi:10.1093/nar/gku1075
108. Berlin J. D., Adak S., Vaughn D. J., Flinker D., Blaszkowsky L., Harris J. E. *et al.* (2000) A phase II study of gemcitabine and 5-fluorouracil in metastatic pancreatic cancer: an Eastern Cooperative Oncology Group Study (E3296). *Oncology* 58 (3):215-218. doi:12103
109. Roehrig S., Wein A., Albrecht H., Konturek P. C., Reulbach U., Mannlein G. *et al.* (2010) Palliative first-line treatment with weekly high-dose 5-fluorouracil as 24h-infusion and gemcitabine in metastatic pancreatic cancer (UICC IV). *Med Sci Monit* 16 (3):CR124-131
110. Pelzer U., Arnold D., Reitzig P., Herrenberger J., Korsten F. W., Kindler M. *et al.* (2011) First-line treatment of pancreatic cancer patients with the combination of 5-fluorouracil/folinic acid plus gemcitabine: a multicenter phase II trial by the CONKO-study group. *Cancer Chemother Pharmacol* 68 (5):1173-1178. doi:10.1007/s00280-011-1602-3
111. Berlin J. D., Catalano P., Thomas J. P., Kugler J. W., Haller D. G., Benson A. B., 3rd (2002) Phase III study of gemcitabine in combination with fluorouracil versus gemcitabine alone in patients with advanced pancreatic carcinoma: Eastern Cooperative Oncology Group Trial E2297. *J Clin Oncol* 20 (15):3270-3275

112. Heinemann V., Wilke H., Mergenthaler H. G., Clemens M., König H., Illiger H. J. *et al.* (2000) Gemcitabine and cisplatin in the treatment of advanced or metastatic pancreatic cancer. *Annals of Oncology* 11 (11):1399-1403
113. Philip P. A., Zalupski M. M., Vaitkevicius V. K., Arlauskas P., Chaplen R., Heilbrun L. K. *et al.* (2001) Phase II study of gemcitabine and cisplatin in the treatment of patients with advanced pancreatic carcinoma. *Cancer* 92 (3):569-577
114. Kulke M. H., Tempero M. A., Niedzwiecki D., Hollis D. R., Kindler H. L., Cusnir M. *et al.* (2009) Randomized phase II study of gemcitabine administered at a fixed dose rate or in combination with cisplatin, docetaxel, or irinotecan in patients with metastatic pancreatic cancer: CALGB 89904. *J Clin Oncol* 27 (33):5506-5512. doi:10.1200/JCO.2009.22.1309
115. Heinemann V., Quietzsch D., Gieseler F., Gonnermann M., Schonekas H., Rost A. *et al.* (2006) Randomized phase III trial of gemcitabine plus cisplatin compared with gemcitabine alone in advanced pancreatic cancer. *J Clin Oncol* 24 (24):3946-3952. doi:10.1200/JCO.2005.05.1490
116. Colucci G., Labianca R., Di Costanzo F., Gebbia V., Carteni G., Massidda B. *et al.* (2010) Randomized phase III trial of gemcitabine plus cisplatin compared with single-agent gemcitabine as first-line treatment of patients with advanced pancreatic cancer: the GIP-1 study. *J Clin Oncol* 28 (10):1645-1651. doi:10.1200/JCO.2009.25.4433
117. Reni M., Passoni P., Panucci M. G., Nicoletti R., Galli L., Balzano G. *et al.* (2001) Definitive results of a phase II trial of cisplatin, epirubicin, continuous-infusion fluorouracil, and gemcitabine in stage IV pancreatic adenocarcinoma. *J Clin Oncol* 19 (10):2679-2686
118. Reni M., Cordio S., Milandri C., Passoni P., Bonetto E., Oliani C. *et al.* (2005) Gemcitabine versus cisplatin, epirubicin, fluorouracil, and gemcitabine in advanced pancreatic cancer: a randomised controlled multicentre phase III trial. *Lancet Oncol* 6 (6):369-376. doi:10.1016/S1470-2045(05)70175-3
119. Rocha Lima C. M., Savarese D., Bruckner H., Dudek A., Eckardt J., Hainsworth J. *et al.* (2002) Irinotecan plus gemcitabine induces both radiographic and CA 19-9 tumor marker responses in patients with previously untreated advanced pancreatic cancer. *J Clin Oncol* 20 (5):1182-1191
120. Stathopoulos G. P., Rigatos S. K., Dimopoulos M. A., Giannakakis T., Foutzilas G., Kouroussis C. *et al.* (2003) Treatment of pancreatic cancer with a combination of irinotecan (CPT-11) and gemcitabine: a multicenter phase II study by the Greek Cooperative Group for Pancreatic Cancer. *Annals of Oncology* 14 (3):388-394
121. Rocha Lima C. M., Green M. R., Rotche R., Miller W. H., Jr., Jeffrey G. M., Cisar L. A. *et al.* (2004) Irinotecan plus gemcitabine results in no survival advantage compared with gemcitabine monotherapy in patients with locally advanced or metastatic pancreatic cancer despite increased tumor response rate. *J Clin Oncol* 22 (18):3776-3783. doi:10.1200/JCO.2004.12.082
122. Stathopoulos G. P., Syrigos K., Aravantinos G., Polyzos A., Papakotoulas P., Fountzilas G. *et al.* (2006) A multicenter phase III trial comparing irinotecan-gemcitabine (IG) with gemcitabine (G) monotherapy as first-line treatment in patients

with locally advanced or metastatic pancreatic cancer. *British Journal of Cancer* 95 (5):587-592. doi:10.1038/sj.bjc.6603301

123. Louvet C., Andre T., Lledo G., Hammel P., Bleiberg H., Bouleuc C. *et al.* (2002) Gemcitabine combined with oxaliplatin in advanced pancreatic adenocarcinoma: final results of a GERCOR multicenter phase II study. *J Clin Oncol* 20 (6):1512-1518

124. Afchain P., Chibaudel B., Lledo G., Selle F., Bengrine-Lefevre L., Nguyen S. *et al.* (2009) First-line simplified GEMOX (S-GemOx) versus classical GEMOX in metastatic pancreatic cancer (MPA): results of a GERCOR randomized phase II study. *Bull Cancer* 96 (5):E18-22. doi:10.1684/bdc.2009.0871

125. Lee K. H., Kim M. K., Kim Y. H., Ryoo B. Y., Lim H. Y., Song H. S. *et al.* (2009) Gemcitabine and oxaliplatin combination as first-line treatment for advanced pancreatic cancer: a multicenter phase II study. *Cancer Chemother Pharmacol* 64 (2):317-325. doi:10.1007/s00280-008-0873-9

126. Louvet C., Labianca R., Hammel P., Lledo G., Zampino M. G., Andre T. *et al.* (2005) Gemcitabine in combination with oxaliplatin compared with gemcitabine alone in locally advanced or metastatic pancreatic cancer: results of a GERCOR and GISCAD phase III trial. *J Clin Oncol* 23 (15):3509-3516. doi:10.1200/JCO.2005.06.023

127. Poplin E., Feng Y., Berlin J., Rothenberg M. L., Hochster H., Mitchell E. *et al.* (2009) Phase III, randomized study of gemcitabine and oxaliplatin versus gemcitabine (fixed-dose rate infusion) compared with gemcitabine (30-minute infusion) in patients with pancreatic carcinoma E6201: a trial of the Eastern Cooperative Oncology Group. *J Clin Oncol* 27 (23):3778-3785. doi:10.1200/JCO.2008.20.9007

128. Kindler H. L. (2002) Pemetrexed in pancreatic cancer. *Semin Oncol* 29 (6 Suppl 18):49-53. doi:10.1053/sonc.2002.37472

129. Oettle H., Richards D., Ramanathan R. K., van Laethem J. L., Peeters M., Fuchs M. *et al.* (2005) A phase III trial of pemetrexed plus gemcitabine versus gemcitabine in patients with unresectable or metastatic pancreatic cancer. *Annals of Oncology* 16 (10):1639-1645. doi:10.1093/annonc/mdi309

130. Bramhall S. R., Schulz J., Nemunaitis J., Brown P. D., Baillet M., Buckels J. A. (2002) A double-blind placebo-controlled, randomised study comparing gemcitabine and marimastat with gemcitabine and placebo as first line therapy in patients with advanced pancreatic cancer. *British Journal of Cancer* 87 (2):161-167. doi:10.1038/sj.bjc.6600446

131. Scheithauer W., Schull B., Ulrich-Pur H., Schmid K., Raderer M., Haider K. *et al.* (2003) Biweekly high-dose gemcitabine alone or in combination with capecitabine in patients with metastatic pancreatic adenocarcinoma: a randomized phase II trial. *Annals of Oncology* 14 (1):97-104

132. Herrmann R., Bodoky G., Ruhstaller T., Glimelius B., Bajetta E., Schuller J. *et al.* (2007) Gemcitabine plus capecitabine compared with gemcitabine alone in advanced pancreatic cancer: a randomized, multicenter, phase III trial of the Swiss Group for Clinical Cancer Research and the Central European Cooperative Oncology Group. *J Clin Oncol* 25 (16):2212-2217. doi:10.1200/JCO.2006.09.0886

133. Cunningham D., Chau I., Stocken D. D., Valle J. W., Smith D., Steward W. *et al.* (2009) Phase III randomized comparison of gemcitabine versus gemcitabine plus capecitabine in patients with advanced pancreatic cancer. *J Clin Oncol* 27 (33):5513-5518. doi:10.1200/JCO.2009.24.2446
134. Van Cutsem E., van de Velde H., Karasek P., Oettle H., Vervenne W. L., Szawlowski A. *et al.* (2004) Phase III trial of gemcitabine plus tipifarnib compared with gemcitabine plus placebo in advanced pancreatic cancer. *J Clin Oncol* 22 (8):1430-1438. doi:10.1200/JCO.2004.10.112
135. Abou-Alfa G. K., Letourneau R., Harker G., Modiano M., Hurwitz H., Tchekmedyian N. S. *et al.* (2006) Randomized phase III study of exatecan and gemcitabine compared with gemcitabine alone in untreated advanced pancreatic cancer. *J Clin Oncol* 24 (27):4441-4447. doi:10.1200/JCO.2006.07.0201
136. Xiong H. Q., Rosenberg A., LoBuglio A., Schmidt W., Wolff R. A., Deutsch J. *et al.* (2004) Cetuximab, a monoclonal antibody targeting the epidermal growth factor receptor, in combination with gemcitabine for advanced pancreatic cancer: a multicenter phase II Trial. *J Clin Oncol* 22 (13):2610-2616. doi:10.1200/JCO.2004.12.040
137. Philip P. A., Benedetti J., Corless C. L., Wong R., O'Reilly E. M., Flynn P. J. *et al.* (2010) Phase III study comparing gemcitabine plus cetuximab versus gemcitabine in patients with advanced pancreatic adenocarcinoma: Southwest Oncology Group-directed intergroup trial S0205. *J Clin Oncol* 28 (22):3605-3610. doi:10.1200/JCO.2009.25.7550
138. Kindler H. L., Friberg G., Singh D. A., Locker G., Nattam S., Kozloff M. *et al.* (2005) Phase II trial of bevacizumab plus gemcitabine in patients with advanced pancreatic cancer. *J Clin Oncol* 23 (31):8033-8040. doi:10.1200/JCO.2005.01.9661
139. Kindler H. L., Niedzwiecki D., Hollis D., Sutherland S., Schrag D., Hurwitz H. *et al.* (2010) Gemcitabine plus bevacizumab compared with gemcitabine plus placebo in patients with advanced pancreatic cancer: phase III trial of the Cancer and Leukemia Group B (CALGB 80303). *J Clin Oncol* 28 (22):3617-3622. doi:10.1200/JCO.2010.28.1386
140. Kindler H. L., Wroblewski K., Wallace J. A., Hall M. J., Locker G., Nattam S. *et al.* (2012) Gemcitabine plus sorafenib in patients with advanced pancreatic cancer: a phase II trial of the University of Chicago Phase II Consortium. *Invest New Drugs* 30 (1):382-386. doi:10.1007/s10637-010-9526-z
141. El-Khoueiry A. B., Ramanathan R. K., Yang D. Y., Zhang W., Shibata S., Wright J. J. *et al.* (2012) A randomized phase II of gemcitabine and sorafenib versus sorafenib alone in patients with metastatic pancreatic cancer. *Invest New Drugs* 30 (3):1175-1183. doi:10.1007/s10637-011-9658-9
142. Goncalves A., Gilibert M., Francois E., Dahan L., Perrier H., Lamy R. *et al.* (2012) BAYPAN study: a double-blind phase III randomized trial comparing gemcitabine plus sorafenib and gemcitabine plus placebo in patients with advanced pancreatic cancer. *Annals of Oncology* 23 (11):2799-2805. doi:10.1093/annonc/mds135

143. Yi S. Y., Park Y. S., Kim H. S., Jun H. J., Kim K. H., Chang M. H. *et al.* (2009) Irinotecan monotherapy as second-line treatment in advanced pancreatic cancer. *Cancer Chemother Pharmacol* 63 (6):1141-1145. doi:10.1007/s00280-008-0839-y
144. Ch'ang H. J., Huang C. L., Wang H. P., Shiah H. S., Chang M. C., Jan C. M. *et al.* (2009) Phase II study of biweekly gemcitabine followed by oxaliplatin and simplified 48-h infusion of 5-fluorouracil/leucovorin (GOFL) in advanced pancreatic cancer. *Cancer Chemother Pharmacol* 64 (6):1173-1179. doi:10.1007/s00280-009-0980-2
145. Yoo C., Hwang J. Y., Kim J. E., Kim T. W., Lee J. S., Park D. H. *et al.* (2009) A randomised phase II study of modified FOLFIRI.3 vs modified FOLFOX as second-line therapy in patients with gemcitabine-refractory advanced pancreatic cancer. *British Journal of Cancer* 101 (10):1658-1663. doi:10.1038/sj.bjc.6605374
146. Zaniboni A., Aitini E., Barni S., Ferrari D., Cascinu S., Catalano V. *et al.* (2012) FOLFIRI as second-line chemotherapy for advanced pancreatic cancer: a GISCAD multicenter phase II study. *Cancer Chemother Pharmacol* 69 (6):1641-1645. doi:10.1007/s00280-012-1875-1
147. Saif M. W., Podoltsev N. A., Rubin M. S., Figueroa J. A., Lee M. Y., Kwon J. *et al.* (2010) Phase II clinical trial of paclitaxel loaded polymeric micelle in patients with advanced pancreatic cancer. *Cancer Invest* 28 (2):186-194. doi:10.3109/07357900903179591
148. Melnik M. K., Webb C. P., Richardson P. J., Luttenton C. R., Campbell A. D., Monroe T. J. *et al.* (2010) Phase II trial to evaluate gemcitabine and etoposide for locally advanced or metastatic pancreatic cancer. *Mol Cancer Ther* 9 (8):2423-2429. doi:10.1158/1535-7163.MCT-09-0854
149. Hess V., Pratsch S., Potthast S., Lee L., Winterhalder R., Widmer L. *et al.* (2010) Combining gemcitabine, oxaliplatin and capecitabine (GEMOXEL) for patients with advanced pancreatic carcinoma (APC): a phase I/II trial. *Annals of Oncology* 21 (12):2390-2395. doi:10.1093/annonc/mdq242
150. Xenidis N., Chelis L., Amarantidis K., Chamalidou E., Dimopoulos P., Courcoutsakis N. *et al.* (2012) Docetaxel plus gemcitabine in combination with capecitabine as treatment for inoperable pancreatic cancer: a phase II study. *Cancer Chemother Pharmacol* 69 (2):477-484. doi:10.1007/s00280-011-1717-6
151. Reni M., Cereda S., Rognone A., Belli C., Ghidini M., Longoni S. *et al.* (2012) A randomized phase II trial of two different 4-drug combinations in advanced pancreatic adenocarcinoma: cisplatin, capecitabine, gemcitabine plus either epirubicin or docetaxel (PEXG or PDXG regimen). *Cancer Chemother Pharmacol* 69 (1):115-123. doi:10.1007/s00280-011-1680-2
152. Ozaka M., Matsumura Y., Ishii H., Omuro Y., Itoi T., Mouri H. *et al.* (2012) Randomized phase II study of gemcitabine and S-1 combination versus gemcitabine alone in the treatment of unresectable advanced pancreatic cancer (Japan Clinical Cancer Research Organization PC-01 study). *Cancer Chemother Pharmacol* 69 (5):1197-1204. doi:10.1007/s00280-012-1822-1
153. Nakai Y., Isayama H., Sasaki T., Sasahira N., Tsujino T., Toda N. *et al.* (2012) A multicentre randomised phase II trial of gemcitabine alone vs gemcitabine and S-1 combination therapy in advanced pancreatic cancer: GEMSAP study. *British Journal of Cancer* 106 (12):1934-1939. doi:10.1038/bjc.2012.183

154. Song H., Han B., Park C. K., Kim J. H., Jeon J. Y., Kim I. G. *et al.* (2013) Phase II trial of gemcitabine and S-1 for patients with advanced pancreatic cancer. *Cancer Chemother Pharmacol* 72 (4):845-852. doi:10.1007/s00280-013-2265-z
155. Ueno H., Ioka T., Ikeda M., Ohkawa S., Yanagimoto H., Boku N. *et al.* (2013) Randomized phase III study of gemcitabine plus S-1, S-1 alone, or gemcitabine alone in patients with locally advanced and metastatic pancreatic cancer in Japan and Taiwan: GEST study. *J Clin Oncol* 31 (13):1640-1648. doi:10.1200/JCO.2012.43.3680
156. Poplin E., Wasan H., Rolfe L., Raponi M., Ikeda T., Bondarenko I. *et al.* (2013) Randomized, multicenter, phase II study of CO-101 versus gemcitabine in patients with metastatic pancreatic ductal adenocarcinoma: including a prospective evaluation of the role of hENT1 in gemcitabine or CO-101 sensitivity. *J Clin Oncol* 31 (35):4453-4461. doi:10.1200/JCO.2013.51.0826
157. Ko A. H., Tempero M. A., Shan Y. S., Su W. C., Lin Y. L., Dito E. *et al.* (2013) A multinational phase 2 study of nanoliposomal irinotecan sucrosofate (PEP02, MM-398) for patients with gemcitabine-refractory metastatic pancreatic cancer. *British Journal of Cancer* 109 (4):920-925. doi:10.1038/bjc.2013.408
158. Saxby A. J., Nielsen A., Scarlett C. J., Clarkson A., Morey A., Gill A. *et al.* (2005) Assessment of HER-2 status in pancreatic adenocarcinoma: correlation of immunohistochemistry, quantitative real-time RT-PCR, and FISH with aneuploidy and survival. *Am J Surg Pathol* 29 (9):1125-1134
159. Cardin D. B., Goff L., Li C. I., Shyr Y., Winkler C., DeVore R. *et al.* (2014) Phase II trial of sorafenib and erlotinib in advanced pancreatic cancer. *Cancer Med* 3 (3):572-579. doi:10.1002/cam4.208
160. Hage C., Rausch V., Giese N., Giese T., Schonsiegel F., Labsch S. *et al.* (2013) The novel c-Met inhibitor cabozantinib overcomes gemcitabine resistance and stem cell signaling in pancreatic cancer. *Cell Death Dis* 4:e627. doi:10.1038/cddis.2013.158
161. Jin H., Yang R., Zheng Z., Romero M., Ross J., Bou-Reslan H. *et al.* (2008) MetMAb, the one-armed 5D5 anti-c-Met antibody, inhibits orthotopic pancreatic tumor growth and improves survival. *Cancer Research* 68 (11):4360-4368. doi:10.1158/0008-5472.CAN-07-5960
162. Delitto D., Vertes-George E., Hughes S. J., Behrns K. E., Trevino J. G. (2014) c-Met signaling in the development of tumorigenesis and chemoresistance: potential applications in pancreatic cancer. *World Journal of Gastroenterology* 20 (26):8458-8470. doi:10.3748/wjg.v20.i26.8458
163. Hingorani S. R., Petricoin E. F., Maitra A., Rajapakse V., King C., Jacobetz M. A. *et al.* (2003) Preinvasive and invasive ductal pancreatic cancer and its early detection in the mouse. *Cancer Cell* 4 (6):437-450
164. von Figura G., Fukuda A., Roy N., Liku M. E., Morris Iv J. P., Kim G. E. *et al.* (2014) The chromatin regulator Brg1 suppresses formation of intraductal papillary mucinous neoplasm and pancreatic ductal adenocarcinoma. *Nat Cell Biol* 16 (3):255-267. doi:10.1038/ncb2916
165. Siveke J. T., Einwachter H., Sipos B., Lubeseder-Martellato C., Kloppel G., Schmid R. M. (2007) Concomitant pancreatic activation of Kras(G12D) and Tgfa

results in cystic papillary neoplasms reminiscent of human IPMN. *Cancer Cell* 12 (3):266-279. doi:10.1016/j.ccr.2007.08.002

166. Bardeesy N., Aguirre A. J., Chu G. C., Cheng K. H., Lopez L. V., Hezel A. F. *et al.* (2006) Both p16(Ink4a) and the p19(Arf)-p53 pathway constrain progression of pancreatic adenocarcinoma in the mouse. *Proceedings of the National Academy of Sciences of the United States of America* 103 (15):5947-5952. doi:10.1073/pnas.0601273103

167. Hingorani S. R., Wang L., Multani A. S., Combs C., Deramaudt T. B., Hruban R. H. *et al.* (2005) Trp53R172H and KrasG12D cooperate to promote chromosomal instability and widely metastatic pancreatic ductal adenocarcinoma in mice. *Cancer Cell* 7 (5):469-483. doi:10.1016/j.ccr.2005.04.023

168. Mazur P. K., Einwachter H., Lee M., Sipos B., Nakhai H., Rad R. *et al.* (2010) Notch2 is required for progression of pancreatic intraepithelial neoplasia and development of pancreatic ductal adenocarcinoma. *Proceedings of the National Academy of Sciences of the United States of America* 107 (30):13438-13443. doi:10.1073/pnas.1002423107

169. Bardeesy N., Cheng K. H., Berger J. H., Chu G. C., Pahler J., Olson P. *et al.* (2006) Smad4 is dispensable for normal pancreas development yet critical in progression and tumor biology of pancreas cancer. *Genes & Development* 20 (22):3130-3146. doi:10.1101/gad.1478706

170. Ijichi H., Chytil A., Gorska A. E., Aakre M. E., Fujitani Y., Fujitani S. *et al.* (2006) Aggressive pancreatic ductal adenocarcinoma in mice caused by pancreas-specific blockade of transforming growth factor-beta signaling in cooperation with active Kras expression. *Genes & Development* 20 (22):3147-3160. doi:10.1101/gad.1475506

171. Skoulidis F., Cassidy L. D., Pisupati V., Jonasson J. G., Bjarnason H., Eyfjord J. E. *et al.* (2010) Germline Brca2 heterozygosity promotes Kras(G12D) -driven carcinogenesis in a murine model of familial pancreatic cancer. *Cancer Cell* 18 (5):499-509. doi:10.1016/j.ccr.2010.10.015

172. Saborowski M., Saborowski A., Morris J. P. th, Bosbach B., Dow L. E., Pelletier J. *et al.* (2014) A modular and flexible ESC-based mouse model of pancreatic cancer. *Genes & Development* 28 (1):85-97. doi:10.1101/gad.232082.113

173. Jancik S, Drabek J, Berkovcova J, Xu YZ, Stankova M, Klein J, Kolek V, Skarda J, Tichy T, Grygarkova I, Radzioch D, Hajduch M. (2012) A comparison of Direct sequencing, Pyrosequencing, High resolution melting analysis, TheraScreen DxS, and the K-ras StripAssay for detecting KRAS mutations in non small cell lung carcinomas. *J Exp Clin Cancer Res* 31:79

174. Afify A. M., al-Khafaji B. M., Kim B., Scheiman J. M. (2003) Endoscopic ultrasound-guided fine needle aspiration of the pancreas. Diagnostic utility and accuracy. *Acta Cytol* 47 (3):341-348

175. Eloubeidi M. A., Varadarajulu S., Desai S., Shirley R., Heslin M. J., Mehra M. *et al.* (2007) A prospective evaluation of an algorithm incorporating routine preoperative endoscopic ultrasound-guided fine needle aspiration in suspected pancreatic cancer. *J Gastrointest Surg* 11 (7):813-819. doi:10.1007/s11605-007-0151-x

176. Puli S. R., Bechtold M. L., Buxbaum J. L., Eloubeidi M. A. (2013) How good is endoscopic ultrasound-guided fine-needle aspiration in diagnosing the correct etiology for a solid pancreatic mass?: A meta-analysis and systematic review. *Pancreas* 42 (1):20-26. doi:10.1097/MPA.0b013e3182546e79
177. Turner B. G., Cizginer S., Agarwal D., Yang J., Pitman M. B., Brugge W. R. (2010) Diagnosis of pancreatic neoplasia with EUS and FNA: a report of accuracy. *Gastrointest Endosc* 71 (1):91-98. doi:10.1016/j.gie.2009.06.017
178. Chen J., Yang R., Lu Y., Xia Y., Zhou H. (2012) Diagnostic accuracy of endoscopic ultrasound-guided fine-needle aspiration for solid pancreatic lesion: a systematic review. *J Cancer Res Clin Oncol* 138 (9):1433-1441. doi:10.1007/s00432-012-1268-1
179. Mavrogenis G., Weynand B., Sibille A., Hassaini H., Deprez P., Gillain C. *et al.* (2015) 25-gauge histology needle versus 22-gauge cytology needle in endoscopic ultrasonography-guided sampling of pancreatic lesions and lymphadenopathy. *Endosc Int Open* 3 (1):E63-68. doi:10.1055/s-0034-1390889
180. Yang M. J., Yim H., Hwang J. C., Lee D., Kim Y. B., Lim S. G. *et al.* (2015) Endoscopic ultrasound-guided sampling of solid pancreatic masses: 22-gauge aspiration versus 25-gauge biopsy needles. *BMC Gastroenterol* 15:122. doi:10.1186/s12876-015-0352-9
181. Vilmann P., Saftoiu A., Hollerbach S., Skov B. G., Linnemann D., Popescu C. F. *et al.* (2013) Multicenter randomized controlled trial comparing the performance of 22 gauge versus 25 gauge EUS-FNA needles in solid masses. *Scand J Gastroenterol* 48 (7):877-883. doi:10.3109/00365521.2013.799222
182. Bang J. Y., Hawes R., Varadarajulu S. (2015) A meta-analysis comparing ProCore and standard fine-needle aspiration needles for endoscopic ultrasound-guided tissue acquisition. *Endoscopy*. doi:10.1055/s-0034-1393354
183. Yachida S., Jones S., Bozic I., Antal T., Leary R., Fu B. *et al.* (2010) Distant metastasis occurs late during the genetic evolution of pancreatic cancer. *Nature* 467 (7319):1114-1117
184. Bruna A., Rueda O. M., Greenwood W., Batra A. S., Callari M., Batra R. N. *et al.* (2016) A Biobank of Breast Cancer Explants with Preserved Intra-tumor Heterogeneity to Screen Anticancer Compounds. *Cell* 167 (1):260-274 e222. doi:10.1016/j.cell.2016.08.041
185. Izumchenko E., Paz K., Ciznadija D., Sloma I., Katz A., Vasquez-Dunddel D. *et al.* (2017) Patient-derived xenografts effectively capture responses to oncology therapy in a heterogeneous cohort of patients with solid tumors. *Annals of Oncology* 28 (10):2595-2605. doi:10.1093/annonc/mdx416
186. Cabanero M., Sangha R., Sheffield B. S., Sukhai M., Pakkal M., Kamel-Reid S. *et al.* (2017) Management of EGFR-mutated non-small-cell lung cancer: practical implications from a clinical and pathology perspective. *Curr Oncol* 24 (2):111-119. doi:10.3747/co.24.3524
187. Schultheis B., Reuter D., Ebert M. P., Siveke J., Kerkhoff A., Berdel W. E. *et al.* (2017) Gemcitabine combined with the monoclonal antibody nimotuzumab is an active first-line regimen in KRAS wildtype patients with locally advanced or metastatic

pancreatic cancer: a multicenter, randomized phase IIb study. *Annals of Oncology* 28 (10):2429-2435. doi:10.1093/annonc/mdx343

188. Boj S. F., Hwang C. I., Baker L. A., Chio, II, Engle D. D., Corbo V. *et al.* (2015) Organoid models of human and mouse ductal pancreatic cancer. *Cell* 160 (1-2):324-338. doi:10.1016/j.cell.2014.12.021

189. Starr T (2012) Cell: Organoid culture. http://www1.med.umn.edu/starrlab_deleteme/prod/groups/med/@pub/@med/@starrlab/documents/content/med_content_416910.html. Accessed Dec, 2016 2016

190. Ben-David U., Ha G., Tseng Y. Y., Greenwald N. F., Oh C., Shih J. *et al.* (2017) Patient-derived xenografts undergo mouse-specific tumor evolution. *Nat Genet* 49 (11):1567-1575. doi:10.1038/ng.3967

191. Eirew P., Steif A., Khattra J., Ha G., Yap D., Farahani H. *et al.* (2015) Dynamics of genomic clones in breast cancer patient xenografts at single-cell resolution. *Nature* 518 (7539):422-426. doi:10.1038/nature13952

192. MacDonald F., Zaiss D. M. W. (2017) The Immune System's Contribution to the Clinical Efficacy of EGFR Antagonist Treatment. *Front Pharmacol* 8:575. doi:10.3389/fphar.2017.00575

193. Broutier L., Andersson-Rolf A., Hindley C. J., Boj S. F., Clevers H., Koo B. K. *et al.* (2016) Culture and establishment of self-renewing human and mouse adult liver and pancreas 3D organoids and their genetic manipulation. *Nat Protoc* 11 (9):1724-1743. doi:10.1038/nprot.2016.097

194. Sato T., Stange D. E., Ferrante M., Vries R. G., Van Es J. H., Van den Brink S. *et al.* (2011) Long-term expansion of epithelial organoids from human colon, adenoma, adenocarcinoma, and Barrett's epithelium. *Gastroenterology* 141 (5):1762-1772. doi:10.1053/j.gastro.2011.07.050

195. Xia J., Hu Z., Yoshihara S., Li Y., Jin C. H., Tan S. *et al.* (2016) Modeling Human Leukemia Immunotherapy in Humanized Mice. *EBioMedicine* 10:101-108. doi:10.1016/j.ebiom.2016.06.028

196. Ji M., Jin X., Phillips P., Yi S. (2012) A humanized mouse model to study human immune response in xenotransplantation. *Hepatobiliary Pancreat Dis Int* 11 (5):494-498

197. Lee H. S., Lee J. G., Yeom H. J., Chung Y. S., Kang B., Hurh S. *et al.* (2016) The Introduction of Human Heme Oxygenase-1 and Soluble Tumor Necrosis Factor-alpha Receptor Type I With Human IgG1 Fc in Porcine Islets Prolongs Islet Xenograft Survival in Humanized Mice. *Am J Transplant* 16 (1):44-57. doi:10.1111/ajt.13467

198. Vakkila J., Lotze M. T. (2004) Inflammation and necrosis promote tumour growth. *Nature Reviews Immunology* 4 (8):641-648

199. Kawai T., Akira S. (2010) The role of pattern-recognition receptors in innate immunity: update on Toll-like receptors. *Nat Immunol* 11 (5):373-384. doi:10.1038/ni.1863

200. Morse D. L., Balagurunathan Y., Hostetter G., Trissal M., Tafreshi N. K., Burke N. *et al.* (2010) Identification of novel pancreatic adenocarcinoma cell-surface targets

by gene expression profiling and tissue microarray. *Biochem Pharmacol* 80 (5):748-754. doi:10.1016/j.bcp.2010.05.018

201. West A. C., Tang K., Tye H., Yu L., Deng N., Najdovska M. *et al.* (2017) Identification of a TLR2-regulated gene signature associated with tumor cell growth in gastric cancer. *Oncogene*. doi:10.1038/onc.2017.121

202. Tye H., Kennedy C. L., Najdovska M., McLeod L., McCormack W., Hughes N. *et al.* (2012) STAT3-driven upregulation of TLR2 promotes gastric tumorigenesis independent of tumor inflammation. *Cancer Cell* 22 (4):466-478. doi:10.1016/j.ccr.2012.08.010

203. Schneider C., Schmidt T., Ziske C., Tiemann K., Lee K. M., Uhlinsky V. *et al.* (2004) Tumour suppression induced by the macrophage activating lipopeptide MALP-2 in an ultrasound guided pancreatic carcinoma mouse model. *Gut* 53 (3):355-361

204. Schmidt J., Welsch T., Jager D., Muhlradt P. F., Buchler M. W., Marten A. (2007) Intratumoural injection of the toll-like receptor-2/6 agonist 'macrophage-activating lipopeptide-2' in patients with pancreatic carcinoma: a phase I/II trial. *British Journal of Cancer* 97 (5):598-604. doi:10.1038/sj.bjc.6603903

205. Shi W Su L, Li Q, Sun L, Lv J, Li J, Cheng B. (2014) Suppression of toll-like receptor 2 expression inhibits the bioactivity of human hepatocellular carcinoma. *Tumour Biol* 35:9627-9637

206. Conti L Lanzardo S, Arigoni M, Antonazzo R, Radaelli E, Cantarella D, Calogero RA, Cavallo F. (2013) The noninflammatory role of high mobility group box 1/Toll-like receptor 2 axis in the self-renewal of mammary cancer stem cells. *FASEB J* 27:4731-4744

207. Reilly M Miller RM, Thomson MH, Patris V, Ryle P, McLoughlin L, Mutch P, Gilboy P, Miller C, Broekema M, Keogh B, McCormack W, van de Wetering de Rooij J. (2013) Randomized, double-blind, placebo-controlled, dose-escalating phase I, healthy subjects study of intravenous OPN-305, a humanized anti-TLR2 antibody. *Clin Pharmacol Ther* 94:593-600